JAERI-M
84-008

ROSA-III 200% DOUBLE-ENDED BREAK INTEGRAL TEST RUN 926

(HPCS FAILURE)

February 1984

Hideo NAKAMURA, Kanji TASAKA, Yasuo KOIZUMI
Yoshinari ANODA, Hiroshige KUMAMARU, Hideo MURATA
Mitsuhiro SUZUKI, Masanori IRIKO* and Masayoshi SHIBA

日本原子力研究所
Japan Atomic Energy Research Institute

JAERI-M レポートは，日本原子力研究所が不定期に公刊している研究報告書です。
入手の問合わせは，日本原子力研究所技術情報部情報資料課（〒319-11茨城県那珂郡東海村）あて，お申しこしください。なお，このほかに財団法人原子力弘済会資料センター（〒319-11 茨城県那珂郡東海村日本原子力研究所内）で複写による実費頒布をおこなっております。

JAERI-M reports are issued irregularly.
Inquiries about availability of the reports should be addressed to Information Section, Division of Technical Information, Japan Atomic Energy Research Institute, Tokai-mura, Naka-gun, Ibaraki-ken 319-11, Japan.

編集兼発行　日本原子力研究所
印　　刷　いばらき印刷㈱

JAERI-M 84-008

ROSA-III 200% Double-ended Break Integral Test RUN 926 (HPCS Failure)

Hideo NAKAMURA, Kanji TASAKA, Yasuo KOIZUMI
Yoshinari ANODA, Hiroshige KUMAMARU, Hideo MURATA
Mitsuhiro SUZUKI, Masanori IRIKO* and Masayoshi SHIBA

Department of Nuclear Safety Research,
Tokai Research Establishment, JAERI

(Received January 11, 1984)

This report presents the test data of ROSA-III test RUN 926 that simulated a 200% double-ended break in the recirculation line with failure of HPCS. The ROSA-III test facility is a volumetrically scaled (1/424) model of the BWR/6 primary system, and is equipped with the electrically heated core, a break simulators and a scaled ECCS. RUN 926 was conducted successfully as designed. A peak cladding temperature (PCT) 783.5 K was reached at 118.5 s after the break, during the reflooding phase. Whole the core was completely quenched and cooled by ECCS, and the effectiveness of ECCS was confirmed.

The primary test results of RUN 926 are compared in this report with that of RUN 901, which was another 200% double-ended break test with full ECCS available, to investigate the effect of HPCS. In RUN 901 with HPCS available, PCT was reached during the initial blowdown phase. Although the time of PCT was different between two tests, the obtained PCTs were almost identical.

Keywords: BWR, LOCA, ECCS, Integral Test, ROSA-III Program, 200% Double-Ended Break, PCT, Fuel Assembly No. 4, HPCS Failure

---

* On leave from Computer Sevices Co. (CSK)

JAERI－M 84－008

ROSA－Ⅲ 200％両端破断総合実験；RUN 926
（HPCS故障）

日本原子力研究所東海研究所安全工学部
中村　秀夫・田坂　完二・小泉　安郎
安濃田良成・熊丸　博滋・村田　秀男
鈴木　光弘・入子　真規*・斯波　正誼

（1984年1月11日受理）

本報は，ROSA－Ⅲ実験装置を用い，HPCS故障を仮定して行った再循環ポンプ入口配管での200％両端破断総合実験RUN 926の実験結果について記述したものである。ROSA－Ⅲ実験装置は，BWR／6型原子炉の炉心を電気加熱ヒーターで模擬した実炉比（1／424）の装置である。RUN 926では，破断口はノズルにより模擬され，また実験は予定通り行われた。RUN 926の最高被覆管温度PCTは783.5 Kで，炉心再冠水時118.5秒に燃料棒A 71のポジション4に生じた。全炉心はECCS作動後クエンチされ，ECC注入効果が確認された。

本報では，RUN 926の主な実験結果が，同じく200％両端破断実験で，全ECCS作動と仮定したRUN 901の実験結果と比較されている。RUN 901では，下部プレナムフラッシング（LPF）鎮静後，RUN 926程燃料表面温度は上昇しなかった。これは，RUN 901で作動したHPCSの効果である。ただし，RUN 901のPCTはブローダウンの際に生じ，780 Kであったがこれは RUN 926でのPCTとほとんど同じ値であった。

＊ 出向職員：コンピューターサービス（株）（CSK）

Contents

目　　次

LIST OF TABLES

LIST OF FIGURES

ABBREVIATIONS

ADS	Automatic Depressurization System
AT	Air Tank
AV	Air Actuation Valve
(2)B	(2) inches pipe of Schedule 80
BN	Boron Nitride
BWR	Boiling Water Reactor
CA	Chromel-Alumel
CCFL	Counter Current Flow Limiting
CHV	Check Valve
CP	Conductivity Prove
CV	Control Valve
CWT	Cooling Water Tank
D	Differential Pressure
d	Diameter
DF	Density of Fluid
DL(+100)	Elevation (+100 mm) from the bottom of PV
ECCS	Emergency Core Cooling System
ESF	Engineered Safety Features
EX	Heat Exchanger
F	Flow Rate
Fig.	Figure
FS	Full Scale
FW	Feedwater
FWLF	Feedwater Line Flashing
FWP	Feedwater Pump
FWT	Feedwater Tank
HPCS	High Pressure Core Spray
HPCSP	High Pressure Core Spray Pump
HPCST	High Pressure Core Spary Tank

HPWP	High Pressure Water Pump
ID	Inner diameter
INC 600	Inconel 600
JP	Jet Pump
K	Kelvin
kg	Kilogram
kPa	Kilopascal
kW	Kilowatt
L	Liter
LB	Liquid Level in Channel Box
LBWR	Large Boiling Water Reactor
LL	Liquid Level
LOCA	Loss-of-Coolant Accident
LOCE	Loss-of-Coolant Experiment
LP	Lower Plenum
LPCI	Low Pressure Coolant Injection
LPCIP	Low Pressure Coolant Injection Pump
LPCIT	Low Pressure Coolant Injection Tank
LPCS	Low Pressure Core Spray
LPCSP	Low Pressure Core Spary Pump
LPCST	Low Pressure Core Spary Tank
LPF	Lower Plenum Flashing
LTP	Lower Tie Plate
M	Momentum Flux
m	Meter
mm	Milimeter
MLHR	Maximum Linear Heat Rate
MPa	Megapascal
MRP	Main Recirculation Pump
MSIV	Main Steam Isolation Valve
MSL	Main Steam Line

MW	Megawatt
N	Rotation Speed
OR	Orifice
P	Pressure
	Power
PCT	Peak Cladding Temperature
PV	Pressure Vessel
PWT	Pure Water Tank
QOBV	Quick Opening Blowdown Valve
QSV	Quick Shut-off Valve
RCN	Rapid Condencer
ROSA	Rig of Safety Assessment
rpm	Revolution per Minute
S	Signal
s	Second
Sch	Schedule
SUS	Stainless Steel
T	Temperature
T/C	Thermocouple
TC	Temperature of Fluid
TF	Temperature of Fuel
TS	Temperature of Structure Material
UTP	Upper Tie Plate
V	Valve
VF	Void Fraction
W	Watt
WL	Water Level
WSP	Water Supply Pump

1. Introduction

The Rig of Safety Assessment (ROSA)-III program was initiated in 1976 to study the thermal-hydraulic behavior of a Boiling Water Reactor (BWR) during a posturated Loss of Coolant Accident (LOCA) with the Emergency Core Cooling System (ECCS) actuation and to provide the data base to evaluate the predictability of computer codes developed for reactor safety analysis. The ROSA-III test facility was fabricated in 1978 and consisted of the volumetrically scaled (1/424) primary system of a 3800 MW BWR/6-251 with the electrically heated core, the break simulator and the scaled ECCS[1].

Special emphasis is made on the following objectives in the ROSA-III program:

(1) to provide the system data required to improve and evaluate the analytical methods currently used to predict the LOCA response of large BWRs. The performance of the Engineered Safety Features (ESFs), with particular emphasis on ECCSs, and the quantitative margins of safety inherent in performance of the ESFs are of primary interest.

(2) To identify and investigate any unexpected event(s) or threshold(s) in the response of either the plant or the ESFs and develop analytical techniques that adequately describe and account for such unexpected behavior.

The information acquired from Loss of Coolant Experiments (LOCEs) is thus used for evaluation and development of LOCA analytical methods and assesment for the qualitative margins of safety of ESFs in response to a LOCA.

RUN 926, conducted on October 29, 1981, was the third 200% break LOCA test of ROSA-III with use of the fuel assembly No. 4. The test simulated a double-ended shear break in the recirculation pump suction line with failure of HPCS.

The specific objectives of RUN 926 are as follows:

(1) To provide data of a 200% double-ended break test in the recirculation pump suction line with failure of HPCS.

(2) To evaluate the performance of the Emergency Core Cooling System (ECCS) by comparing the test results with those of other 200% double-ended break tests.

In this report, all the data obtained in RUN 926 are presented and the primary test results are compared with those of RUN 901 that was the 200% double-ended break LOCA test assuming that all of ECCS functioned as designed. The processed data like mass inventory in the pressure vessel are also given.

2. ROSA-III Test Facility

The ROSA-III test facility is a volumetrically scaled (1/424) BWR system with an electrically heated core designed to study the response of the primary system, the core and the ECCS during the postulated LOCA. The test facility is instrumented such that various thermal-hydraulic parameters are measured and recorded during the test. Details of the instrumentation are described in Section 3.

The test facility consists of four subsystems. These subsystems are : (a) the pressure vessel, (b) the steam line and the feedwater line, (c) the recirculation loops and (d) the ECCS. Figures 2.1 through 2.3 illustrate configuration of the test facility, the pressure vessel internals and the piping schematics, respectively. Table 2.1 compares the major dimensions of the ROSA-III test facility to the corresponding dimensions of the reference BWR system.

The ROSA-III pressure vessel includes various components in it simulating the internal structures of the reactor vessel in the BWR system as shown in Fig. 2.4. The interior of the vessel is divided into the core, the lower plenum, the upper plenum, the downcomer annulus, the steam separator, the steam dome and the steam dryer. The core is consisted of four model fuel assemblies of half length and a control rod simulator. Each fuel assembly contains 62 heater rods (Fig. 2.5) and 2 water rods spaced in a 8 x 8 square array and supported by spacers and upper and lower tie plates. The heater rod is heated electrically with chopped cosine power distribution along the axis as shown in Fig. 2.6. The effective heated length is 1880 mm, one half of the active length of a BWR fuel rod. The electric power supplied to the model fuel assembly "A" is 1.4 times larger than the power supplied to each of the other assemblies. The heater rods in each assembly are divided into three groups in terms of heat generation rate as shown in Fig. 2.7. The relative power generation rate of a heater rod in each group is 1.1,

1.0, and 0.875 respectively. The orifice plates are inserted at the core inlet to control the core inlet flow[1].

The steam line is connected to the steam dome of the pressure vessel. A control valve is installed in the steam line to control the steam dome pressure in steady state before the initiation of the tests. The steam line has a branch in which the automatic depressurization system is installed. The operation of valves in the steam line is described in Sec. 4. The feedwater is supplied from the feedwater tank (FWT) through the feedwater line and the feedwater sparger below the steam separator.

Figure 2.8 shows the recirculation lines consisted of two loops. Each line is furnished with a pump and two jet pumps. The jet pumps are installed outside the pressure vessel to simulte the relative volume and the relative height to the core. Two break simulators and a quick shut-off valve (QSV) are installed in one of these loops to simulate the various break conditions. Each break simulator consists of a nozzle or a orifice to determine the break size and a quick opening blowdown valve (QOBV) to initiate the test. The break mode (double-ended or split), the break size and the break location can be changed. The diameter of the largest nozzle and orifice available is 26.2 mm. Figure 2.8 shows two QOBVs, a QSV and flow nozzles installed upstream of the QOBVs. Several flow nozzles and orifices of different size are prepared to vary the break size.

The ROSA-III test facility is furnished with all kinds of the ECCS available in the BWR system, i.e., the High Pressure Core Spray (HPCS), the Low Pressure Core Spray (LPCS), the Low Pressure Coolant Injection (LPCI), and the Automatic Depressurization System (ADS). The HPCS and the LPCS provide the cooling water from the top of the core. The LPCI injects the cooling water into the core bypass. Each ECCS consists of a pump, a tank, piping, and a control system.

Reference (1) serves more detailed information on the facility.

3. Instrumentation

The instrumentation of the ROSA-III is designed to obtain thermal-hydraulic data during the simulated BWR LOCA. The data obtained from the experiments will contribute to the assessment of the analytical computer code. Table 3.1 summarizes instrumentation used in RUN 926.

Tables 3.2 and 3.3 show the measurement list of RUN 926 and the core instrumentation list, respectively. Instrumentation locations are shown in Fig. 3.1 through Fig. 3.7.

Typical measured parameters in the ROSA-III are pressure, differential pressure, flow rate, electric power, pump speed, fluid and metal temperatures, collapsed liquid level, two-phase mixture level, coolant fluid density, on-off type signals and so on.

Pressure and differential pressure transducers are two-wire, direct-current type which convert diaphragm displacement to electric capacitance. The pressure lead pipes are either the standard single, cylindrical pipes used in conjunction with condensate pots, or dual concentric cylinders capable of the circulation of cooling water to prevent flashing of the fluid.

The flow rate is measured either by an orifice or a venturi type flow meter depending on the fluid condition and measurement location.

The temperatures of the fluid, structural material and fuel rod cladding are measured with Chromel-Alumel thermocouples (CA T/C) of 1.6 or 0.5 mm ϕ.

Liquid levels are measured by either differential pressure transducers, described above or needle type electrical conductivity probes (CP) developed in the ROSA-III program. The probes are distributed along the vessel hight to detect the existence of water or vapor at different levels.

The electric power supplied to the simulated fuel rods is controlled to follow the predetermined function of time and measured by

a fast response electric power meter.

Pump speed is measured by a pulse generator integral of the pump. On-off signals such as selected valve positions, decay heat and pump coastdown simulation initiations and so on are detected in order to record the exact actuation time.

Fluid density in the pipe is measured by means of gamma densitometers. Preliminary studies indicate that a three-beam densitometer should be used to determine the flow regime. Figures 3.7 and 3.8 show the beam directions of the three-beam and the two-beam gamma densitometers, respectively. The gamma-ray source is ^{137}Cs and the detector is a water cooled NaI(Tl) scintillation counter.

Momentum flux is measured by a drag disk as shown in Fig. 3.9. The combination of signals from a drag disk and a gamma densitometer is used to determine the two-phase flow rate as shown in Fig. 3.10.

The data acquisition system (DATAC 2000B, Iwasaki Tsūshinki Co.) scans all the 700 channels of signals with the frequency up to 30 Hz. The data recorded on magnetic tape are processed by the FACOM M200 system computer at JAERI by off-line control. After evaluation, for example by comparing the initial and final pressure values with standard values, the data is reprocessed using the correct conversion factors as determined from the consistency examination.

More detailed information on the instrumentation and the data processing procedure are available in Reference (2).

4. Test Conditions and Procedure

RUN 926 is a 200% double ended large break test at the recirculation pump suction in the recirculation line. The break area is determined by inserting an nozzle upstream of the QOBV as shown in Figs. 4.1 and 3.9. Blowdown is initiated by opening the QOBV and closing the QSV placed between the two break simulators. The initial conditions of the test are as follows: The steam dome pressure is 7.37 MPa, the lower plenum temperature is 553 K giving the subcooling of 10.0 K, the core inlet flow rate is 16.3 kg/s, the core heat generating rate is 3.967 MW. The estimated quality at the core outlet is 13.9%. The detailed conditions are summerized in Table 4.1.

To conduct the test, makeup water (pure water) is pumped into the primary system of the test facility and electric power is supplied to the core to heat the water in the system and to achieve the saturation condition in the upper portion of the pressure vessel. The core power is 3.967 MW before the break initiation and is 44% of the steady state power 9 MW based on the conservation of the power to volume ratio in the reference BWR. The core power is changed during the transient after the break initiation as shown in Fig. 4.2. The power is kept constant for the first 9.0 seconds and reduced along the curve shown in the figure which simulated the total heat transfer rate in the core of the reference BWR (the delayed neutron fission power, the decay power of fission products and actinides and the stored heat in the nuclear fuel) neglecting the stored heat of ROSA-III heater rod[3]. The maximum linear heat rate of the peak power rod is 16.69 kW/m before the break initiation.

The schematics of the main steam line and the feedwater line are shown in Figs. 4.3 and 4.4. The main steam line of the ROSA-III has three branches: (1) steady flow branch, (2) ADS branch and (3) transient branch. Before the break initiation CV-130 in the steady flow branch

controls the steam flow to maintain the steam dome pressure constant and CV-1 and CV-2 are opened to provide steam to the heat exchanger to heat the feedwater. At the break initiation, CV-1 and 2 as closed and CV-130 is fully opened limiting the steam flow by an orifice OR-3 of 18 mm ID (inside diameter) at the upstream of CV-130. The main steam isolation valve (MSIV) is simulated by CV-130 after the break. Tables 4.2 and 4.3 show the characteristics and the control sequence of steam discharge line valves in the present test, respectively.

The details of the feedwater line is shown in Fig. 4.5. The feedwater is terminated at 2 s after the break by closing AV-112 in the feedwater line. However, the feedwater remained in the piping between the valve AV-112 and the feedwater sparger below the steam separator in the pressure vessel.

The coolant recirculation pumps are tripped to start coasting dowm at the break initiation.

The liquid level signal in the dowmcomer is used to actuate the ECCS and to close the MSIV. The downcomer level in the steady state operation is set at the scram level L3 (5.00 meters above the bottom of the pressure vessel) and L1 and L2 levels are 4.25 meters and 4.76 meters, respectively. The L2 level signal is used to close the MSIV with a time delay of 3 s and to actuate the HPCS with time delay of 27 s. The L1 level signal is used to actuate the LPCS, the LPCI and the ADS with time delay of 40 s, 40 s and 120 s, respectively. The above lag times of 3 s , 27 s, 40 s and 120 s are used in a safety analysis of the reference BWR[4]. The LPCI and the LPCS could inject cooling water after the primary system pressure is reduced below 2.16 MPa and 1.57 MPa, respectively. Specified system pressures for actuating the LPCS and the LPCI were decided from the pump characteristics used in the safety analysis of the reference BWR [5]. The test was terminated after all the core is quenched at 188 s after the break initiation.

5. Data Processing

In RUN 926, the data acquisition by DATAC 2000B was started 117 s before the break initiation and terminated 688 s after the break initiation. The data acquisition frequency was 10 Hz. The test data was processed and reduced to 1000 data points for computer plotting. The time span and frequency of the reduced data for plotting were 500 s and 2.0 Hz, respectively.

The test data are shown in Figs. 5.1 through 5.229. In these figures, the measured quantity is identified by the channel number and the alphabetic characters (Ref. Table 3.2).

The major test sequences and events observed in RUN 926 are summarized in Table 5.1.

Figures 5.1 through 5.7 show the pressure data in the pressure vessel and in the recirculation loop. Figures 5.8 through 5.37 show differential pressure data between various positions in the pressure vessel and the recirculation loop. Figures 5.38 and 5.39 show the liquid levels in the pressure vessel and in the tanks. Figures 5.40 through 5.46 show the flow rates. Differential pressures across orilfices and venturies shown in Figs. 5.47 through 5.57, are useful to check out the flow rate instrumentations. Figure 5.58 shows the power supplies to the core with the maximum capacities of 2100 and 3150 kW. The revolution speeds of the recirculation pumps are shown in Fig. 5.59. On-off signals such as the break initiation signal and the valve positioning signals are shown in Figs. 5.60, 5.61 and 5.62. Figures 5.63 through 5.72 show the fluid densities measured by the gamma densitometer. Figures 5.73 through 5.78 show momentum fluxes measured by drag disks. Figures 5.79 through 5.87 show the fluid temperatures at various positions in the loops. The fuel rod cladding temperature and the surface temperatures of the water rods and the channel boxes measured at Positions 1 through 7 are given in Figs. 5. 88 through 5.120. Figures 5.121 through 5.167 show the fuel rod

cladding temperatures in a different manner. Figures 5.168 through 5.170 show the fluid temperatures at the inlet and outlet of the channel box. Figures 5.171 through 5.198 show the fluid temperatures measured above and below the opeenings of the upper tie plate. The surface temperatures of the channel box are shown in Figs. 5.199 through 5.205, comparing the data at the same elevation. Figures 5.206, 5.207 and 5.208 show the fluid temperature in the lower plenum. The liquid level signals in the core, the upper and lower plena, the guide tube and the downcomer are shown in Fig. 5.209 through 5.229. Table 5.2 gives the maximum cladding temperature distribution in the core.

Quantities obtained from reduction of the test data are shown in Fig. 5.230 through 5.261.

Figures 5.230 shows the estimated liquid level in the pressure vessel obtained by reducing the conductivity probe signals in Figs. 5.209 through 5.229. Figures 5.231 and 5.232 show transients of the dryout front and the quenching front. Figures 5.233 through 5.236 show the average density claculated from the data measured by the three-beam or two-beam gamma densitometers. The beam configurations of gamma densitometers installed in the ROSA-III facility are shown in Figs. 3.7 and 3.8. The average density is claculated as an arithmetic mean of the densities in multi directions with the weight of the cord length.

For the three beam densitometer at the jet pump outlet spool piece,

$$\rho_{av} = 0.3221\rho_A + 0.43\rho_B + 0.2479\rho_C \qquad (5.1)$$

where,

ρ_{av} : average density obtained from the three-beam gamma densitometer,

ρ_A : density measured by beam A (bottom),

ρ_B : density measured by beam B (middle),

ρ_C : density measured by beam C (top).

For the two-beam densitometer at the break spool piece,

$$\rho_{av} = 0.5863\rho_A + 0.4137\rho_B \tag{5.2}$$

where,

ρ_{av} : average density obtained from the two-beam gamma densitometer,

ρ_A : density measured by beam A (bottom),

ρ_B : density measured by beam B (top).

Figures 5.237 through 5.240 show the flow rates at upstream sides of the break in the recirculation loop. The flow rate is computed from the drag disk data and the gamma densitometer data using the following equation,

$$G = C_D A\sqrt{\rho_{av} \cdot \rho_v^2} \tag{5.3}$$

where,

G : mass flow rate,

C_D : drag coefficient (=1.13),

A : flow area ($=1.923 \times 10^{-3}$ m^2),

ρ_{av} : average density from gamma densitometer,

ρ_v^2 : momentum flux from drag disk.

The break flow is derived from the flow rate in the recirculation loop as follows,

$$G_B = G_P + G_V \tag{5.4}$$

where,

G_B : break flow,

G_P : flow rate at the pump side of the break,

G_V : flow rate at the vessel side of the break.

The break flow rate based on the low and the high range drag disk data is shown in Fig. 5.241 and Fig. 5.242, respectively.

Figures 5.243 through 5.253 show the fluid flow rates at the main

steam line (MSL), the channel inlet orifices, the bypass hole and the jet pump outlets. The fluid flow rates are calculated from the test data which are the pressure drop across the orifices or venturi flow meters and the liquid density obtained from the temperature and the pressure condition. The equation used for the calculation is as follows:

$$G = C_D A\sqrt{2g \rho_\ell \Delta P} \qquad (5.5)$$

where,

G : flow rate (kg/s)

ΔP : pressure drop (mmH_2O)

C_D : discharge coefficient,

= 0.6552 (the orifice to measure the steam discharge flow rate)

= 0.4761 (the channel inlet orifice)

= 0.8032 (the bypass hole)

= 0.7383 (the orifice to measure the jet pump outlet flow rate)

= 1.1260 (the venturi tube to measure the jet pump outlet flow rate)

A : flow area (m^2)

= 2.875×10^{-3} (the orifice to measure the steam discharge flow rate)

= 1.521×10^{-3} (the channel inlet orifice)

= 1.758×10^{-4} (the bypass hole)

= 1.133×10^{-3} (the orifice to measure the jet pump outlet flow rate)

= 9.095×10^{-4} (the venturi tube to measure the jet pump outlet flow rate)

g : gravitational acceleration (=9.807 m/s^2)

ρ_ℓ : density of the single-phase fluid (kg/m^3)

This calculation method is not applicable for two-phase flow condition after the LPF initiation at the channel inlet orifice, the bypass hole and the jet pump outlet. The calculated value shows only a trend in

two-phase flow condition. Total channel inlet flow rate presents the sum of four channel inlet flow rates.

Figure 5.254 and 5.255 show the collapsed water level outside and inside the shrond. The collapped water level is obtained from the differential pressure in the pressure vessel. The differential pressure may include the flow resistance effect, however, the flow resistance becomes negligible after completion of the recirculation pump coastdown.

Figures 5.256, 5.257 and 5.258 show the fluid mass inventories in the pressure vessel. The fluid mass inventory is determined from the density and the volumes of liquid outside and inside the shroud,

$$M = \rho_\ell \cdot Q \tag{5.6}$$

where,

M : fluid inventory,

ρ_ℓ : liquid density estimated from the satulation temperature and/or pressure,

Q : liquid volume calculated from the liquid level.

The volume Q (m^3) outside the shroud is given below as a function of height.

$$\begin{aligned}
Q &= 0 && (\quad L \leq 0.494) \\
Q &= 0.0225\,L - 0.0111 && (0.494 \leq L \leq 1.384) \\
Q &= 0.0697\,L - 0.0769 && (0.384 \leq L \leq 1.519) \\
Q &= 0.0801\,L - 0.1980 && (3.355 \leq L \leq 4.250) \\
Q &= 0.2443\,L - 0.8959 && (4.250 \leq L \leq 4.413) \\
Q &= 0.2611\,L - 0.9700 && (4.413 \leq L \leq 4.578) \\
Q &= 0.2504\,L - 0.9211 && (4.578 \leq L \leq 4.654) \\
Q &= 0.2375\,L - 0.8610 && (4.654 \leq L \leq 4.815) \\
Q &= 0.2866\,L - 1.0974 && (4.815 \leq L \leq 4.915) \\
Q &= 0.3396\,L - 1.3580 && (4.915 \leq L \leq 5.143) \\
Q &= 0.3607\,L - 1.4665 && (5.143 \leq L \leq 5.365)
\end{aligned} \tag{5.7}$$

$Q = 0.3848\ L - 1.5960 \quad (5.365 \leq L \leq 5.955)$

$Q = 0.7111 \quad (5.955 \leq L)$

The volume Q (m^3) inside the shroud is given below as a function of height.

$Q = 0 \quad (L \leq 0.0)$

$Q = 0.2350\ L \quad (0.0 \leq L \leq 0.497)$

$Q = 0.1245\ L + 0.0549 \quad (0.497 \leq L \leq 1.354)$

$Q = 0.0698\ L + 0.1290 \quad (1.354 \leq L \leq 3.589)$

$Q = 0.1648\ L - 0.2120 \quad (3.589 \leq L \leq 3.744)$

$Q = 0.1963\ L - 0.3299 \quad (3.744 \leq L \leq 4.243)$

$Q = 0.0196\ L + 0.4199 \quad (4.243 \leq L \leq 4.578)$ (5.8)

$Q = 0.0186\ L + 0.4244 \quad (4.578 \leq L \leq 4.654)$

$Q = 0.0410\ L + 0.3201 \quad (4.654 \leq L \leq 5.099)$

$Q = 0.0196\ L + 0.4292 \quad (5.099 \leq L \leq 5.365)$

$Q = 0.5344\ L \quad (5.365 \leq L)$

The total fluid mass inventory in the pressure vessel is obtained as the summation of the mass inventory outside and inside the shround. The initial mass inventory before the break initiation is estimated as 640 kg.

Figure 5.259 shows the mass decrease by the fluid discharge from the break and the fluid mass recovery by the ECCS water and the feedwater injections. The variation of fluid mass inventory with time is calculated by the following equation,

$$M = \int_0^t \left\{ G + \rho_1 \cdot (W_H + W_L + W_I) + \rho_2 \cdot W_F \right\} dt \qquad (5.9)$$

where,

M : mass accumulation,

G : steam discharge flow rate,

ρ_1 : density of satulated liquid at 315 K,

ρ_2 : density of satulated liquid at 489 K,

W_H : volumetric flow rate of the HPCS,

W_L : volumetric flow rate of the LPCS,

W_I : volumetric flow rate of the LPCI,

W_F : volumetric flow rate of the feedwater

Figure 5.260 shows the fluid mass discharged from the break. The fluid mass discharge M_B is calculated as follows neglecting the change of the fluid mass inventory in the loops,

$$M_B = (M_P)_i - M_P + M_F \tag{5.10}$$

where,

M_B : fluid mass discharged from the break,

$(M_P)_i$: fluid mass inventory in the pressure vessel (= 640 kg),

M_P : fluid mass inventory in the pressure vessel,

M_F : net fluid mass increase by the ECCS, the feedwater flow and the steam discharge flow.

Figure 5.261 shows the break flow calculated from the fluid mass inventory in the pressure vessel. The break flow is estimated from the mass inventory as follows,

$$G_B = \frac{d}{dt} M_B \tag{5.11}$$

where,

G_B : break flow,

M_B : fluid mass discharge from the break.

6. Test Results and Comparison with those of RUN 901

This section presents interpretation of the RUN 926 test data, as well as comparison of the RUN 926 data with that of RUN 901. RUN 901 was the first 200% double-ended break test with use of the fuel assembly No.4, and simulated all of ECCS functioning as designed. The effect of HPCS can be evaluated by comparing the results of these two tests.

6.1 Test Conditions

Table 6.1 compares the test initial conditions and the sequence of major events in two tests. The differences between test conditions of two tests, except for that in the HPCS availability, primarily resulted from differences in the initial core power and in the MSL valve control sequence.

Figures 6.1 through 6.3 show the electric core power, the steam discharge flow rate and the feedwater flow rate in two tests, respectively. Initially the steam discharge flow rate and the feedwater flow rate in RUN 901 were a little higher than those in RUN 926 because of the higher initial core power in RUN 901. The steam discharge flow rate in RUN 926 decreased temporarily after the break, because CV1 and CV2, shown in Figs.4.3 and 4.4, closed earlier than full opening of CV130. In RUN 901 the steam discharge flow rate also decreased temporarily after the break as the steam flow rate was switched.

6.2 System Pressure

The lower plenum pressures in RUNs 926 and 901 are compared in Figs. 6.4. The pressure represents typical system pressure response in two tests. The pressure transients in two tests show very similar trends: After the initial decrease, the pressure began to recover when MSIV was closed, and to decrease again as the recirculation line was uncovered. The MSIV, simulated by CV-130 in RUN 926 and by AV 165 in RUN 901, initiated to close 5.4s in RUN 926, 2.0s earlier than in RUN 901. The temporary pressure increase after the MSIV closure was larger in RUN 926 than in RUN 901, because the MSIV closed earlier in RUN 926. The lower plenum flashing (LPF) started at 17s in two tests as the system depressurized to the saturation pressure corresponding to the lower plenum fluid temperature. The pressure in RUN 901 decreased a little faster

than that in RUN 926 after the HPCS was actuated at 31.5s, because steam in the upper plenum was condensed by the cold (313K) HPCS liquid. Therefore, the feedwater line flashing (FWLF) in RUN 901 occurred a little earlier than in RUN 926 as shown in Fig.6.3. After the FWLF initiation the system pressure showed similar trend as shown in Fig.6.4. LPCS, LPCI and ADS affected the pressure transient little.

6.3 Differential Pressure

The differential pressures between the top and bottom of the pressure vessel in two tests are compared in Fig.6.5. The differential pressures in two tests were similar to the FWLF. The differential pressure decreased rapidly after the break, and became nearly constant before the LPF. An upward flow and a downward flow were observed in the shroud when the LPF and the FWLF occurred, respectively. HPCS, actuated at 31.5s in RUN 901, did not markedly affect the decreasing trend of the differential pressure shown in Fig.6.5. LPCS halted the decrease of the differential pressure. After LPCS was actuated, the difference between two tests became more pronounced. The collapsed liquid levels in the downcomer calculated from the downcomer differential pressure are shown in Fig.6.6. Measuring range is separated as ECC spray line nozzle elevation (3900mm) as shown in Fig.3.2. The collapsed liquid levels in two tests showed very similar behaviors. Since the liquid level in the upper downcomer is used for tripping ECCS including ADS, similar level behaviors in two tests resulted in nearly the same timings of actuation of ADS in two tests as shown in Table 6.1. Considerable influence of fluid acceleration on the lower downcomer differential pressure was observed immediately after the break in both tests; the downward acceleration of the downcomer fluid reduced the measured differential pressure.

6.4 Coolant Flow Rate

The coolant flow rate through the channel inlet orifices and the bypass holes were calculated from the differential pressures across these flow paths as mentioned in section 5. The total channel inlet flow rate in RUN 926, shown in Fig.5.249, is compared with that in RUN 901 in Fig.6.7. The total channel inlet flow rates in two tests show nearly the same behavior until the FWLF. The flow rate decreased rapidly to one corresponding to the natural circulation. The flow rate decreased again to nearly zero after the liquid level in the downcomer decreased

to the jet pump suction level. After the LPF initiation the flow rate increased temporarily. However, when the flow through the orifices became two phase, the calculated flow rates became incorrect giving only the trend. After the FWLF initiation the core flow was reversed to the downward direction temporarily. That is because the rapid steam generation in the feedwater line reduced the system depressurization rate, and reduced the steam generation in the lower plenum. In RUN 926 the core was wholly uncovered at 70s, 2s after the FWLF initiation, as shown in Figs.5.230 snd 6.9. At 80s the liquid level above the channel inlet orifice disappeared. Then, upward steam flow rate in RUN 926 was larger than that in RUN 901 until 100s, because the upward flow at the channel inlet orifice in RUN 901 was restriced by the CCFL.

Figure 6.8 shows the ECCS injection rates in RUNs 926 and 901. The core spray flow rate was five times as large as the LPCI injection rate. LPCS and LPCI actuated later in RUN 926 than in RUN 901 because of the slower depressurization in RUN 926 than in RUN 901.

6.5 Liquid Level

Liquid levels inside the core shroud in RUNs 926 and 901 are compared in Fig.6.9. These liquid levels shown are estimated from signals obtained from the conductivity probes installed in the fuel assembly. Liquid levels only in channel A are shown in Fig.6.9 as those in the core.

The difference in the core mass inventory between RUNs 926 and 901 became notable after HPCS is actuated in RUN 901. The core liquid levels in two tests began to drop simultaneously at 40s from the upper tie plate as LPF moderated. But, the liquid level in RUN 926 dropped to the lower tie plate after the initiation of FWLF, whereas the liquid level in RUN 901 dropped only to the position 6 and then began to recover soon. When LPCI was actuated, the whole core including the channel inlet was uncovered in RUN 926 but the liquid level in RUN 901 had already recovered above position 3 in the core. HPCS in RUN 901 prevented a whole core uncovery and made the core uncovery time much shorter than that in RUN 926.

CCFL was observed at both upper tie plate and the channel inlet orifice. CCFL pushed the mixture level in the lower plenum down. In RUN 926 the CCFL affected the mixture level especially after 105s.

In RUN 926 the liquid level in the lower plenum disappeared at 165s, because the CCFL at the channel inlet orifices broke down. The CCFL

breakdown at the channel inlet orifices caused flow reversal at the channel inlet orifices and a temporary decrease of level in the upper core. This was observed particularly in channel D as shown in Figs.5.213 and 5.247.

The liquid level in the downcomer shown in Fig.5.230 decreased steeply after the break. The jet pump suction and recirculation line nozzle were uncovered at 10.0s and 13.0s, respectively.

6.6 Fuel Rod Surface Temperature

Dryout and quenching behaviors in channels A and C in RUN 926 are shown in Figs.5.231 and 5.232. These behaviors were estimated from the fuel rod surface temperature histories shown in Figs.5.88, 5.90, 5.92, 5.94, 5.104, 5.105, 5.106 and 5.107. The mixture levels in channels A and C are also presented in Figs.5.231 and 5.232, respectively.

The dryout and quenching behaviors corresponded closely to the mixture levels in the channel box: The dryout front followed the falling liquid level, and the quench front followed the recovering liquid level. In RUN 926 major liquid level fall in the core occurred twice. The first was the temporary level fall before the LPF initiation and the second was a whole core uncovery occurred after the LPF had moderated and before the bottom-up core reflooding initiated.

The fuel rod surface temperature rose faster in the first level fall than in the second, because the core power was higher during the first level fall. In RUN 901 the peak cladding temperature (PCT) was 780K and was reached at 18.3s, during the first level fall, at position 2 of A11 rod in the peak power channel A as shown in Fig.6.10. In RUN 926 the fuel rod surface temperature also rose as high as in RUN 901 in the first level fall especially at position 2 of corner rods A11 and A88 in the peak power channel A. But, the PCT in RUN 926 was reached at 118.5s, during the second level fall, at midplane of the fuel rod A71 in the peak power channel A. The duration of the second level fall in RUN 926 was much longer than in RUN 901 due to the HPCS failure and the rod surface temperature in the second level fall became much higher than in the first level fall. The PCT in RUN 926 was 783.5K and was almost identical to that in RUN 901.

After the FWLF initiation top-down quenching was observed in the upper part of the core in RUN 926. At the same time, the lower part of the core was quenched by the falling down LPCS liquid through the core.

The fuel rod surfaces were finally quenched by reflooding after LPCI was actuated. But the quenching in the upper part of the core was delayed from the core uncovering by reflooding.

6.7 Density, Momentum Flux and Discharge Flow

Density, momentum flux and discharge flow rate from the break obtained in RUN 926 showed nearly the same tendency as those obtained in RUN 901.[6]

The area-averaged fluid densities measured at the JP outlet in the intact and broken loops and upstream the MRP side and PV side of the break are shown in Figs.5.233 through 5.236.

The densities at the JP outlet in intact and broken loops showed the same tendency: The density began to decrease after the LPF initiation at 17.0s and recovered temporarily when the FWLF initiated at 68.0s. It took much time to recover the density to that of the single phase liquid after LPCI was actuated because of the continuous flashing at the jet pump outlet as shown in Figs.5.63 through 5.68.

The density at the MRP side of the break decreased after the break, because of depressurization and flashing in the recirculation line between the break and the jet pump drive nozzles. The density at the PV side of the break stayed at the single phase liquid value until the recirculation pump suction line was uncovered at 13.0s. After 140s the density at the PV side of the break began to increase gradually as the coolant flowing out from the core shroud reached to the break.

Figures 5.75 through 5.78 show the momentum flux at the break measured by drag disks. The low range drag disks saturated during the initial blowdown phase. Also the high range drag disk showed abnormal values until 14s. Since the break flow rates shown in Figs.5.237 through 5.242 were calculated from the measured momentum flux, the calculated break flow rate is incorrect when the drag disks were saturated or operated abnormally. The steady state flow directions were defined as negative at the MRP side of the break and as positive at the PV side of the break. The flow direction at the MRP side of the break was reversed immediately after the break initiation.

These break flow rates obtained from the measurements with the drag disks and gamma densitometers include an error of at least $\pm$20%.

The total break flow rate was also calculated differentiating the vessel mass inventory with respect to time and is shown in Fig.5.261. This estimation was affected by the acceleration effects on the measure-

ment of differential pressure, which was used for calculation of the vessel mass inventory.

7. Conclusion

In this report, all the available test data obtained in ROSA-III test RUN 926 have been presented. RUN 926 simulated a 200% double-ended shear break in the MRP suction line LOCA with failure of HPCS. Some informations on the ROSA-III test facility, instrumentation and test procedure, and brief interpretation of the test results have also been presented.

RUN 926 was conducted successfully as previously planned. From evaluation of the test results of RUN 926 and comparison between the test results of RUN 926 and RUN 901 which simulated a 200% double-ended break LOCA with full ECCS available, the following conclusions were derived:

(1) The PCT was reached during the core reflooding phase. This was in contract to that PCT in RUN 901 was reached during the initial blowdown phase. However the absolute values of PCT were almost identical in two tests: 783.5K in RUN 926 reached at Pos.4 of A71 rod, and 780K in RUN 901 reached at Pos.2 of A11 rod.

(2) The core was wholly uncovered by the FWLF. In RUN 901, with intact HPCS, the core was not wholly uncovered even after the FWLF. The whole core uncovering in RUN 926 resulted in much longer core dryout than in RUN 901.

(3) HPCS condensed steam in the upper plenum and accelerated the system depressurization.

(4) All the heater rods were quenched with LPCS and LPCI, and the effectiveness of ECCS for core cooling has been confirmed in RUN 926.

(5) The CCFL was observed at both the channel inlet orifices and the upper tie plate.

(6) The LPF and the FWLF induced upward and downward flows in the core shroud respectively.

Acknowledgment

The authors are grateful to H. Asahi, T. Odaira, T. takayasu, S. Sekiguchi, Y. Kitano and T. Numata of Nuclear Engineering Corporation for their assistance in conducting the experiment and K. Yamano, H. Gotoh and K. Hiyama of Information System Laboratory Corpolation for preparing the data plots and T. Kurosawa of Nihon Computer Bureau Corporation for preparing the report. The authors are also indebted to M. Akinaga of Nippon Atomic Industry Group Corporation Co., Ltd. for his valuable discussion in preparing the report. They are grateful to Dr. Y. Kukita for reviewing the manuscript.

References

(1) ANODA, Y., et. al., "ROSA-III System Description for Fuel Assembly No. 4", JAERI-M 9363 (1981).

(2) SOBAJIMA, M., et. al., "Instrumentation and Data Processing for ROSA-III Test" (in Japanese), JAERI-M 8499 (1979).

(3) ABE, N., et. al., "Electric Power Transient Curve for ROSA-III Tests", JAERI-M 8728 (1980).

(4) "General Electric Standard Safety Analysis Report, BWR/6", DOCKET-STN-50531-22, General Electric Company.

(5) "BWR Blowdown Emergency Core Cooling Program, Preliminary Facility Description Report for the BT/ECC1A Test Phase", GEAP-23592, NRC-2 (1977).

(6) Nakamura, H., et. al., "200% Double-ended Break Integral Test RUN 901", JAERI-M (1983), to be published.

Acknowledgment

The authors are grateful to H. Asahi, T. Odaira, T. takayasu, S. Sekiguchi, Y. Kitano and T. Numata of Nuclear Engineering Corporation for their assistance in conducting the experiment and K. Yamano, H. Gotoh and K. Hiyama of Information System Laboratory Corpolation for preparing the data plots and T. Kurosawa of Nihon Computer Bureau Corporation for preparing the report. The authors are also indebted to M. Akinaga of Nippon Atomic Industry Group Corporation Co., Ltd. for his valuable discussion in preparing the report. They are grateful to Dr. Y. Kukita for reviewing the manuscript.

References

(1) ANODA, Y., et. al., "ROSA-III System Description for Fuel Assembly No. 4", JAERI-M 9363 (1981).

(2) SOBAJIMA, M., et. al., "Instrumentation and Data Processing for ROSA-III Test" (in Japanese), JAERI-M 8499 (1979).

(3) ABE, N., et. al., "Electric Power Transient Curve for ROSA-III Tests", JAERI-M 8728 (1980).

(4) "General Electric Standard Safety Analysis Report, BWR/6", DOCKET-STN-50531-22, General Electric Company.

(5) "BWR Blowdown Emergency Core Cooling Program, Preliminary Facility Description Report for the BT/ECC1A Test Phase", GEAP-23592, NRC-2 (1977).

(6) Nakamura, H., et. al., "200% Double-ended Break Integral Test RUN 901", JAERI-M (1983), to be published.

Table 2.1 Primary Characteristics of BWR/6 and ROSA-III

	BWR*	ROSA-III	BWR/ROSA-III
Number of Recirc. Loops	2	2	1
Number of Jet Pumps	24	4	6
Number of Separators	251	1	251
Number of Fuel Assemblies	848	4	212
Active Fuel Length (m)	3.76	1.88	2
Total Volume (m^3)	621	1.42	437
Power (MW)	3,800	4.40	864
Pressure (MPa)	7.23	7.23	1
Core Flow (kg/s)	1.54×10^4	36.4	424
Recirculation Flow (l/s)	2,970	7.01	424
Feedwater Flow (kg/s)	2,060	4.86	424
Feedwater Temp. (K)	489	489	1

* BWR/6-251

Table 3.1 ROSA-III Instrumentation List

ITEM	SENSOR	NUMBER	NOTE
Pressure	Pressure Transducer	20	
Differential Pressure	DP Cell	60	PV and Loop 44 Level Measurement 5 Flow Meter 11
Fluid Temperature	CA Thermocouple	129	Primary Loop 23 DTT 4 Tie Rod 28 Upper Plenum 10 Lower Plenum 10 Tie Plate 40 Bypass 14
Fuel Rod Temperature	CA Thermocouple	213	
Slab Surface Temperature	CA Thermocouple	70	Core Barrel 24 Pressure Vessel 3 Channel Box 35 Shroud Support 8
Slab Inner Temperature	CA Thermocouple	9	JP Diffuser 4 PV Wall 5
Volumetric Flow Rate	Turbine Flow Meter Venturi Flow Meter Orifice Flow Meter	3 4 6	ECCS Loop 3 Primary Loop 10
Mass Flow Rate	Turbine Flow Meter Orifice Flow Meter	4 3	Recirculation Loop 4 Main Steam Line 3
Liquid Level	Conductivity Probe Capacitance Probe	138 2	
Density	Gamma Densitometer	10	2 Beam GD 2 3 Beam GD 2
Momentum Flux	Drag Disk	4	JP Spool Piece 2 Break Spool Piece 4 Break Orifice 1
Signal	ON/OFF Switch	14	
Pump Speed	Revolution Counter	2	
Electric Core Power	VA Meter	2	
TOTAL		693	

Table 3.2 Measurement List for RUN 926

1Ch.- 50Ch.

Ch.	Item	Symbol	ID.		Location	Fig.No.	Range			Unit	Accuracy
1	Press.	P- 1	PA	1	Lower Plenum	Fig.5. 1	0.100	-	10.0	MPa	1.08%FS
2	Press.	P- 2	PA	2	Upper Plenum	Fig.5. 1	0.100	-	10.0	MPa	1.08%FS
3	Press.	P- 3	PA	3	Steam Dome	Fig.5. 1	0.100	-	10.0	MPa	1.08%FS
4	Press.	P- 4	PA	4	Downcomer Bottom	Fig.5. 1	0.100	-	10.0	MPa	1.08%FS
5	Press.	P- 5	PA	5	JP-3 Drive	Fig.5. 2	0.100	-	10.0	MPa	1.08%FS
6	Press.	P- 6	PA	6	JP-4 Drive	Fig.5. 2	0.100	-	10.0	MPa	1.08%FS
7	Press.	P- 7	PA	7	JP-3 Suction	Fig.5. 2	0.100	-	10.0	MPa	1.08%FS
8	Press.	P- 8	PA	8	JP-4 Suction	Fig.5. 2	0.100	-	10.0	MPa	1.08%FS
9	Press.	P- 9	PA	9	MRP-1 Suction	Fig.5. 3	0.100	-	10.0	MPa	1.08%FS
10	Press.	P-10	PA	10	MRP-2 Suction	Fig.5. 3	0.100	-	10.0	MPa	1.08%FS
11	Press.	P-11	PA	11	MRP-2 Delivery	Fig.5. 3	0.100	-	10.0	MPa	1.08%FS
12	Press.	P-12	PA	12	Break A Upstream	Failure	0.100	-	10.0	MPa	1.08%FS
13	Press.	P-13	PA	13	Break A Downstream	Fig.5. 4	0.100	-	10.0	MPa	1.08%FS
14	Press.	P-14	PA	14	Break B Upstream	Fig.5. 5	0.100	-	10.0	MPa	1.08%FS
15	Press.	P-15	PA	15	Break B Downstream	Fig.5. 5	0.100	-	10.0	MPa	1.08%FS
16	Press.	P-16	PA	16	Steam Line	Fig.5. 6	0.100	-	10.0	MPa	1.08%FS
17	Press.	P-17	PA	17	JP-1,2 Outlet Spool	Fig.5. 7	0.100	-	10.0	MPa	1.08%FS
18	Press.	P-18	PA	18	JP-3,4 Outlet Spool	Fig.5. 7	0.100	-	10.0	MPa	1.08%FS
19	Press.	P-19	PA	19	Break A Spool Piece	Fig.5. 4	0.100	-	10.0	MPa	1.08%FS
20	Press.	P-30	PA	20	Break B Spool Piece	Fig.5. 5	0.100	-	10.0	MPa	1.08%FS
21	Diff.P.	D- 1	PD	21	Lower Pl.-Upper Pl.	Fig.5. 8	-50.0	-	350.	kPa	0.63%FS
22	Diff.P.	D- 2	PD	22	Upper Pl.-Steam Dome	Fig.5. 9	-10.0	-	90.0	kPa	0.63%FS
23	Diff.P.	D- 3	PD	23	Lower Plenum Head	Not Measured					
24	Diff.P.	D- 4	PD	24	Downcomer Head	Fig.5.10	0.0	-	100.	kPa	0.63%FS
25	Diff.P.	D- 5	PD	25	PV Bottom-Top	Fig.5.11	-100.	-	900.	kPa	0.63%FS
26	Diff.P.	D- 6	PD	26	JP-1 Disch.-Suction	Fig.5.12	-100.	-	300.	kPa	0.63%FS
27	Diff.P.	D- 7	PD	27	JP-1 Drive -Suction	Fig.5.13	0.0	-	2.50	MPa	0.63%FS
28	Diff.P.	D- 8	PD	28	JP-2 Disch.-Suction	Fig.5.12	-100.	-	300.	kPa	0.63%FS
29	Diff.P.	D- 9	PD	29	JP-2 Drive -Suction	Fig.5.13	0.0	-	2.50	MPa	0.63%FS
30	Diff.P.	D-10	PD	30	JP-3 Disch.-Suction	Fig.5.14	-100.	-	300.	kPa	0.63%FS
31	Diff.P.	D-11	PD	31	JP-3 Drive -Suction	Fig.5.15	-4.00	-	2.00	MPa	0.63%FS
32	Diff.P.	D-12	PD	32	JP-4 Disch.-Suction	Fig.5.14	-100.	-	300.	kPa	0.63%FS
33	Diff.P.	D-13	PD	33	JP-4 Drive -Suction	Fig.5.15	-4.00	-	2.00	MPa	0.63%FS
34	Diff.P.	D-14	PD	34	MRP-1 Deliv.-Suction	Fig.5.16	-0.100	-	2.50	MPa	0.63%FS
35	Diff.P.	D-15	PD	35	MRP-2 Deliv.-Suction	Fig.5.16	-0.100	-	2.50	MPa	0.63%FS
36	Diff.P.	D-16	PD	36	DC Bottom- MRP-1 Suc.	Fig.5.17	-50.0	-	50.0	kPa	0.63%FS
37	Diff.P.	D-17	PD	37	MRP1 Deliv.-JP1 Drive	Fig.5.18	0.0	-	250.	kPa	0.63%FS
38	Diff.P.	D-18	PD	38	MRP1 Deliv.-JP2 Drive	Fig.5.18	0.0	-	250.	kPa	0.63%FS
39	Diff.P.	D-19	PD	39	DC Middle-JP1 Suction	Fig.5.19	0.0	-	250.	kPa	0.63%FS
40	Diff.P.	D-20	PD	40	DC Middle-JP2 Suction	Fig.5.19	0.0	-	250.	kPa	0.63%FS
41	Diff.P.	D-21	PD	41	JP1 Disch.-Lower Pl.	Fig.5.20	-100.	-	100.	kPa	0.63%FS
42	Diff.P.	D-22	PD	42	JP2 Disch.-Lower Pl.	Fig.5.20	-100.	-	100.	kPa	0.63%FS
43	Diff.P.	D-23	PD	43	DC Bottom- Break B	Fig.5.21	-60.0	-	540.	kPa	0.63%FS
44	Diff.P.	D-24	PD	44	Break B- Break A	Fig.5.22	0.0	-	100.	kPa	0.63%FS
45	Diff.P.	D-25	PD	45	Break A- MRP2 Suction	Fig.5.23	-500.	-	100.	kPa	0.63%FS
46	Diff.P.	D-26	PD	46	MRP2 Deliv.-JP3 Drive	Fig.5.24	-500.	-	500.	kPa	0.63%FS
47	Diff.P.	D-27	PD	47	MRP2 Deliv.-JP4 Drive	Fig.5.24	-500.	-	500.	kPa	0.63%FS
48	Diff.P.	D-28	PD	48	DC Middle-JP3 Suction	Fig.5.25	-250.	-	250.	kPa	0.63%FS
49	Diff.P.	D-29	PD	49	DC Middle-JP4 Suction	Fig.5.25	-250.	-	250.	kPa	0.63%FS
50	Diff.P.	D-30	PD	50	JP3 Disch.-Confluence	Fig.5.26	-100.	-	100.	kPa	0.63%FS

Table 3.2 Measurement List for RUN 926 (Continued)

51Ch.- 100Ch.

Ch.	Item	Symbol	ID.		Location	Fig.No.	Range			Unit	Accuracy
51	Diff.P.	D-31	PD	51	JP4 Disch.-Confluence	Fig.5.26	-100.	-	100.	kPa	0.63%FS
52	Diff.P.	D-32	PD	52	Confluence -Lower Pl.	Fig.5.27	-50.0	-	50.0	kPa	0.63%FS
53	Diff.P.	D-33	PD	53	Lower Pl.-DC Middle	Fig.5.28	-250.	-	250.	kPa	0.63%FS
54	Diff.P.	D-34	PD	54	Lower Pl.-DC Bottom	Fig.5.29	-250.	-	250.	kPa	0.63%FS
55	Diff.P.	D-35	PD	55	DC Bottom-DC Middle	Fig.5.30	-50.0	-	50.0	kPa	0.63%FS
56	Diff.P.	D-36	PD	56	DC Middle-Steam Dome	Fig.5.31	-50.0	-	50.0	kPa	0.63%FS
57	Diff.P.	D-37	PD	57	Lower Pl.Mid-Upper PL	Not Measured					
58	Diff.P.	D-38	PD	58	Lower Pl.Bottom-Mid.	Fig.5.32	0.0	-	50.0	kPa	0.63%FS
59	Diff.P.	D-39	PD	59	Upper Pl.-DC High	Not Used	-20.0	-	100.	kPa	0.63%FS
60	Diff.P.	D-40	PD	60	Channel Orifice A	Fig.5.33	-50.0	-	50.0	kPa	0.63%FS
61	Diff.P.	D-41	PD	61	Channel Orifice B	Fig.5.34	-50.0	-	50.0	kPa	0.63%FS
62	Diff.P.	D-42	PD	62	Channel Orifice C	Fig.5.35	-25.0	-	75.0	kPa	0.63%FS
63	Diff.P.	D-43	PD	63	Channel Orifice D	Fig.5.36	-50.0	-	50.0	kPa	0.63%FS
64	Diff.P.	D-44	PD	64	Lower Plenum Head	Fig.5.37	-100.	-	100.	kPa	0.63%FS
65	Level	WL- 1	LM	65	HPCS Tank	Not Used	0.0	-	2.30	m	1.00%FS
66	Level	WL- 2	LM	66	LPCS Tank	Fig.5.38	0.0	-	2.30	m	1.00%FS
67	Level	WL- 3	LM	67	LPCI Tank	Fig.5.38	0.0	-	4.25	m	1.00%FS
68	Level	WL- 4	LM	68	Upper Downcomer	Fig.5.39	3.90	-	6.04	m	1.00%FS
69	Level	WL- 5	LM	69	Lower Downcomer	Fig.5.39	0.938	-	3.90	m	1.00%FS
70	Mass.F.	F- 1	FM	70	Steam Line (Low Range)	Fig.5.40	0.0	-	1.13	kg/s	0.92%FS
71	Mass.F.	F- 2	FM	71	Steam Line(High Range)	Fig.5.40	0.0	-	3.00	kg/s	0.92%FS
72	Mass.F.	F- 3	FM	72	Steam Line (Mid Range)	Fig.5.40	0.0	-	1.94	kg/s	1.40%FS
73	Vol.F.	F- 7	FV	73	HPCS (Upper Plenum)	Not Used	0.0	-	0.250E-02	m3/s	0.79%FS
74	Vol.F.	F- 9	FV	74	LPCS (Upper Plenum)	Fig.5.41	0.0	-	0.250E-02	m3/s	0.79%FS
75	Vol.F.	F-11	FV	75	LPCI (Core Bypass)	Fig.5.41	0.0	-	0.830E-02	m3/s	0.79%FS
76	Vol.F.	F-15	FV	76	Feedwater	Fig.5.42	0.0	-	0.100E-01	m3/s	0.79%FS
77	Vol.F.	F-16	FV	77	PWT Flow	NOT USED	0.0	-	0.420E-02	m3/s	0.79%FS
78	Vol.F.	F-17	FV	78	JP1 Discharge	Fig.5.43	0.0	-	0.170E-01	m3/s	0.88%FS
79	Vol.F.	F-18	FV	79	JP2 Discharge	Fig.5.43	0.0	-	0.170E-01	m3/s	0.88%FS
80	Vol.F.	F-19	FV	80	JP3 Disch. Positive	Fig.5.44	0.0	-	0.170E-01	m3/s	0.92%FS
81	Vol.F.	F-20	FV	81	JP3 Disch. Negative	Fig.5.45	0.0	-	0.500E-02	m3/s	0.92%FS
82	Vol.F.	F-21	FV	82	JP4 Disch. Positive	Fig.5.44	0.0	-	0.170E-01	m3/s	0.92%FS
83	Vol.F.	F-22	FV	83	JP4 Disch. Negative	Fig.5.45	0.0	-	0.500E-02	m3/s	0.92%FS
84	Mass.F.	F-23	FM	84	JP1,2 Outlet Spool	Not Measured	0.0	-	30.0	kg/s	1.40%FS
85	Mass.F.	F-24	FM	85	JP3,4 Outlet Spool	Not Measured	0.0	-	30.0	kg/s	1.40%FS
86	Mass.F.	F-25	FM	86	Break A Spool Piece	Not Measured	0.0	-	30.0	kg/s	1.40%FS
87	Mass.F.	F-26	FM	87	Break B Spool Piece	Not Measured	0.0	-	30.0	kg/s	1.40%FS
88	Vol.F.	F-27	FV	88	MRP-1	Fig.5.46	0.0	-	0.120E-01	m3/s	0.88%FS
89	Vol.F.	F-28	FV	89	MRP-2	Fig.5.46	0.0	-	0.120E-01	m3/s	0.63%FS
90	Diff.P.	D-F1	PD	90	F1 Orifice	Fig.5.47	0.0	-	4.90	kPa	0.63%FS
91	Diff.P.	D-F2	PD	91	F2 Orifice	Fig.5.48	0.0	-	34.9	kPa	0.63%FS
92	Diff.P.	D-F3	PD	92	F3 Orifice	Fig.5.49	0.0	-	14.6	kPa	0.63%FS
93	Diff.P.	D-F17	PD	93	F17 Venturi	Fig.5.50	0.0	-	98.1	kPa	0.63%FS
94	Diff.P.	D-F18	PD	94	F18 Venturi	Fig.5.51	0.0	-	98.1	kPa	0.63%FS
95	Diff.P.	D-F19	PD	95	F19 Orifice	Fig.5.52	0.0	-	147.	kPa	0.63%FS
96	Diff.P.	D-F20	PD	96	F20 Orifice	Fig.5.53	0.0	-	13.2	kPa	0.63%FS
97	Diff.P.	D-F21	PD	97	F21 Orifice	Fig.5.54	0.0	-	147.	kPa	0.63%FS
98	Diff.P.	D-F22	PD	98	F22 Orifice	Fig.5.55	0.0	-	13.2	kPa	0.63%FS
99	Diff.P.	D-F27	PD	99	F27 Venturi	Fig.5.56	0.0	-	200.	kPa	0.63%FS
100	Diff.P.	D-F28	PD	100	F28 Venturi	Fig.5.57	0.0	-	200.	kPa	0.63%FS

Table 3.2 Measurement List for RUN 926 (Continued)

101Ch.- 150Ch.

Ch.	Item	Symbol	ID.		Location	Fig.No.	Range			Unit	Accuracy
101	Power	W- 1	WE	101	2100 kW Power Supplier	Fig.5.58	0.0	-	0.210E+04	kW	1.00%FS
102	Power	W- 2	WE	102	3150 kW Power Supplier	Fig.5.58	0.0	-	0.315E+04	kW	1.00%FS
103											
104	Rev.	N- 1	SR	104	MRP-1 Revolution	Fig.5.59	0.0	-	0.500E+04	RPM	1.08%FS
105	Rev.	N- 2	SR	105	MRP-2 Revolution	Fig.5.59	0.0	-	0.500E+04	RPM	1.08%FS
106	Signal	S- 1	EV	106	Break Signal A	Fig.5.60					
107	Signal	S- 2	EV	107	Break Signal B	Fig.5.60					
108	Signal	S- 3	EV	108	QSV Signal	Fig.5.60					
109	Signal	S- 6	EV	109	HPCS Valve	Fig.5.61					
110	Signal	S- 7	EV	110	LPCS Valve	Fig.5.61					
111	Signal	S- 8	EV	111	LPCI Valve	Fig.5.61					
112	Signal	S- 9	EV	112	Feedwater Control	Fig.5.60					
113	Signal	S-10	EV	113	MSIV Signal	Fig.5.60					
114	Signal	S-11	EV	114	Steam Line Valve	Fig.5.60					
115	Signal	S-12	EV	115	ADS Valve	Fig.5.61					
116	Signal	S-13	EV	116	MRP-1 Power OFF	Fig.5.62					
117	Signal	S-14	EV	117	MRP-2 Power OFF	Fig.5.62					
118	Signal	RD- 1	EV	118	MRP-1 Rev. Direction	Failure					
119	Signal	RD- 2	EV	119	MRP-2 Rev. Direction	Fig.5.62					
120	Density	DF- 1	DE	120	JP1,2 Outlet Beam A	Fig.5.63	0.0	-	0.100E+04	kg/m3	1.00%FS
121	Density	DF- 2	DE	121	JP1,2 Outlet Beam B	Fig.5.64	0.0	-	0.100E+04	kg/m3	1.00%FS
122	Density	DF- 3	DE	122	JP1,2 Outlet Beam C	Fig.5.65	0.0	-	0.100E+04	kg/m3	1.00%FS
123	Density	DF- 4	DE	123	JP3,4 Outlet Beam A	Fig.5.66	0.0	-	0.100E+04	kg/m3	1.00%FS
124	Density	DF- 5	DE	124	JP3,4 Outlet Beam B	Fig.5.67	0.0	-	0.100E+04	kg/m3	1.00%FS
125	Density	DF- 6	DE	125	JP3,4 Outlet Beam C	Fig.5.68	0.0	-	0.100E+04	kg/m3	1.00%FS
126	Density	DF- 7	DE	126	Break A Beam A	Fig.5.69	0.0	-	0.100E+04	kg/m3	1.00%FS
127	Density	DF- 8	DE	127	Break A Beam B	Fig.5.70	0.0	-	0.100E+04	kg/m3	1.00%FS
128	Density	DF- 9	DE	128	Break B Beam A	Fig.5.71	0.0	-	0.100E+04	kg/m3	1.00%FS
129	Density	DF-10	DE	129	Break B Beam B	Fig.5.72	0.0	-	0.100E+04	kg/m3	1.00%FS
130	Mo.Flux	M- 1	MF	130	JP1,2 Outlet Spool	Fig.5.73	0.0	-	0.220E+05	kg/ms2	1.00%FS
131	Mo.Flux	M- 2	MF	131	JP3,4 Outlet Spool	Fig.5.74	0.0	-	0.220E+05	kg/ms2	1.00%FS
132	Mo.Flux	M- 3	MF	132	Break A (Low Range)	Fig.5.75	0.0	-	0.220E+05	kg/ms2	1.00%FS
133	Mo.Flux	M- 4	MF	133	Break B (Low Range)	Fig.5.76	0.0	-	0.220E+05	kg/ms2	1.00%FS
134	Mo.Flux	M- 5	MF	134	Break A (High Range)	Fig.5.77	0.0	-	0.220E+06	kg/ms2	1.00%FS
135	Mo.Flux	M- 6	MF	135	Break B (High Range)	Fig.5.78	0.0	-	0.220E+06	kg/ms2	1.00%FS
136	Mo.Flux	M- 7	MF	136	Break Orifice	Not Measured	0.0	-	0.220E+05	kg/ms2	1.00%FS
137											
138	Fluid T.	T- 1	TE	138	Lower Plenum	Fig.5.79	273.	-	673.	K	0.64%FS
139	Fluid T.	T- 2	TE	139	Upper Plenum	Fig.5.79	273.	-	673.	K	0.64%FS
140	Fluid T.	T- 3	TE	140	Steam Dome	Fig.5.80	273.	-	673.	K	0.64%FS
141	Fluid T.	T- 4	TE	141	Upper Downcomer	Fig.5.81	273.	-	673.	K	0.64%FS
142	Fluid T.	T- 5	TE	142	Lower Downcomer	Fig.5.81	273.	-	673.	K	0.64%FS
143	Fluid T.	T- 6	TE	143	JP-1 Drive	Fig.5.82	273.	-	673.	K	0.64%FS
144	Fluid T.	T- 7	TE	144	JP-2 Drive	Fig.5.82	273.	-	673.	K	0.64%FS
145	Fluid T.	T- 8	TE	145	JP-3 Drive	Fig.5.83	273.	-	673.	K	0.64%FS
146	Fluid T.	T- 9	TE	146	JP-4 Drive	Fig.5.83	273.	-	673.	K	0.64%FS
147	Fluid T.	T-10	TE	147	JP-1 Discharge	Fig.5.84	273.	-	673.	K	0.64%FS
148	Fluid T.	T-11	TE	148	JP-2 Discharge	Fig.5.84	273.	-	673.	K	0.64%FS
149	Fluid T.	T-12	TE	149	JP-3 Discharge	Fig.5.85	273.	-	673.	K	0.64%FS
150	Fluid T.	T-13	TE	150	JP-4 Discharge	Fig.5.85	273.	-	673.	K	0.64%FS

Table 3.2 Measurement List for RUN 926 (Continued)

151Ch.- 200Ch.

Ch.	Item	Symbol	ID.		Location	Fig.No.	Range			Unit	Accuracy
151	Fluid T.	T-14	TE	151	MRP-1 Suction	Fig.5.82	273.	-	673.	K	0.64%FS
152	Fluid T.	T-15	TE	152	MRP-1 Delivery	Fig.5.82	273.	-	673.	K	0.64%FS
153	Fluid T.	T-16	TE	153	MRP-2 Suction	Fig.5.83	273.	-	673.	K	0.64%FS
154	Fluid T.	T-17	TE	154	MRP-2 Delivery	Fig.5.83	273.	-	673.	K	0.64%FS
155	Fluid T.	T-18	TE	155	Break A Upstream	Fig.5.86	273.	-	673.	K	0.64%FS
156	Fluid T.	T-19	TE	156	Break B Upstream	Fig.5.86	273.	-	673.	K	0.64%FS
157	Fluid T.	T-20	TE	157	RCN A Condenced Water	Not Used	273.	-	698.	K	0.64%FS
158	Fluid T.	T-21	TE	158	RCN B Condenced Water	Not Used	273.	-	698.	K	0.64%FS
159	Fluid T.	T-22	TE	159	Discharged Steam	Fig.5.80	273.	-	673.	K	0.64%FS
160	Fluid T.	T-24	TE	160	JP-1,2 Outlet Spool	Fig.5.84	273.	-	763.	K	0.64%FS
161	Fluid T.	T-25	TE	161	JP-3,4 Outlet Spool	Fig.5.85	273.	-	763.	K	0.64%FS
162	Fluid T.	T-26	TE	162	Break A Spool Piece	Fig.5.86	273.	-	763.	K	0.64%FS
163	Fluid T.	T-37	TE	163	Break B Spool Piece	Fig.5.86	273.	-	763.	K	0.64%FS
164	Fluid T.	T-38	TE	164	Feedwater	Fig.5.87	273.	-	673.	K	0.64%FS
165	Slab T.	TS- 1	TE	165	Core Barrel C Pos.1	Not Measured	273.	-	673.	K	0.64%FS
166	Slab T.	TS- 2	TE	166	Core Barrel C Pos.2	Not Measured	273.	-	673.	K	0.64%FS
167	Slab T.	TS- 3	TE	167	Core Barrel C Pos.3	Not Measured	273.	-	673.	K	0.64%FS
168	Slab T.	TS- 4	TE	168	Core Barrel C Pos.4	Not Measured	273.	-	673.	K	0.64%FS
169	Slab T.	TS- 5	TE	169	Core Barrel C Pos.5	Not Measured	273.	-	673.	K	0.64%FS
170	Slab T.	TS- 6	TE	170	Core Barrel C Pos.6	Not Measured	273.	-	673.	K	0.64%FS
171	Slab T.	TS- 7	TE	171	Core Barrel A Pos.1	Not Measured	273.	-	673.	K	0.64%FS
172	Slab T.	TS- 8	TE	172	Core Barrel A Pos.2	Not Measured	273.	-	673.	K	0.64%FS
173	Slab T.	TS- 9	TE	173	Core Barrel A Pos.3	Not Measured	273.	-	673.	K	0.64%FS
174	Slab T.	TS-10	TE	174	Core Barrel A Pos.4	Not Measured	273.	-	673.	K	0.64%FS
175	Slab T.	TS-11	TE	175	Core Barrel A Pos.5	Not Measured	273.	-	673.	K	0.64%FS
176	Slab T.	TS-12	TE	176	Core Barrel A Pos.6	Not Measured	273.	-	673.	K	0.64%FS
177	Slab T.	TS-13	TE	177	Filler Block C Pos.1	Not Measured	273.	-	673.	K	0.64%FS
178	Slab T.	TS-14	TE	178	Filler Block C Pos.2	Not Measured	273.	-	673.	K	0.64%FS
179	Slab T.	TS-15	TE	179	Filler Block C Pos.3	Not Measured	273.	-	673.	K	0.64%FS
180	Slab T.	TS-16	TE	180	Filler Block C Pos.4	Not Measured	273.	-	673.	K	0.64%FS
181	Slab T.	TS-17	TE	181	Filler Block C Pos.5	Not Measured	273.	-	673.	K	0.64%FS
182	Slab T.	TS-18	TE	182	Filler Block C Pos.6	Not Measured	273.	-	673.	K	0.64%FS
183	Slab T.	TS-19	TE	183	Filler Block A Pos.1	Not Measured	273.	-	673.	K	0.64%FS
184	Slab T.	TS-20	TE	184	Filler Block A Pos.2	Not Measured	273.	-	673.	K	0.64%FS
185	Slab T.	TS-21	TE	185	Filler Block A Pos.3	Not Measured	273.	-	673.	K	0.64%FS
186	Slab T.	TS-22	TE	186	Filler Block A Pos.4	Not Measured	273.	-	673.	K	0.64%FS
187	Slab T.	TS-23	TE	187	Filler Block A Pos.5	Not Measured	273.	-	673.	K	0.64%FS
188	Slab T.	TS-24	TE	188	Filler Block A Pos.6	Not Measured	273.	-	673.	K	0.64%FS
189	Slab T.	TS-25	TE	189	JP-1 Diffuser Wall	Not Measured	273.	-	673.	K	0.64%FS
190	Slab T.	TS-26	TE	190	JP-2 Diffuser Wall	Not Measured	273.	-	673.	K	0.64%FS
191	Slab T.	TS-27	TE	191	JP-3 Diffuser Wall	Not Measured	273.	-	673.	K	0.64%FS
192	Slab T.	TS-28	TE	192	JP-4 Diffuser Wall	Not Measured	273.	-	673.	K	0.64%FS
193	Slab T.	TS-29	TE	193	PV Wall Inside 1-1	Not Measured	273.	-	673.	K	0.64%FS
194	Slab T.	TS-30	TE	194	PV Inner Surface 1-2	Not Measured	273.	-	673.	K	0.64%FS
195	Slab T.	TS-31	TE	195	PV Inner Surface 1-3	Not Measured	273.	-	673.	K	0.64%FS
196	Slab T.	TS-32	TE	196	PV Wall Inside 2	Not Measured	273.	-	673.	K	0.64%FS
197	Slab T.	TS-33	TE	197	PV Wall Inside 3	Not Measured	273.	-	673.	K	0.64%FS
198	Slab T.	TS-34	TE	198	PV Wall Inside 4	Not Measured	273.	-	673.	K	0.64%FS
199	Slab T.	TS-35	TE	199	L.P. Inner Surface	Not Measured	273.	-	673.	K	0.64%FS
200	Slab T.	TS-36	TE	200	L.P. Wall Inside	Not Measured	273.	-	673.	K	0.64%FS

Table 3.2 Measurement List for RUN 926 (Continued)

201Ch.- 250Ch.

Ch.	Item	Symbol	ID.	Location	Fig.No.	Range	Unit	Accuracy
201	Temp.	TF- 1	TE 201	A11 Fuel Rod Pos.1	FIG.5.88, 147	273. - 0.147E+04	K	0.64%FS
202	Temp.	TF- 2	TE 202	A11 Fuel Rod Pos.2	FIG.5.88, 148	273. - 0.147E+04	K	0.64%FS
203	Temp.	TF- 3	TE 203	A11 Fuel Rod Pos.3	FIG.5.88, 149	273. - 0.147E+04	K	0.64%FS
204	Temp.	TF- 4	TE 204	A11 Fuel Rod Pos.4	FIG.5.88, 150	273. - 0.147E+04	K	0.64%FS
205	Temp.	TF- 5	TE 205	A11 Fuel Rod Pos.5	FIG.5.88, 151	273. - 0.147E+04	K	0.64%FS
206	Temp.	TF- 6	TE 206	A11 Fuel Rod Pos.6	FIG.5.88, 152	273. - 0.147E+04	K	0.64%FS
207	Temp.	TF- 7	TE 207	A11 Fuel Rod Pos.7	FIG.5.88, 153	273. - 0.147E+04	K	0.64%FS
208	Temp.	TF- 8	TE 208	A12 Fuel Rod Pos.1	FIG.5.89, 147	273. - 0.147E+04	K	0.64%FS
209	Temp.	TF- 9	TE 209	A12 Fuel Rod Pos.2	FIG.5.89, 148	273. - 0.147E+04	K	0.64%FS
210	Temp.	TF- 10	TE 210	A12 Fuel Rod Pos.3	FIG.5.89, 149	273. - 0.147E+04	K	0.64%FS
211	Temp.	TF- 11	TE 211	A12 Fuel Rod Pos.4	FIG.5.89, 150	273. - 0.147E+04	K	0.64%FS
212	Temp.	TF- 12	TE 212	A12 Fuel Rod Pos.5	FIG.5.89, 151	273. - 0.147E+04	K	0.64%FS
213	Temp.	TF- 13	TE 213	A12 Fuel Rod Pos.6	FIG.5.89, 152	273. - 0.147E+04	K	0.64%FS
214	Temp.	TF- 14	TE 214	A12 Fuel Rod Pos.7	FIG.5.89, 153	273. - 0.147E+04	K	0.64%FS
215	Temp.	TF- 15	TE 215	A13 Fuel Rod Pos.1	FIG.5.90, 147	273. - 0.147E+04	K	0.64%FS
216	Temp.	TF- 16	TE 216	A13 Fuel Rod Pos.2	FIG.5.90, 148	273. - 0.147E+04	K	0.64%FS
217	Temp.	TF- 17	TE 217	A13 Fuel Rod Pos.3	FIG.5.90, 149	273. - 0.147E+04	K	0.64%FS
218	Temp.	TF- 18	TE 218	A13 Fuel Rod Pos.4	FIG.5.90, 150	273. - 0.147E+04	K	0.64%FS
219	Temp.	TF- 19	TE 219	A13 Fuel Rod Pos.5	FIG.5.90, 151	273. - 0.147E+04	K	0.64%FS
220	Temp.	TF- 20	TE 220	A13 Fuel Rod Pos.6	FIG.5.90, 152	273. - 0.147E+04	K	0.64%FS
221	Temp.	TF- 21	TE 221	A13 Fuel Rod Pos.7	FIG.5.90, 153	273. - 0.147E+04	K	0.64%FS
222	Temp.	TF- 22	TE 222	A14 Fuel Rod Pos.1	Fig.5.91	273. - 0.147E+04	K	0.64%FS
223	Temp.	TF- 23	TE 223	A14 Fuel Rod Pos.2	Fig.5.91	273. - 0.147E+04	K	0.64%FS
224	Temp.	TF- 24	TE 224	A14 Fuel Rod Pos.3	Fig.5.91	273. - 0.147E+04	K	0.64%FS
225	Temp.	TF- 25	TE 225	A14 Fuel Rod Pos.4	Fig.5.91	273. - 0.147E+04	K	0.64%FS
226	Temp.	TF- 26	TE 226	A14 Fuel Rod Pos.5	Fig.5.91	273. - 0.147E+04	K	0.64%FS
227	Temp.	TF- 27	TE 227	A14 Fuel Rod Pos.6	Fig.5.91	273. - 0.147E+04	K	0.64%FS
228	Temp.	TF- 28	TE 228	A14 Fuel Rod Pos.7	Fig.5.91	273. - 0.147E+04	K	0.64%FS
229	Temp.	TF- 29	TE 229	A15 Fuel Rod Pos.1	FIG.5.121	273. - 0.147E+04	K	0.64%FS
230	Temp.	TF- 30	TE 230	A15 Fuel Rod Pos.4	FIG.5.121	273. - 0.147E+04	K	0.64%FS
231	Temp.	TF- 31	TE 231	A17 Fuel Rod Pos.1	FIG.5.122	273. - 0.147E+04	K	0.64%FS
232	Temp.	TF- 32	TE 232	A17 Fuel Rod Pos.4	FIG.5.122	273. - 0.147E+04	K	0.64%FS
233	Temp.	TF- 33	TE 233	A22 Fuel Rod Pos.1	Failure	273. - 0.147E+04	K	0.64%FS
234	Temp.	TF- 34	TE 234	A22 Fuel Rod Pos.2	FIG.5.92, 155	273. - 0.147E+04	K	0.64%FS
235	Temp.	TF- 35	TE 235	A22 Fuel Rod Pos.3	FIG.5.92, 156	273. - 0.147E+04	K	0.64%FS
236	Temp.	TF- 36	TE 236	A22 Fuel Rod Pos.4	FIG.5.92, 157	273. - 0.125E+04	K	0.64%FS
237	Temp.	TF- 37	TE 237	A22 Fuel Rod Pos.5	FIG.5.92, 158	273. - 0.125E+04	K	0.64%FS
238	Temp.	TF- 38	TE 238	A22 Fuel Rod Pos.6	FIG.5.92, 159	273. - 0.125E+04	K	0.64%FS
239	Temp.	TF- 39	TE 239	A22 Fuel Rod Pos.7	FIG.5.92, 160	273. - 0.125E+04	K	0.64%FS
240	Temp.	TF- 40	TE 240	A24 Fuel Rod Pos.1	Fig.5.93	273. - 0.125E+04	K	0.64%FS
241	Temp.	TF- 41	TE 241	A24 Fuel Rod Pos.2	Fig.5.93	273. - 0.125E+04	K	0.64%FS
242	Temp.	TF- 42	TE 242	A24 Fuel Rod Pos.3	Fig.5.93	273. - 0.125E+04	K	0.64%FS
243	Temp.	TF- 43	TE 243	A24 Fuel Rod Pos.4	Fig.5.93	273. - 0.125E+04	K	0.64%FS
244	Temp.	TF- 44	TE 244	A24 Fuel Rod Pos.5	Fig.5.93	273. - 0.125E+04	K	0.64%FS
245	Temp.	TF- 45	TE 245	A24 Fuel Rod Pos.6	Fig.5.93	273. - 0.125E+04	K	0.64%FS
246	Temp.	TF- 46	TE 246	A24 Fuel Rod Pos.7	Fig.5.93	273. - 0.125E+04	K	0.64%FS
247	Temp.	TF- 47	TE 247	A26 Fuel Rod Pos.1	FIG.5.123	273. - 0.125E+04	K	0.64%FS
248	Temp.	TF- 48	TE 248	A26 Fuel Rod Pos.2	FIG.5.123	273. - 0.125E+04	K	0.64%FS
249	Temp.	TF- 49	TE 249	A28 Fuel Rod Pos.1	FIG.5.124	273. - 0.125E+04	K	0.64%FS
250	Temp.	TF- 50	TE 250	A28 Fuel Rod Pos.4	FIG.5.124	273. - 0.125E+04	K	0.64%FS

Table 3.2 Measurement List for RUN 926 (Continued)

251Ch.- 300Ch.

Ch.	Item	Symbol	ID.	Location	Fig.No.	Range	Unit	Accuracy
251	Temp.	TF- 51	TE 251	A31 Fuel Rod Pos.1	FIG.5.125	273. - 0.125E+04	K	0.64%FS
252	Temp.	TF- 52	TE 252	A31 Fuel Rod Pos.4	FIG.5.125	273. - 0.125E+04	K	0.64%FS
253	Temp.	TF- 53	TE 253	A33 Fuel Rod Pos.1	FIG.5.94	273. - 0.125E+04	K	0.64%FS
254	Temp.	TF- 54	TE 254	A33 Fuel Rod Pos.2	FIG.5.94	273. - 0.125E+04	K	0.64%FS
255	Temp.	TF- 55	TE 255	A33 Fuel Rod Pos.3	FIG.5.94	273. - 0.125E+04	K	0.64%FS
256	Temp.	TF- 56	TE 256	A33 Fuel Rod Pos.4	FIG.5.94	273. - 0.125E+04	K	0.64%FS
257	Temp.	TF- 57	TE 257	A33 Fuel Rod Pos.5	FIG.5.94	273. - 0.125E+04	K	0.64%FS
258	Temp.	TF- 58	TE 258	A33 Fuel Rod Pos.6	FIG.5.94	273. - 0.125E+04	K	0.64%FS
259	Temp.	TF- 59	TE 259	A33 Fuel Rod Pos.7	FIG.5.94	273. - 0.125E+04	K	0.64%FS
260	Temp.	TF- 60	TE 260	A34 Fuel Rod Pos.1	FIG.5.95	273. - 0.125E+04	K	0.64%FS
261	Temp.	TF- 61	TE 261	A34 Fuel Rod Pos.2	FIG.5.95	273. - 0.125E+04	K	0.64%FS
262	Temp.	TF- 62	TE 262	A34 Fuel Rod Pos.3	FIG.5.95	273. - 0.125E+04	K	0.64%FS
263	Temp.	TF- 63	TE 263	A34 Fuel Rod Pos.4	FIG.5.95	273. - 0.125E+04	K	0.64%FS
264	Temp.	TF- 64	TE 264	A34 Fuel Rod Pos.5	FIG.5.95	273. - 0.125E+04	K	0.64%FS
265	Temp.	TF- 65	TE 265	A34 Fuel Rod Pos.6	FIG.5.95	273. - 0.125E+04	K	0.64%FS
266	Temp.	TF- 66	TE 266	A34 Fuel Rod Pos.7	FIG.5.95	273. - 0.125E+04	K	0.64%FS
267	Temp.	TF- 67	TE 267	A37 Fuel Rod Pos.1	FIG.5.126	273. - 0.125E+04	K	0.64%FS
268	Temp.	TF- 68	TE 268	A37 Fuel Rod Pos.4	FIG.5.126	273. - 0.125E+04	K	0.64%FS
269	Temp.	TF- 69	TE 269	A42 Fuel Rod Pos.1	FIG.5.127	273. - 0.125E+04	K	0.64%FS
270	Temp.	TF- 70	TE 270	A42 Fuel Rod Pos.4	FIG.5.127	273. - 0.125E+04	K	0.64%FS
271	Temp.	TF- 71	TE 271	A44 Fuel Rod Pos.1	FIG.5.96	273. - 0.125E+04	K	0.64%FS
272	Temp.	TF- 72	TE 272	A44 Fuel Rod Pos.2	FIG.5.96	273. - 0.125E+04	K	0.64%FS
273	Temp.	TF- 73	TE 273	A44 Fuel Rod Pos.3	FIG.5.96	273. - 0.125E+04	K	0.64%FS
274	Temp.	TF- 74	TE 274	A44 Fuel Rod Pos.4	FIG.5.96	273. - 0.125E+04	K	0.64%FS
275	Temp.	TF- 75	TE 275	A44 Fuel Rod Pos.5	FIG.5.96	273. - 0.125E+04	K	0.64%FS
276	Temp.	TF- 76	TE 276	A44 Fuel Rod Pos.6	FIG.5.96	273. - 0.125E+04	K	0.64%FS
277	Temp.	TF- 77	TE 277	A44 Fuel Rod Pos.7	FIG.5.96	273. - 0.125E+04	K	0.64%FS
278	Temp.	TF- 78	TE 278	A48 Fuel Rod Pos.1	FIG.5.128	273. - 0.125E+04	K	0.64%FS
279	Temp.	TF- 79	TE 279	A48 Fuel Rod Pos.4	FIG.5.128	273. - 0.125E+04	K	0.64%FS
280	Temp.	TF- 80	TE 280	A51 Fuel Rod Pos.1	FIG.5.129	273. - 0.125E+04	K	0.64%FS
281	Temp.	TF- 81	TE 281	A51 Fuel Rod Pos.4	FIG.5.129	273. - 0.125E+04	K	0.64%FS
282	Temp.	TF- 82	TE 282	A53 Fuel Rod Pos.1	FIG.5.130	273. - 0.125E+04	K	0.64%FS
283	Temp.	TF- 83	TE 283	A53 Fuel Rod Pos.4	FIG.5.130	273. - 0.125E+04	K	0.64%FS
284	Temp.	TF- 84	TE 284	A57 Fuel Rod Pos.1	FIG.5.131	273. - 0.125E+04	K	0.64%FS
285	Temp.	TF- 85	TE 285	A57 Fuel Rod Pos.4	FIG.5.131	273. - 0.125E+04	K	0.64%FS
286	Temp.	TF- 86	TE 286	A62 Fuel Rod Pos.1	FIG.5.132	273. - 0.125E+04	K	0.64%FS
287	Temp.	TF- 87	TE 287	A62 Fuel Rod Pos.4	FIG.5.132	273. - 0.125E+04	K	0.64%FS
288	Temp.	TF- 88	TE 288	A66 Fuel Rod Pos.1	FIG.5.133	273. - 0.125E+04	K	0.64%FS
289	Temp.	TF- 89	TE 289	A66 Fuel Rod Pos.4	FIG.5.133	273. - 0.125E+04	K	0.64%FS
290	Temp.	TF- 90	TE 290	A68 Fuel Rod Pos.1	FIG.5.134	273. - 0.125E+04	K	0.64%FS
291	Temp.	TF- 91	TE 291	A68 Fuel Rod Pos.4	FIG.5.134	273. - 0.125E+04	K	0.64%FS
292	Temp.	TF- 92	TE 292	A71 Fuel Rod Pos.1	FIG.5.135	273. - 0.125E+04	K	0.64%FS
293	Temp.	TF- 93	TE 293	A71 Fuel Rod Pos.4	FIG.5.135	273. - 0.125E+04	K	0.64%FS
294	Temp.	TF- 94	TE 294	A73 Fuel Rod Pos.1	FIG.5.136	273. - 0.125E+04	K	0.64%FS
295	Temp.	TF- 95	TE 295	A73 Fuel Rod Pos.4	FIG.5.136	273. - 0.125E+04	K	0.64%FS
296	Temp.	TF- 96	TE 296	A75 Fuel Rod Pos.1	FIG.5.137	273. - 0.125E+04	K	0.64%FS
297	Temp.	TF- 97	TE 297	A75 Fuel Rod Pos.4	FIG.5.137	273. - 0.125E+04	K	0.64%FS
298	Temp.	TF- 98	TE 298	A77 Fuel Rod Pos.1	FIG.5.97, 161	273. - 0.125E+04	K	0.64%FS
299	Temp.	TF- 99	TE 299	A77 Fuel Rod Pos.2	FIG.5.97, 162	273. - 0.125E+04	K	0.64%FS
300	Temp.	TF-100	TE 300	A77 Fuel Rod Pos.3	FIG.5.97, 163	273. - 0.125E+04	K	0.64%FS

Table 3.2 Measurement List for RUN 926 (Continued)

301Ch.- 350Ch.

Ch.	Item	Symbol	ID.	Location	Fig.No.	Range	Unit	Accuracy
301	Temp.	TF-101	TE 301	A77 Fuel Rod Pos.4	FIG.5.97, 164	273. - 0.125E+04	K	0.64%FS
302	Temp.	TF-102	TE 302	A77 Fuel Rod Pos.5	FIG.5.97, 165	273. - 0.125E+04	K	0.64%FS
303	Temp.	TF-103	TE 303	A77 Fuel Rod Pos.6	FIG.5.97, 166	273. - 0.125E+04	K	0.64%FS
304	Temp.	TF-104	TE 304	A77 Fuel Rod Pos.7	Failure	273. - 0.125E+04	K	0.64%FS
305	Temp.	TF-105	TE 305	A82 Fuel Rod Pos.1	FIG.5.138	273. - 0.125E+04	K	0.64%FS
306	Temp.	TF-106	TE 306	A82 Fuel Rod Pos.4	FIG.5.138	273. - 0.125E+04	K	0.64%FS
307	Temp.	TF-107	TE 307	A84 Fuel Rod Pos.1	FIG.5.139	273. - 0.125E+04	K	0.64%FS
308	Temp.	TF-108	TE 308	A84 Fuel Rod Pos.4	FIG.5.139	273. - 0.125E+04	K	0.64%FS
309	Temp.	TF-109	TE 309	A85 Fuel Rod Pos.1	Fig.5.98	273. - 0.125E+04	K	0.64%FS
310	Temp.	TF-110	TE 310	A85 Fuel Rod Pos.2	Fig.5.98	273. - 0.125E+04	K	0.64%FS
311	Temp.	TF-111	TE 311	A85 Fuel Rod Pos.3	Fig.5.98	273. - 0.125E+04	K	0.64%FS
312	Temp.	TF-112	TE 312	A85 Fuel Rod Pos.4	Fig.5.98	273. - 0.125E+04	K	0.64%FS
313	Temp.	TF-113	TE 313	A85 Fuel Rod Pos.5	Fig.5.98	273. - 0.125E+04	K	0.64%FS
314	Temp.	TF-114	TE 314	A85 Fuel Rod Pos.6	Fig.5.98	273. - 0.125E+04	K	0.64%FS
315	Temp.	TF-115	TE 315	A85 Fuel Rod Pos.7	Fig.5.98	273. - 0.125E+04	K	0.64%FS
316	Temp.	TF-116	TE 316	A87 Fuel Rod Pos.1	FIG.5.99, 147	273. - 0.125E+04	K	0.64%FS
317	Temp.	TF-117	TE 317	A87 Fuel Rod Pos.2	FIG.5.99, 148	273. - 0.125E+04	K	0.64%FS
318	Temp.	TF-118	TE 318	A87 Fuel Rod Pos.3	FIG.5.99, 149	273. - 0.125E+04	K	0.64%FS
319	Temp.	TF-119	TE 319	A87 Fuel Rod Pos.4	FIG.5.99, 150	273. - 0.125E+04	K	0.64%FS
320	Temp.	TF-120	TE 320	A87 Fuel Rod Pos.5	FIG.5.99, 151	273. - 0.125E+04	K	0.64%FS
321	Temp.	TF-121	TE 321	A87 Fuel Rod Pos.6	FIG.5.99, 152	273. - 0.125E+04	K	0.64%FS
322	Temp.	TF-122	TE 322	A87 Fuel Rod Pos.7	FIG.5.99, 153	273. - 0.125E+04	K	0.64%FS
323	Temp.	TF-123	TE 323	A88 Fuel Rod Pos.1	FIG.5.100, 147	273. - 0.125E+04	K	0.64%FS
324	Temp.	TF-124	TE 324	A88 Fuel Rod Pos.2	FIG.5.100, 148	273. - 0.125E+04	K	0.64%FS
325	Temp.	TF-125	TE 325	A88 Fuel Rod Pos.3	FIG.5.100, 149	273. - 0.125E+04	K	0.64%FS
326	Temp.	TF-126	TE 326	A88 Fuel Rod Pos.4	FIG.5.100, 150	273. - 0.125E+04	K	0.64%FS
327	Temp.	TF-127	TE 327	A88 Fuel Rod Pos.5	FIG.5.100, 151	273. - 0.125E+04	K	0.64%FS
328	Temp.	TF-128	TE 328	A88 Fuel Rod Pos.6	FIG.5.100, 152	273. - 0.125E+04	K	0.64%FS
329	Temp.	TF-129	TE 329	A88 Fuel Rod Pos.7	FIG.5.100, 153	273. - 0.125E+04	K	0.64%FS
330	Temp.	TF-130	TE 330	B11 Fuel Rod Pos.1	FIG.5.101	273. - 0.125E+04	K	0.64%FS
331	Temp.	TF-131	TE 331	B11 Fuel Rod Pos.2	FIG.5.101	273. - 0.125E+04	K	0.64%FS
332	Temp.	TF-132	TE 332	B11 Fuel Rod Pos.3	FIG.5.101	273. - 0.125E+04	K	0.64%FS
333	Temp.	TF-133	TE 333	B11 Fuel Rod Pos.4	FIG.5.101	273. - 0.125E+04	K	0.64%FS
334	Temp.	TF-134	TE 334	B11 Fuel Rod Pos.5	FIG.5.101	273. - 0.125E+04	K	0.64%FS
335	Temp.	TF-135	TE 335	B11 Fuel Rod Pos.6	FIG.5.101	273. - 0.125E+04	K	0.64%FS
336	Temp.	TF-136	TE 336	B11 Fuel Rod Pos.7	Failure	273. - 0.125E+04	K	0.64%FS
337	Temp.	TF-137	TE 337	B13 Fuel Rod Pos.4	FIG.5.140	273. - 0.125E+04	K	0.64%FS
338	Temp.	TF-138	TE 338	B22 Fuel Rod Pos.1	FIG.5.102, 154	273. - 0.125E+04	K	0.64%FS
339	Temp.	TF-139	TE 339	B22 Fuel Rod Pos.2	FIG.5.102, 155	273. - 0.125E+04	K	0.64%FS
340	Temp.	TF-140	TE 340	B22 Fuel Rod Pos.3	FIG.5.102, 156	273. - 0.125E+04	K	0.64%FS
341	Temp.	TF-141	TE 341	B22 Fuel Rod Pos.4	FIG.5.102, 157	273. - 0.125E+04	K	0.64%FS
342	Temp.	TF-142	TE 342	B22 Fuel Rod Pos.5	FIG.5.102, 158	273. - 0.125E+04	K	0.64%FS
343	Temp.	TF-143	TE 343	B22 Fuel Rod Pos.6	FIG.5.102, 159	273. - 0.125E+04	K	0.64%FS
344	Temp.	TF-144	TE 344	B22 Fuel Rod Pos.7	FIG.5.102, 160	273. - 0.125E+04	K	0.64%FS
345	Temp.	TF-145	TE 345	B31 Fuel Rod Pos.4	FIG.5.140	273. - 0.125E+04	K	0.64%FS
346	Temp.	TF-146	TE 346	B33 Fuel Rod Pos.4	FIG.5.141	273. - 0.125E+04	K	0.64%FS
347	Temp.	TF-147	TE 347	B51 Fuel Rod Pos.4	FIG.5.142	273. - 0.125E+04	K	0.64%FS
348	Temp.	TF-148	TE 348	B53 Fuel Rod Pos.4	FIG.5.141	273. - 0.125E+04	K	0.64%FS
349	Temp.	TF-149	TE 349	B66 Fuel Rod Pos.4	FIG.5.141	273. - 0.125E+04	K	0.64%FS
350	Temp.	TF-150	TE 350	B77 Fuel Rod Pos.1	FIG.5.103, 161	273. - 0.125E+04	K	0.64%FS

Table 3.2 Measurement List for RUN 926 (Continued)

351Ch.- 400Ch.

Ch.	Item	Symbol	ID.		Location	Fig.No.	Range			Unit	Accuracy
351	Temp.	TF-151	TE	351	B77 Fuel Rod Pos.2	FIG.5.103, 162	273.	-	0.125E+04	K	0.64%FS
352	Temp.	TF-152	TE	352	B77 Fuel Rod Pos.3	FIG.5.103, 163	273.	-	0.125E+04	K	0.64%FS
353	Temp.	TF-153	TE	353	B77 Fuel Rod Pos.4	FIG.5.103, 164	273.	-	0.125E+04	K	0.64%FS
354	Temp.	TF-154	TE	354	B77 Fuel Rod Pos.5	FIG.5.103, 165	273.	-	0.125E+04	K	0.64%FS
355	Temp.	TF-155	TE	355	B77 Fuel Rod Pos.6	FIG.5.103, 166	273.	-	0.125E+04	K	0.64%FS
356	Temp.	TF-156	TE	356	B77 Fuel Rod Pos.7	FIG.5.103, 167	273.	-	0.125E+04	K	0.64%FS
357	Temp.	TF-157	TE	357	B86 Fuel Rod Pos.4	FIG.5.140	273.	-	0.125E+04	K	0.64%FS
358	Temp.	TF-158	TE	358	C11 Fuel Rod Pos.1	FIG.5.104	273.	-	0.125E+04	K	0.64%FS
359	Temp.	TF-159	TE	359	C11 Fuel Rod Pos.2	FIG.5.104	273.	-	0.125E+04	K	0.64%FS
360	Temp.	TF-160	TE	360	C11 Fuel Rod Pos.3	FIG.5.104	273.	-	0.125E+04	K	0.64%FS
361	Temp.	TF-161	TE	361	C11 Fuel Rod Pos.4	FIG.5.104	273.	-	0.125E+04	K	0.64%FS
362	Temp.	TF-162	TE	362	C11 Fuel Rod Pos.5	FIG.5.104	273.	-	0.125E+04	K	0.64%FS
363	Temp.	TF-163	TE	363	C11 Fuel Rod Pos.6	FIG.5.104	273.	-	0.125E+04	K	0.64%FS
364	Temp.	TF-164	TE	364	C11 Fuel Rod Pos.7	FIG.5.104	273.	-	0.125E+04	K	0.64%FS
365	Temp.	TF-165	TE	365	C13 Fuel Rod Pos.1	FIG.5.105	273.	-	0.125E+04	K	0.64%FS
366	Temp.	TF-166	TE	366	C13 Fuel Rod Pos.2	FIG.5.105	273.	-	0.125E+04	K	0.64%FS
367	Temp.	TF-167	TE	367	C13 Fuel Rod Pos.3	FIG.5.105	273.	-	0.125E+04	K	0.64%FS
368	Temp.	TF-168	TE	368	C13 Fuel Rod Pos.4	FIG.5.105	273.	-	0.125E+04	K	0.64%FS
369	Temp.	TF-169	TE	369	C13 Fuel Rod Pos.5	FIG.5.105	273.	-	0.125E+04	K	0.64%FS
370	Temp.	TF-170	TE	370	C13 Fuel Rod Pos.6	FIG.5.105	273.	-	0.125E+04	K	0.64%FS
371	Temp.	TF-171	TE	371	C13 Fuel Rod Pos.7	FIG.5.105	273.	-	0.125E+04	K	0.64%FS
372	Temp.	TF-172	TE	372	C15 Fuel Rod Pos.4	FIG.5.142	273.	-	0.125E+04	K	0.64%FS
373	Temp.	TF-173	TE	373	C22 Fuel Rod Pos.1	FIG.5.106	273.	-	0.125E+04	K	0.64%FS
374	Temp.	TF-174	TE	374	C22 Fuel Rod Pos.2	FIG.5.106	273.	-	0.125E+04	K	0.64%FS
375	Temp.	TF-175	TE	375	C22 Fuel Rod Pos.3	FIG.5.106	273.	-	0.125E+04	K	0.64%FS
376	Temp.	TF-176	TE	376	C22 Fuel Rod Pos.4	FIG.5.106	273.	-	0.125E+04	K	0.64%FS
377	Temp.	TF-177	TE	377	C22 Fuel Rod Pos.5	FIG.5.106	273.	-	0.125E+04	K	0.64%FS
378	Temp.	TF-178	TE	378	C22 Fuel Rod Pos.6	FIG.5.106	273.	-	0.125E+04	K	0.64%FS
379	Temp.	TF-179	TE	379	C22 Fuel Rod Pos.7	FIG.5.106	273.	-	0.125E+04	K	0.64%FS
380	Temp.	TF-180	TE	380	C31 Fuel Rod Pos.4	FIG.5.143	273.	-	0.125E+04	K	0.64%FS
381	Temp.	TF-181	TE	381	C33 Fuel Rod Pos.1	FIG.5.107	273.	-	0.125E+04	K	0.64%FS
382	Temp.	TF-182	TE	382	C33 Fuel Rod Pos.2	FIG.5.107	273.	-	0.125E+04	K	0.64%FS
383	Temp.	TF-183	TE	383	C33 Fuel Rod Pos.3	FIG.5.107	273.	-	0.125E+04	K	0.64%FS
384	Temp.	TF-184	TE	384	C33 Fuel Rod Pos.4	FIG.5.107	273.	-	0.125E+04	K	0.64%FS
385	Temp.	TF-185	TE	385	C33 Fuel Rod Pos.5	FIG.5.107	273.	-	0.125E+04	K	0.64%FS
386	Temp.	TF-186	TE	386	C33 Fuel Rod Pos.6	FIG.5.107	273.	-	0.125E+04	K	0.64%FS
387	Temp.	TF-187	TE	387	C33 Fuel Rod Pos.7	FIG.5.107	273.	-	0.125E+04	K	0.64%FS
388	Temp.	TF-188	TE	388	C35 Fuel Rod Pos.4	FIG.5.144	273.	-	0.125E+04	K	0.64%FS
389	Temp.	TF-189	TE	389	C66 Fuel Rod Pos.4	FIG.5.144	273.	-	0.125E+04	K	0.64%FS
390	Temp.	TF-190	TE	390	C68 Fuel Rod Pos.4	FIG.5.143	273.	-	0.125E+04	K	0.64%FS
391	Temp.	TF-191	TE	391	C77 Fuel Rod Pos.1	FIG.5.108, 161	273.	-	0.125E+04	K	0.64%FS
392	Temp.	TF-192	TE	392	C77 Fuel Rod Pos.2	FIG.5.108, 162	273.	-	0.125E+04	K	0.64%FS
393	Temp.	TF-193	TE	393	C77 Fuel Rod Pos.3	FIG.5.108, 163	273.	-	0.125E+04	K	0.64%FS
394	Temp.	TF-194	TE	394	C77 Fuel Rod Pos.4	FIG.5.108, 164	273.	-	0.125E+04	K	0.64%FS
395	Temp.	TF-195	TE	395	C77 Fuel Rod Pos.5	FIG.5.108, 165	273.	-	0.125E+04	K	0.64%FS
396	Temp.	TF-196	TE	396	C77 Fuel Rod Pos.6	FIG.5.108, 166	273.	-	0.125E+04	K	0.64%FS
397	Temp.	TF-197	TE	397	C77 Fuel Rod Pos.7	FIG.5.108, 167	273.	-	0.125E+04	K	0.64%FS
398	Temp.	TF-198	TE	398	D11 Fuel Rod Pos.4	FIG.5.145	273.	-	0.125E+04	K	0.64%FS
399	Temp.	TF-199	TE	399	D13 Fuel Rod Pos.4	FIG.5.145	273.	-	0.125E+04	K	0.64%FS
400	Temp.	TF-200	TE	400	D22 Fuel Rod Pos.1	FIG.5.109	273.	-	0.125E+04	K	0.64%FS

Table 3.2 Measurement List for RUN 926 (Continued)

401Ch.- 450Ch.

Ch.	Item	Symbol	ID.	Location	Fig.No.	Range			Unit	Accuracy
401	Temp.	TF-201	TE 401	D22 Fuel Rod Pos.2	FIG.5.109	273.	-	0.125E+04	K	0.64%FS
402	Temp.	TF-202	TE 402	D22 Fuel Rod Pos.3	FIG.5.109	273.	-	0.125E+04	K	0.64%FS
403	Temp.	TF-203	TE 403	D22 Fuel Rod Pos.4	FIG.5.109	273.	-	0.125E+04	K	0.64%FS
404	Temp.	TF-204	TE 404	D22 Fuel Rod Pos.5	FIG.5.109	273.	-	0.125E+04	K	0.64%FS
405	Temp.	TF-205	TE 405	D22 Fuel Rod Pos.6	FIG.5.109	273.	-	0.125E+04	K	0.64%FS
406	Temp.	TF-206	TE 406	D22 Fuel Rod Pos.7	FIG.5.109	273.	-	0.125E+04	K	0.64%FS
407	Temp.	TF-207	TE 407	D31 Fuel Rod Pos.4	FIG.5.145	273.	-	0.125E+04	K	0.64%FS
408	Temp.	TF-208	TE 408	D33 Fuel Rod Pos.4	FIG.5.146	273.	-	0.125E+04	K	0.64%FS
409	Temp.	TF-209	TE 409	D51 Fuel Rod Pos.4	FIG.5.142	273.	-	0.125E+04	K	0.64%FS
410	Temp.	TF-210	TE 410	D53 Fuel Rod Pos.4	FIG.5.146	273.	-	0.125E+04	K	0.64%FS
411	Temp.	TF-211	TE 411	D66 Fuel Rod Pos.4	FIG.5.146	273.	-	0.125E+04	K	0.64%FS
412	Temp.	TF-212	TE 412	D77 Fuel Rod Pos.4	FIG.5.142	273.	-	0.125E+04	K	0.64%FS
413	Temp.	TF-213	TE 413	D86 Fuel Rod Pos.4	FIG.5.145	273.	-	0.125E+04	K	0.64%FS
414	Fluid T.	TW- 1	TE 414	A45 Tie Rod Pos.1	FIG.5.110	273.	-	0.125E+04	K	0.64%FS
415	Fluid T.	TW- 2	TE 415	A45 Tie Rod Pos.2	FIG.5.110	273.	-	0.125E+04	K	0.64%FS
416	Fluid T.	TW- 3	TE 416	A45 Tie Rod Pos.3	FIG.5.110	273.	-	0.125E+04	K	0.64%FS
417	Fluid T.	TW- 4	TE 417	A45 Tie Rod Pos.4	FIG.5.110	273.	-	0.125E+04	K	0.64%FS
418	Fluid T.	TW- 5	TE 418	A45 Tie Rod Pos.5	FIG.5.110	273.	-	0.125E+04	K	0.64%FS
419	Fluid T.	TW- 6	TE 419	A45 Tie Rod Pos.6	FIG.5.110	273.	-	0.125E+04	K	0.64%FS
420	Fluid T.	TW- 7	TE 420	A45 Tie Rod Pos.7	FIG.5.110	273.	-	0.125E+04	K	0.64%FS
421	Fluid T.	TW- 8	TE 421	B45 Tie Rod Pos.1	FIG.5.111	273.	-	0.125E+04	K	0.64%FS
422	Fluid T.	TW- 9	TE 422	B45 Tie Rod Pos.2	FIG.5.111	273.	-	0.125E+04	K	0.64%FS
423	Fluid T.	TW-10	TE 423	B45 Tie Rod Pos.3	FIG.5.111	273.	-	0.125E+04	K	0.64%FS
424	Fluid T.	TW-11	TE 424	B45 Tie Rod Pos.4	FIG.5.111	273.	-	0.125E+04	K	0.64%FS
425	Fluid T.	TW-12	TE 425	B45 Tie Rod Pos.5	FIG.5.111	273.	-	0.125E+04	K	0.64%FS
426	Fluid T.	TW-13	TE 426	B45 Tie Rod Pos.6	FIG.5.111	273.	-	0.125E+04	K	0.64%FS
427	Fluid T.	TW-14	TE 427	B45 Tie Rod Pos.7	FIG.5.111	273.	-	0.125E+04	K	0.64%FS
428	Fluid T.	TW-15	TE 428	C45 Tie Rod Pos.1	FIG.5.112	273.	-	0.125E+04	K	0.64%FS
429	Fluid T.	TW-16	TE 429	C45 Tie Rod Pos.2	FIG.5.112	273.	-	0.125E+04	K	0.64%FS
430	Fluid T.	TW-17	TE 430	C45 Tie Rod Pos.3	FIG.5.112	273.	-	0.125E+04	K	0.64%FS
431	Fluid T.	TW-18	TE 431	C45 Tie Rod Pos.4	FIG.5.112	273.	-	0.125E+04	K	0.64%FS
432	Fluid T.	TW-19	TE 432	C45 Tie Rod Pos.5	FIG.5.112	273.	-	0.125E+04	K	0.64%FS
433	Fluid T.	TW-20	TE 433	C45 Tie Rod Pos.6	FIG.5.112	273.	-	0.125E+04	K	0.64%FS
434	Fluid T.	TW-21	TE 434	C45 Tie Rod Pos.7	FIG.5.112	273.	-	0.125E+04	K	0.64%FS
435	Fluid T.	TW-22	TE 435	D45 Tie Rod Pos.1	FIG.5.113	273.	-	0.125E+04	K	0.64%FS
436	Fluid T.	TW-23	TE 436	D45 Tie Rod Pos.2	FIG.5.113	273.	-	0.125E+04	K	0.64%FS
437	Fluid T.	TW-24	TE 437	D45 Tie Rod Pos.3	Not Measured	273.	-	0.125E+04	K	0.64%FS
438	Fluid T.	TW-25	TE 438	D45 Tie Rod Pos.4	Not Measured	273.	-	0.125E+04	K	0.64%FS
439	Fluid T.	TW-26	TE 439	D45 Tie Rod Pos.5	Not Measured	273.	-	0.125E+04	K	0.64%FS
440	Fluid T.	TW-27	TE 440	D45 Tie Rod Pos.6	Not Measured	273.	-	0.125E+04	K	0.64%FS
441	Fluid T.	TW-28	TE 441	D45 Tie Rod Pos.7	Not Measured	273.	-	0.125E+04	K	0.64%FS
442	Fluid T.	TC- 1	TE 442	Channel Box A Inlet	FIG.5.168	273.	-	0.125E+04	K	0.64%FS
443	Fluid T.	TC- 2	TE 443	Channel Box B Inlet	FIG.5.168	273.	-	0.125E+04	K	0.64%FS
444	Fluid T.	TC- 3	TE 444	Channel Box C Inlet	FIG.5.168	273.	-	0.125E+04	K	0.64%FS
445	Fluid T.	TC- 4	TE 445	Channel Box D Inlet	FIG.5.168	273.	-	0.125E+04	K	0.64%FS
446	Fluid T.	TC- 5	TE 446	Channel Box Outlet A-1	FIG.5.169	273.	-	0.125E+04	K	0.64%FS
447	Fluid T.	TC- 6	TE 447	Channel Box Outlet A-2	FIG.5.169	273.	-	0.125E+04	K	0.64%FS
448	Fluid T.	TC- 7	TE 448	Channel Box Outlet A-3	FIG.5.169	273.	-	0.125E+04	K	0.64%FS
449	Fluid T.	TC- 8	TE 449	Channel Box Outlet A-4	FIG.5.169	273.	-	0.125E+04	K	0.64%FS
450	Fluid T.	TC- 9	TE 450	Channel Box Outlet A-6	FIG.5.169	273.	-	0.125E+04	K	0.64%FS

Table 3.2 Measurement List for RUN 926 (Continued)

451Ch.- 500Ch.

Ch.	Item	Symbol	ID.	Location	Fig.No.	Range	Unit	Accuracy
451	Fluid T.	TC-10	TE 451	Channel Box Outlet C-1	FIG.5.170	273. - 0.125E+04	K	0.64%FS
452	Fluid T.	TC-11	TE 452	Channel Box Outlet C-2	FIG.5.170	273. - 0.125E+04	K	0.64%FS
453	Fluid T.	TC-12	TE 453	Channel Box Outlet C-3	FIG.5.170	273. - 0.125E+04	K	0.64%FS
454	Fluid T.	TC-13	TE 454	Channel Box Outlet C-4	FIG.5.170	273. - 0.125E+04	K	0.64%FS
455	Fluid T.	TC-14	TE 455	Channel Box Outlet C-6	FIG.5.170	273. - 0.125E+04	K	0.64%FS
456	Fluid T.	TG- 1	TE 456	Upper Tieplate A Up.1	FIG.5.171, 175	273. - 0.125E+04	K	0.64%FS
457	Fluid T.	TG- 2	TE 457	Upper Tieplate A Up.2	FIG.5.171, 176	273. - 0.125E+04	K	0.64%FS
458	Fluid T.	TG- 3	TE 458	Upper Tieplate A Up.3	FIG.5.171, 177	273. - 0.125E+04	K	0.64%FS
459	Fluid T.	TG- 4	TE 459	Upper Tieplate A Up.4	FIG.5.171, 178	273. - 0.125E+04	K	0.64%FS
460	Fluid T.	TG- 5	TE 460	Upper Tieplate A Up.5	FIG.5.171, 179	273. - 0.125E+04	K	0.64%FS
461	Fluid T.	TG- 6	TE 461	Upper Tieplate A Up.6	FIG.5.172, 180	273. - 0.125E+04	K	0.64%FS
462	Fluid T.	TG- 7	TE 462	Upper Tieplate A Up.7	FIG.5.172, 181	273. - 0.125E+04	K	0.64%FS
463	Fluid T.	TG- 8	TE 463	Upper Tieplate A Up.8	FIG.5.172, 182	273. - 0.125E+04	K	0.64%FS
464	Fluid T.	TG- 9	TE 464	Upper Tieplate A Up.9	FIG.5.172 183	273. - 0.125E+04	K	0.64%FS
465	Fluid T.	TG-10	TE 465	Upper Tieplate A Up.10	FIG.5.172, 184	273. - 0.125E+04	K	0.64%FS
466	Fluid T.	TG-11	TE 466	Upper Tieplate A Lo.1	FIG.5.173, 175	273. - 0.125E+04	K	0.64%FS
467	Fluid T.	TG-12	TE 467	Upper Tieplate A Lo.2	FIG.5.173, 176	273. - 0.125E+04	K	0.64%FS
468	Fluid T.	TG-13	TE 468	Upper Tieplate A Lo.3	FIG.5.173, 177	273. - 0.125E+04	K	0.64%FS
469	Fluid T.	TG-14	TE 469	Upper Tieplate A Lo.4	FIG.5.173, 178	273. - 0.125E+04	K	0.64%FS
470	Fluid T.	TG-15	TE 470	Upper Tieplate A Lo.5	FIG.5.173, 179	273. - 0.125E+04	K	0.64%FS
471	Fluid T.	TG-16	TE 471	Upper Tieplate A Lo.6	FIG.5.174, 180	273. - 0.125E+04	K	0.64%FS
472	Fluid T.	TG-17	TE 472	Upper Tieplate A Lo.7	FIG.5.174, 181	273. - 0.125E+04	K	0.64%FS
473	Fluid T.	TG-18	TE 473	Upper Tieplate A Lo.8	FIG.5.174, 182	273. - 0.125E+04	K	0.64%FS
474	Fluid T.	TG-19	TE 474	Upper Tieplate A Lo.9	FIG.5.174, 183	273. - 0.125E+04	K	0.64%FS
475	Fluid T.	TG-20	TE 475	Upper Tieplate A Lo.10	FIG.5.174, 184	273. - 0.125E+04	K	0.64%FS
476	Fluid T.	TG-21	TE 476	Upper Tieplate C Up.1	FIG.5.185, 189	273. - 0.125E+04	K	0.64%FS
477	Fluid T.	TG-22	TE 477	Upper Tieplate C Up.2	FIG.5.185, 190	273. - 0.125E+04	K	0.64%FS
478	Fluid T.	TG-23	TE 478	Upper Tieplate C Up.3	FIG.5.185, 191	273. - 0.125E+04	K	0.64%FS
479	Fluid T.	TG-24	TE 479	Upper Tieplate C Up.4	FIG.5.185, 192	273. - 0.125E+04	K	0.64%FS
480	Fluid T.	TG-25	TE 480	Upper Tieplate C Up.5	FIG.5.185, 193	273. - 0.125E+04	K	0.64%FS
481	Fluid T.	TG-26	TE 481	Upper Tieplate C Up.6	FIG.5.186, 194	273. - 0.125E+04	K	0.64%FS
482	Fluid T.	TG-27	TE 482	Upper Tieplate C Up.7	FIG.5.186, 195	273. - 0.125E+04	K	0.64%FS
483	Fluid T.	TG-28	TE 483	Upper Tieplate C Up.8	FIG.5.186, 196	273. - 0.125E+04	K	0.64%FS
484	Fluid T.	TG-29	TE 484	Upper Tieplate C Up.9	FIG.5.186, 197	273. - 0.125E+04	K	0.64%FS
485	Fluid T.	TG-30	TE 485	Upper Tieplate C Up.10	FIG.5.186, 198	273. - 0.125E+04	K	0.64%FS
486	Fluid T.	TG-31	TE 486	Upper Tieplate C Lo.1	FIG.5.187, 189	273. - 0.125E+04	K	0.64%FS
487	Fluid T.	TG-32	TE 487	Upper Tieplate C Lo.2	FIG.5.187, 190	273. - 0.125E+04	K	0.64%FS
488	Fluid T.	TG-33	TE 488	Upper Tieplate C Lo.3	FIG.5.187, 191	273. - 0.125E+04	K	0.64%FS
489	Fluid T.	TG-34	TE 489	Upper Tieplate C Lo.4	FIG.5.187, 192	273. - 0.125E+04	K	0.64%FS
490	Fluid T.	TG-35	TE 490	Upper Tieplate C Lo.5	FIG.5.187, 193	273. - 0.125E+04	K	0.64%FS
491	Fluid T.	TG-36	TE 491	Upper Tieplate C Lo.6	FIG.5.181, 194	273. - 0.125E+04	K	0.64%FS
492	Fluid T.	TG-37	TE 492	Upper Tieplate C Lo.7	FIG.5.188, 195	273. - 0.125E+04	K	0.64%FS
493	Fluid T.	TG-38	TE 493	Upper Tieplate C Lo.8	FIG.5.188, 196	273. - 0.125E+04	K	0.64%FS
494	Fluid T.	TG-39	TE 494	Upper Tieplate C Lo.9	FIG.5.188, 197	273. - 0.125E+04	K	0.64%FS
495	Fluid T.	TG-40	TE 495	Upper Tieplate C Lo.10	FIG.5.188, 198	273. - 0.125E+04	K	0.64%FS
496	Slab T.	TB- 1	TE 496	C.B. A1 Inner ,Pos.1	FIG.5.114, 199	273. - 0.125E+04	K	0.64%FS
497	Slab T.	TB- 2	TE 497	C.B. A1 Inner ,Pos.2	FIG.5.114, 200	273. - 0.125E+04	K	0.64%FS
498	Slab T.	TB- 3	TE 498	C.B. A1 Inner ,Pos.3	FIG.5.114, 201	273. - 0.125E+04	K	0.64%FS
499	Slab T.	TB- 4	TE 499	C.B. A1 Inner ,Pos.4	FIG.5.114, 202	273. - 0.125E+04	K	0.64%FS
500	Slab T.	TB- 5	TE 500	C.B. A1 Inner ,Pos.5	FIG.5.114, 203	273. - 0.125E+04	K	0.64%FS

Table 3.2 Measurement List for RUN 926 (Continued)

501Ch.- 550Ch.

Ch.	Item	Symbol	ID.	Location	Fig.No.	Range		Unit	Accuracy
501	Slab T.	TB- 6	TE 501	C.B. A1 Inner ,Pos.6	FIG.5.114, 204	273.	- 0.125E+04	K	0.64%FS
502	Slab T.	TB- 7	TE 502	C.B. A1 Inner ,Pos.7	FIG.5.114, 205	273.	- 0.125E+04	K	0.64%FS
503	Slab T.	TB- 8	TE 503	C.B. A2 Inner ,Pos.1	Failure	273.	- 0.125E+04	K	0.64%FS
504	Slab T.	TB- 9	TE 504	C.B. A2 Inner ,Pos.2	FIG.5.115, 200	273.	- 0.125E+04	K	0.64%FS
505	Slab T.	TB-10	TE 505	C.B. A2 Inner ,Pos.3	FIG.5.115, 201	273.	- 0.125E+04	K	0.64%FS
506	Slab T.	TB-11	TE 506	C.B. A2 Inner ,Pos.4	FIG.5.115, 202	273.	- 0.125E+04	K	0.64%FS
507	Slab T.	TB-12	TE 507	C.B. A2 Inner ,Pos.5	FIG.5.115, 203	273.	- 0.125E+04	K	0.64%FS
508	Slab T.	TB-13	TE 508	C.B. A2 Inner ,Pos.6	FIG.5.115, 204	273.	- 0.125E+04	K	0.64%FS
509	Slab T.	TB-14	TE 509	C.B. A2 Inner ,Pos.7	FIG.5.115, 205	273.	- 0.125E+04	K	0.64%FS
510	Slab T.	TB-15	TE 510	C.B. B Inner ,Pos.1	FIG.5.116, 199	273.	- 0.125E+04	K	0.64%FS
511	Slab T.	TB-16	TE 511	C.B. B Inner ,Pos.2	FIG.5.116, 200	273.	- 0.125E+04	K	0.64%FS
512	Slab T.	TB-17	TE 512	C.B. B Inner ,Pos.3	FIG.5.116, 201	273.	- 0.125E+04	K	0.64%FS
513	Slab T.	TB-18	TE 513	C.B. B Inner ,Pos.4	FIG.5.116, 202	273.	- 0.125E+04	K	0.64%FS
514	Slab T.	TB-19	TE 514	C.B. B Inner ,Pos.5	FIG.5.116, 203	273.	- 0.125E+04	K	0.64%FS
515	Slab T.	TB-20	TE 515	C.B. B Inner ,Pos.6	FIG.5.116, 204	273.	- 0.125E+04	K	0.64%FS
516	Slab T.	TB-21	TE 516	C.B. B Inner ,Pos.7	FIG.5.116, 205	273.	- 0.125E+04	K	0.64%FS
517	Slab T.	TB-22	TE 517	C.B. C Inner ,Pos.1	FIG.5.117, 199	273.	- 0.125E+04	K	0.64%FS
518	Slab T.	TB-23	TE 518	C.B. C Inner ,Pos.2	FIG.5.117, 200	273.	- 0.125E+04	K	0.64%FS
519	Slab T.	TB-24	TE 519	C.B. C Inner ,Pos.3	FIG.5.117, 201	273.	- 0.125E+04	K	0.64%FS
520	Slab T.	TB-25	TE 520	C.B. C Inner ,Pos.4	FIG.5.117, 202	273.	- 0.125E+04	K	0.64%FS
521	Slab T.	TB-26	TE 521	C.B. C Inner ,Pos.5	FIG.5.117, 203	273.	- 0.125E+04	K	0.64%FS
522	Slab T.	TB-27	TE 522	C.B. C Inner ,Pos.6	FIG.5.117, 204	273.	- 0.125E+04	K	0.64%FS
523	Slab T.	TB-28	TE 523	C.B. C Inner ,Pos.7	FIG.5.117, 205	273.	- 0.125E+04	K	0.64%FS
524	Slab T.	TB-29	TE 524	C.B. D Inner ,Pos.1	FIG.5.118, 199	273.	- 0.125E+04	K	0.64%FS
525	Slab T.	TB-30	TE 525	C.B. D Inner ,Pos.2	FIG.5.118, 200	273.	- 0.125E+04	K	0.64%FS
526	Slab T.	TB-31	TE 526	C.B. D Inner ,Pos.3	FIG.5.118, 201	273.	- 0.125E+04	K	0.64%FS
527	Slab T.	TB-32	TE 527	C.B. D Inner ,Pos.4	FIG.5.118, 202	273.	- 0.125E+04	K	0.64%FS
528	Slab T.	TB-33	TE 528	C.B. D Inner ,Pos.5	FIG.5.118, 203	273.	- 0.125E+04	K	0.64%FS
529	Slab T.	TB-34	TE 529	C.B. D Inner ,Pos.6	FIG.5.118, 204	273.	- 0.125E+04	K	0.64%FS
530	Slab T.	TB-35	TE 530	C.B. D Inner ,Pos.7	FIG.5.118, 205	273.	- 0.125E+04	K	0.64%FS
531	Fluid T.	TB-36	TE 531	C.B. A Outer ,Pos.1	FIG.5.119, 199	273.	- 0.125E+04	K	0.64%FS
532	Fluid T.	TB-37	TE 532	C.B. A Outer ,Pos.2	FIG.5.119, 200	273.	- 0.125E+04	K	0.64%FS
533	Fluid T.	TB-38	TE 533	C.B. A Outer ,Pos.3	FIG.5.119, 201	273.	- 0.125E+04	K	0.64%FS
534	Fluid T.	TB-39	TE 534	C.B. A Outer ,Pos.4	FIG.5.119, 202	273.	- 0.125E+04	K	0.64%FS
535	Fluid T.	TB-40	TE 535	C.B. A Outer ,Pos.5	FIG.5.119, 203	273.	- 0.125E+04	K	0.64%FS
536	Fluid T.	TB-41	TE 536	C.B. A Outer ,Pos.6	FIG.5.119, 204	273.	- 0.125E+04	K	0.64%FS
537	Fluid T.	TB-42	TE 537	C.B. A Outer ,Pos.7	FIG.5.119, 205	273.	- 0.125E+04	K	0.64%FS
538	Fluid T.	TB-43	TE 538	C.B. C Outer ,Pos.1	FIG.5.120, 199	273.	- 0.125E+04	K	0.64%FS
539	Fluid T.	TB-44	TE 539	C.B. C Outer ,Pos.2	FIG.5.120, 200	273.	- 0.125E+04	K	0.64%FS
540	Fluid T.	TB-45	TE 540	C.B. C Outer ,Pos.3	FIG.5.120, 201	273.	- 0.125E+04	K	0.64%FS
541	Fluid T.	TB-46	TE 541	C.B. C Outer ,Pos.4	FIG.5.120, 202	273.	- 0.125E+04	K	0.64%FS
542	Fluid T.	TB-47	TE 542	C.B. C Outer ,Pos.5	FIG.5.120, 203	273.	- 0.125E+04	K	0.64%FS
543	Fluid T.	TB-48	TE 543	C.B. C Outer ,Pos.6	FIG.5.120, 204	273.	- 0.125E+04	K	0.64%FS
544	Fluid T.	TB-49	TE 544	C.B. C Outer ,Pos.7	FIG.5.120, 205	273.	- 0.125E+04	K	0.64%FS
545	Fluid T.	TP- 1	TE 545	Lower Pl. Center 1	Fig.5.206	273.	- 0.125E+04	K	0.64%FS
546	Fluid T.	TP- 2	TE 546	Lower Pl. Center 2	Fig.5.206	273.	- 0.125E+04	K	0.64%FS
547	Fluid T.	TP- 3	TE 547	Lower Pl. Center 3	Fig.5.206	273.	- 0.125E+04	K	0.64%FS
548	Fluid T.	TP- 4	TE 548	Lower Pl. Center 4	Fig.5.206	273.	- 0.125E+04	K	0.64%FS
549	Fluid T.	TP- 5	TE 549	Lower Pl. Center 5	Fig.5.206	273.	- 0.125E+04	K	0.64%FS
550	Fluid T.	TP- 6	TE 550	Lower Pl. Center 7	Fig.5.206	273.	- 0.125E+04	K	0.64%FS

Table 3.2 Measurement List for RUN 926 (Continued)

551Ch.- 600Ch.

Ch.	Item	Symbol	ID.		Location		Fig.No.	Range			Unit	Accuracy
551	Slab T.	TP- 7	TE	551	Lower Pl. North	1	Fig.5.207	273.	-	0.125E+04	K	0.64%FS
552	Slab T.	TP- 8	TE	552	Lower Pl. North	2	Fig.5.207	273.	-	673.	K	0.64%FS
553	Slab T.	TP- 9	TE	553	Lower Pl. North	4	Fig.5.207	273.	-	673.	K	0.64%FS
554	Slab T.	TP-10	TE	554	Lower Pl. North	6	Fig.5.207	273.	-	673.	K	0.64%FS
555	Slab T.	TP-11	TE	555	Lower Pl. South	1	Fig.5.208	273.	-	673.	K	0.64%FS
556	Slab T.	TP-12	TE	556	Lower Pl. South	2	Fig.5.208	273.	-	673.	K	0.64%FS
557	Slab T.	TP-13	TE	557	Lower Pl. South	4	Fig.5.208	273.	-	673.	K	0.64%FS
558	Slab T.	TP-14	TE	558	Lower Pl. South	6	Fig.5.208	273.	-	673.	K	0.64%FS
559	Level	LB- 1	LM	559	C.B.Liquid Level	A1-1	Fig.5.209					
560	Level	LB- 2	LM	560	C.B.Liquid Level	A1-2	Failure					
561	Level	LB- 3	LM	561	C.B.Liquid Level	A1-3	Fig.5.209					
562	Level	LB- 4	LM	562	C.B.Liquid Level	A1-4	Fig.5.209					
563	Level	LB- 5	LM	563	C.B.Liquid Level	A1-5	Fig.5.209					
564	Level	LB- 6	LM	564	C.B.Liquid Level	A1-6	Fig.5.209					
565	Level	LB- 7	LM	565	C.B.Liquid Level	A1-7	Fig.5.209					
566	Level	LB- 8	LM	566	C.B.Liquid Level	A2-1	Fig.5.210					
567	Level	LB- 9	LM	567	C.B.Liquid Level	A2-2	Failure					
568	Level	LB-10	LM	568	C.B.Liquid Level	A2-3	Fig.5.210					
569	Level	LB-11	LM	569	C.B.Liquid Level	A2-4	Fig.5.210					
570	Level	LB-12	LM	570	C.B.Liquid Level	A2-5	Fig.5.210					
571	Level	LB-13	LM	571	C.B.Liquid Level	A2-6	Fig.5.210					
572	Level	LB-14	LM	572	C.B.Liquid Level	A2-7	Fig.5.210					
573	Level	LB-15	LM	573	C.B.Liquid Level	B-1	Fig.5.211					
574	Level	LB-16	LM	574	C.B.Liquid Level	B-2	Fig.5.211					
575	Level	LB-17	LM	575	C.B.Liquid Level	B-3	Fig.5.211					
576	Level	LB-18	LM	576	C.B.Liquid Level	B-4	Fig.5.211					
577	Level	LB-19	LM	577	C.B.Liquid Level	B-5	Fig.5.211					
578	Level	LB-20	LM	578	C.B.Liquid Level	B-6	Fig.5.211					
579	Level	LB-21	LM	579	C.B.Liquid Level	B-7	Fig.5.211					
580	Level	LB-22	LM	580	C.B.Liquid Level	C-1	Fig.5.212					
581	Level	LB-23	LM	581	C.B.Liquid Level	C-2	Fig.5.212					
582	Level	LB-24	LM	582	C.B.Liquid Level	C-3	Fig.5.212					
583	Level	LB-25	LM	583	C.B.Liquid Level	C-4	Fig.5.212					
584	Level	LB-26	LM	584	C.B.Liquid Level	C-5	Fig.5.212					
585	Level	LB-27	LM	585	C.B.Liquid Level	C-6	Fig.5.212					
586	Level	LB-28	LM	586	C.B.Liquid Level	C-7	Fig.5.212					
587	Level	LB-29	LM	587	C.B.Liquid Level	D-1	Fig.5.213					
588	Level	LB-30	LM	588	C.B.Liquid Level	D-2	Fig.5.213					
589	Level	LB-31	LM	589	C.B.Liquid Level	D-3	Fig.5.213					
590	Level	LB-32	LM	590	C.B.Liquid Level	D-4	Fig.5.213					
591	Level	LB-33	LM	591	C.B.Liquid Level	D-5	Fig.5.213					
592	Level	LB-34	LM	592	C.B.Liquid Level	D-6	Fig.5.213					
593	Level	LB-35	LM	593	C.B.Liquid Level	D-7	Fig.5.213					
594	Level	LL- 1	LM	594	Ch.Box Outlet	A1-5	Fig.5.214					
595	Level	LL- 2	LM	595	Ch.Box Outlet	A1-6	Fig.5.214					
596	Level	LL- 3	LM	596	Ch.Box Outlet	A1-7	Failure					
597	Level	LL- 4	LM	597	Ch.Box Outlet	A2-5	Fig.5.215					
598	Level	LL- 5	LM	598	Ch.Box Outlet	A2-6	Fig.5.215					
599	Level	LL- 6	LM	599	Ch.Box Outlet	A2-7	Fig.5.215					
600	Level	LL- 7	LM	600	Ch.Box Outlet	A-1	Fig.5.216					

Table 3.2 Measurement List for RUN 926 (Continued)

601Ch.- 650Ch.

Ch.	Item	Symbol	ID.	Location	Fig.No.	Range	Unit	Accuracy
601	Level	LL- 8	LM 601	Ch.Box Outlet A-2	Failure			
602	Level	LL- 9	LM 602	Ch.Box Outlet A-3	Fig.5.216			
603	Level	LL-10	LM 603	Ch.Box Outlet A-4	Fig.5.216			
604	Level	LL-11	LM 604	Ch.Box Outlet A-6	Fig.5.216			
605	Level	LL-12	LM 605	Ch.Box Outlet C1-5	Fig.5.217			
606	Level	LL-13	LM 606	Ch.Box Outlet C1-6	Fig.5.217			
607	Level	LL-14	LM 607	Ch.Box Outlet C1-7	Fig.5.217			
608	Level	LL-15	LM 608	Ch.Box Outlet C2-5	Fig.5.218			
609	Level	LL-16	LM 609	Ch.Box Outlet C2-6	Fig.5.218			
610	Level	LL-17	LM 610	Ch.Box Outlet C2-7	Fig.5.218			
611	Level	LL-18	LM 611	Ch.Box Outlet C-1	Fig.5.219			
612	Level	LL-19	LM 612	Ch.Box Outlet C-2	Fig.5.219			
613	Level	LL-20	LM 613	Ch.Box Outlet C-3	Fig.5.219			
614	Level	LL-21	LM 614	Ch.Box Outlet C-4	Fig.5.219			
615	Level	LL-22	LM 615	Ch.Box Outlet C-6	Fig.5.219			
616	Level	LL-23	LM 616	Ch.Box Inlet A-1	Fig.5.220			
617	Level	LL-24	LM 617	Ch.Box Inlet A-2	Fig.5.220			
618	Level	LL-25	LM 618	Ch.Box Inlet B-1	Fig.5.221			
619	Level	LL-26	LM 619	Ch.Box Inlet B-2	Fig.5.221			
620	Level	LL-27	LM 620	Ch.Box Inlet C-1	Fig.5.222			
621	Level	LL-28	LM 621	Ch.Box Inlet C-2	Fig.5.222			
622	Level	LL-29	LM 622	Ch.Box Inlet D-1	Fig.5.223			
623	Level	LL-30	LM 623	Ch.Box Inlet D-2	Fig.5.223			
624	Level	LL-31	LM 624	Lower Pl. North 1	Fig.5.224			
625	Level	LL-32	LM 625	Lower Pl. North 2	Fig.5.224			
626	Level	LL-33	LM 626	Lower Pl. North 3	Fig.5.224			
627	Level	LL-34	LM 627	Lower Pl. North 4	Fig.5.224			
628	Level	LL-35	LM 628	Lower Pl. North 5	Fig.5.224			
629	Level	LL-36	LM 629	Lower Pl. North 6	Fig.5.224			
630	Level	LL-37	LM 630	Lower Pl. South 1	Fig.5.225			
631	Level	LL-38	LM 631	Lower Pl. South 2	Fig.5.225			
632	Level	LL-39	LM 632	Lower Pl. South 3	Fig.5.225			
633	Level	LL-40	LM 633	Lower Pl. South 4	Fig.5.225			
634	Level	LL-41	LM 634	Lower Pl. South 5	Fig.5.225			
635	Level	LL-42	LM 635	Lower Pl. South 6	Fig.5.225			
636	Level	LL-43	LM 636	Guide Tube North 0	Fig.5.226			
637	Level	LL-44	LM 637	Guide Tube North 1	Fig.5.226			
638	Level	LL-45	LM 638	Guide Tube North 3	Fig.5.226			
639	Level	LL-46	LM 639	Guide Tube North 6	Fig.5.226			
640	Level	LL-47	LM 640	Guide Tube South 0	Fig.5.227			
641	Level	LL-48	LM 641	Guide Tube South 1	Fig.5.227			
642	Level	LL-49	LM 642	Guide Tube South 3	Fig.5.227			
643	Level	LL-50	LM 643	Guide Tube South 6	Fig.5.227			
644	Level	L- 1	LM 644	Downcomer D-Side 1	Fig.5.228			
645	Level	L- 2	LM 645	Downcomer D-Side 2	Fig.5.228			
646	Level	L- 3	LM 646	Downcomer D-Side 3	Fig.5.228			
647	Level	L- 4	LM 647	Downcomer D-Side 4	Fig.5.228			
648	Level	L- 5	LM 648	Downcomer D-Side 5	Fig.5.228			
649	Level	L- 6	LM 649	Downcomer B-Side 1	Fig.5.229			
650	Level	L- 7	LM 650	Downcomer B-Side 2	Fig.5.229			

Table 3.2 Measurement List for RUN 926 (Continued)

651Ch.- 700Ch.

Ch.	Item	Symbol	ID.		Location	Fig.No.	Range			Unit	Accuracy
651	Level	L- 8	LM	651	Downcomer B-Side 3	Fig.5.229					
652	Level	L- 9	LM	652	Downcomer B-Side 4	Fig.5.229					
653	Level	L-10	LM	653	Downcomer B-Side 5	Failure					
654	Void	VF- 1	VD	654	A54 Tie Rod Pos.1	Not Measured	0.0	-	1.00		
655	Void	VF- 2	VD	655	A54 Tie Rod Pos.2	Not Measured	0.0	-	1.00		
656	Void	VF- 3	VD	656	A54 Tie Rod Pos.3	Not Measured	0.0	-	1.00		
657	Void	VF- 4	VD	657	A54 Tie Rod Pos.4	Not Measured	0.0	-	1.00		
658	Void	VF- 5	VD	658	A54 Tie Rod Pos.5	Not Measured	0.0	-	1.00		
659	Void	VF- 6	VD	659	A54 Tie Rod Pos.6	Not Measured	0.0	-	1.00		
660	Void	VF- 7	VD	660	A54 Tie Rod Pos.7	Not Measured	0.0	-	1.00		
661	Void	VF- 8	VD	661	B54 Tie Rod Pos.1	Not Measured	0.0	-	1.00		
662	Void	VF- 9	VD	662	B54 Tie Rod Pos.2	Not Measured	0.0	-	1.00		
663	Void	VF-10	VD	663	B54 Tie Rod Pos.3	Not Measured	0.0	-	1.00		
664	Void	VF-11	VD	664	B54 Tie Rod Pos.4	Not Measured	0.0	-	1.00		
665	Void	VF-12	VD	665	B54 Tie Rod Pos.5	Not Measured	0.0	-	1.00		
666	Void	VF-13	VD	666	B54 Tie Rod Pos.6	Not Measured	0.0	-	1.00		
667	Void	VF-14	VD	667	B54 Tie Rod Pos.7	Not Measured	0.0	-	1.00		
668	Void	VF-15	VD	668	C54 Tie Rod Pos.1	Not Measured	0.0	-	1.00		
669	Void	VF-16	VD	669	C54 Tie Rod Pos.2	Not Measured	0.0	-	1.00		
670	Void	VF-17	VD	670	C54 Tie Rod Pos.3	Not Measured	0.0	-	1.00		
671	Void	VF-18	VD	671	C54 Tie Rod Pos.4	Not Measured	0.0	-	1.00		
672	Void	VF-19	VD	672	C54 Tie Rod Pos.5	Not Measured	0.0	-	1.00		
673	Void	VF-20	VD	673	C54 Tie Rod Pos.6	Not Measured	0.0	-	1.00		
674	Void	VF-21	VD	674	C54 Tie Rod Pos.7	Not Measured	0.0	-	1.00		
675	Void	VF-22	VD	675	D54 Tie Rod Pos.7	Not Measured	0.0	-	1.00		
676	Void	VF-23	VD	676	D54 Tie Rod Pos.7	Not Measured	0.0	-	1.00		
677	Void	VF-24	VD	677	D54 Tie Rod Pos.7	Not Measured	0.0	-	1.00		
678	Void	VF-25	VD	678	D54 Tie Rod Pos.7	Not Measured	0.0	-	1.00		
679	Void	VF-26	VD	679	D54 Tie Rod Pos.7	Not Measured	0.0	-	1.00		
680	Void	VF-27	VD	680	D54 Tie Rod Pos.7	Not Measured	0.0	-	1.00		
681	Void	VF-28	VD	681	D54 Tie Rod Pos.7	Not Measured	0.0	-	1.00		
682	Void	VE- 1	VD	682	Channel A Outlet 1	Not Measured	0.0	-	1.00		
683	Void	VE- 2	VD	683	Channel A Outlet 2	Not Measured	0.0	-	1.00		
684	Void	VE- 3	VD	684	Channel A Outlet 3	Not Measured	0.0	-	1.00		
685	Void	VE- 4	VD	685	Channel B Outlet 1	Not Measured	0.0	-	1.00		
686	Void	VE- 5	VD	686	Channel B Outlet 2	Not Measured	0.0	-	1.00		
687	Void	VE- 6	VD	687	Channel B Outlet 3	Not Measured	0.0	-	1.00		
688	Void	VE- 7	VD	688	Channel C Outlet 1	Not Measured	0.0	-	1.00		
689	Void	VE- 8	VD	689	Channel C Outlet 2	Not Measured	0.0	-	1.00		
690	Void	VE- 9	VD	690	Channel C Outlet 3	Not Measured	0.0	-	1.00		
691	Void	VE-10	VD	691	Channel D Outlet 1	Not Measured	0.0	-	1.00		
692	Void	VE-11	VD	692	Channel D Outlet 2	Not Measured	0.0	-	1.00		
693	Void	VE-12	VD	693	Channel D Outlet 3	Not Measured	0.0	-	1.00		
694	Void	VE-13	VD	694	Lower Plenum Bottom 1	Not Measured	0.0	-	1.00		
695	Void	VE-14	VD	695	Lower Plenum Bottom 2	Not Measured	0.0	-	1.00		
696	Void	VE-15	VD	696	Lower Plenum Bottom 3	Not Measured	0.0	-	1.00		
697	Void	VP- 1	VD	697	Lower Plenum Inlet	Not Measured	0.0	-	1.00		
698	Void	VP- 2	VD	698	Lower Plenum Inlet	Not Measured	0.0	-	1.00		

Table 3.3 Core Instrumentation List

Item	Pos. / DL / Rod NO.	Core Outlet	Pos.1	Pos.2	Pos.3	Pos.4	Pos.5	Pos.6	Pos.7	Core Inlet
		3660	3417	3114.5	2879.5	2527	2174.5	1939.5	1637	1454
Surface Temp.	A11		TF 1	TF 2	TF 3	TF 4	TF 5	TF 6	TF 7	
	A12		TF 8	TF 9	TF 10	TF 11	TF 12	TF 13	TF 14	
	A13		TF 15	TF 16	TF 17	TF 18	TF 19	TF 20	TF 21	
	A14		TF 22	TF 23	TF 24	TF 25	TF 26	TF 27	TF 28	
	A15		TF 29			TF 30				
	A17		TF 31			TF 32				
	A22		TF 33	TF 34	TF 35	TF 36	TF 37	TF 38	TF 39	
	A23		TF 40	TF 41	TF 42	TF 43	TF 44	TF 45	TF 46	
	A24		TF 47	TF 48	TF 49	TF 50	TF.51	TF 52	TF 53	
	A26		TF 54			TF 55				
	A28		TF 56			TF 57				
	A31		TF 58			TF 59				
	A33		TF 60	TF 61	TF 62	TF 63	TF 64	TF 65	TF 66	
	A34		TF 67	TF 68	TF 69	TF 70	TF 71	TF 72	TF 73	
	A35		TF 74			TF 75				
	A37		TF 76			TF 77				
	A42		TF 78			TF 79				
Fluid Temp.	A44	TC 1	TF180	TF181	TF182	TF183	TF184	TF185	TF186	TC 2
Surface Temp.	A45		TF 80			TF 81				
	A46		TF 82			TF 83				
	A48		TF 84			TF 85				
	A51		TF 86			TF 87				
	A53		TF 88			TF 89				
	A54		TF 90							
	A57		TF 91			TF 92				
	A62		TF 93			TF 94				
	A64		TF 95			TF 96				
	A66		TF 97			TF 98				
	A68		TF 99			TF100				
	A71		TF101			TF102				
	A73		TF103			TF104				
	A75		TF105			TF106				
	A77		TF107			TF108				

Table 3.3 Core Instrumentation List (Continued)

Item	Pos. / DL / Rod NO.	Core Outlet	Pos.1	Pos.2	Pos.3	Pos.4	Pos.5	Pos.6	Pos.7	Core Inlet
		3660	3417	3114.5	2879.5	2527	2174.5	1939.5	1637	1454
Surface Temp.	A82		TF109			TF110				
	A84		TF111			TF112				
	A86		TF113			TF114				
	A88		TF115			TF116				
	B11					TF117				
	B13					TF118				
	B15		TF119	TF120	TF121	TF122	TF123	TF124	TF125	
	B31					TF126				
	B33					TF127				
	B35					TF128				
Fluid Temp.	B44	TC 3	TF187	TF188	TF189	TF190	TF191	TF192	TF193	TC 4
Surface Temp.	B51					TF129				
	B53					TF130				
	B85		TF131	TF132	TF133	TF134	TF135	TF136	TF137	
	C11					TF138				
	C13					TF139				
	C15					TF140				
	C31					TF141				
	C33		TF142	TF143	TF144	TF145	TF146	TF147	TF148	
	C35					TF149				
Fluid Temp.	C44	TC 5	TF194	TF195	TF196	TF197	TF198	TF199	TF200	TC 6
Surface Temp.	C51					TF150				
	C53					TF151				
	C77		TF152	TF153	TF154	TF155	TF156	TF157	TF158	
	D11					TF159				
	D13					TF160				
	D27		TF161	TF162	TF163	TF164	TF165	TF166	TF167	
	D31					TF168				
	D33					TF169				
	D35					TF170				
Fluid Temp.	D44	TC 7	TF201	TF202	TF203	TF204	TF205	TF206	TF207	TC 8
Surface Temp.	D51					TF171				
	D53					TF172				
	D88		TF173	TF174	TF175	TF176	TF177	TF178	TF179	

Table 3.3 Core Instrumentation List (Continued)

Item	Pos. / Rod NO. / DL	Core Outlet	Pos.1	Pos.2	Pos.3	Pos.4	Pos.5	Pos.6	Pos.7	Core Inlet
		3660	3417	3114.5	2879.5	2527	2174.5	1939.5	1673	1454
Void	A55		VF 1	VF 2	VF 3	VF 4	VF 5	VF 6	VF 7	
	B55		VF 8	VF 9	VF 10	VF 11	VF 12	VF 13	VF 14	
	C55		VF 15	VF 16	VF 17	VF 18	VF 19	VF 20	VF 21	
	D55		VF 22	VF 23	VF 24	VF 25	VF 26	VF 27	VF 28	
Channel Box Surface Temp.	A1*		TB 1	TB 2	TB 3	TB 4	TB 5	TB 6	TB 7	
	A2*		TB 8	TB 9	TB 10	TB 11	TB 12	TB 13	TB 14	
	B*		TB 15	TB 16	TB 17	TB 18	TB 19	TB 20	TB 21	
	C*		TB 22	TB 23	TB 24	TB 25	TB 26	TB 27	TB 28	
	D*		TB 29	TB 30	TB 31	TB 32	TB 33	TB 34	TB 35	
Liquid Level in the Channel Box	A1*		LB 1	LB 2	LB 3	LB 4	LB 5	LB 6	LB 7	
	A2*		LB 8	LB 9	LB 10	LB 11	LB 12	LB 13	LB 14	
	B*		LB 15	LB 16	LB 17	LB 18	LB 19	LB 20	LB 21	
	C*		LB 22	LB 23	LB 24	LB 25	LB 26	LB 27	LB 28	
	D*		LB 29	LB 30	LB 31	LB 32	LB 33	LB 34	LB 35	

Table 4.1 Test Conditions of RUN 926

Parameter	Specified Value	Measured Value
Break Conditions		
Location	MRP suction	MRP suction
Type	Double-ended	Double-ended
Break Nozzle Diameter (mm)	26.2/26.2	26.2/26.2
Initial System Conditions		
Steam Dome Pressure (MPa)	7.35	7.37
Lower Plenum Temperature (K)	551.7	553.0
Lower Plenum Subcooling (K)	10.5	10.0
Core Inlet Flow Rate (kg/s)	16.0	16.3
Core Outlet Quality (%)	13.8**	13.9
Power Level (kW)	1260 + 2700	1263 + 2704
Maximum Linear Heat Rate(kW/m)		
Channel A P.F.=1.1	16.65	16.69
P.F.=1.0	15.13	15.17
P.F.=0.875	13.24	13.27
Channel B-D P.F.=1.1	11.89	11.91
P.F.=1.0	10.81	10.83
P.F.=0.875	9.46	9.47
Water Level in PV* (m)	5.0	5.05
Feedwater Conditions		
Temperature (K)	489	489
Flow Rate (kg/s)	2.39	2.03 (cf.Fig.5.42)
Initiation of Line Closure(s)	2.0	1.5 (completely closed at 4.0s)

* note, L3 Level for Scram : 5.0 m from PV Bottom

** not include core bypass flow
core bypass flow is assumed to be 0.8kg/s

Table 4.1 Test Conditions of RUN 926 (Continued)

Parameter	Specified Value	Measured Value
Steam Discharge Conditions		
Steady State Flow Rate(kg/s)	2.39	2.08
Transient Flow Rate (kg/s)	keep steady value	Fig.5.40
Orifice Diameter (mm)	18.0	18.0
Initiation of Line Closure(s)	L2*+3(s)or $P \leq 6.67$ (MPa)**	5.4 s (by level trip signal)
Safety Relief Valve Setting Pressure (MPa)	P = 8.14	not operated
ECCS Conditions		
HPCS	not-used	not-used
LPCS		
Injection Location	Upper Plenum	Upper Plenum
Initiation Conditions	L1*+40(s) and $\leq$ 2.16 (MPa)	71.0 (s) at PV Pressure 2.13 (MPa)
Coolant Temperature (K)	313	313
Injection Flow Rate(m^3/s)	1.13×10^{-3}	Fig.5.41
LPCI		
Injection Location	Top of Core Bypass	Top of Core Bypass
Initiation Conditions	L1*+40(s) and $\leq$ 1.57 (MPa)	96.3 (s) at PV Pressure 1.45 (MPa)
Coolant Temperature (K)	313	313
Injection Flow Rate (m^3/s)	3.50×10^{-3}	Fig.5.41
ADS Conditions		
Initiation Time (s)	L1*+120 (s)	131 (s)
Flow Rate	Scaled Flow of BWR	Fig.5.40
Orifice Diameter (mm)	15.5	15.5

* note : Each trip level is as follows;

L3 Level for Scram : 5.0 m from PV Bottom

L2 Level for MSIV and HPCS : 4.76 m from PV Bottom

L1 Level for LPCS, LPCI and ADS : 4.25 from PV Bottom

** note : System pressure is controlled to maintain at 6.67 MPa before MSIV closure by low level signal (L2 + 3s).

Table 4.2 Valve Characteristics of Steam Discharge Line

Valve	Close to Open (sec)	Open to Close (sec)
AV165	Not Used	Not Used
AV168	-	0.1
AV169	0.3	2.0

Orifice	Diameter (mm)	Area (mm^2)
OR3	18.0	254.5
OR4	15.5	188.7
OR5	Not Used (Blind)	Not Used (Blind)

Table 4.3 Valve Control Sequence of Steam Discharge Line

Time	t < 0 s	t = 0 s (Break)	P ≦ 6.67MPa	L2 + 3 s	---	P ≧ 8.14MPa	---	L1 + 120 s
CV-1	Open	Close (Manual)	Closed	Closed		Closed		Closed
CV-2 (see Fig.2.3)	Open	Close (Manual)	Closed	Closed		Closed		Closed
CV-130	Control to maintain steady state pressure	Open (Manual)	Control to maintain system pressure at 6.67MPa (Auto)	Close (Manual)		Control to maintain system pressure at 8.14MPa (Auto)		Closed
AV-168	Open	Open	Open	Open		Open		Close (Auto)
AV-169 (ADS Line)	Closed	Closed	Closed	Closed		Closed		Open (Auto)

t = 0 s : Break

t = L2 + 3 s : MSIV closure

t = L1 + 120 s : ADS valve opening

Table 5.1 Sequence of Events in RUN 926

Time after Break (s)	Events
0.0	Break
	Initiate core power control
	Terminate intact loop recirculation pump power (simple coastdown)
	Terminate broken loop recirculation pump power (simple coastdown)
1.5	Initiation of feedwater line valve closure
3.0	Liquid level in downcomer decreased to L2 level
4.0	Closure of feedwater line
5.4	Initiation of steam discharge line valve closure
7.8	Liquid level in downcomer decreased to L1 level
9.0	Initiation of core power curve reduction
9.2	Closure of steam discharge line
10.0	Liquid level in downcomer decreased to jet pump suction nozzle
13.0	Liquid level in downcomer decreased to recirculation pump suction line
17.0	Initiation of lower plenum flashing (LPF)
68.0	Initiation of feedwater line flashing (FWLF)
71.0	LPCS initiation (at system pressure 2.13 MPa)
96.3	LPCI initiation (at system pressure 1.45 MPa)
129.5	ADS initiation (at system pressure 0.74 MPa)
188.0	Quench of the whole core
688.0	End of data acquisition

Table 5.2 Maximum Cladding Temperature Distribution in the Core

	Pos.1	Pos.2	Pos.3	Pos.4	Pos.5	Pos.6	Pos.7
A-11 rod	TE 201	TE 202	TE 203	TE 204	TE 205	TE 206	TE 207
PCT (K)	666.7	737.5	731.5	765.1	663.1	623.5	570.7
Time (s)	16.5	19.0	92.0	113.0	92.5	105.5	12.0
A-12 rod	TE 208	TE 209	TE 210	TE 211	TE 212	TE 213	TE 214
PCT (K)	654.7	666.7	713.5	751.9	688.3	607.9	564.8
Time (s)	20.0	16.5	90.5	112.5	111.0	105.0	0.0
A-13 rod	TE 215	TE 216	TE 217	TE 218	TE 219	TE 220	TE 221
PCT (K)	655.9	670.3	715.9	757.9	691.9	605.5	566.1
Time (s)	19.0	83.5	90.5	114.0	107.5	103.5	0.0
A-14 rod	TE 222	TE 223	TE 224	TE 225	TE 226	TE 227	TE 228
PCT (K)	661.9	720.7	744.7	737.5	681.1	603.1	562.4
Time (s)	19.5	130.0	125.0	114.5	112.0	104.0	0.0
A-15 rod	TE 229			TE 230			
PCT (K)	655.9			737.5			
Time (s)	19.0			113.5			
A-17 rod	TE 231			TE 232			
PCT (K)	660.7			753.1			
Time (s)	19.5			114.0			
A-22 rod	TE 233	TE 234	TE 235	TE 236	TE 237	TE 238	TE 239
PCT (K)	------	724.3	754.3	757.2	692.2	601.8	564.5
Time (s)	------	131.0	117.5	118.5	110.5	104.0	0.0
A-24 rod	TE 240	TE 241	TE 242	TE 243	TE 244	TE 245	TE 246
PCT (K)	649.5	734.6	757.2	737.4	678.9	600.8	565.3
Time (s)	19.5	129.5	123.0	118.5	110.5	106.0	11.5
A-26 rod	TE 247			TE 248			
PCT (K)	642.9			739.3			
Time (s)	19.5			114.0			
A-28 rod	TE 249			TE 250			
PCT (K)	673.3			768.5			
Time (s)	18.5			114.0			
A-31 rod	TE 251			TE 252			
PCT (K)	677.1			782.5			
Time (s)	18.5			113.5			
A-33 rod	TE 253	TE 254	TE 255	TE 256	TE 257	TE 258	TE 259
PCT (K)	631.4	648.6	731.8	713.9	620.9	567.2	565.4
Time (s)	19.5	18.5	121.5	114.5	94.5	0.0	0.0
A-34 rod	TE 260	TE 261	TE 262	TE 263	TE 264	TE 265	TE 266
PCT (K)	626.7	713.0	729.9	711.1	654.3	568.1	564.9
Time (s)	19.0	130.5	129.0	114.5	109.0	0.0	0.0
A-37 rod	TE 267			TE 268			
PCT (K)	741.2			635.2			
Time (s)	114.5			18.5			
A-42 rod	TE 269			TE 270			
PCT (K)	641.0			760.0			
Time (s)	19.0			118.5			
A-44 rod	TE 271	TE 272	TE 273	TE 274	TE 275	TE 276	TE 277
PCT (K)	619.0	702.6	721.4	709.2	652.4	581.6	563.6
Time (s)	19.0	128.5	116.5	114.0	109.5	106.0	0.0

Table 5.2 Maximum Cladding Temperature Distribution in the Core (Continued)

	Pos.1	Pos.2	Pos.3	Pos.4	Pos.5	Pos.6	Pos.7
A-48 rod	TE 278			TE 279			
PCT (K)	643.8			739.3			
Time (s)	19.5			114.5			
A-51 rod	TE 280			TE 281			
PCT (K)	665.7			763.8			
Time (s)	20.0			114.0			
A-53 rod	TE 282			TE 283			
PCT (K)	620.0			711.1			
Time (s)	19.0			114.0			
A-57 rod	TE 284			TE 285			
PCT (K)	654.3			745.0			
Time (s)	132.5			114.5			
A-62 rod	TE 286			TE 287			
PCT (K)	640.0			762.8			
Time (s)	18.5			114.5			
A-66 rod	TE 288			TE 289			
PCT (K)	632.4			711.1			
Time (s)	130.5			114.0			
A-68 rod	TE 290			TE 291			
PCT (K)	669.5			764.7			
Time (s)	19.0			118.5			
A-71 rod	TE 292			TE 293			
PCT (K)	678.9			783.5			
Time (s)	19.5			118.5			
A-73 rod	TE 294			TE 295			
PCT (K)	645.7			759.1			
Time (s)	19.0			114.5			
A-75 rod	TE 296			TE 297			
PCT (K)	643.8			740.3			
Time (s)	19.5			114.5			
A-77 rod	TE 298	TE 299	TE 300	TE 301	TE 302	TE 303	TE 304
PCT (K)	670.4	745.0	761.9	738.4	673.3	599.9	------
Time (s)	132.5	130.0	129.0	113.0	108.0	105.0	------
A-82 rod	TE 305			TE 306			
PCT (K)	679.9			781.6			
Time (s)	19.5			114.5			
A-84 rod	TE 307			TE 308			
PCT (K)	662.8			762.8			
Time (s)	19.0			115.0			
A-85 rod	TE 309	TE 310	TE 311	TE 312	TE 313	TE 314	TE 315
PCT (K)	659.0	749.7	768.5	759.1	691.2	615.2	566.2
Time (s)	18.5	130.0	119.5	114.5	109.5	105.0	10.5
A-87 rod	TE 316	TE 317	TE 318	TE 319	TE 320	TE 321	TE 322
PCT (K)	646.7	745.0	773.1	761.9	693.1	616.2	562.4
Time (s)	16.5	130.0	128.5	113.5	109.5	104.5	0.0
A-88 rod	TE 323	TE 324	TE 325	TE 326	TE 327	TE 328	TE 329
PCT (K)	681.8	754.4	776.0	768.5	699.7	617.1	565.6
Time (s)	19.0	19.0	128.5	114.5	111.0	106.0	0.0

Table 5.2 Maximum Cladding Temperature Distribution in the Core (Continued)

	Pos.1	Pos.2	Pos.3	Pos.4	Pos.5	Pos.6	Pos.7
B-11 rod	TE 330	TE 331	TE 332	TE 333	TE 334	TE 335	TE 336
PCT (K)	588.4	666.6	695.0	705.4	643.8	579.7	------
Time (s)	67.5	19.0	99.0	114.5	110.5	107.0	------
B-13 rod				TE 337			
PCT (K)				702.6			
Time (s)				114.0			
B-22 rod	TE 338	TE 339	TE 340	TE 341	TE 342	TE 343	TE 344
PCT (K)	605.6	641.9	659.0	646.7	568.7	566.3	563.3
Time (s)	19.0	18.5	85.0	89.5	0.0	0.0	0.0
B-31 rod				TE 345			
PCT (K)				694.1			
Time (s)				114.5			
B-33 rod				TE 346			
PCT (K)				613.3			
Time (s)				86.5			
B-51 rod				TE 347			
PCT (K)				681.8			
Time (s)				113.5			
B-53 rod				TE 348			
PCT (K)				651.4			
Time (s)				115.0			
B-66 rod				TE 349			
PCT (K)				657.1			
Time (s)				113.5			
B-77 rod	TE 350	TE 351	TE 352	TE 353	TE 354	TE 355	TE 356
PCT (K)	642.9	698.8	720.5	701.6	638.1	577.8	564.9
Time (s)	115.5	115.5	115.0	114.0	108.5	106.5	0.0
B-86 rod				TE 357			
PCT (K)				703.5			
Time (s)				106.5			
C-11 rod	TE 358	TE 359	TE 360	TE 361	TE 362	TE 363	TE 364
PCT (K)	571.0	667.6	721.4	709.2	646.7	587.4	565.3
Time (s)	15.5	95.5	119.0	117.5	110.0	106.5	11.5
C-13 rod	TE 365	TE 366	TE 367	TE 368	TE 369	TE 370	TE 371
PCT (K)	609.5	651.4	692.2	692.2	643.8	568.4	564.7
Time (s)	19.5	83.5	99.5	111.5	108.0	0.0	0.0
C-15 rod				TE 372			
PCT (K)				691.2			
Time (s)				117.0			
C-22 rod	TE 373	TE 374	TE 375	TE 376	TE 377	TE 378	TE 379
PCT (K)	616.2	653.3	691.2	680.8	576.8	569.6	564.6
Time (s)	20.0	95.0	119.0	114.5	83.5	0.0	0.0
C-31 rod				TE 380			
PCT (K)				679.9			
Time (s)				100.0			
C-33 rod	TE 381	TE 382	TE 383	TE 384	TE 385	TE 386	TE 387
PCT (K)	599.9	632.4	654.3	603.7	565.6	564.4	562.3
Time (s)	19.0	18.5	104.5	85.5	0.0	0.0	10.0

Table 5.2 Maximum Cladding Temperature Distribution in the Core (Continued)

	Pos.1	Pos.2	Pos.3	Pos.4	Pos.5	Pos.6	Pos.7
C-35 rod				TE 388			
PCT (K)				661.9			
Time (s)				114.5			
C-66 rod				TE 389			
PCT (K)				653.3			
Time (s)				113.0			
C-68 rod				TE 390			
PCT (K)				712.0			
Time (s)				113.5			
C-77 rod	TE 391	TE 392	TE 393	TE 394	TE 395	TE 396	TE 397
PCT (K)	632.4	694.1	709.2	690.3	634.3	573.9	565.3
Time (s)	120.5	119.0	117.5	113.5	109.0	106.5	12.0
D-11 rod				TE 398			
PCT (K)				747.8			
Time (s)				124.5			
D-13 rod				TE 399			
PCT (K)				747.8			
Time (s)				125.0			
D-22 rod	TE 400	TE 401	TE 402	TE 403	TE 404	TE 405	TE 406
PCT (K)	609.5	718.6	751.5	730.8	581.6	566.0	564.3
Time (s)	18.5	129.5	127.0	125.0	86.0	0.0	11.0
D-31 rod				TE 407			
PCT (K)				747.8			
Time (s)				125.0			
D-33 rod				TE 408			
PCT (K)				683.7			
Time (s)				124.5			
D-51 rod				TE 409			
PCT (K)				728.0			
Time (s)				125.0			
D-53 rod				TE 410			
PCT (K)				696.0			
Time (s)				124.5			
D-66 rod				TE 411			
PCT (K)				682.5			
Time (s)				125.0			
D-77 rod				TE 412			
PCT (K)				705.1			
Time (s)				125.5			
D-86 rod				TE 413			
PCT (K)				717.7			
Time (s)				104.0			

Table 5.2 Maximum Cladding Temperature Distribution in the Core (Continued)

** Order of PCT **

No. 1	A-71 rod	Pos. 4	PCT =	783.5	(K)	Time =	118.5 (s)
No. 2	A-31 rod	Pos. 4	PCT =	782.5	(K)	Time =	113.5 (s)
No. 3	A-82 rod	Pos. 4	PCT =	781.6	(K)	Time =	114.5 (s)
No. 4	A-88 rod	Pos. 3	PCT =	776.0	(K)	Time =	128.5 (s)
No. 5	A-87 rod	Pos. 3	PCT =	773.1	(K)	Time =	128.5 (s)
No. 6	A-28 rod	Pos. 4	PCT =	768.5	(K)	Time =	114.0 (s)
No. 7	A-85 rod	Pos. 3	PCT =	768.5	(K)	Time =	119.5 (s)
No. 8	A-88 rod	Pos. 4	PCT =	768.5	(K)	Time =	114.5 (s)
No. 9	A-11 rod	Pos. 4	PCT =	765.1	(K)	Time =	113.0 (s)
No.10	A-68 rod	Pos. 4	PCT =	764.7	(K)	Time =	118.5 (s)

Table 6.1 Comparison of Initial Conditions and Major Events in RUN 926 and RUN 901

Parameter	RUN 926	RUN 901
Break Nozzle Diameter	26.2/26.2(mm)	26.2/26.2(mm)
ECCS Conditions	LPCS + LPCI	Full ECCS
Initial Core Power	3.967 MW	4.045 MW
Power Curve	see Fig. 6.1	
PCT	783.5 K (A71 rod Pos.4 118.5s)	779.9 K (A11 rod Pos.2 18.3s)
Events	Time after break (s)	
Feedwater Stop	1.5 ∿ 4.0	1.2 ∿ 4.0
MSIV Closure	5.4 ∿ 9.2	7.4 ∿ 9.2
LPF Initiation	17.0	17.0
HPCS Actuation	-	31.5
FWLF Initiation	68.0	64.8
LPCS Actuation	71.0	65.6
LPCI Actuation	96.3	90.9
ADS Actuation	129.5	128.2
Quench of the Whole Core	188.0	127.3

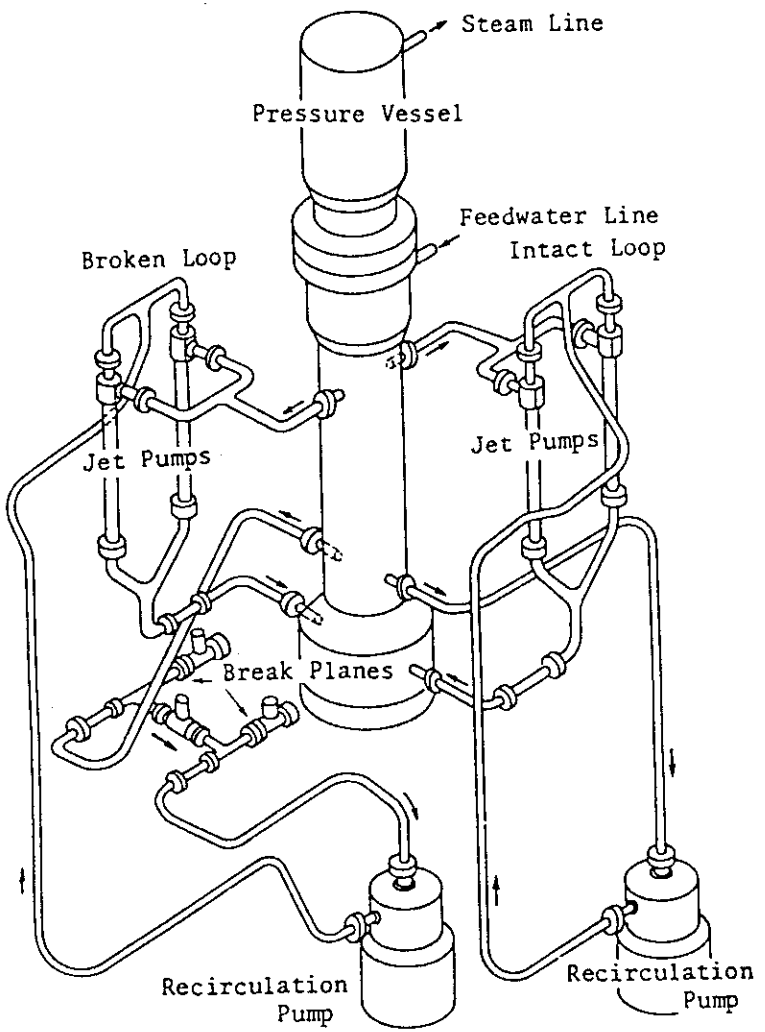

Fig. 2.1 Schematic Diagram of ROSA-III Test Facility

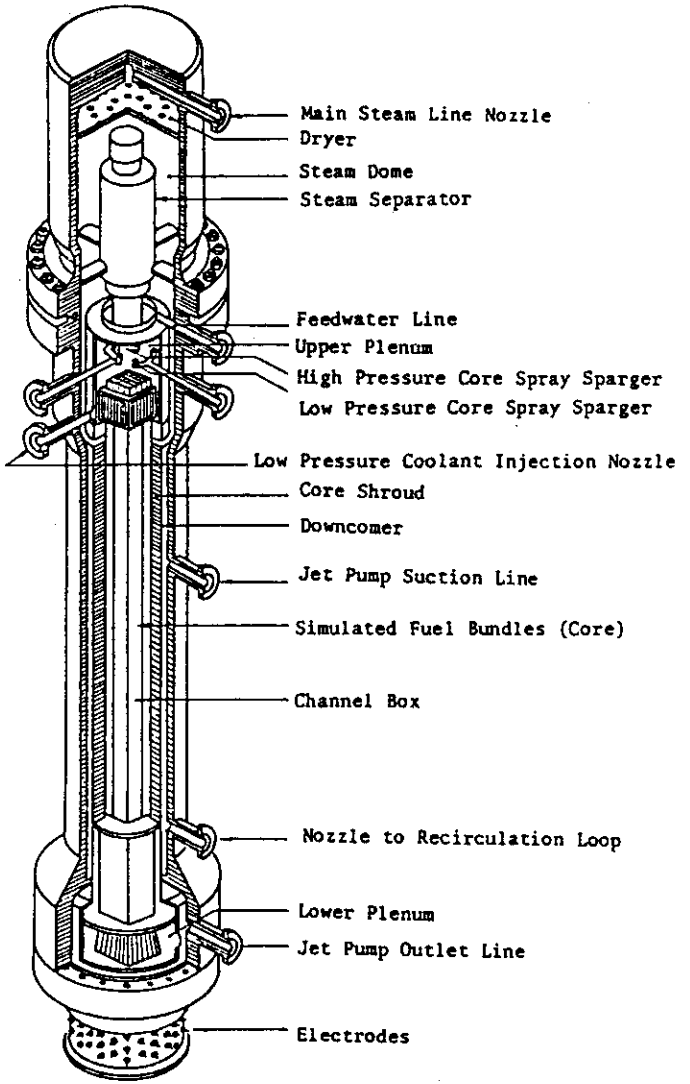

Fig. 2.2 Internal Structure of Pressure Vessel of ROSA-III

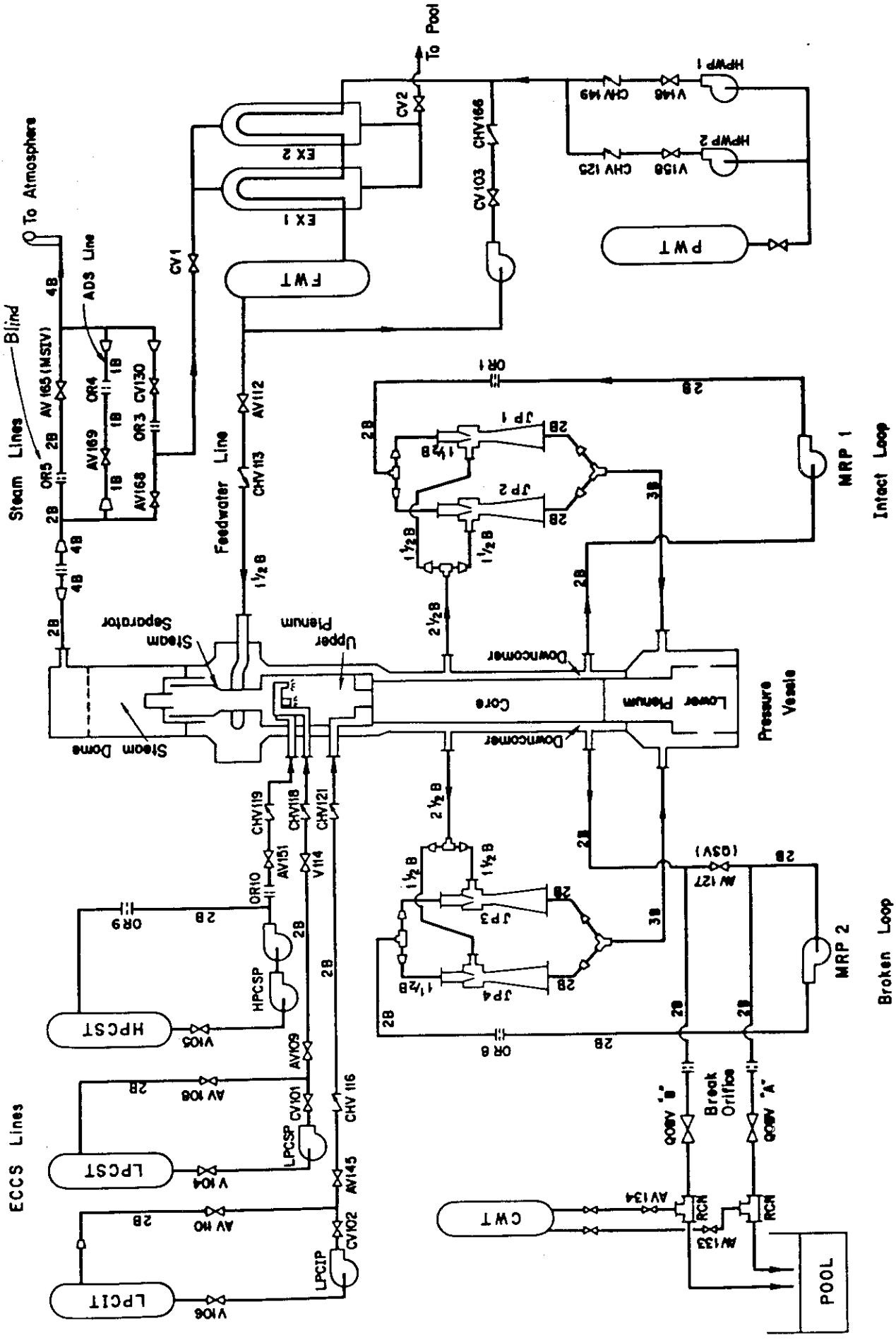

Fig. 2.3 ROSA-III Piping Schematics

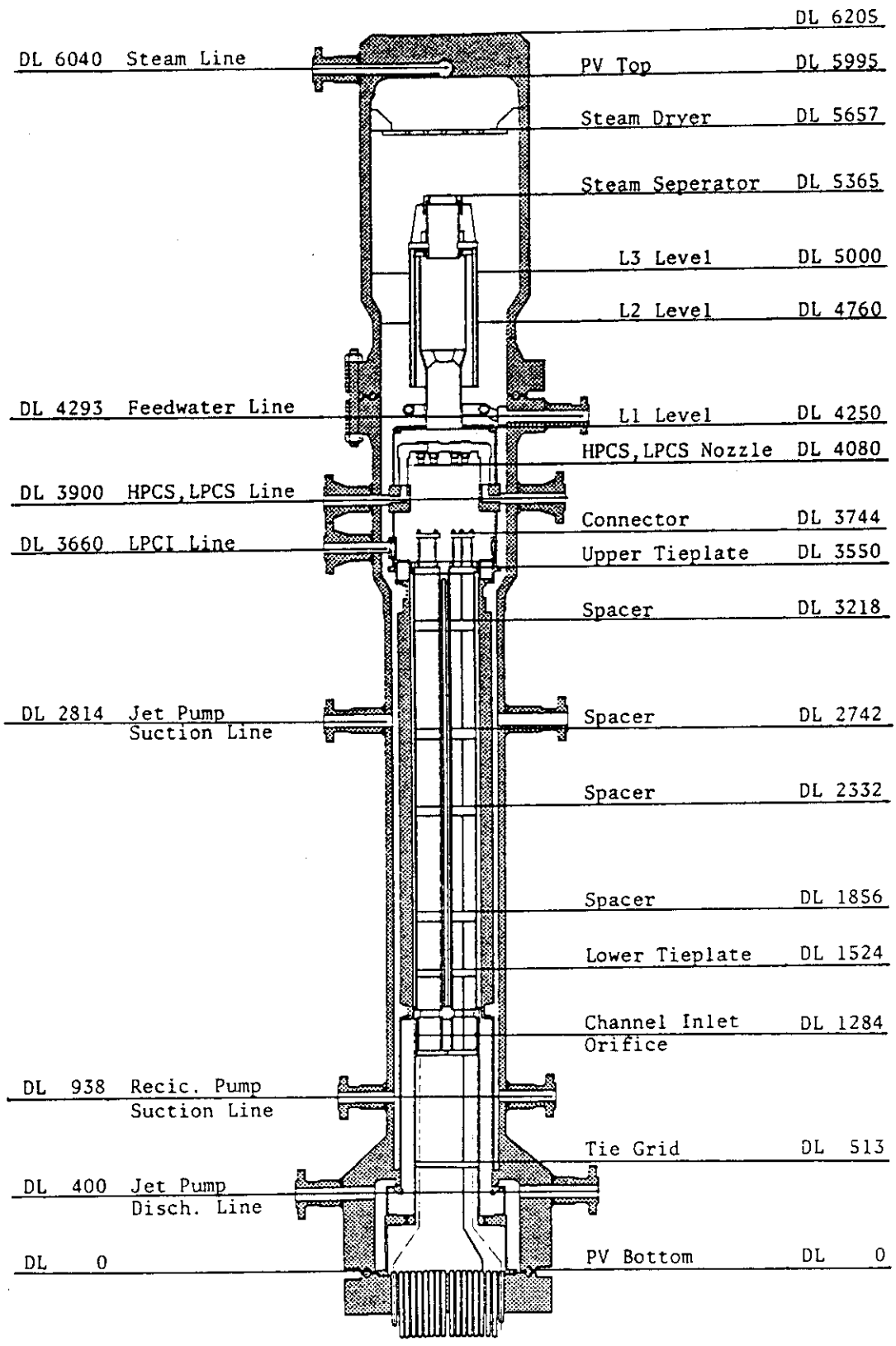

Fig. 2.4 Pressure Vessel Internals Arrangement

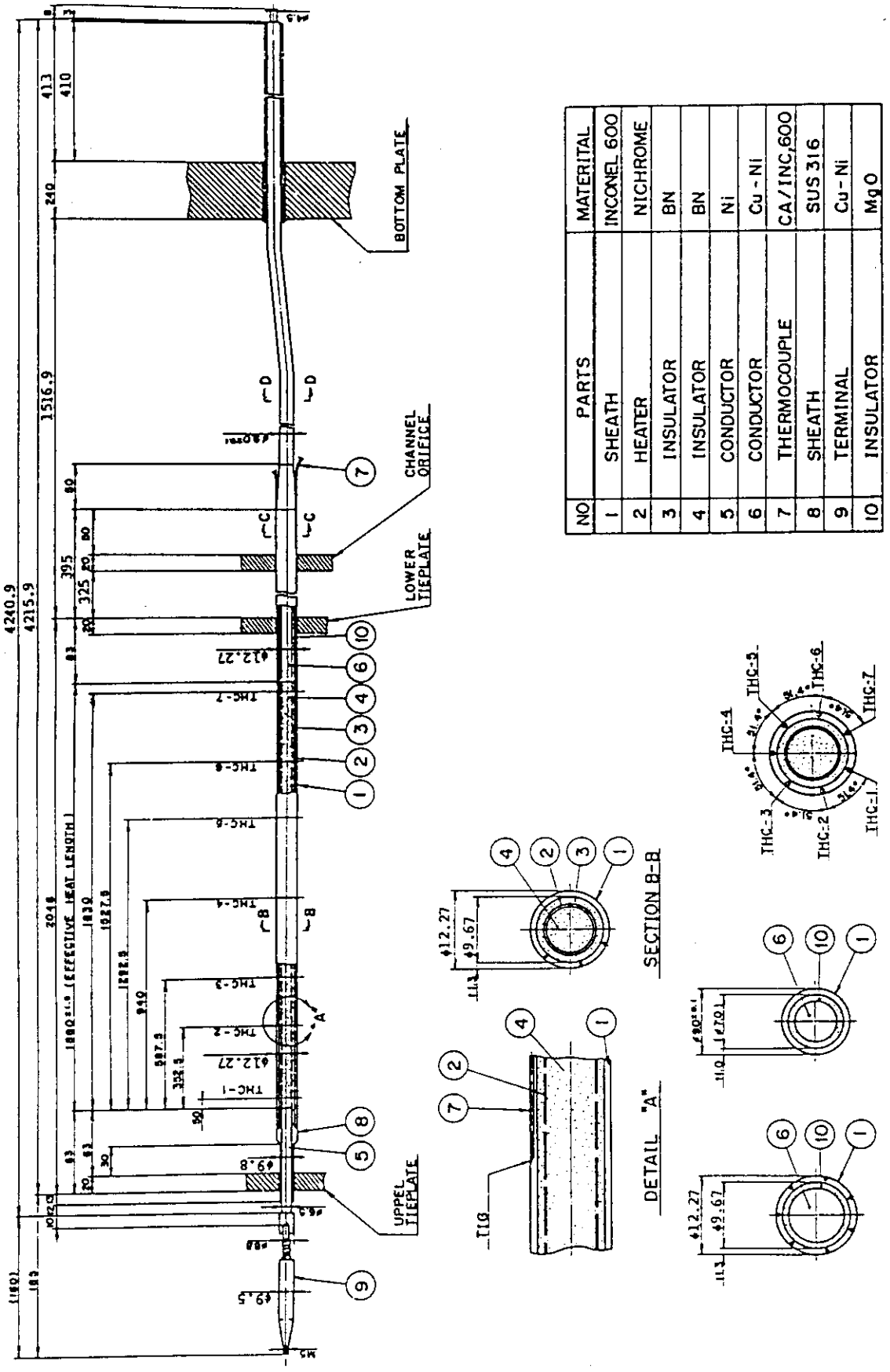

NO	PARTS	MATERITAL
1	SHEATH	INCONEL 600
2	HEATER	NICHROME
3	INSULATOR	BN
4	INSULATOR	BN
5	CONDUCTOR	Ni
6	CONDUCTOR	Cu－Ni
7	THERMOCOUPLE	CA/INC,600
8	SHEATH	SUS 316
9	TERMINAL	Cu－Ni
10	INSULATOR	MgO

Fig. 2.5 Simulated Fuel Rod of ROSA-III

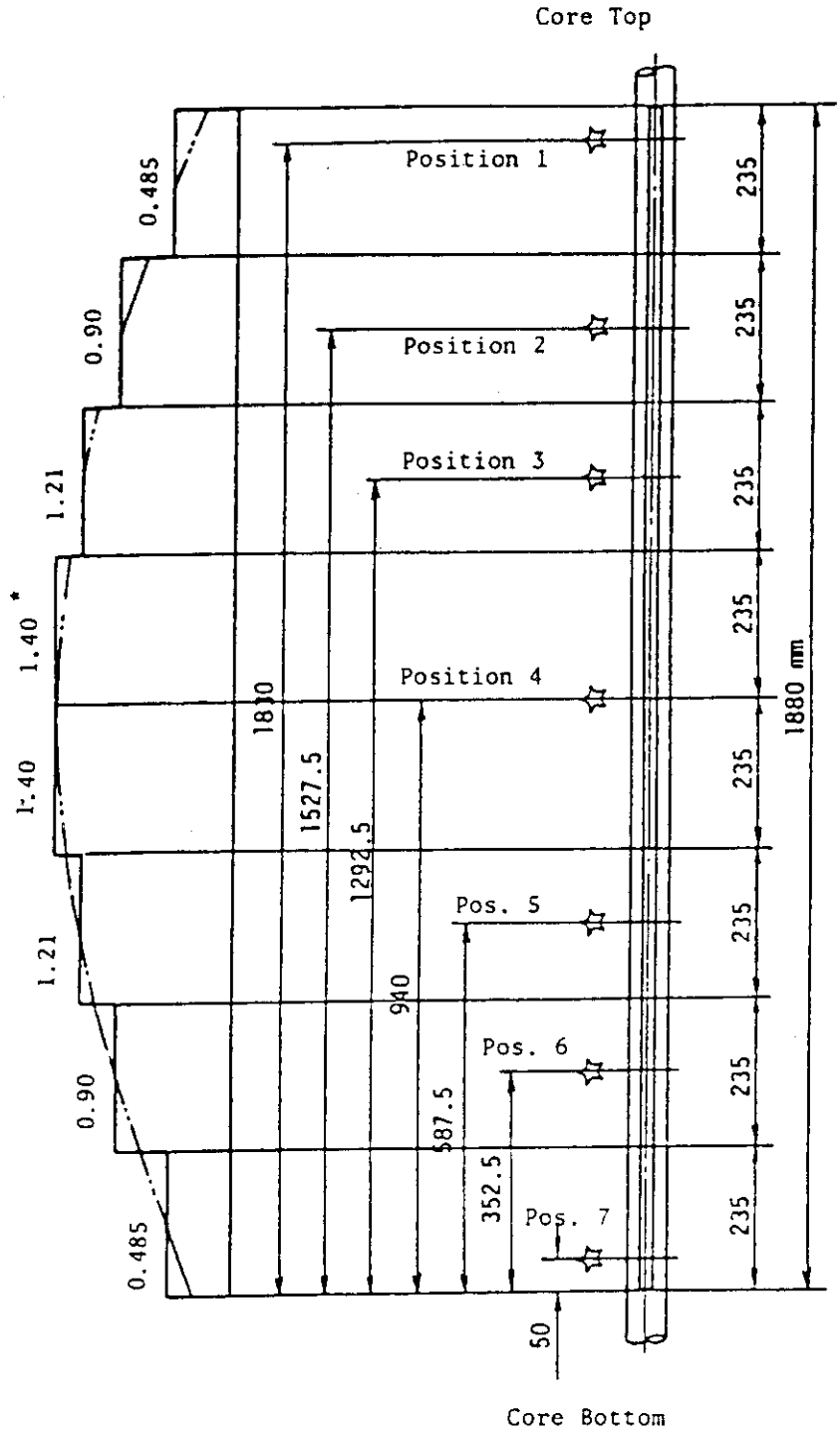

Fig.2.6 Axial Power Distribution of Heater Rod

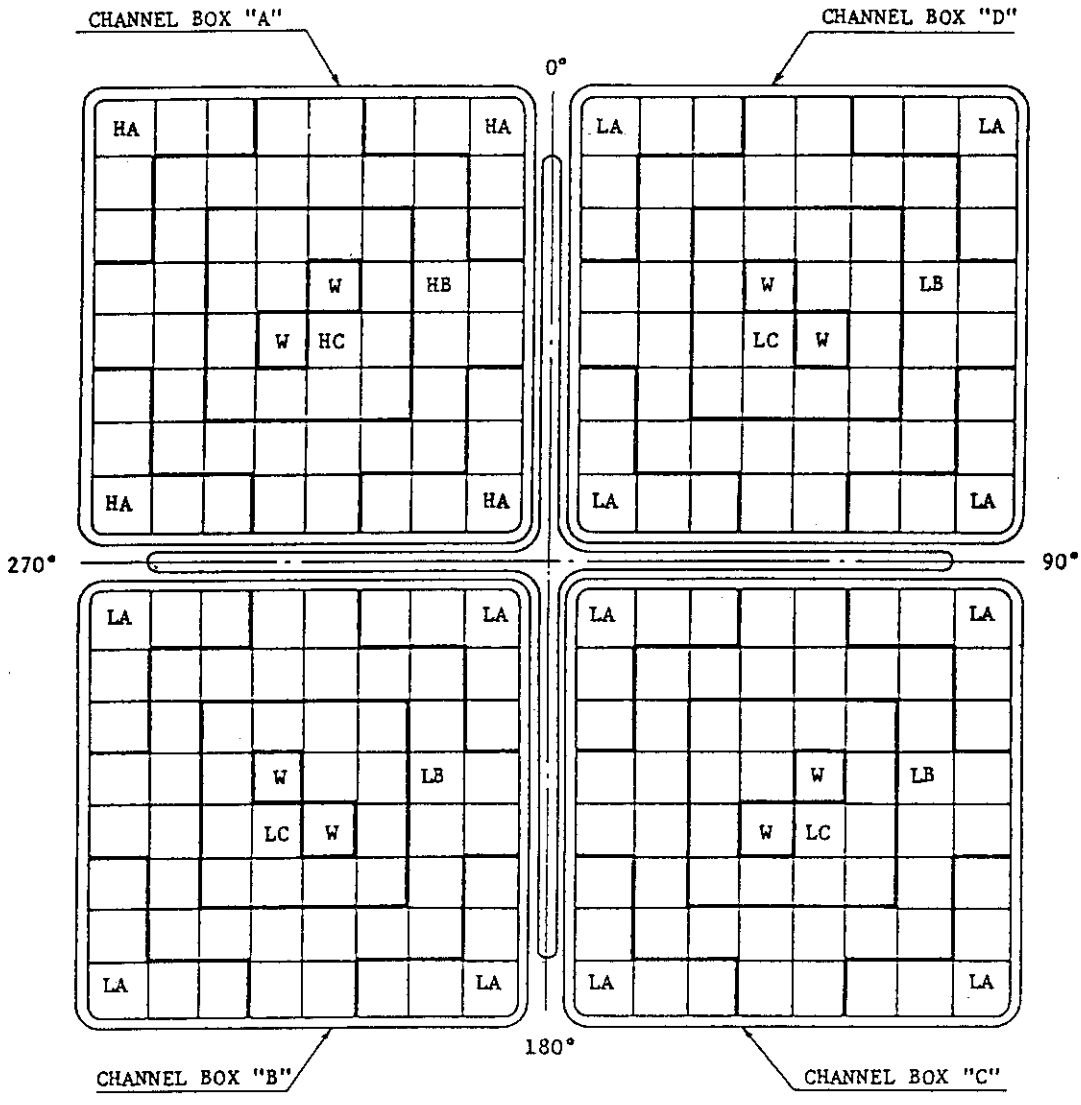

Region	HA	HB	HC	LA	LB	LC	W
Lenear Heat Rate (kW/m)	18.5	16.81	14.41	13.21	12.01	10.29	0.0
Local peaking factor	1.1	1.0	0.875	1.1	1.0	0.875	0.0
No. of Rods	20	28	14	60	84	42	8

* note : Radial peaking factor is 1.4

Fig. 2.7 Radial Power Distribution of Core

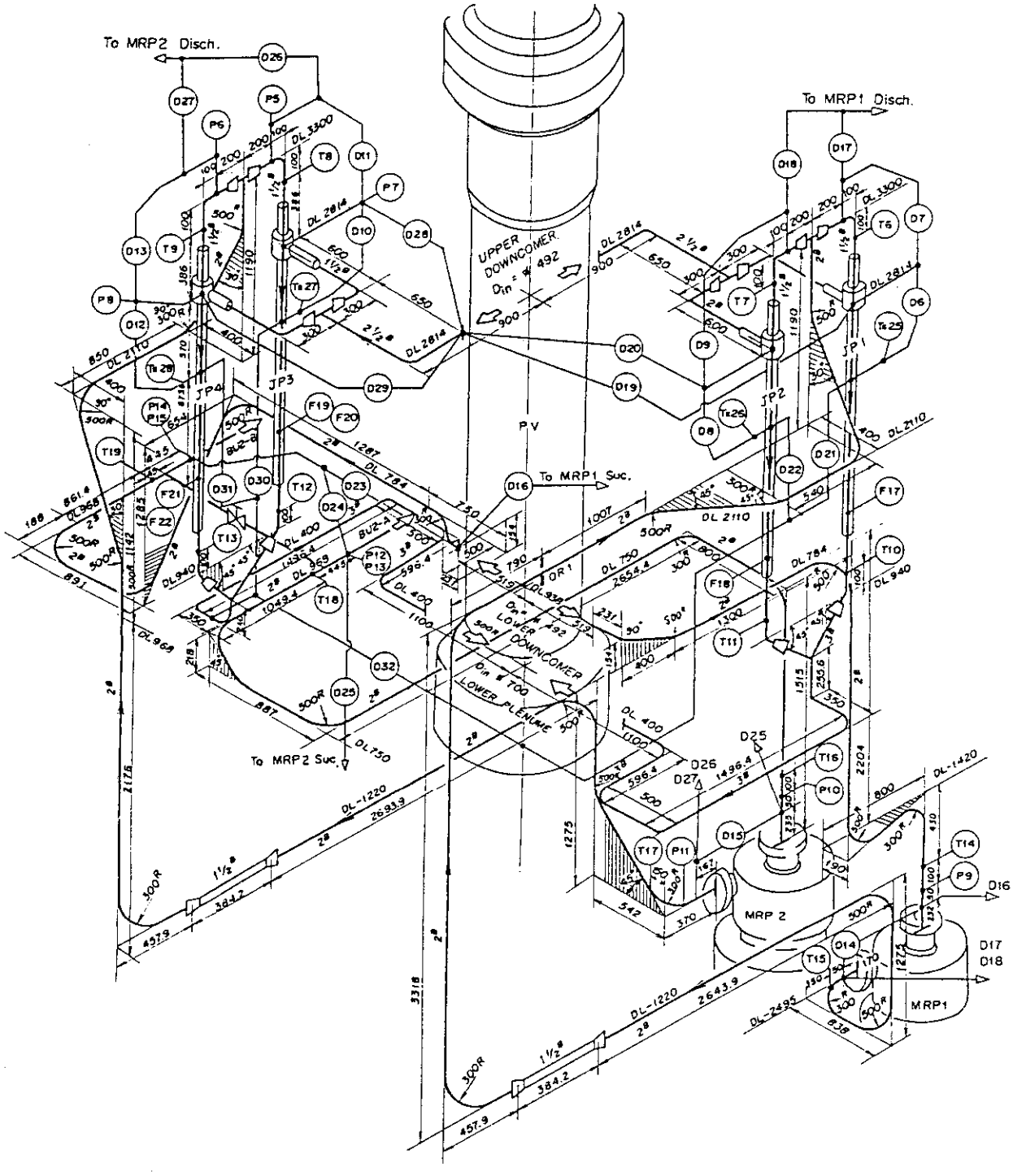

Fig. 2.8 Piping Layout of Recirculation Loops and Jet Pumps

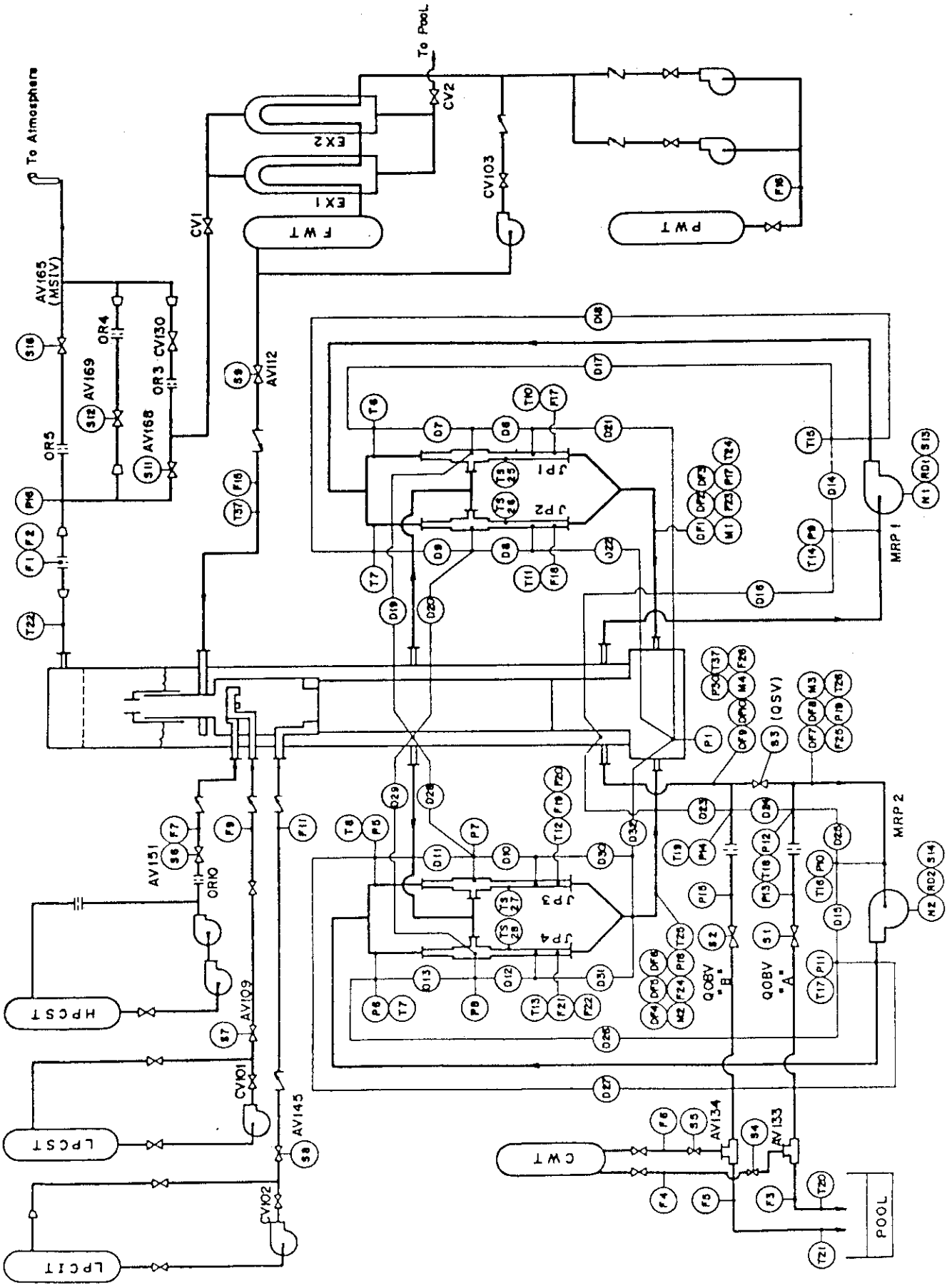

Fig. 3.1 Instrumentation Location of ROSA-III Test Facility

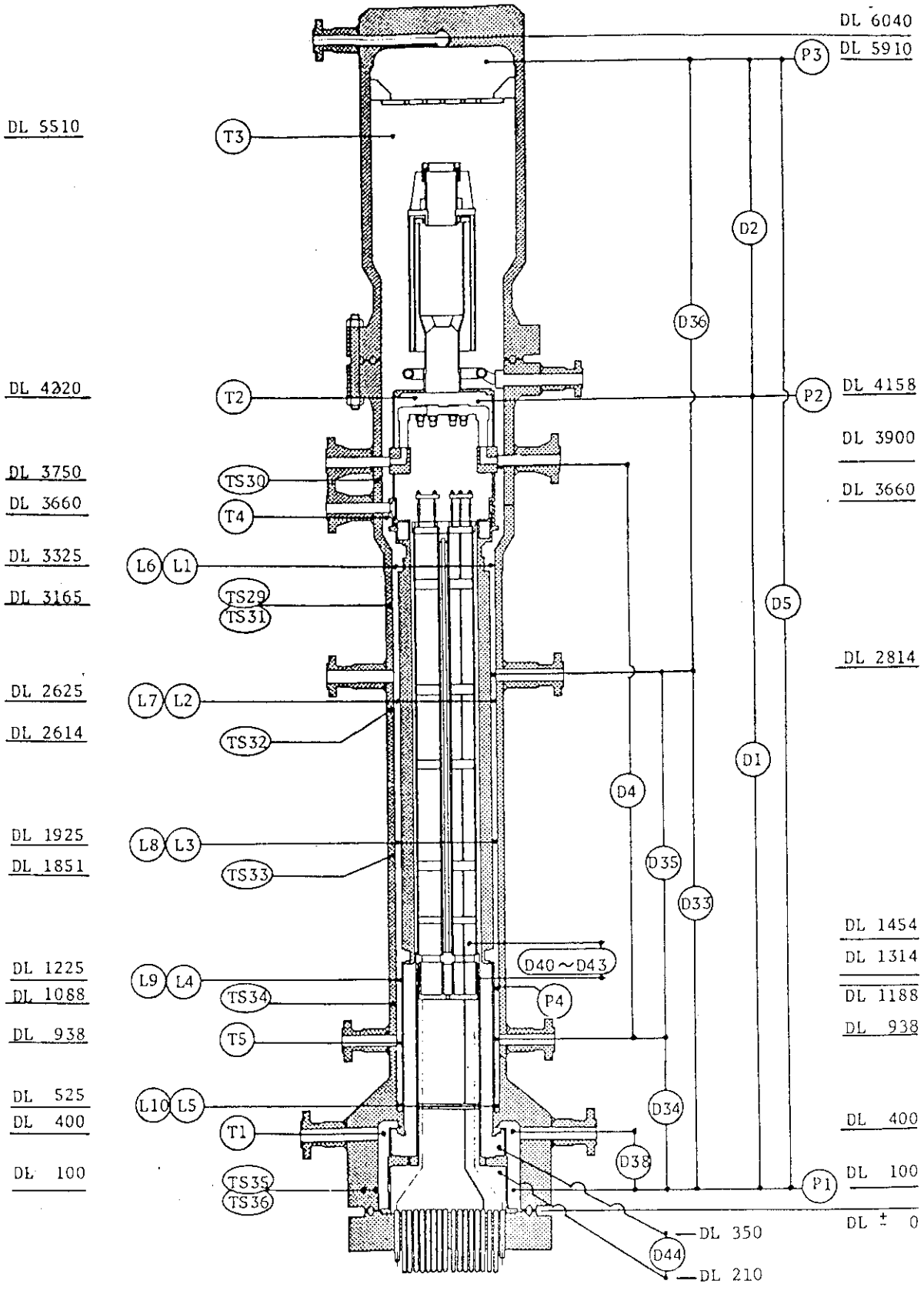

Fig. 3.2 Instrumentation Location in Pressure Vessel

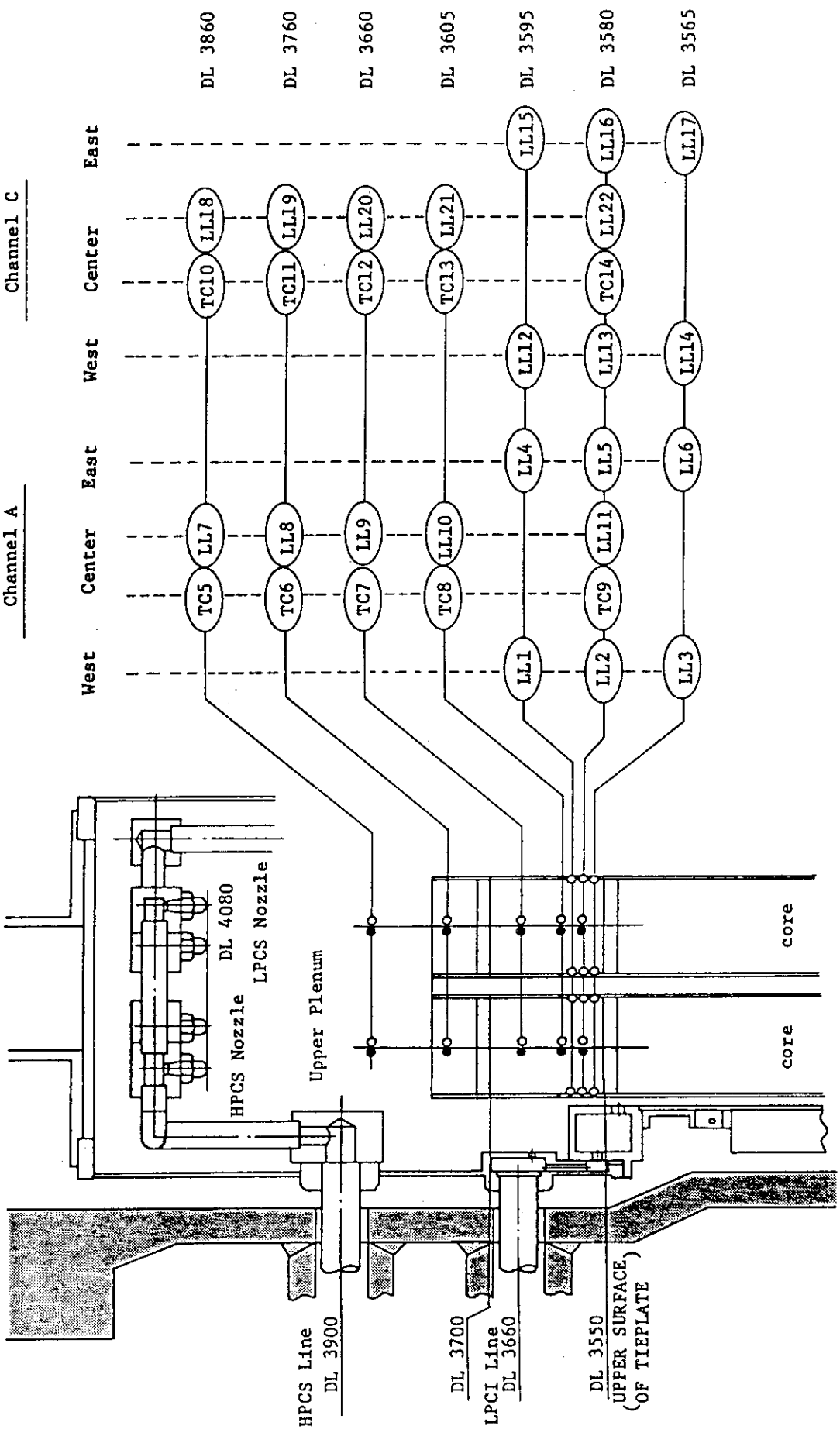

Fig. 3.3 Upper Plenum Instrumentations

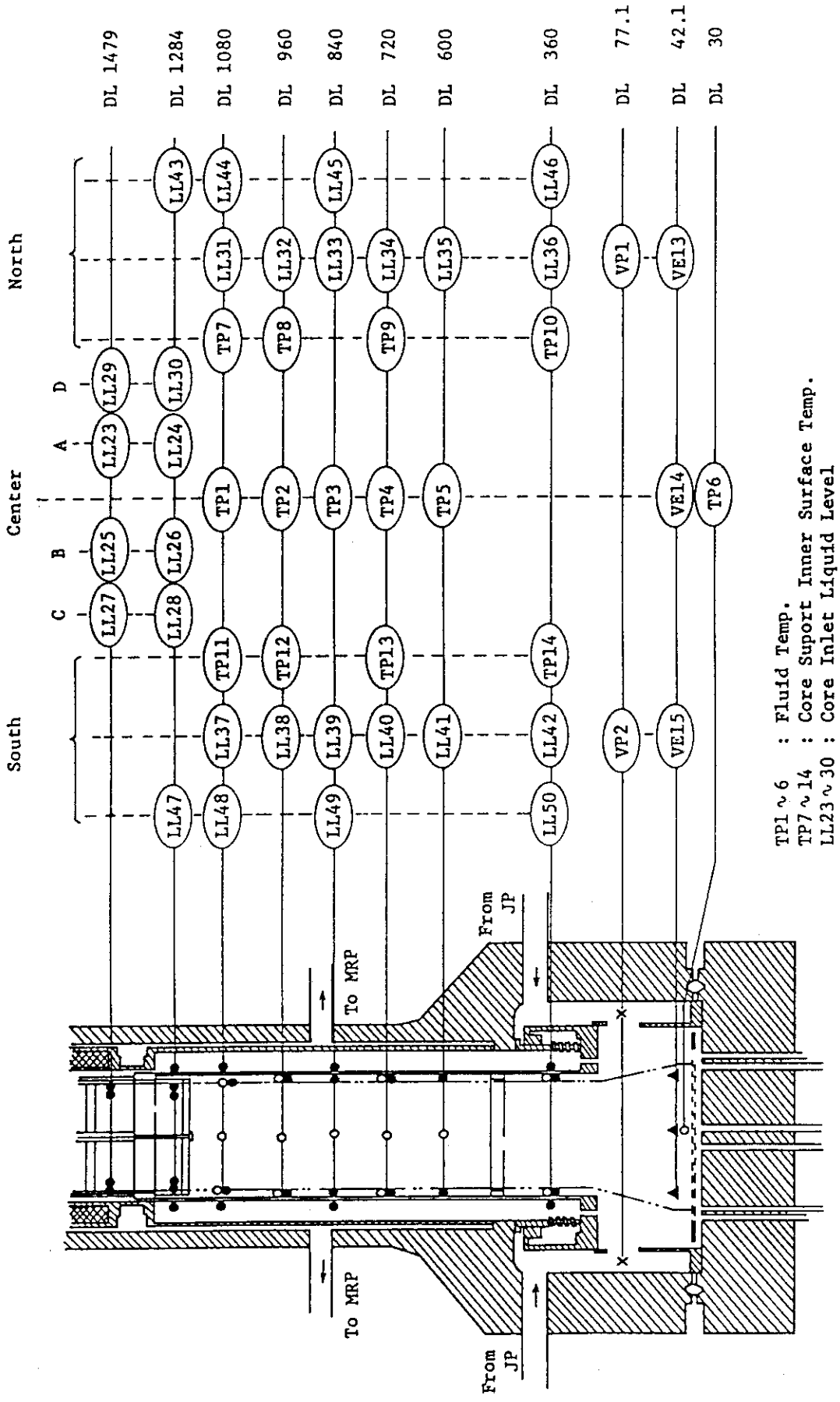

Fig. 3.4 Lower Plenum Instrumentations

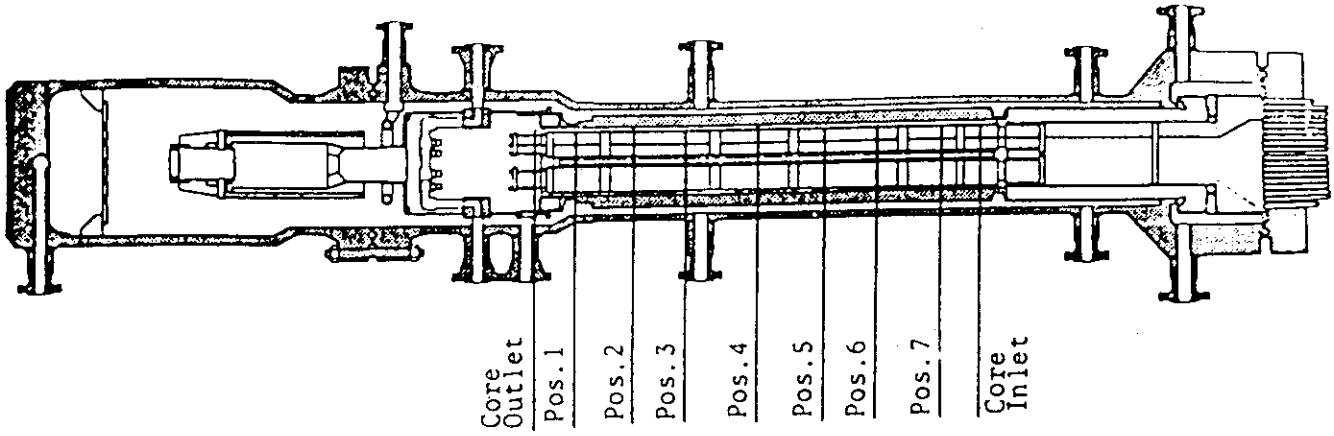

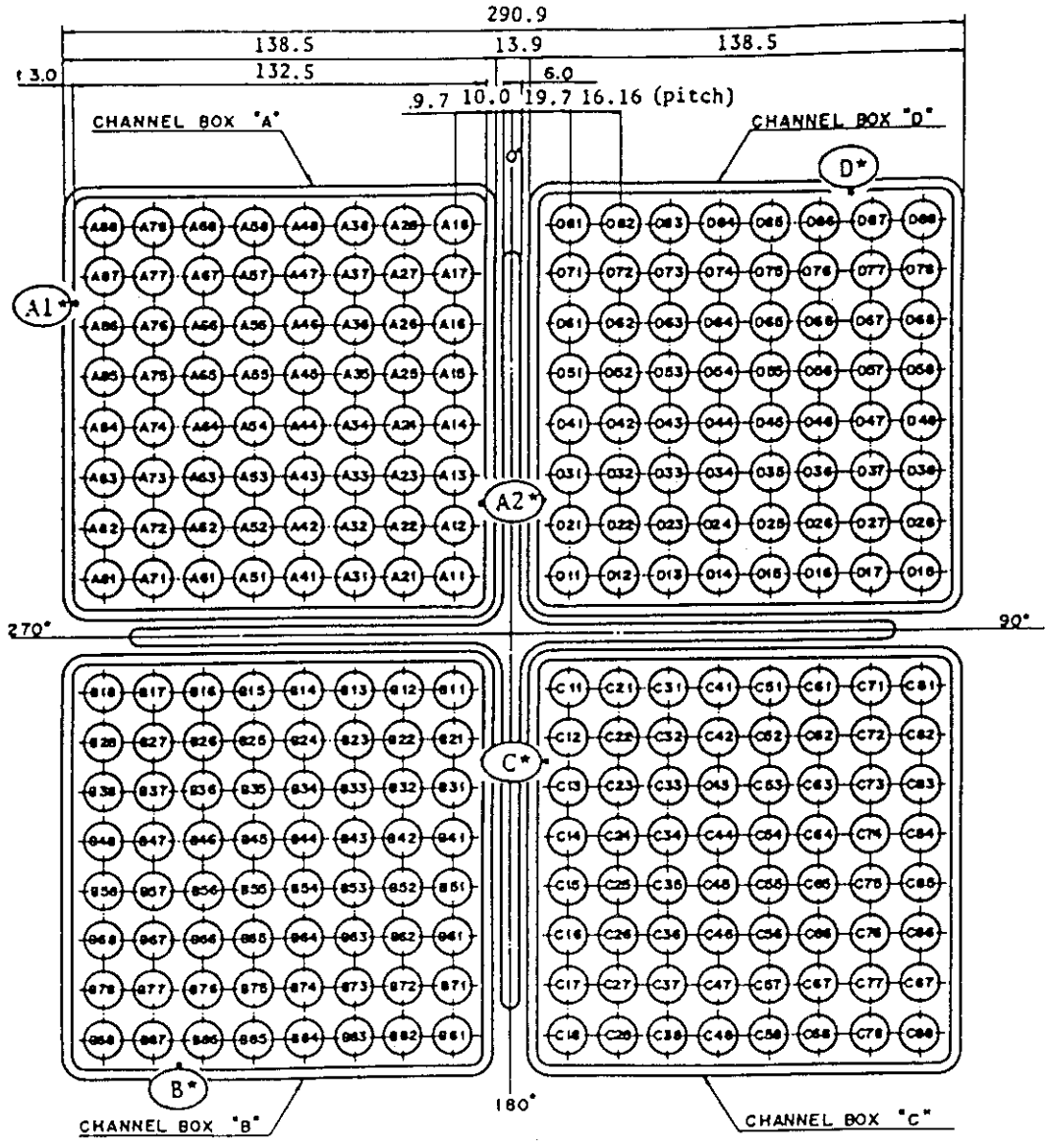

Heater rod O.D. is 12.27mm

A54,B54,C54 and D54 are water rod simulators with void probes, O.D.= 15.01mm

A45,B45,C45 and D45 are water rod simulators with thermocouples, O.D.= 15.01mm

Fig. 3.5 Core Instrumentation (cf. Table 3.3)

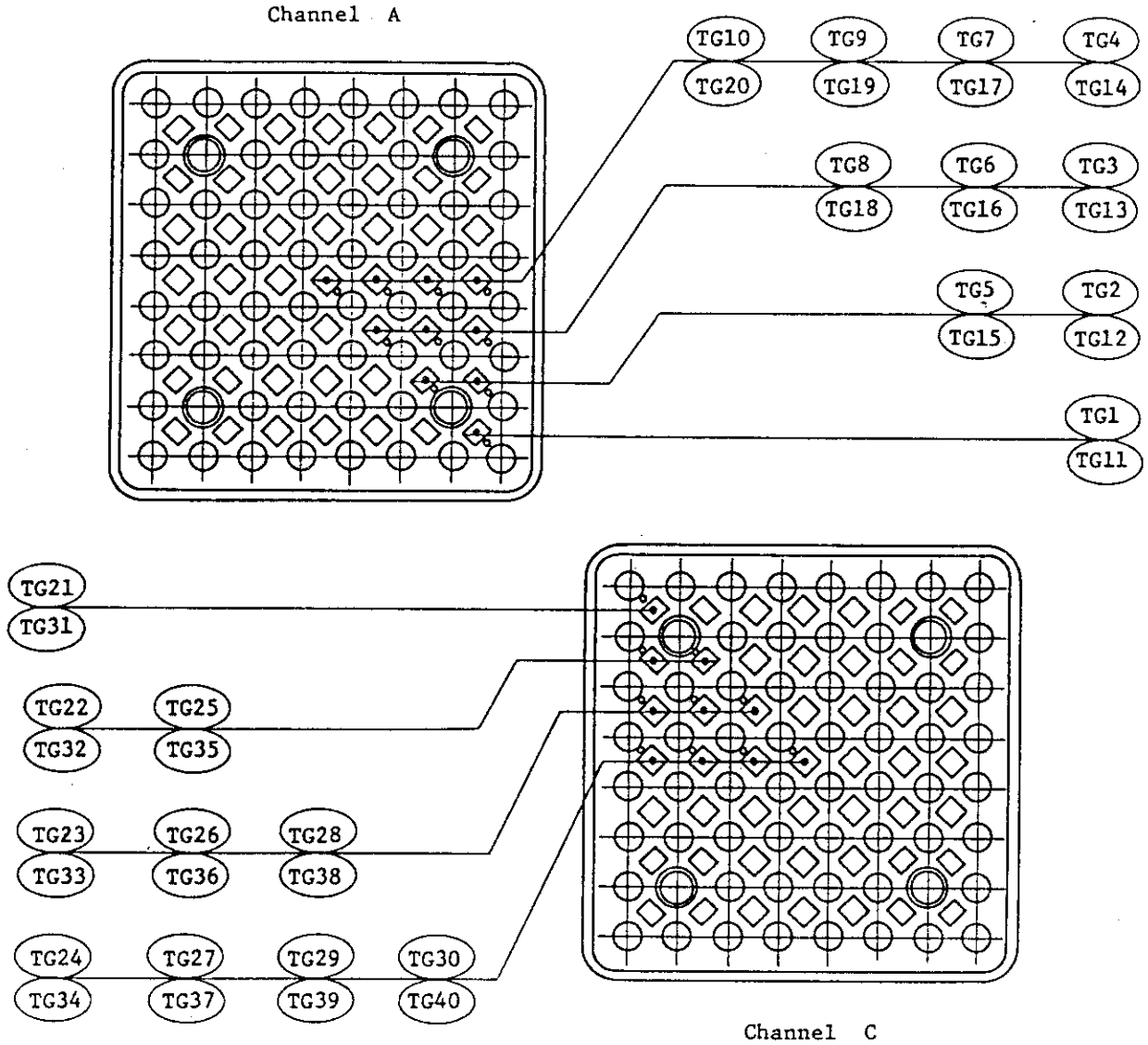

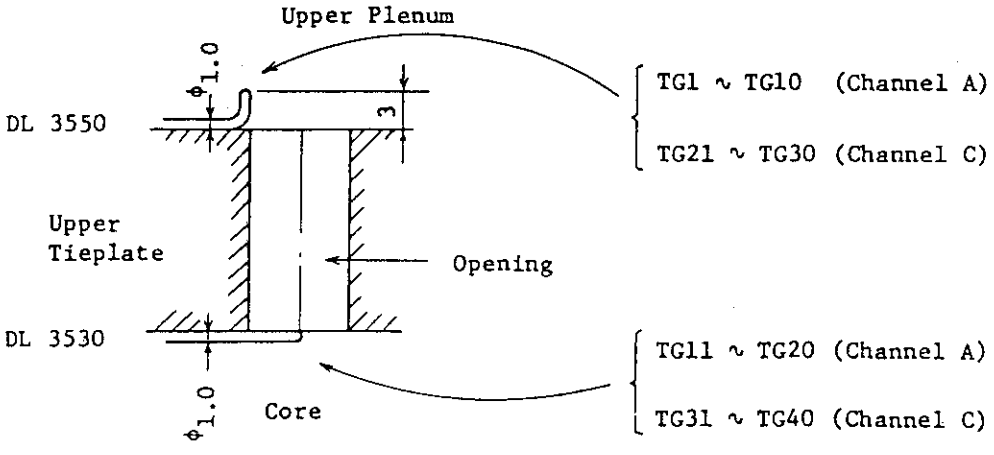

Fig. 3.6 Upper Tieplate Instrumentations

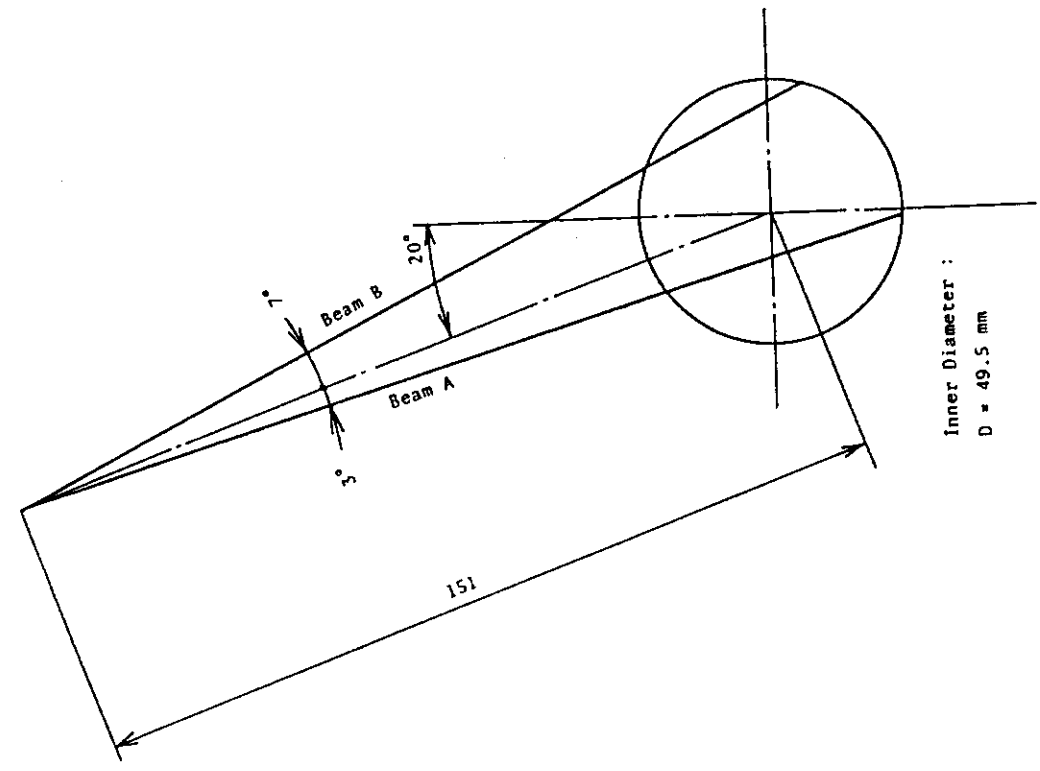

Fig. 3.8 Beam Configuration of Two-Beam Gamma Densitometer

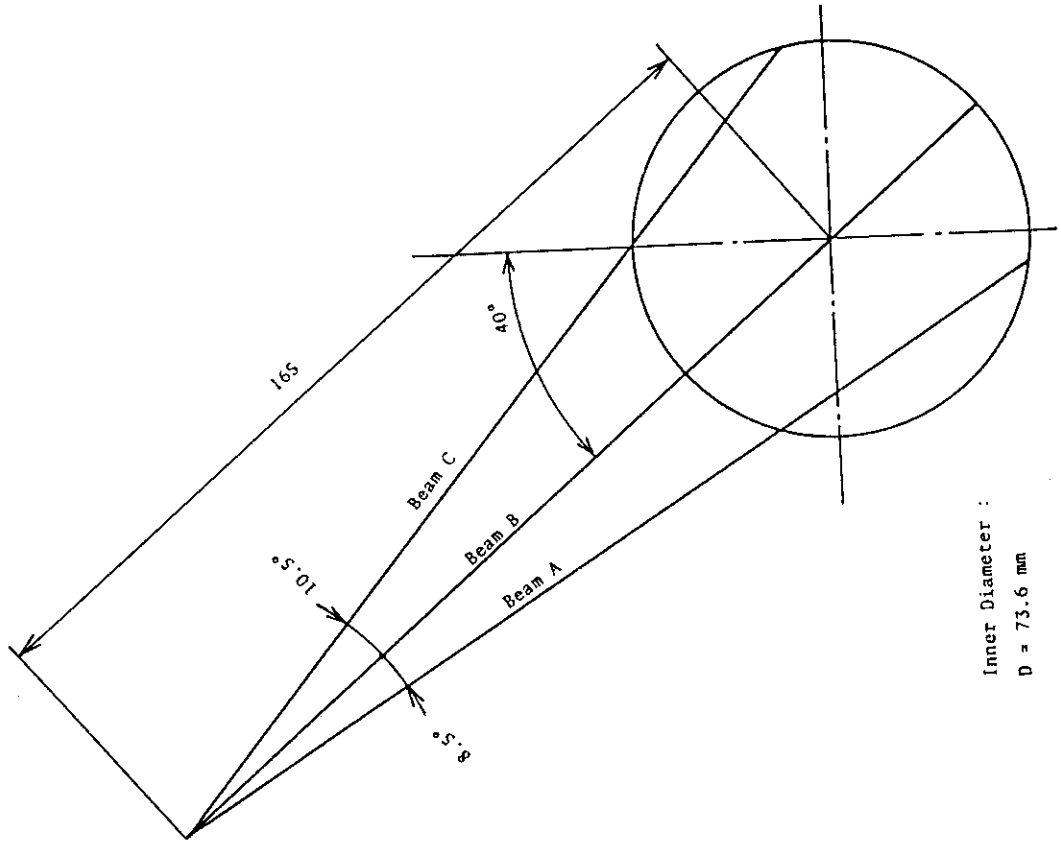

Fig. 3.7 Beam Configuration of Three-Beam Gamma Densitometer

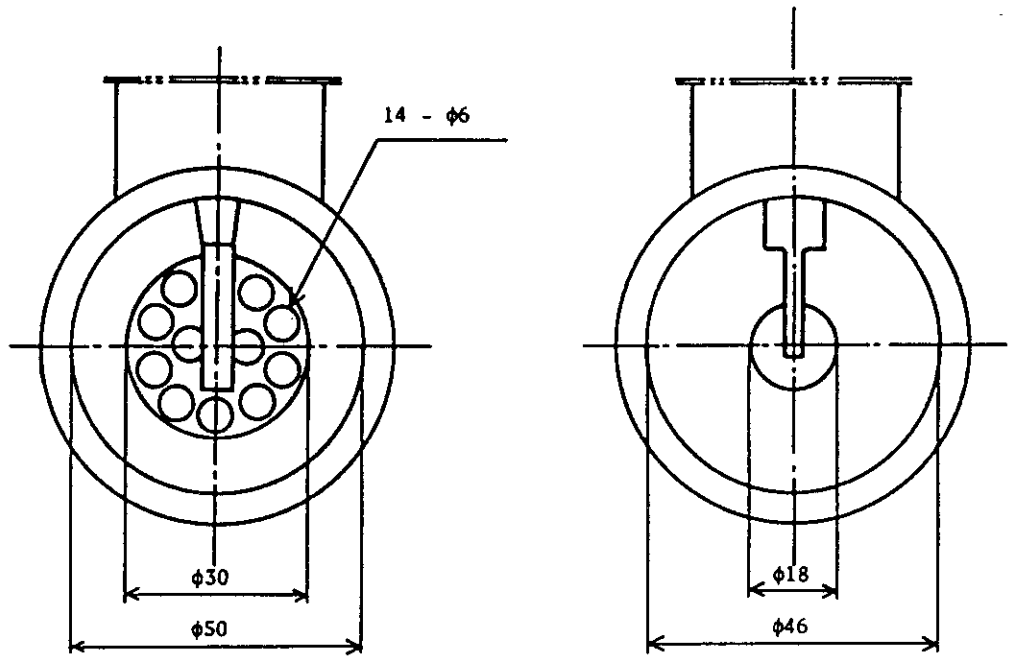

(a) High Range Drag Disc　　(b) Low Range Drag Disc

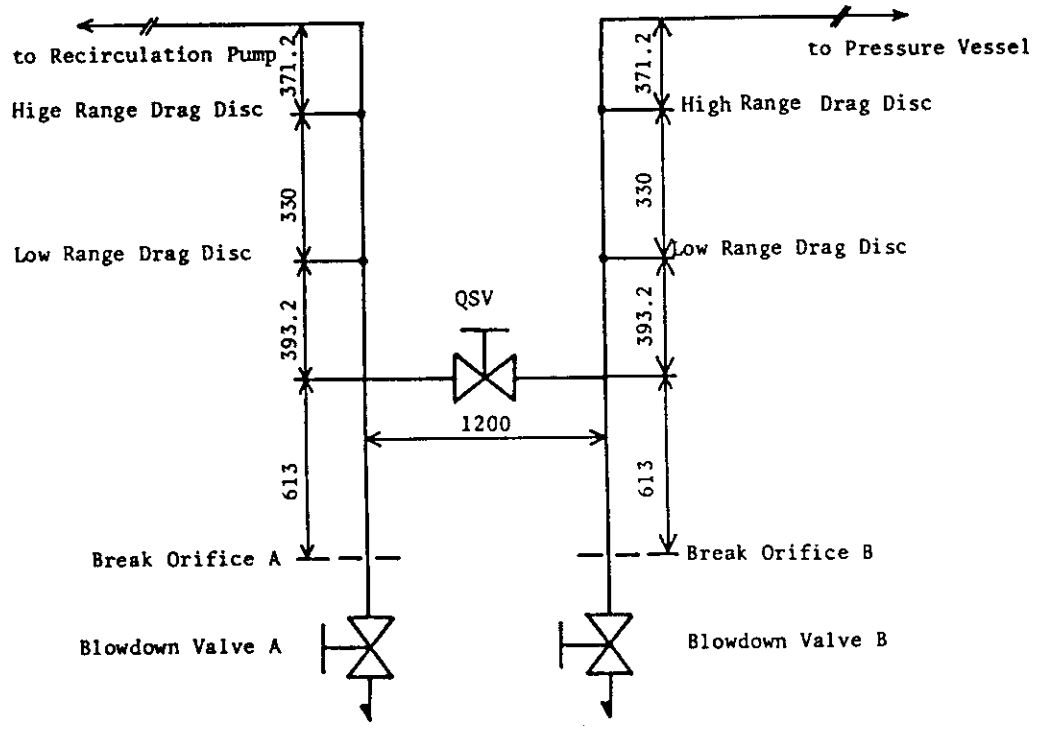

(c) Location of Drag Discs

Fig. 3.9　Configuration and Location of Drag Disks

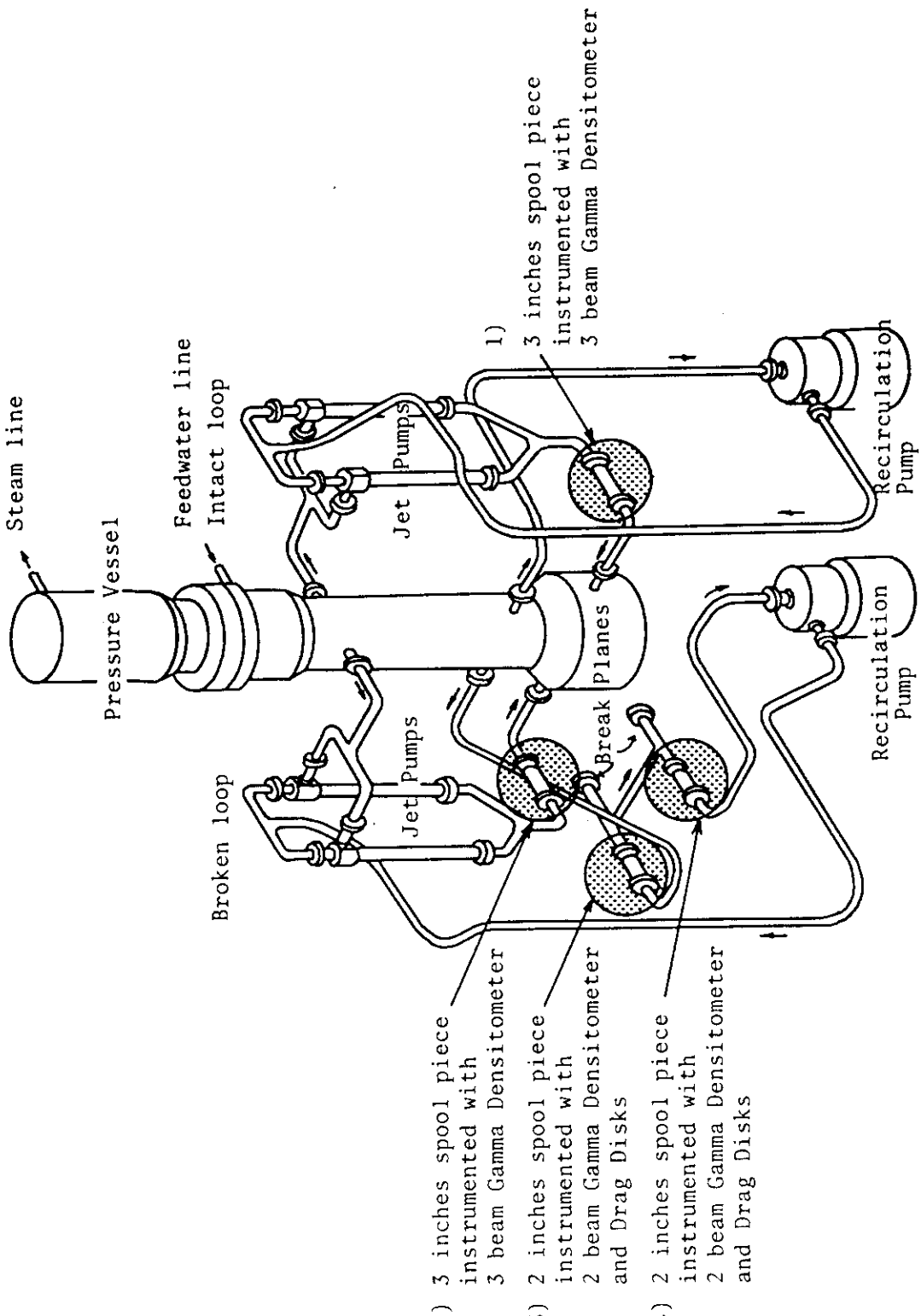

Fig. 3.10 Location of Two-Phase Flow Measurement Spool Pieces

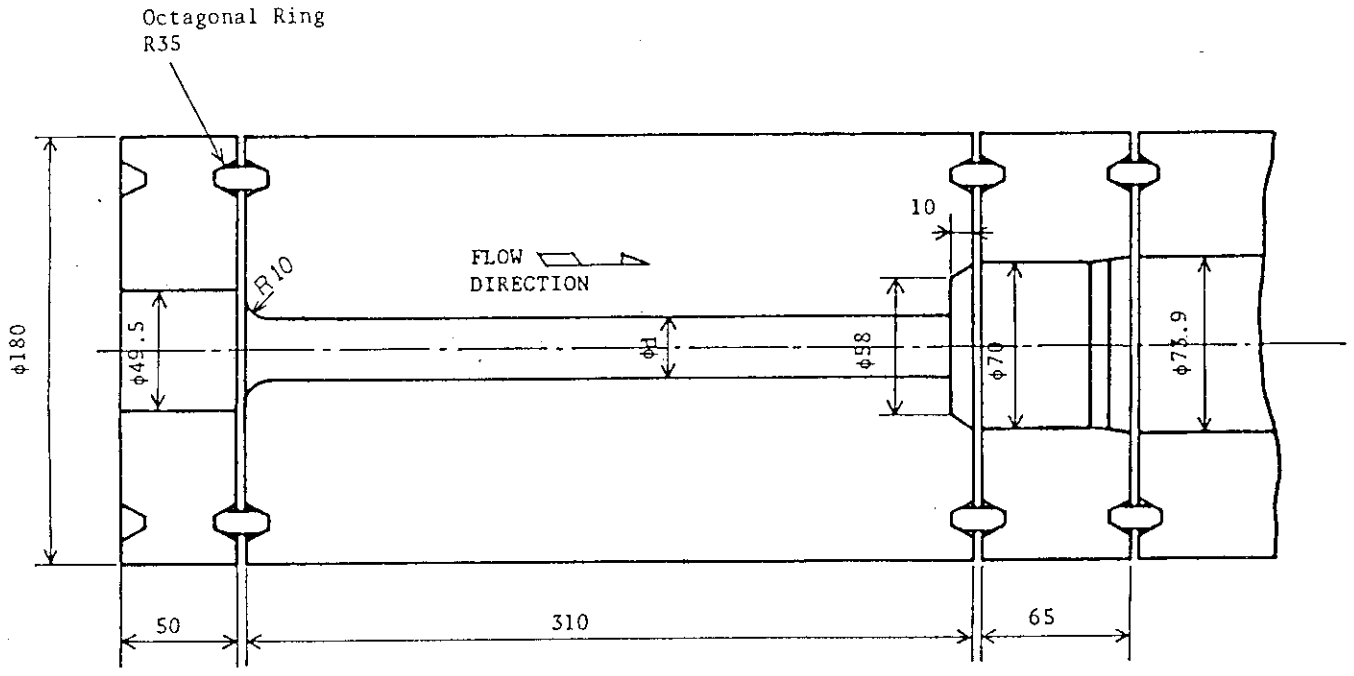

Material SUS304

Dimension in mm

Break area ratio (%)	d (mm)
100	26.2

Fig. 4.1 Break Nozzle Details

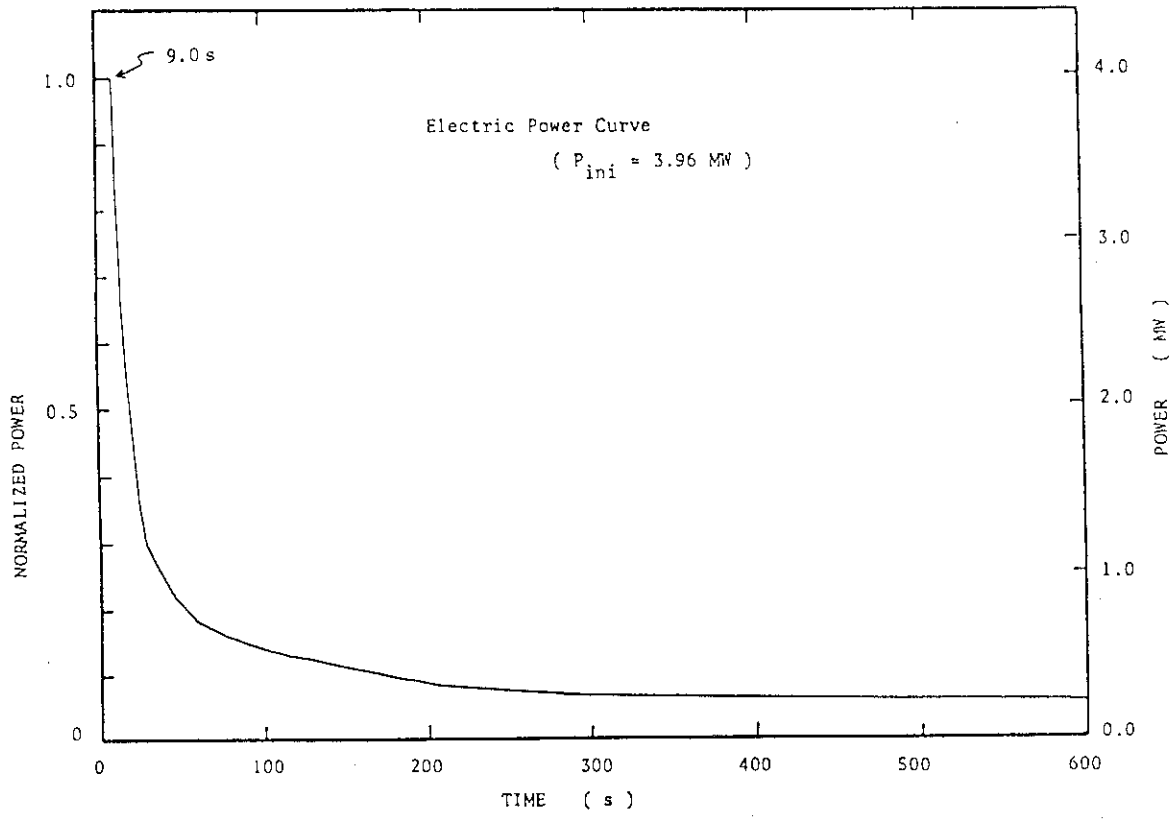

Fig. 4.2 Normalized Power Transient in ROSA-III

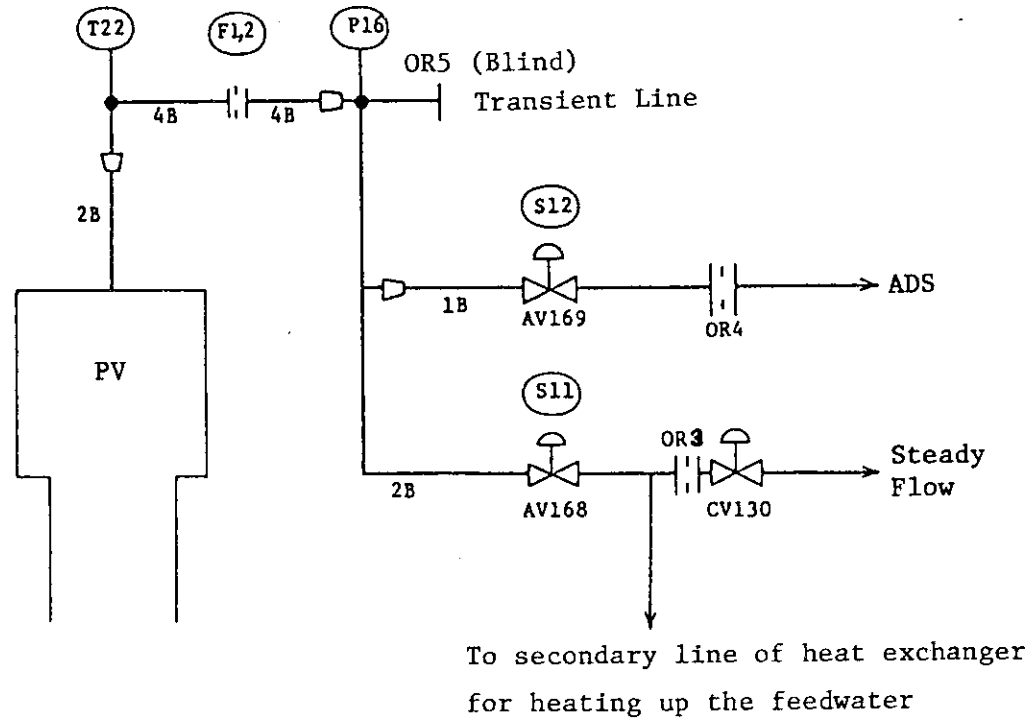

Fig. 4.3 Main Steam Line Schematic

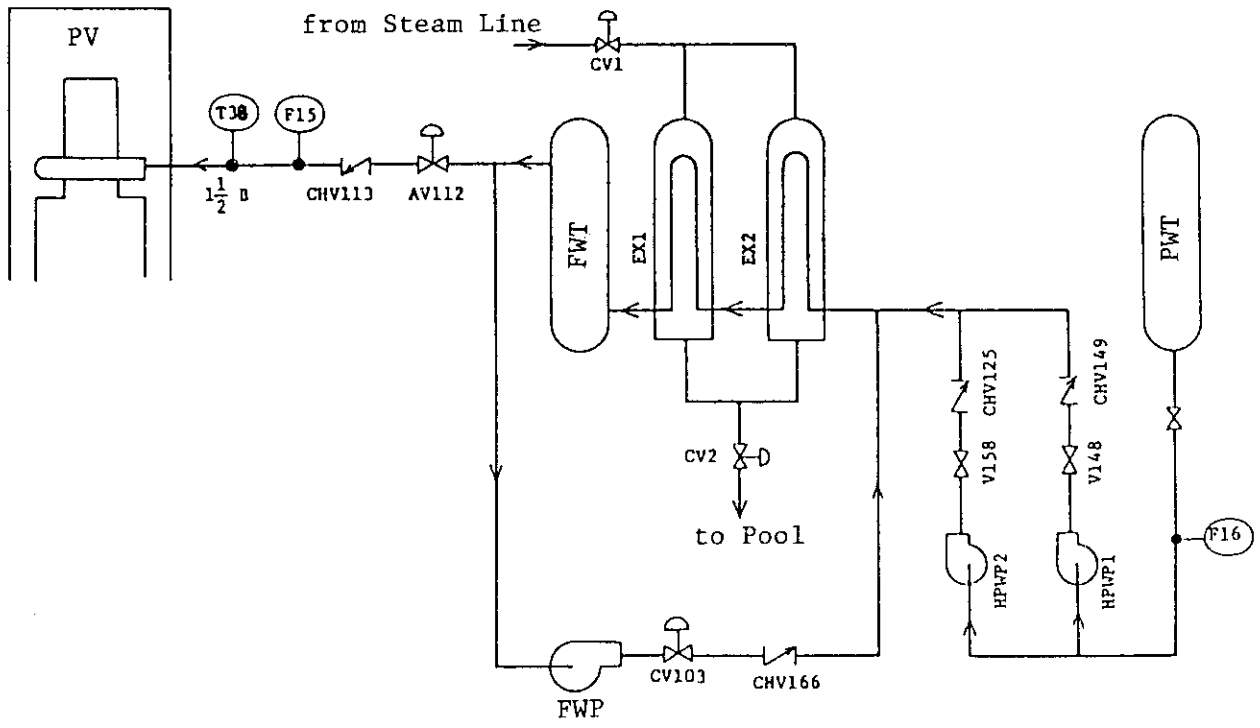

Fig. 4.4 Feedwater Line Schematic

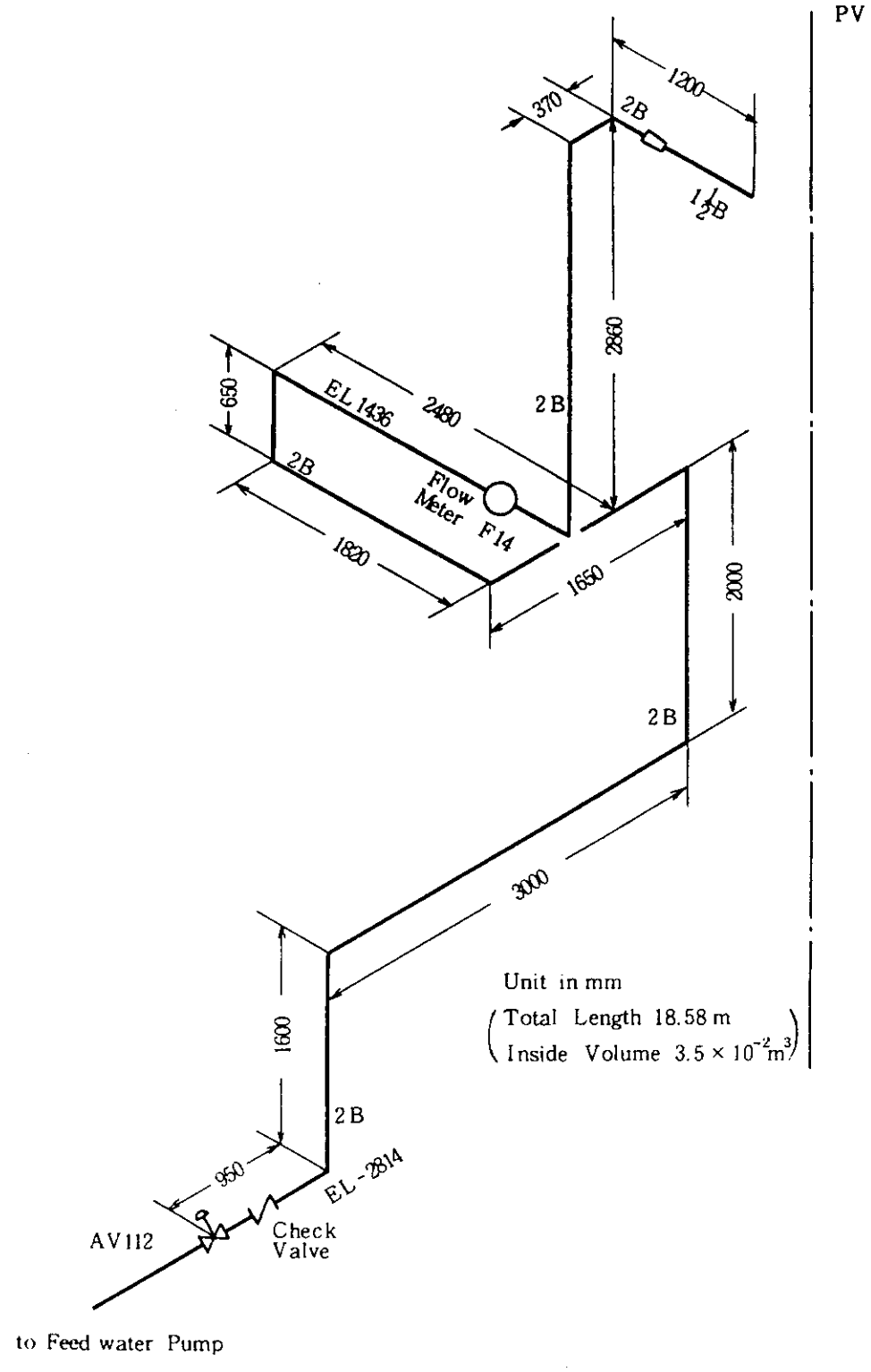

Fig. 4.5 Feedwater Line between AV112 and the Pressure Vessel

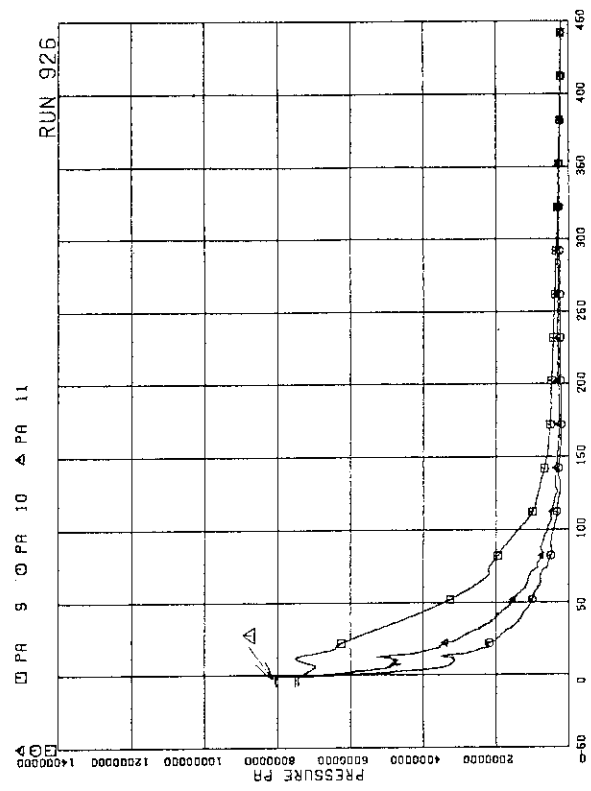

FIG.5. 3 PRESSURE NEAR MRP (MAIN RECIRCULATION PUMP)

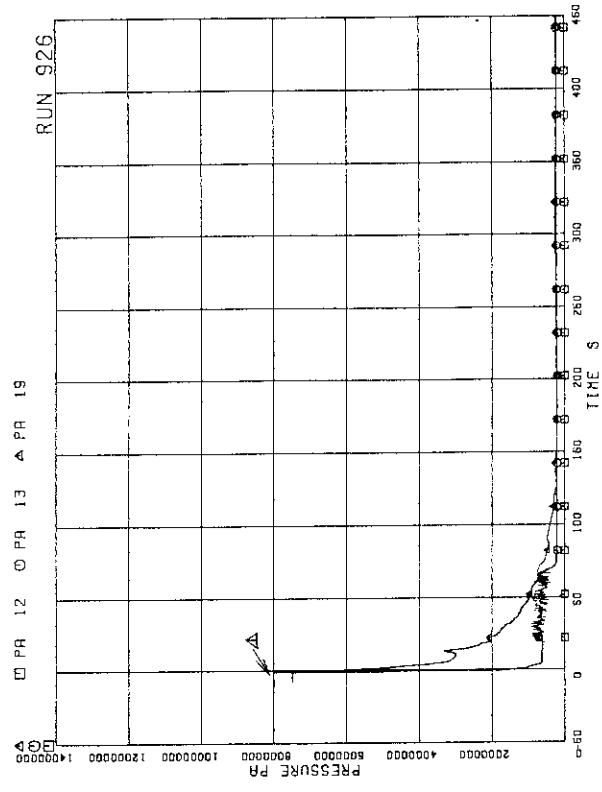

FIG.5. 4 PRESSURE AT MRP SIDE OF BREAK

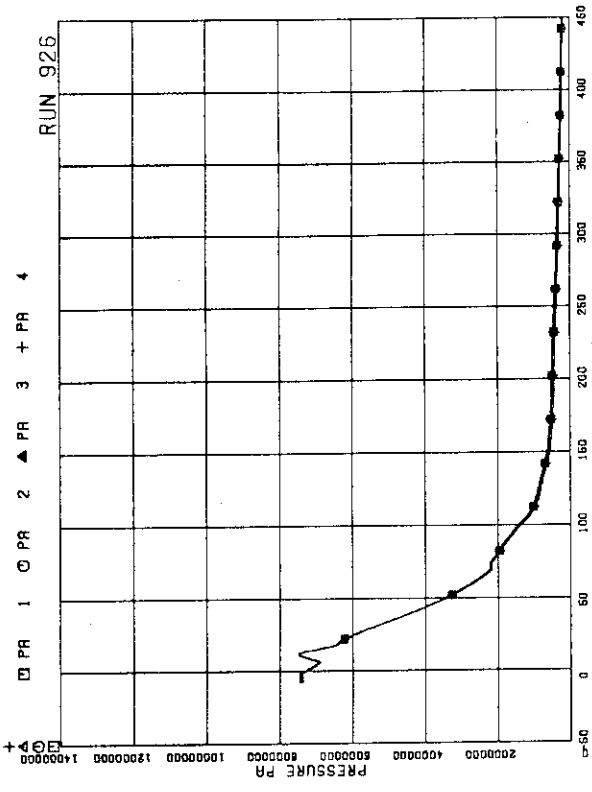

FIG.5. 1 PRESSURE IN PV (PRESSURE VESSEL)

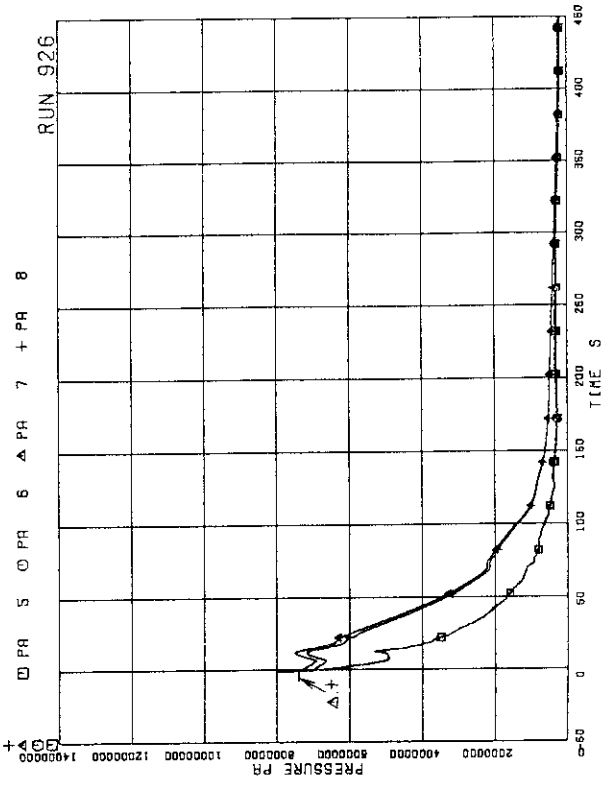

FIG.5. 2 PRESSURE IN BROKEN LOOP JP (JET PUMP)

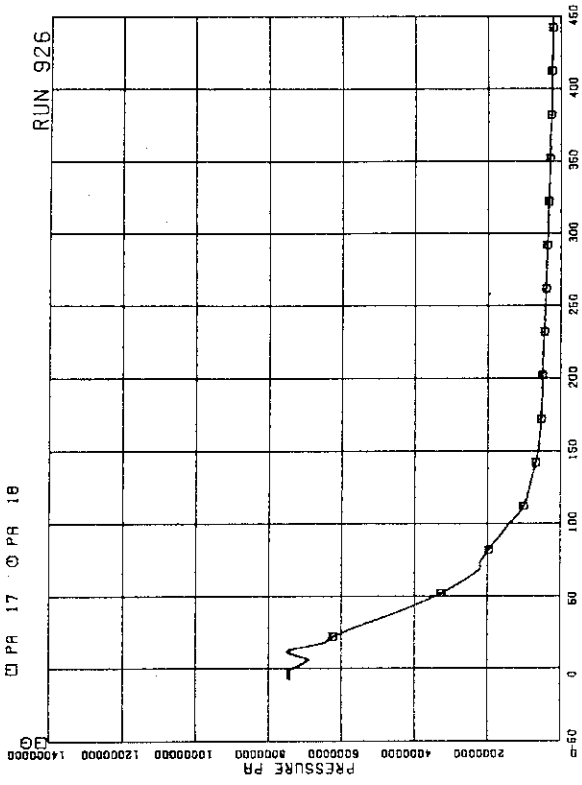

FIG.5. 7 PRESSURE IN JP OUTLET SPOOL

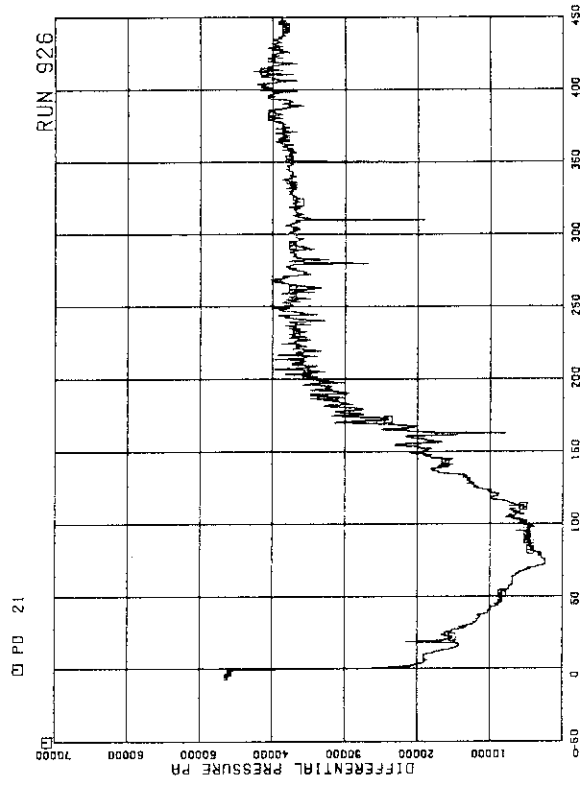

FIG.5. 8 DIFFERENTIAL PRESSURE BETWEEN LOWER PLENUM AND UPPER PLENUM

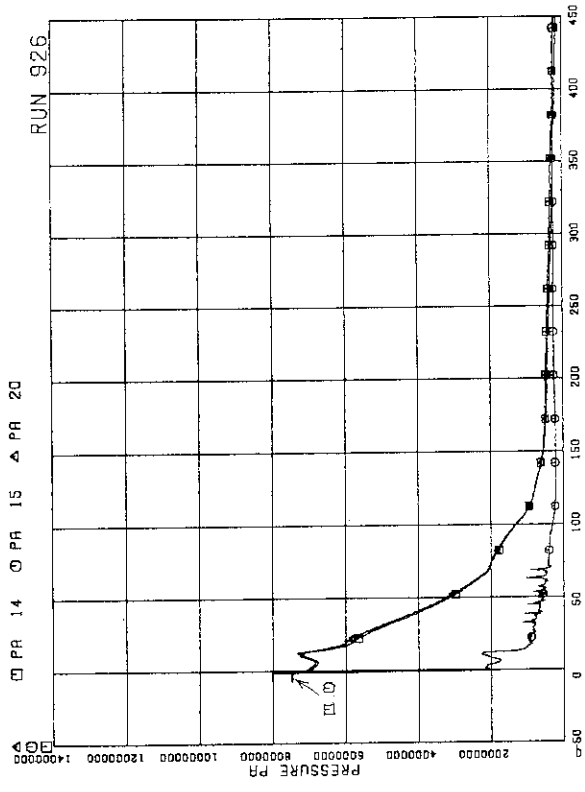

FIG.5. 5 PRESSURE AT PV SIDE OF BREAK

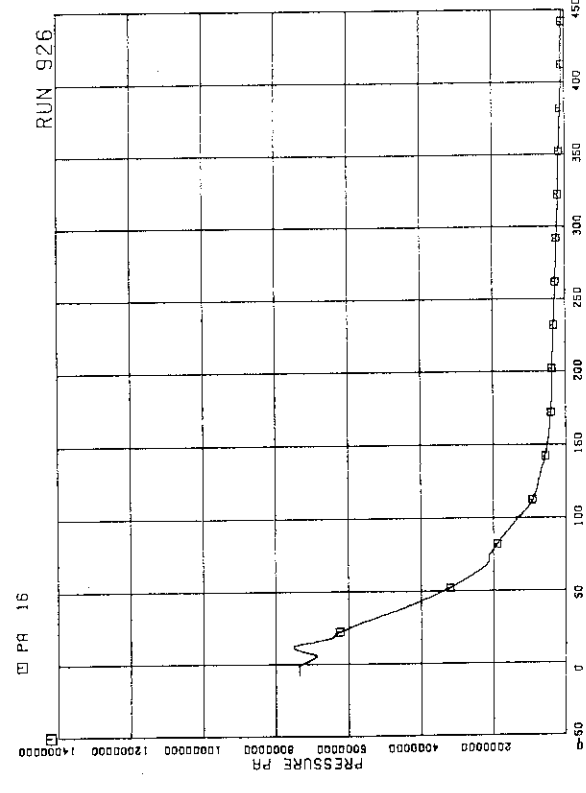

FIG.5. 6 PRESSURE IN MSL (MAIN STEAM LINE)

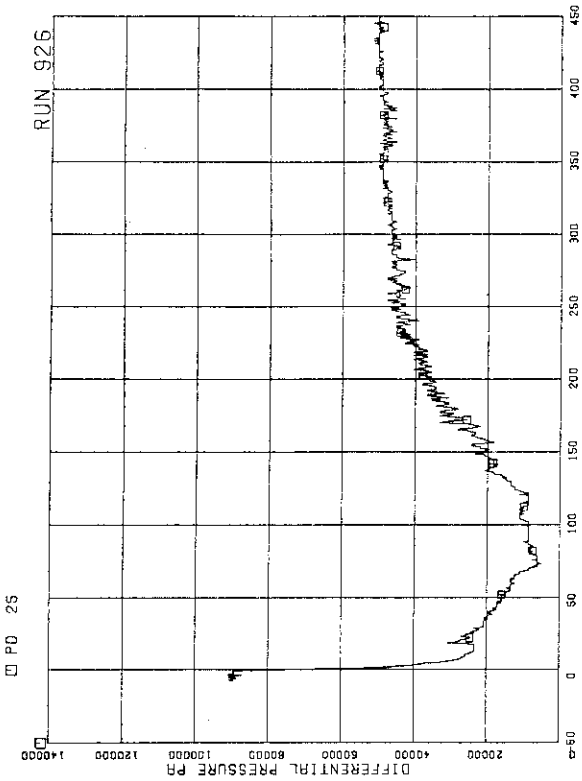

FIG.S. 11 DIFFERENTIAL PRESSURE BETWEEN Pv BOTTOM AND TOP

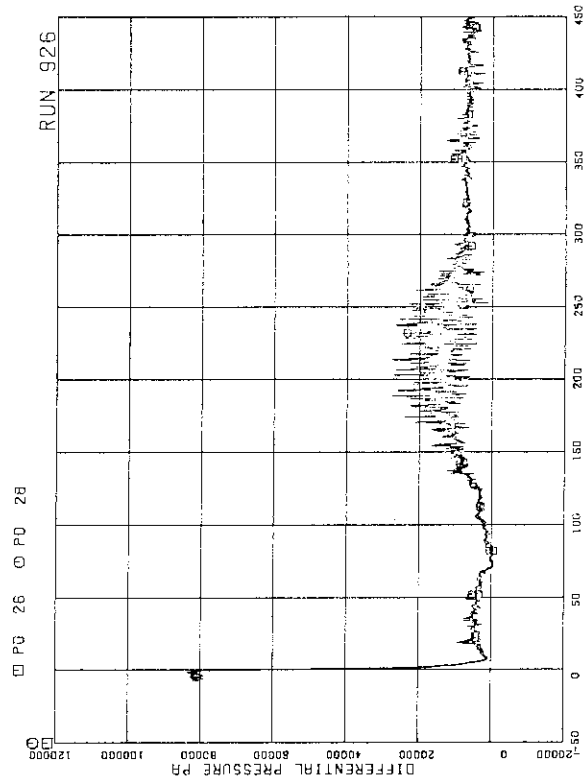

FIG.S. 12 DIFFERENTIAL PRESSURE BETWEEN JP-1.2 DISCHARGE AND SUCTION

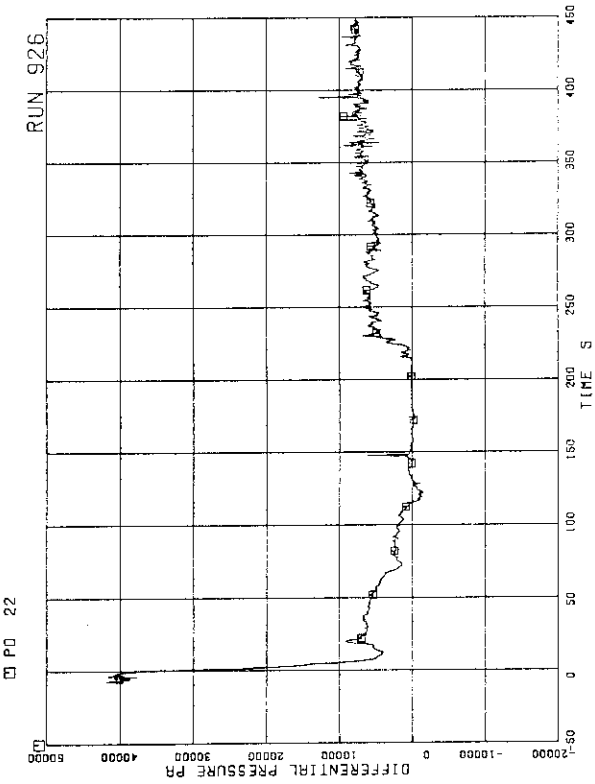

FIG.S. 9 DIFFERENTIAL PRESSURE BETWEEN UPPER PLENUM AND STEAM DOME

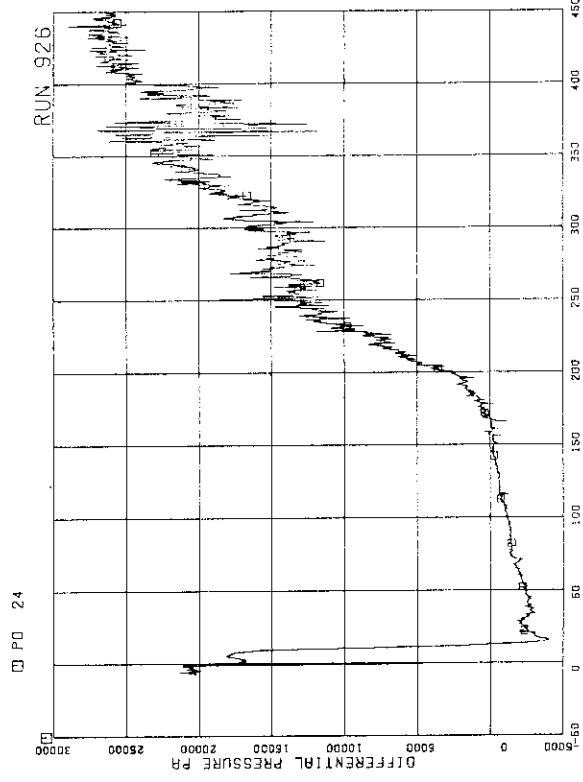

FIG.S. 10 DC (DOWNCOMER) HEAD

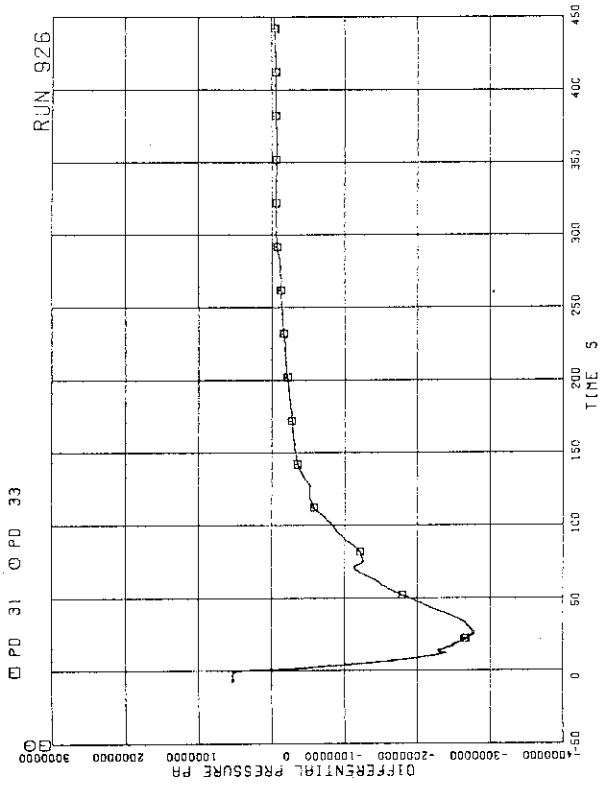

FIG.5. 15 DIFFERENTIAL PRESSURE BETWEEN JP-3.4 DRIVE AND SUCTION

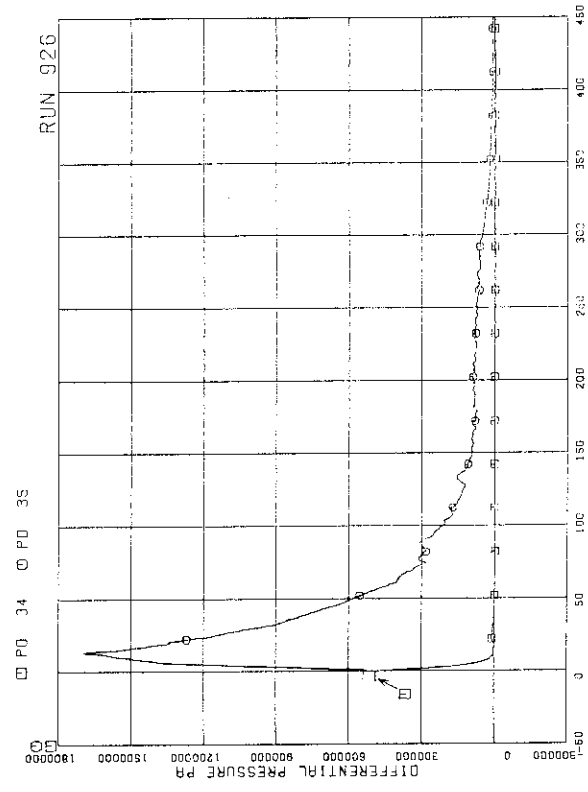

FIG.5. 16 DIFFERENTIAL PRESSURE BETWEEN MAP DELIVERY AND SUCTION

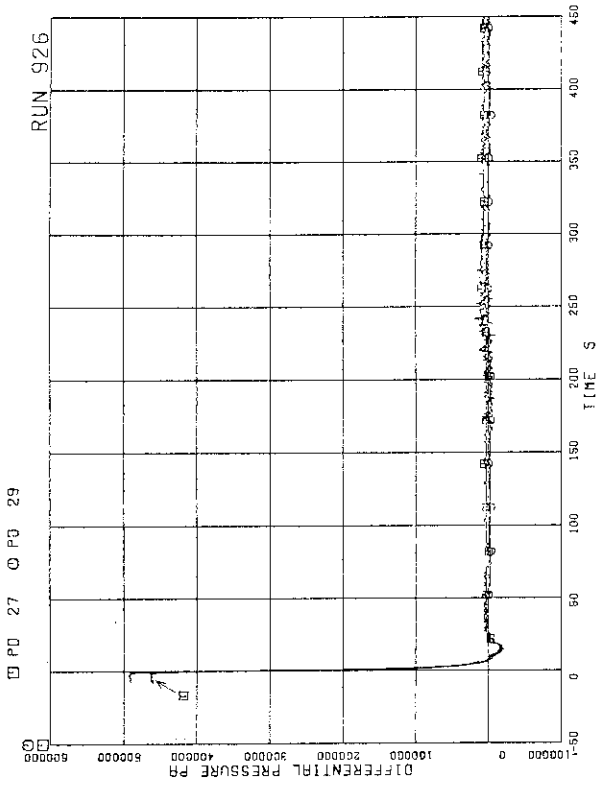

FIG.5. 13 DIFFERENTIAL PRESSURE BETWEEN JP 1,2 DRIVE AND SUCTION

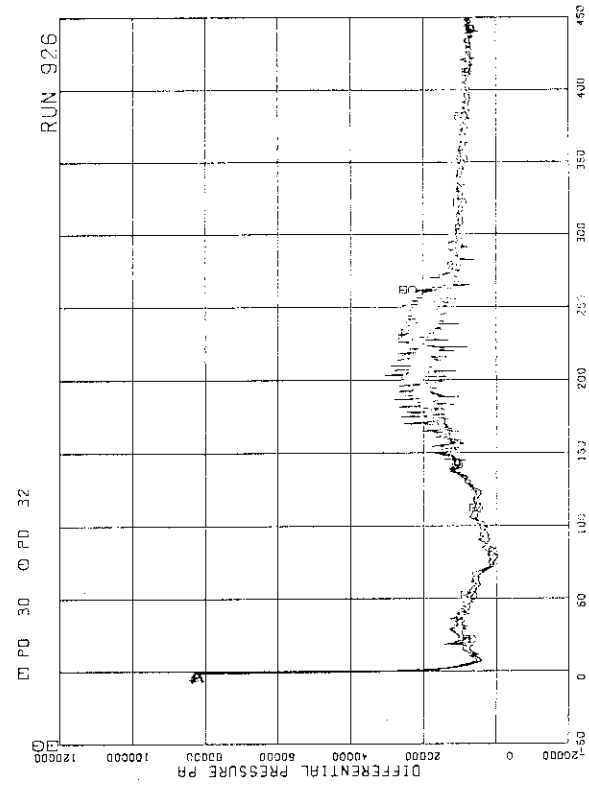

FIG.5. 14 DIFFERENTIAL PRESSURE BETWEEN P-3.4 DISCHARGE AND SUCTION

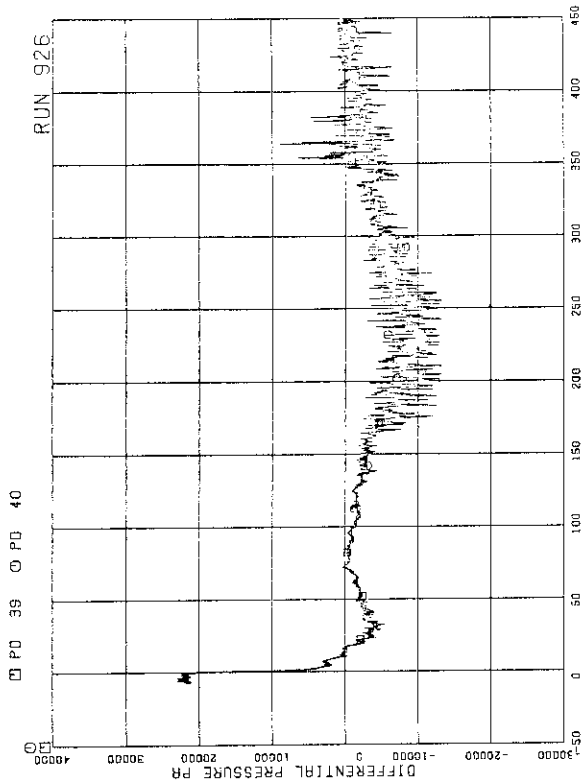

FIG.5. 19 DIFFERENTIAL PRESSURE BETWEEN DOWNCOMER MIDDLE AND JP-1,2 SUCTION

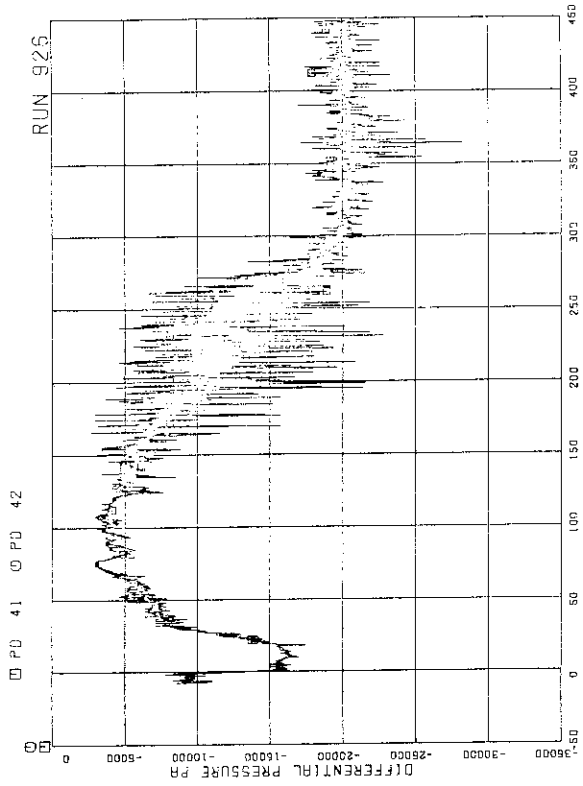

FIG.5. 20 DIFFERENTIAL PRESSURE BETWEEN JP-1,2 DISCHARGE AND LOWER PLENUM

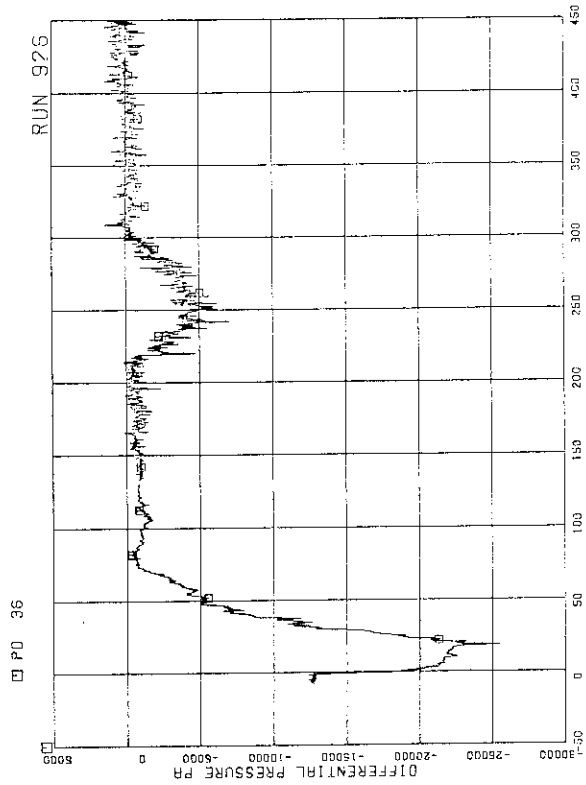

FIG.5. 17 DIFFERENTIAL PRESSURE BETWEEN DOWNCOMER BOTTOM AND MRPI SUCTION

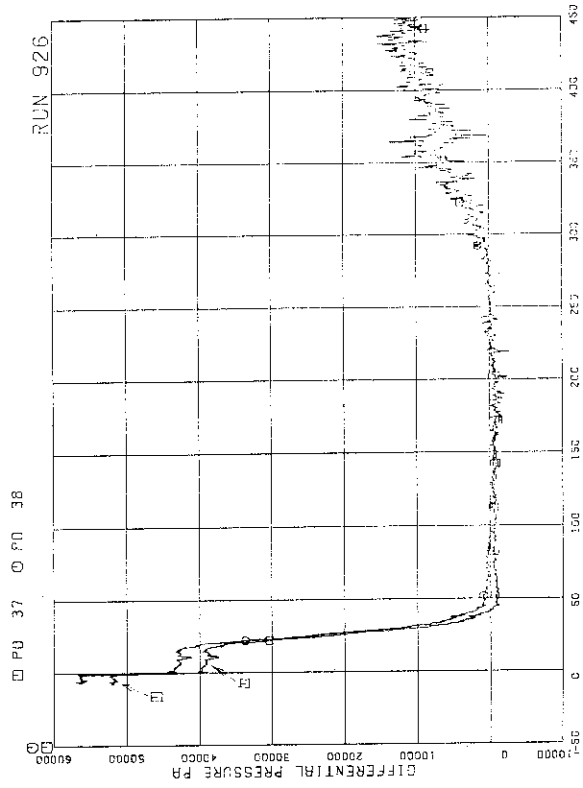

FIG.5. 18 DIFFERENTIAL PRESSURE BETWEEN MRF DELIVERY AND JP-1,2 SUCTION

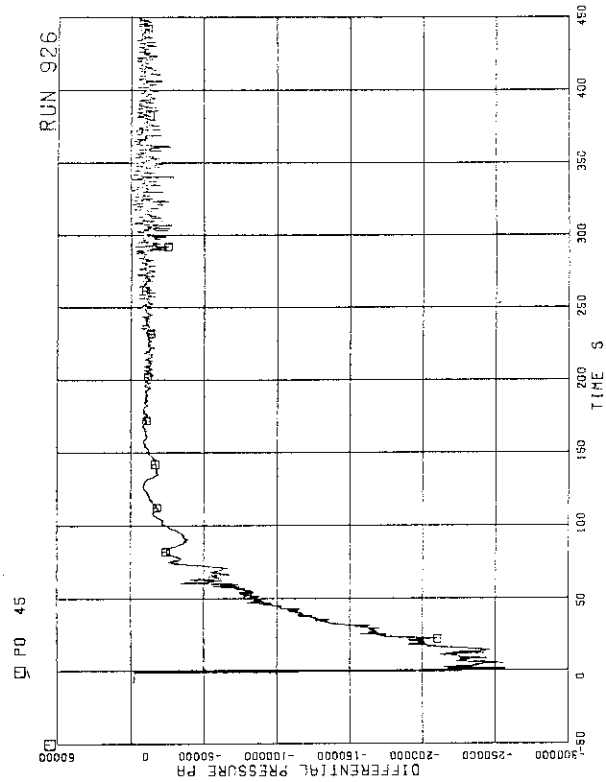

FIG.5. 23 DIFFERENTIAL PRESSURE BETWEEN BREAK A AND MRP2 SUCTION

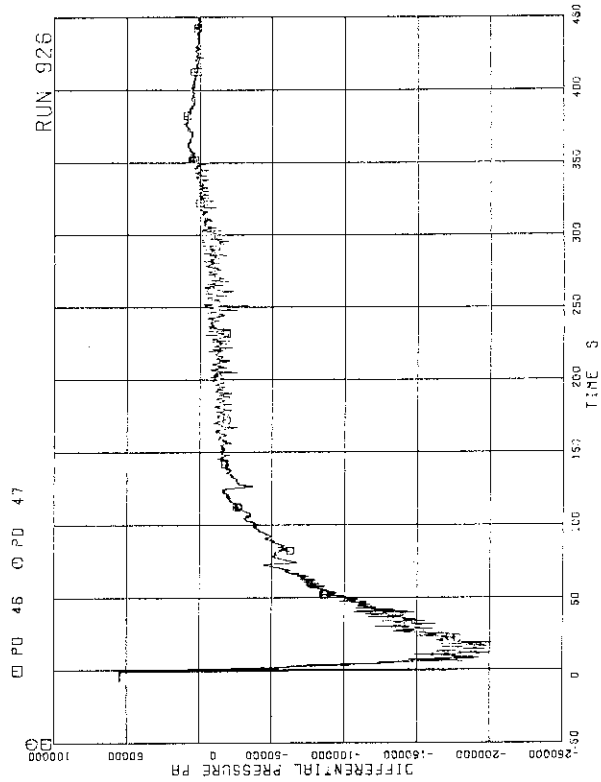

FIG.5. 24 DIFFERENTIAL PRESSURE BETWEEN MRP DELIVERY AND JP-3,4 DRIVE

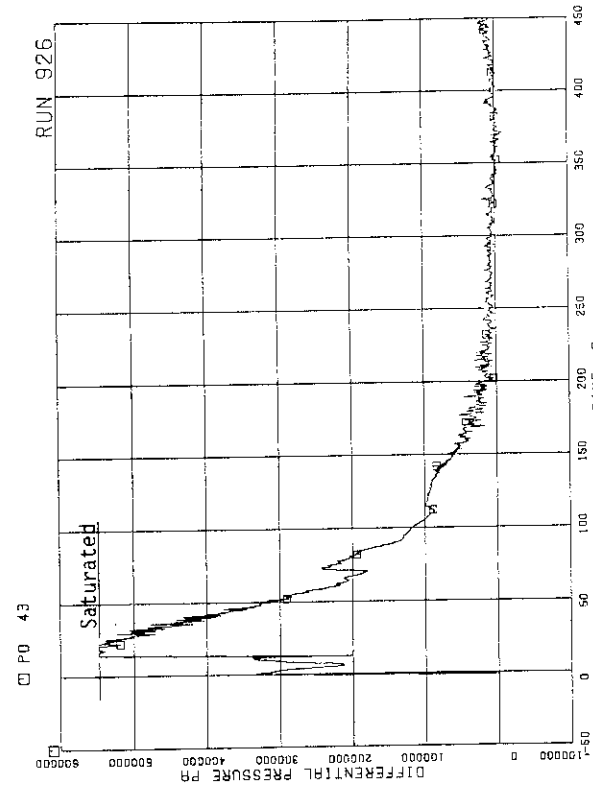

FIG.5. 21 DIFFERENTIAL PRESSURE BETWEEN DOWNCOMER BOTTOM AND BREAK B

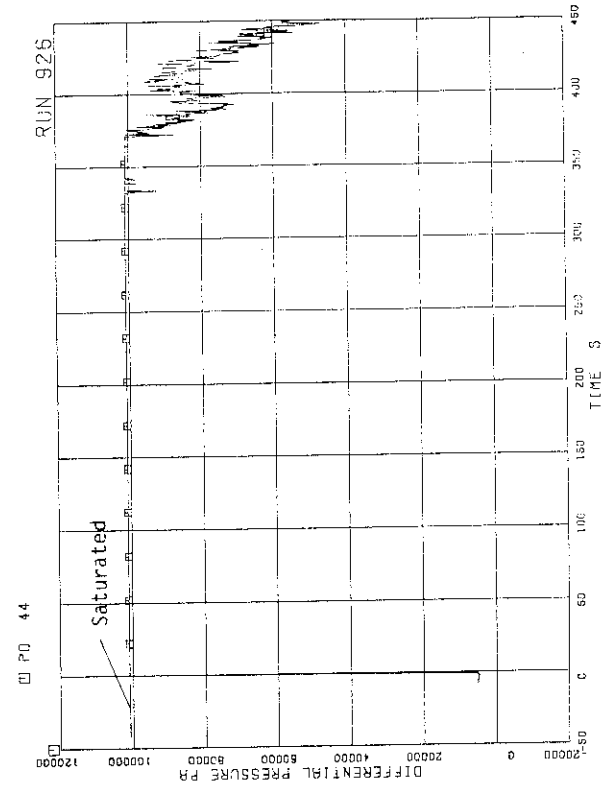

FIG.5. 22 DIFFERENTIAL PRESSURE BETWEEN BREAK A AND B

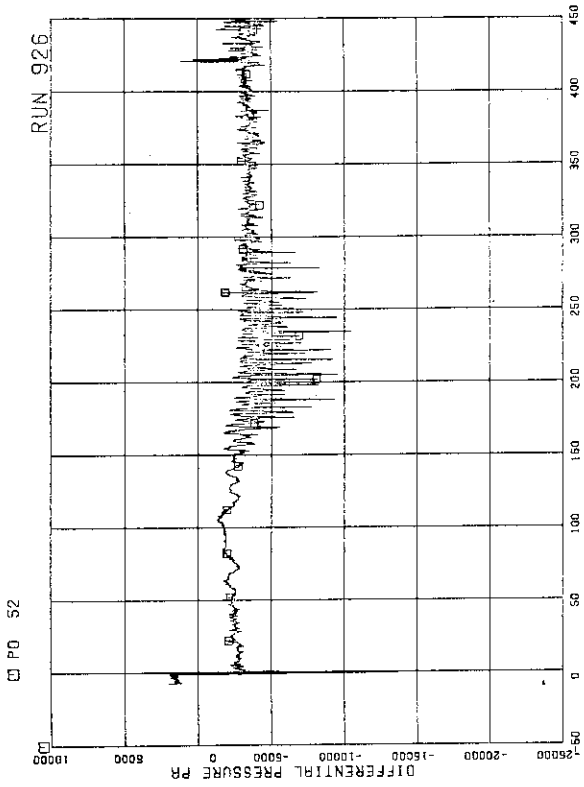

FIG.5. 27 DIFFERENTIAL PRESSURE BETWEEN JP-3,4 CONFLUENCE IN BROKEN LOOP AND LP

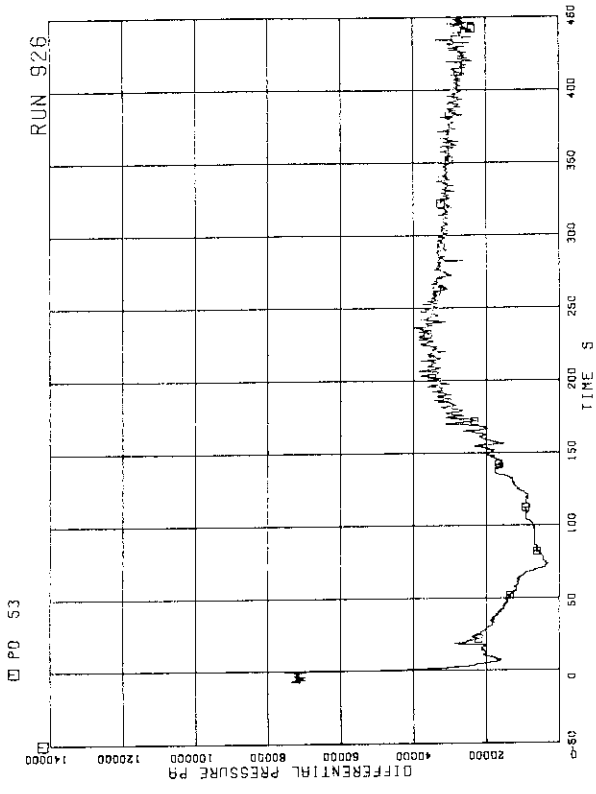

FIG.5. 28 DIFFERENTIAL PRESSURE BETWEEN LOWER PLENUM AND DOWNCOMER MIDDLE

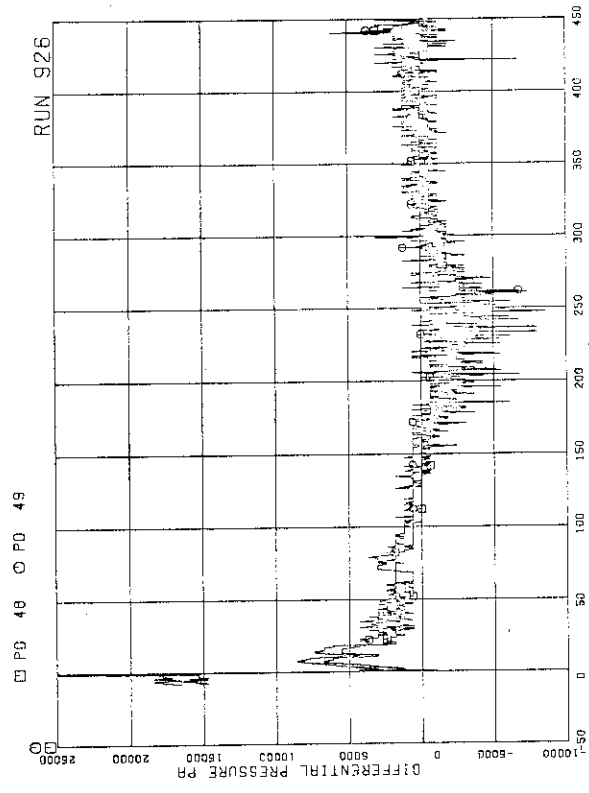

FIG.5. 25 DIFFERENTIAL PRESSURE BETWEEN DOWNCOMER MIDDLE AND JP-3,4 SUCTION

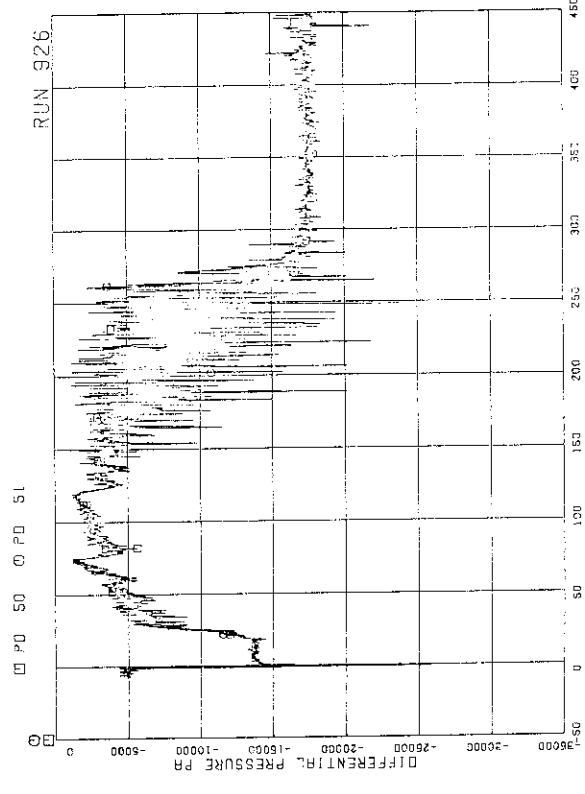

FIG.5. 26 DIFFERENTIAL PRESSURE BETWEEN JP-3,4 DISCHARGE AND CONFLUENCE

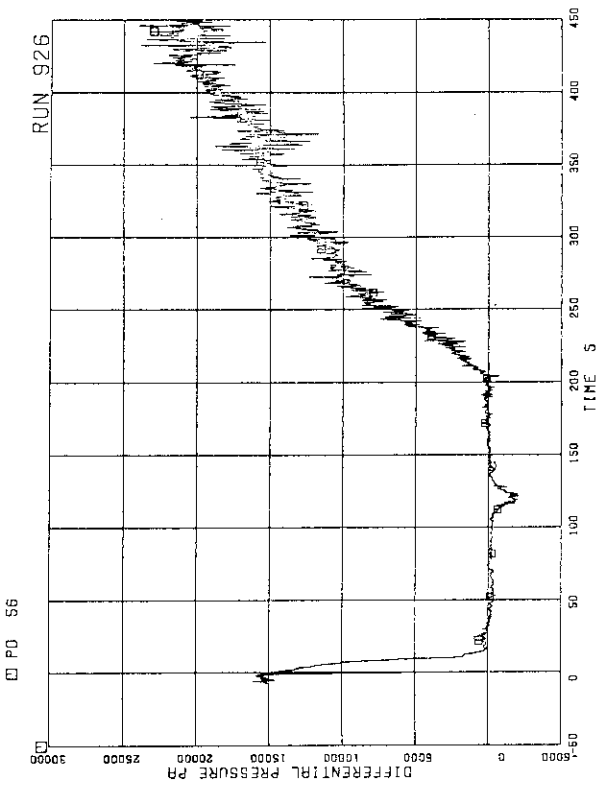

FIG.5. 31 DIFFERENTIAL PRESSURE BETWEEN DOWNCOMER MIDDLE AND STEAM DOME

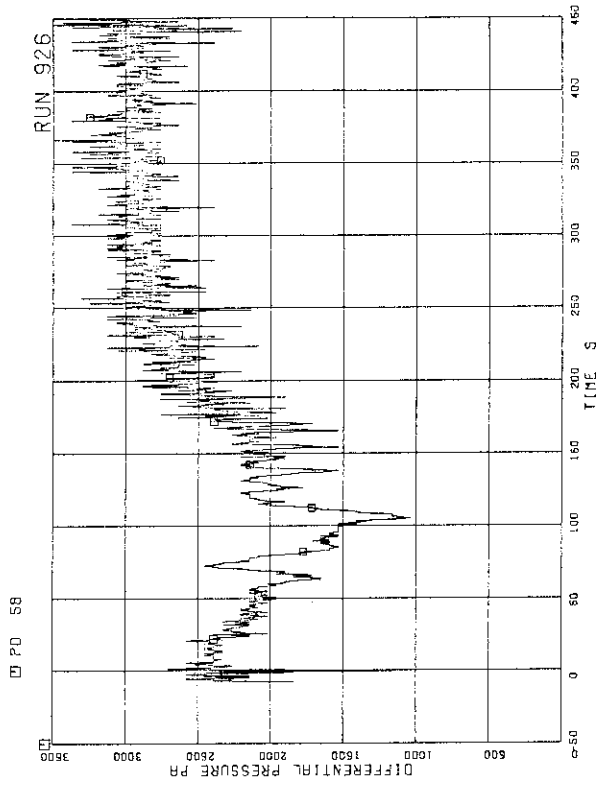

FIG.5. 32 DIFFERENTIAL PRESSURE BETWEEN LP BOTTOM AND LP MIDDLE

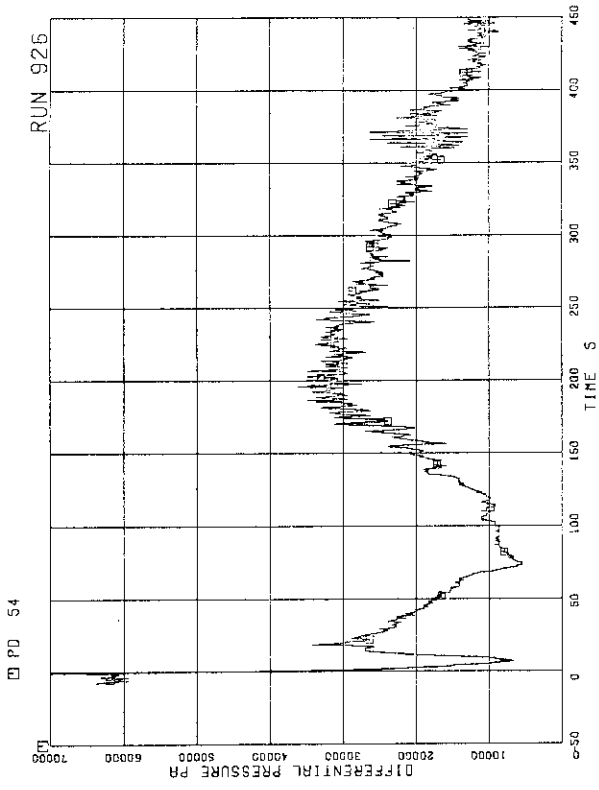

FIG.5. 29 DIFFERENTIAL PRESSURE BETWEEN LOWER PLENUM AND DOWNCOMER BOTTOM

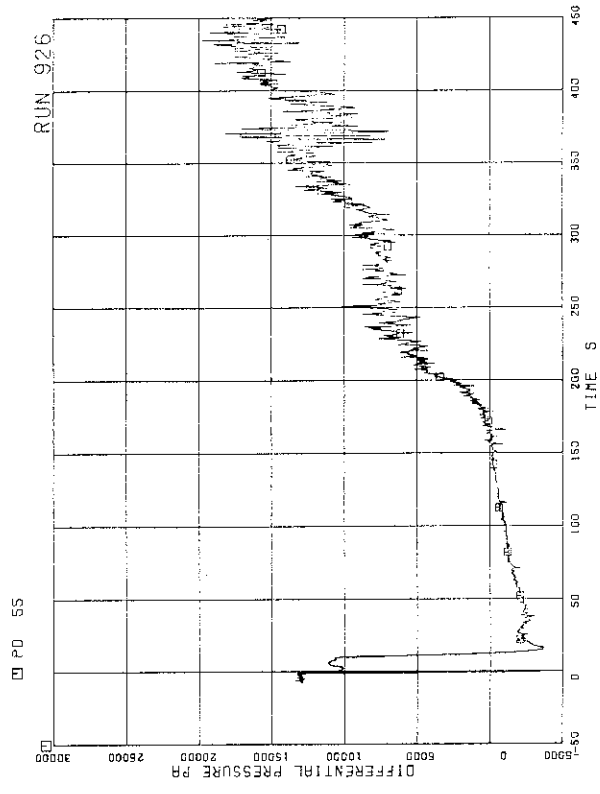

FIG.5. 30 DIFFERENTIAL PRESSURE BETWEEN DOWNCOMER BOTTOM AND DOWNCOMER MIDDLE

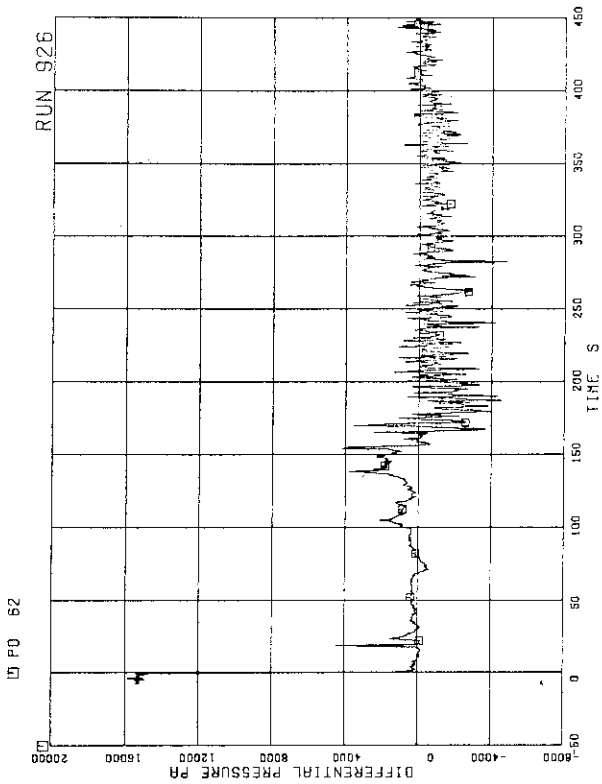

FIG.5. 35 DIFFERENTIAL PRESSURE ACROSS CHANNEL INLET ORIFICE C

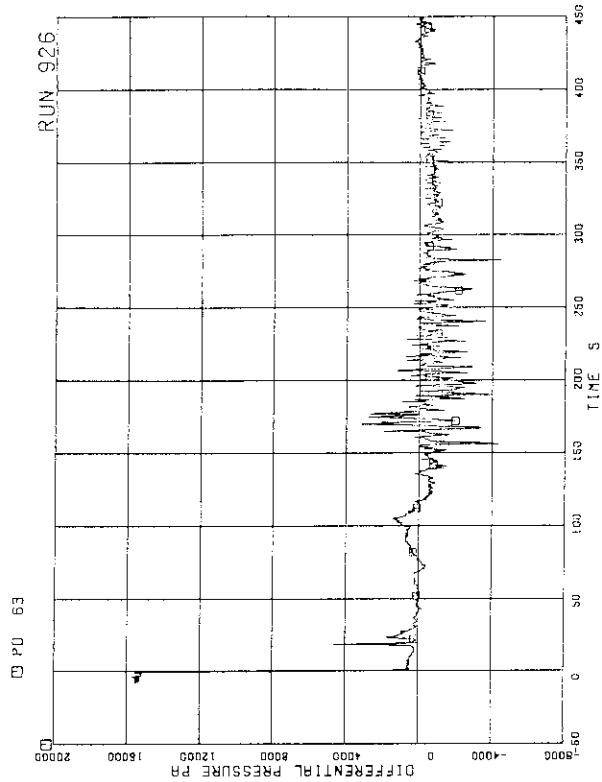

FIG.5. 36 DIFFERENTIAL PRESSURE ACROSS CHANNEL INLET ORIFICE D

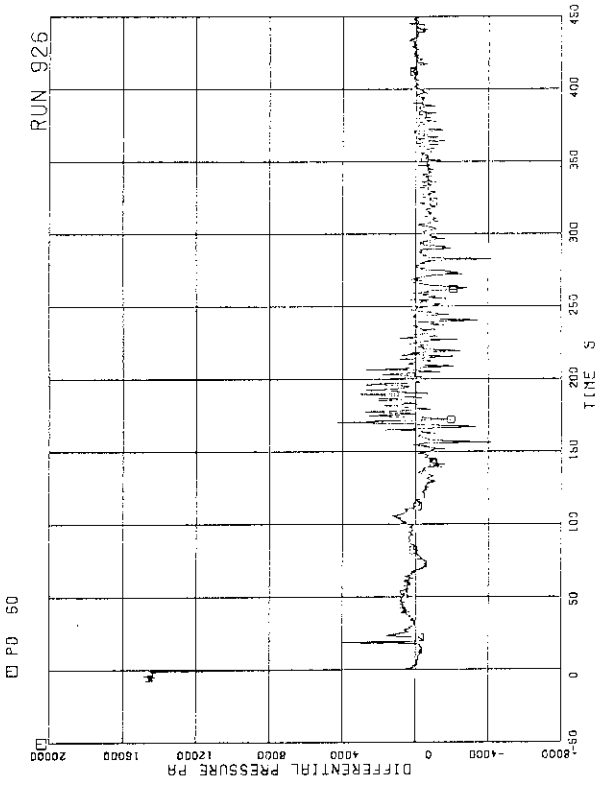

FIG.5. 33 DIFFERENTIAL PRESSURE ACROSS CHANNEL INLET ORIFICE A

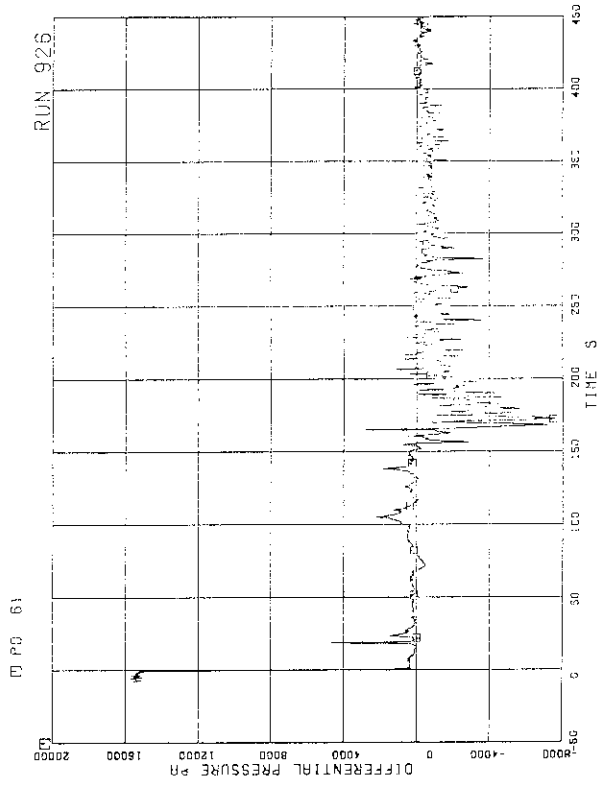

FIG.5. 34 DIFFERENTIAL PRESSURE ACROSS CHANNEL INLET ORIFICE B

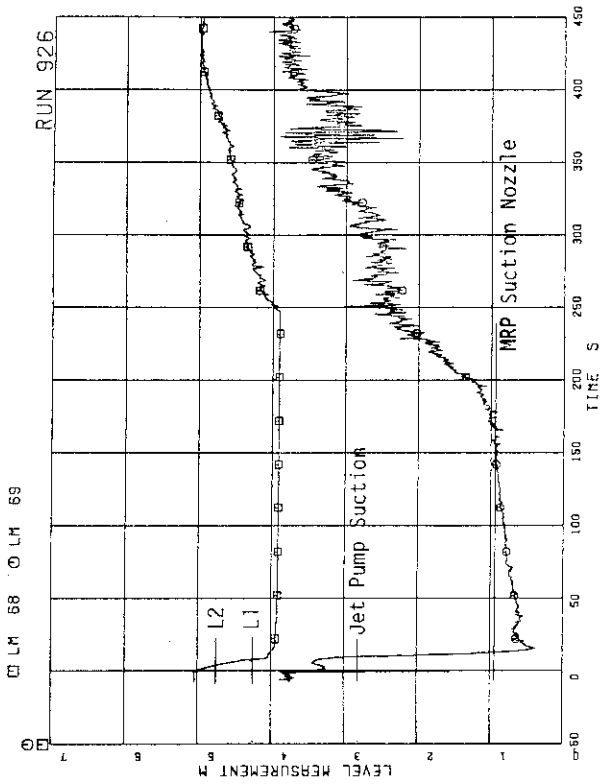

FIG.5.39 LIQUID LEVEL IN DOWNCOMER

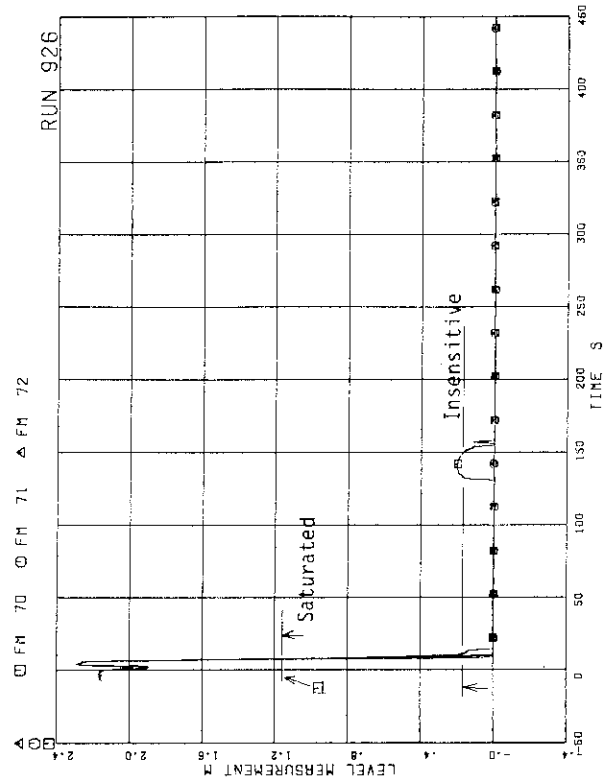

FIG.5.40 MASS FLOW RATE IN MSL

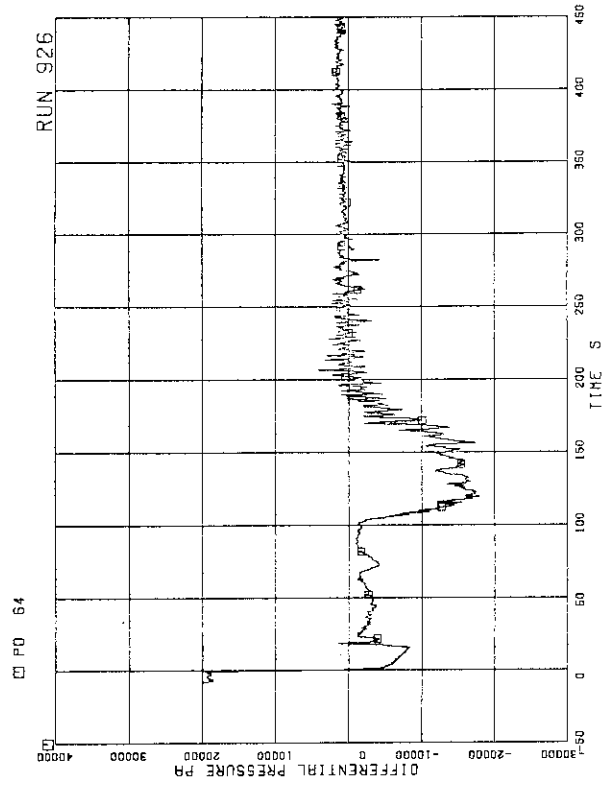

FIG.5.37 DIFFERENTIAL PRESSURE ACROSS BYPASS HOLE

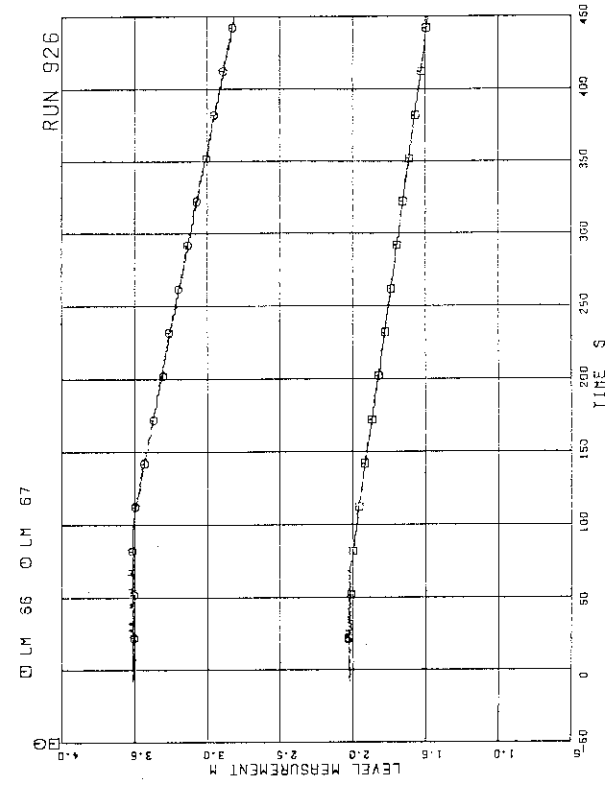

FIG.5.38 LIQUID LEVEL IN ECCS TANKS

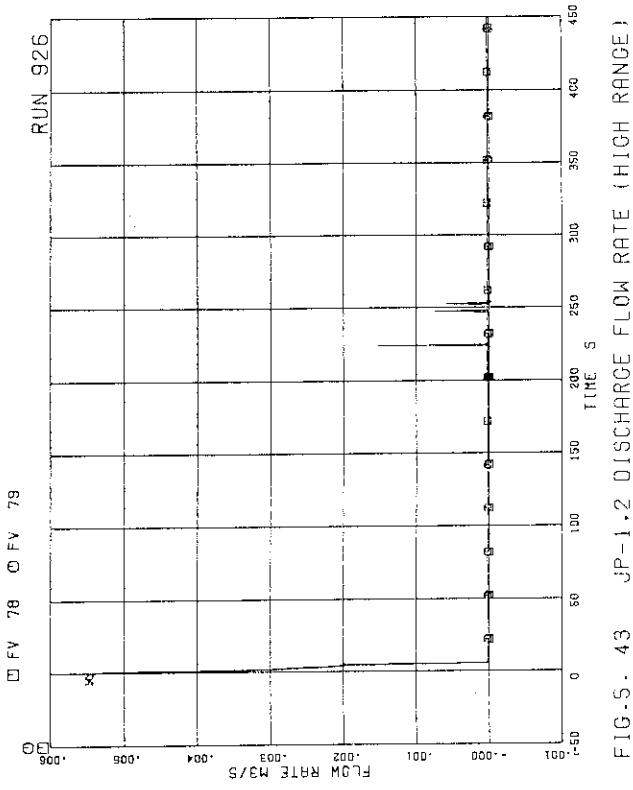

FIG.S. 43 JP-1.2 DISCHARGE FLOW RATE (HIGH RANGE)

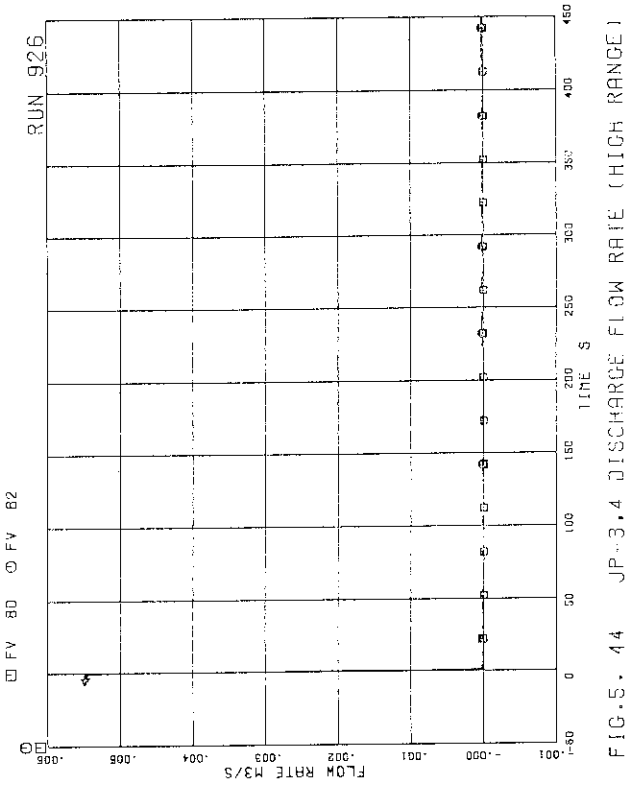

FIG.S. 44 JP-3.4 DISCHARGE FLOW RATE (HIGH RANGE)

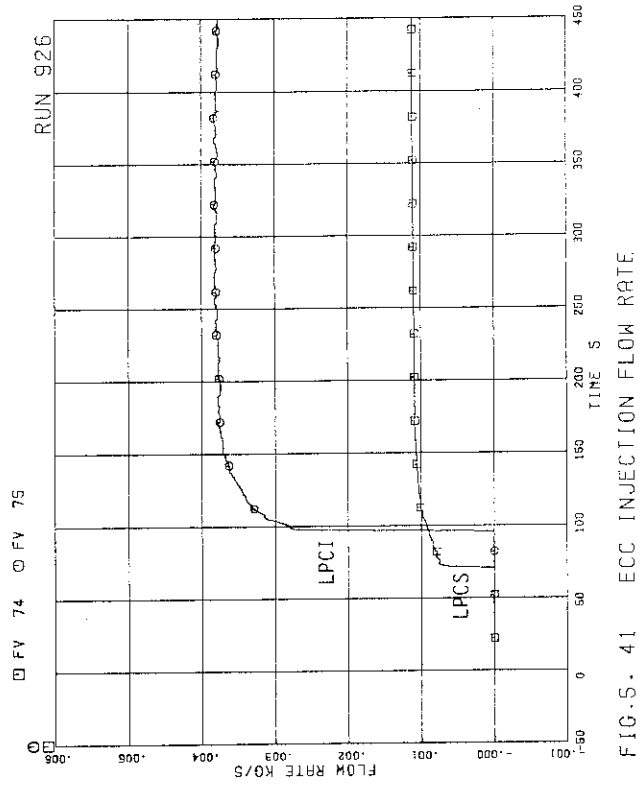

FIG.S. 41 ECC INJECTION FLOW RATE

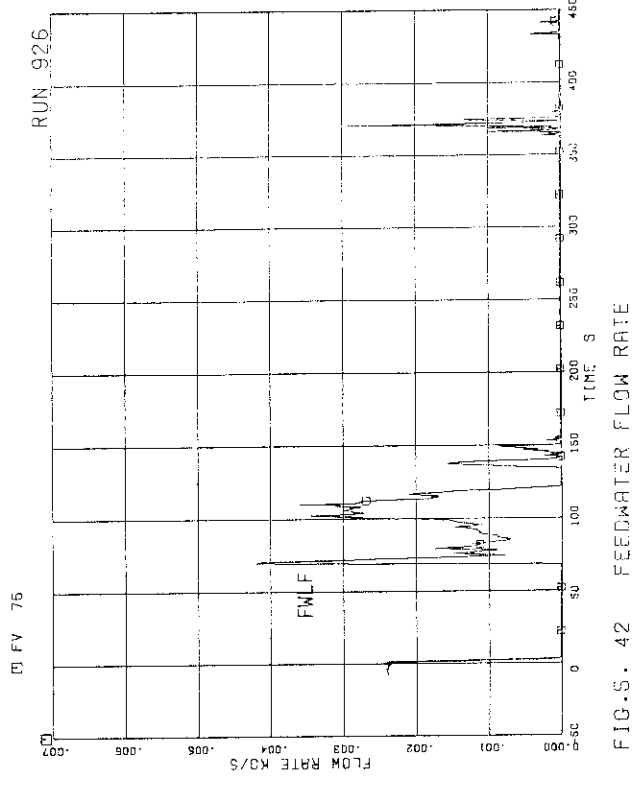

FIG.S. 42 FEEDWATER FLOW RATE

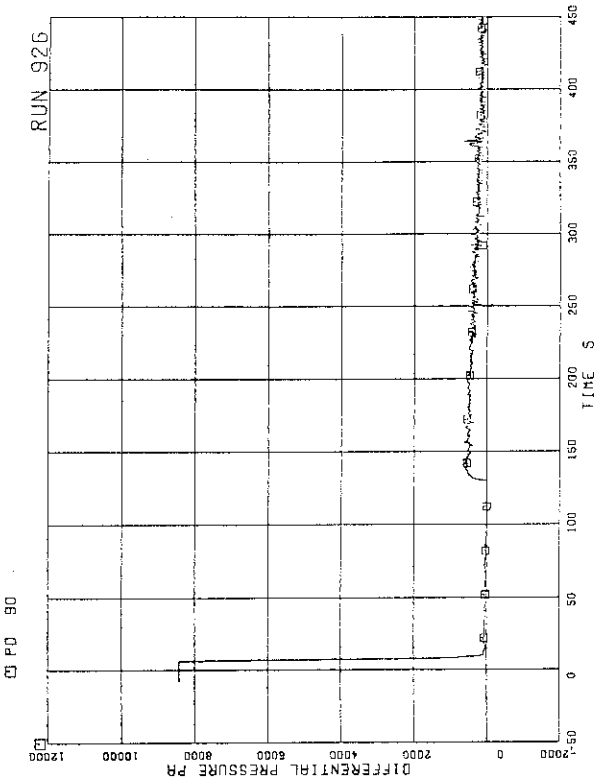

FIG.5. 47 DIFFERENTIAL PRESSURE ACROSS ORIFICE FLOWMETER F-1

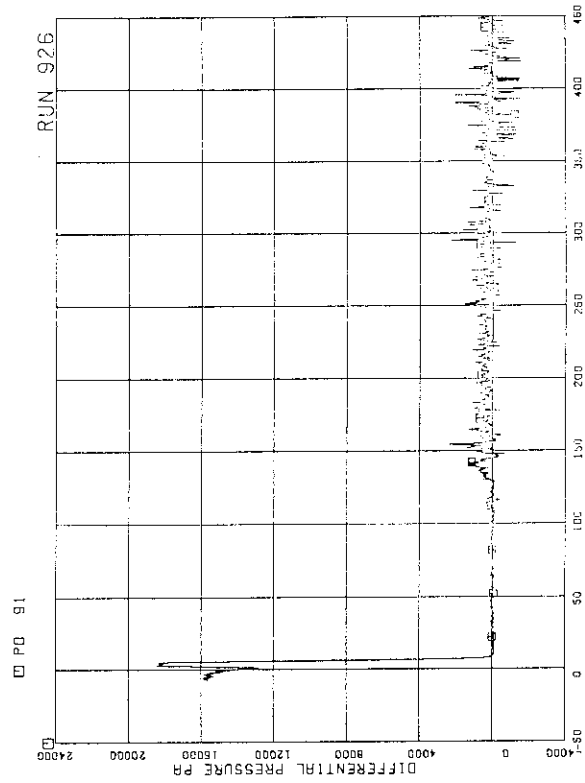

FIG.5. 48 DIFFERENTIAL PRESSURE ACROSS ORIFICE FLOWMETER F-2

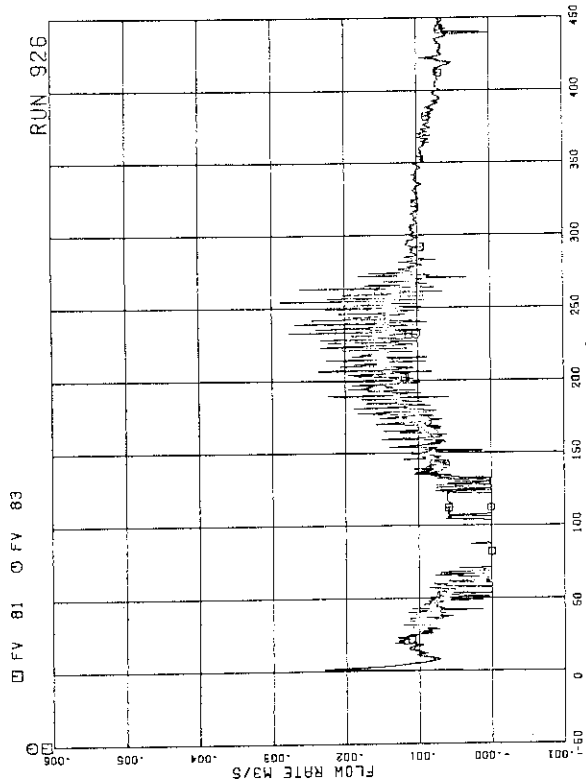

FIG.5. 45 JP-3.4 DISCHARGE FLOW RATE (LOW RANGE)

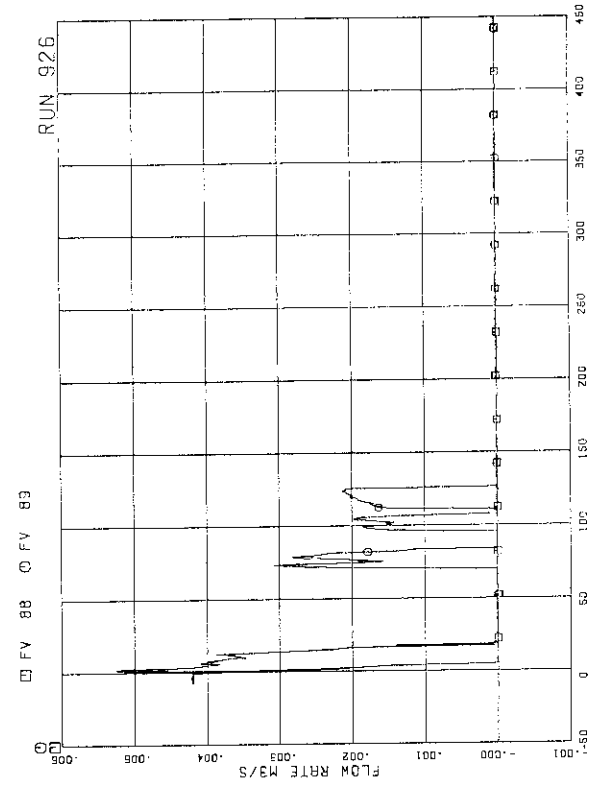

FIG.5. 46 MRP DISCHARGE FLOW RATE

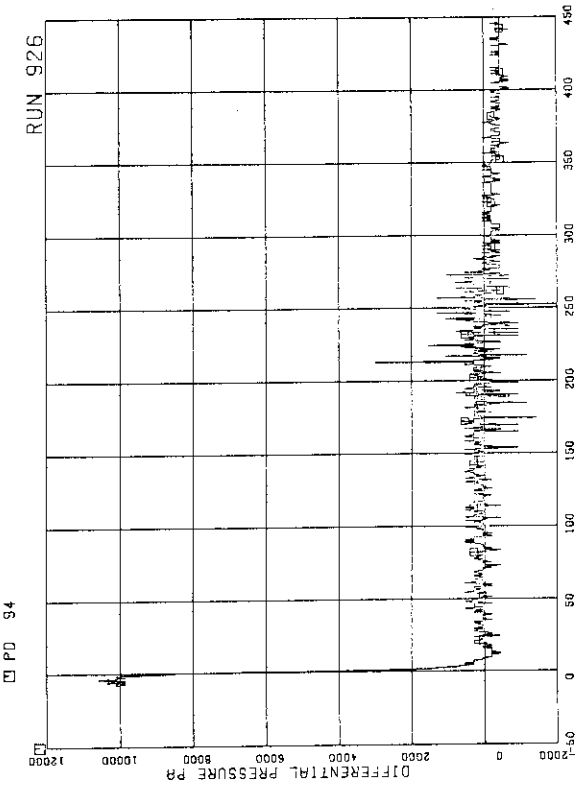

FIG.5. 51 DIFFERENTIAL PRESSURE ACROSS VENTURI FLOWMETER F-18

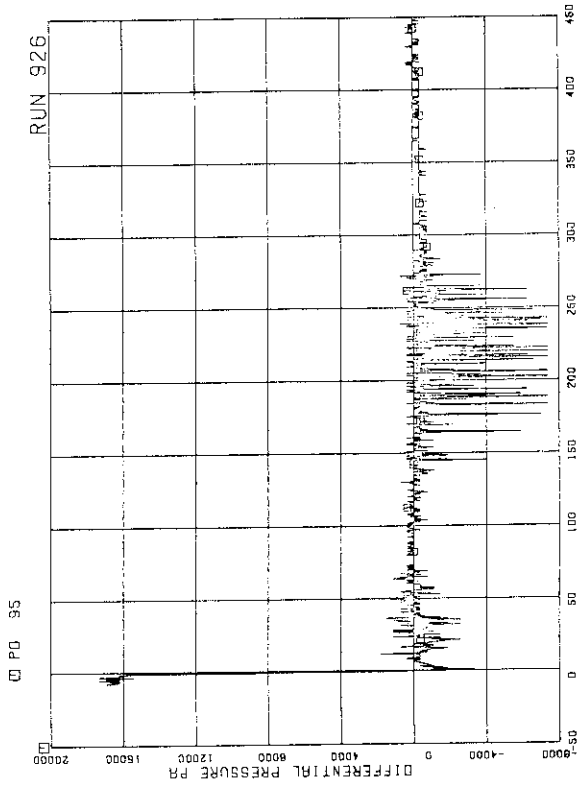

FIG.5. 52 DIFFERENTIAL PRESSURE ACROSS ORIFICE FLOWMETER F-19

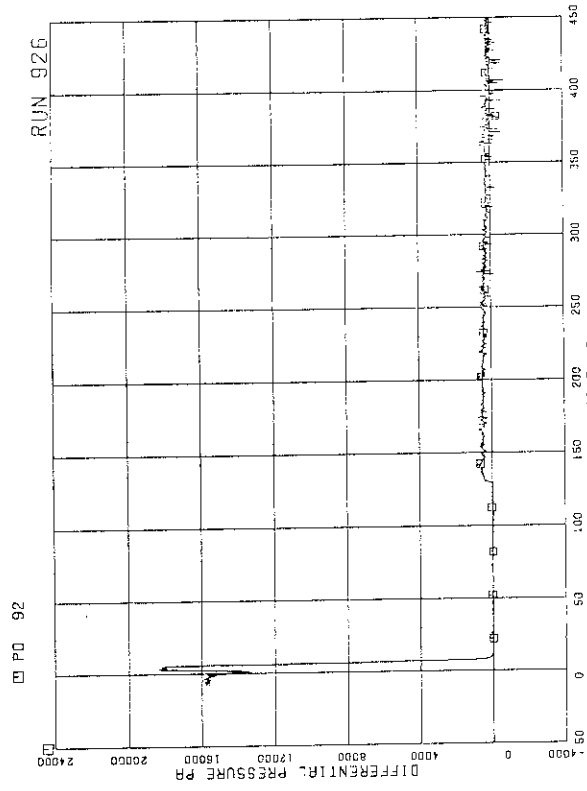

FIG.5. 49 DIFFERENTIAL PRESSURE ACROSS ORIFICE FLOWMETER F-3

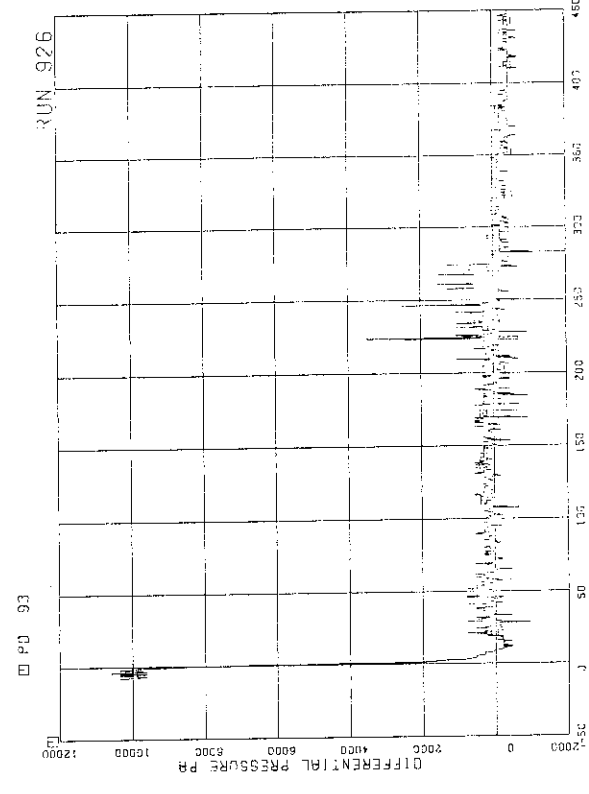

FIG.5. 50 DIFFERENTIAL PRESSURE ACROSS VENTURI FLOWMETER F-17

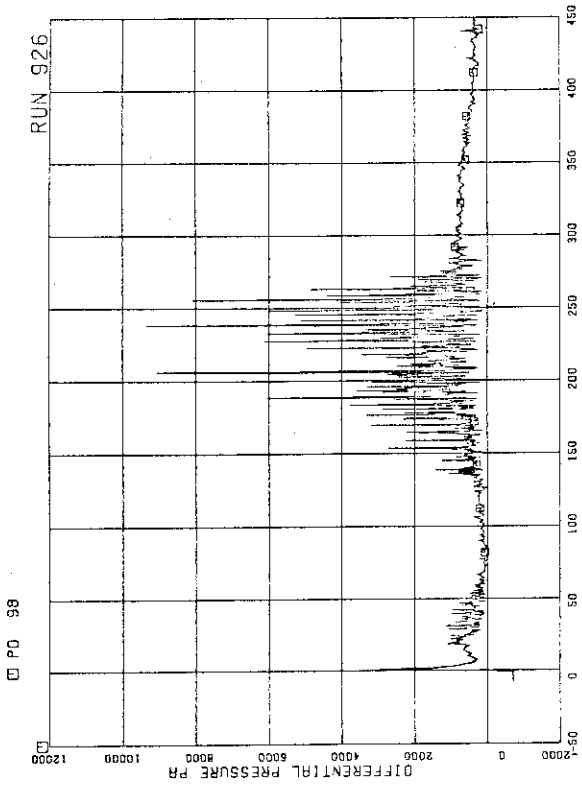

FIG.5. 55 DIFFERENTIAL PRESSURE ACROSS ORIFICE FLOWMETER F-22

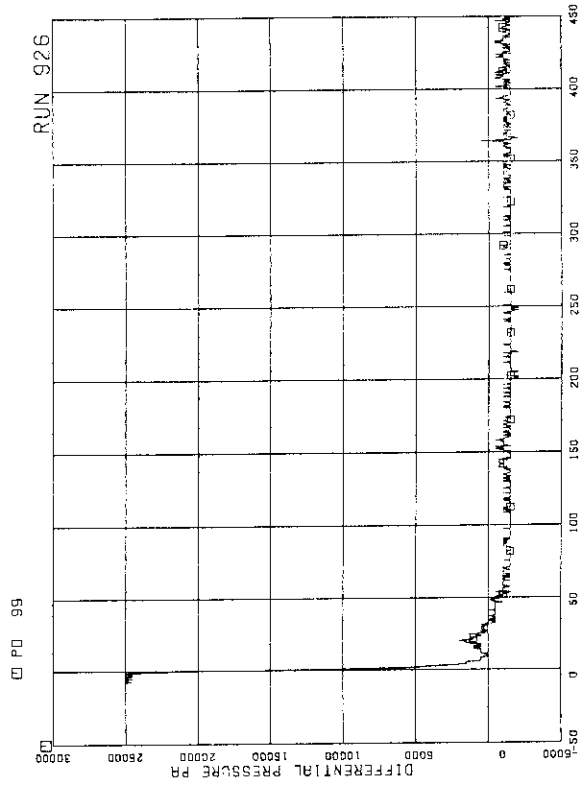

FIG.5. 56 DIFFERENTIAL PRESSURE ACROSS VENTURI FLOWMETER F-27

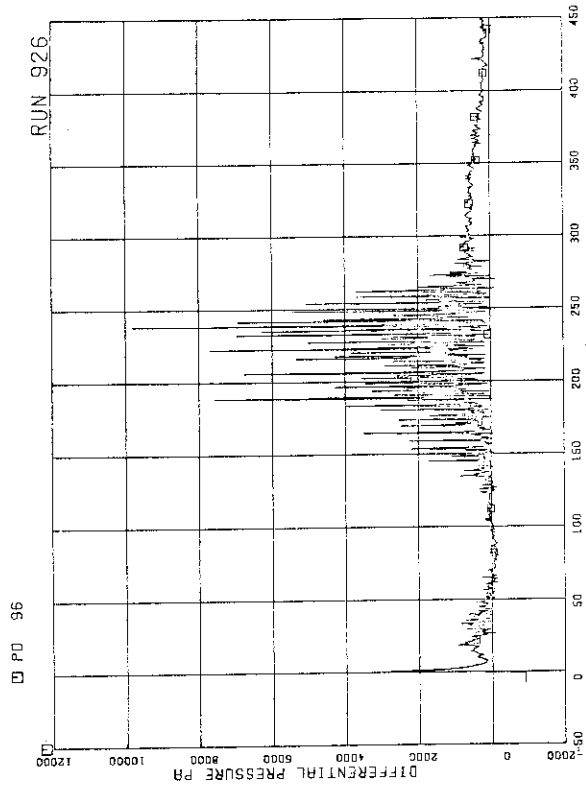

FIG.5. 53 DIFFERENTIAL PRESSURE ACROSS ORIFICE FLOWMETER F-20

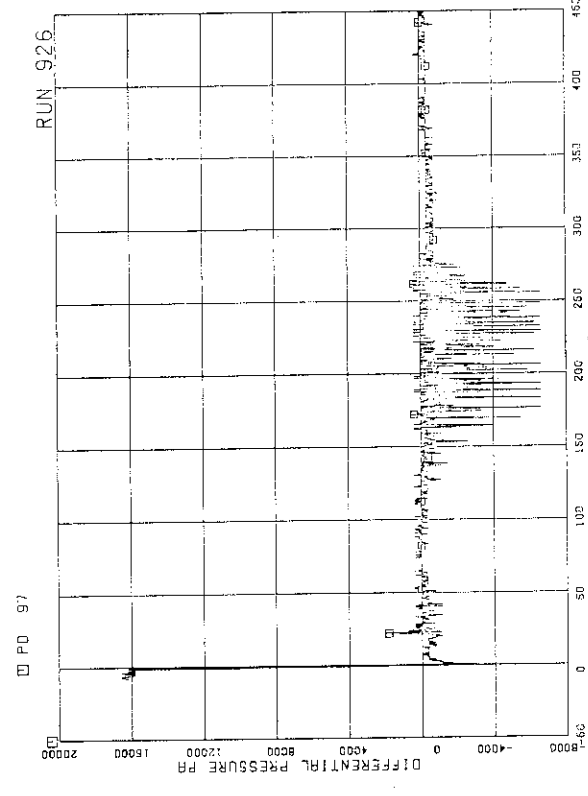

FIG.5. 54 DIFFERENTIAL PRESSURE ACROSS ORIFICE FLOWMETER F-21

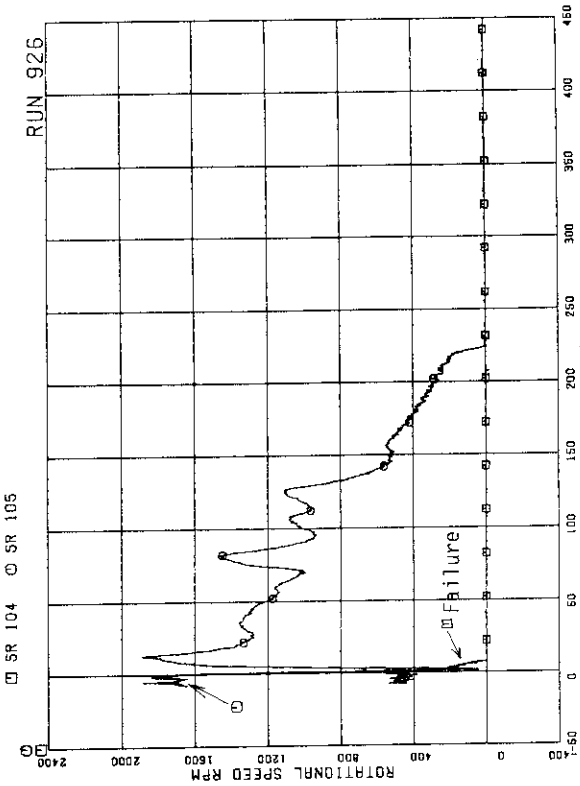

FIG.5. 59 MRP REVOLUTION

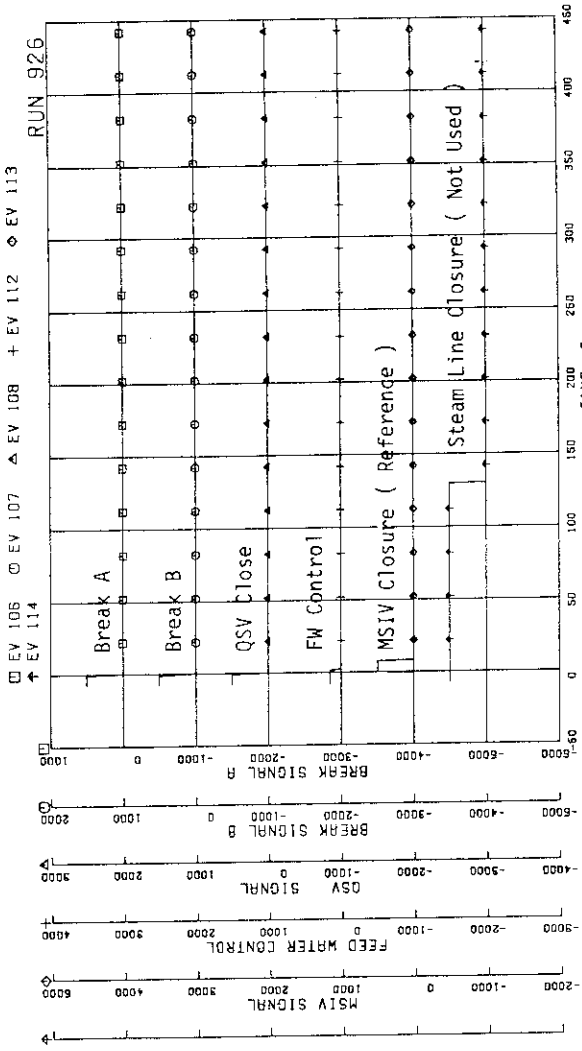

FIG.5. 60 VALVE OPERATION SIGNALS

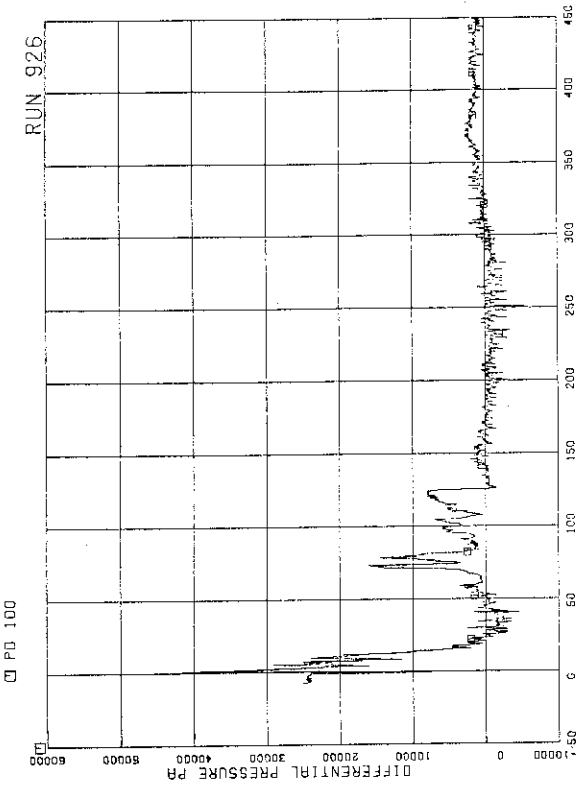

FIG.5. 57 DIFFERENTIAL PRESSURE ACROSS VENTURI FLOWMETER F-28

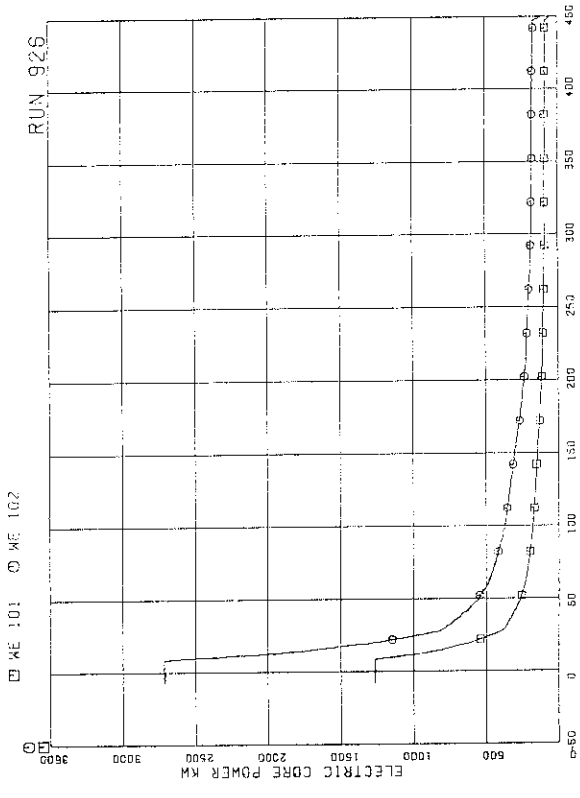

FIG.5. 58 ELECTRIC CORE POWER

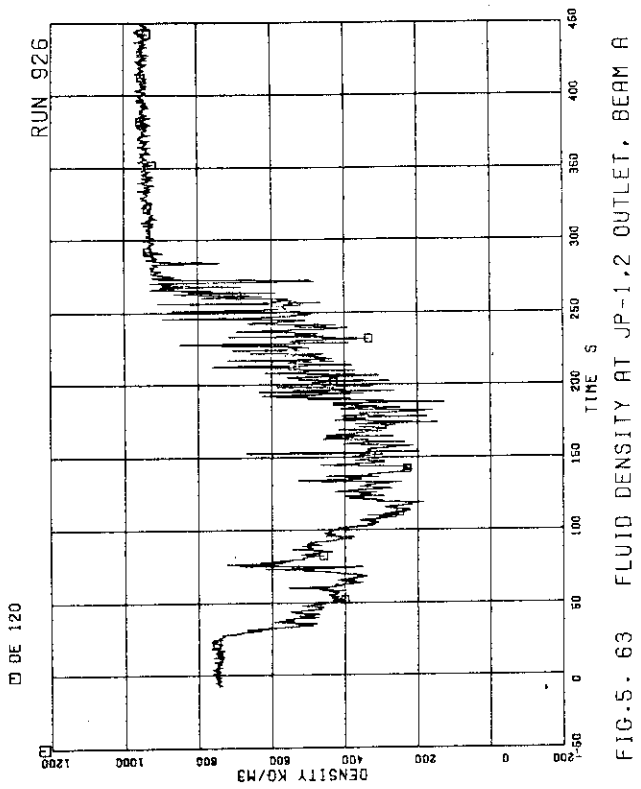

FIG.5. 63 FLUID DENSITY AT JP-1,2 OUTLET, BEAM A

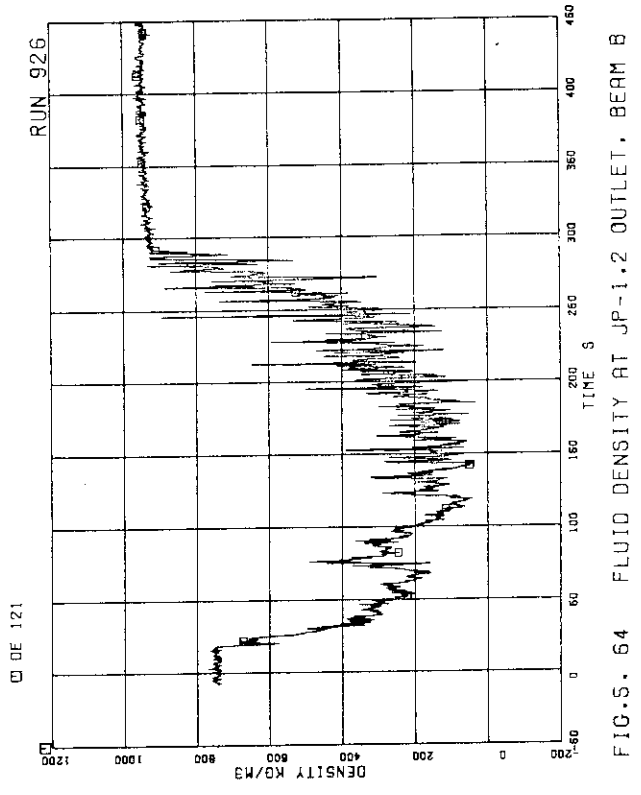

FIG.5. 64 FLUID DENSITY AT JP-1,2 OUTLET, BEAM B

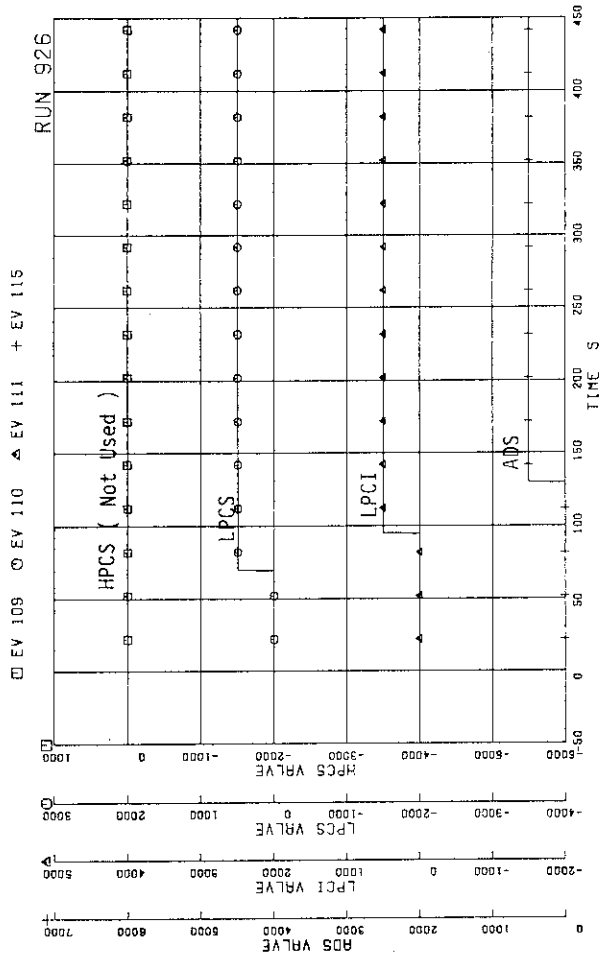

FIG.5. 61 ECCS OPERATION SIGNALS

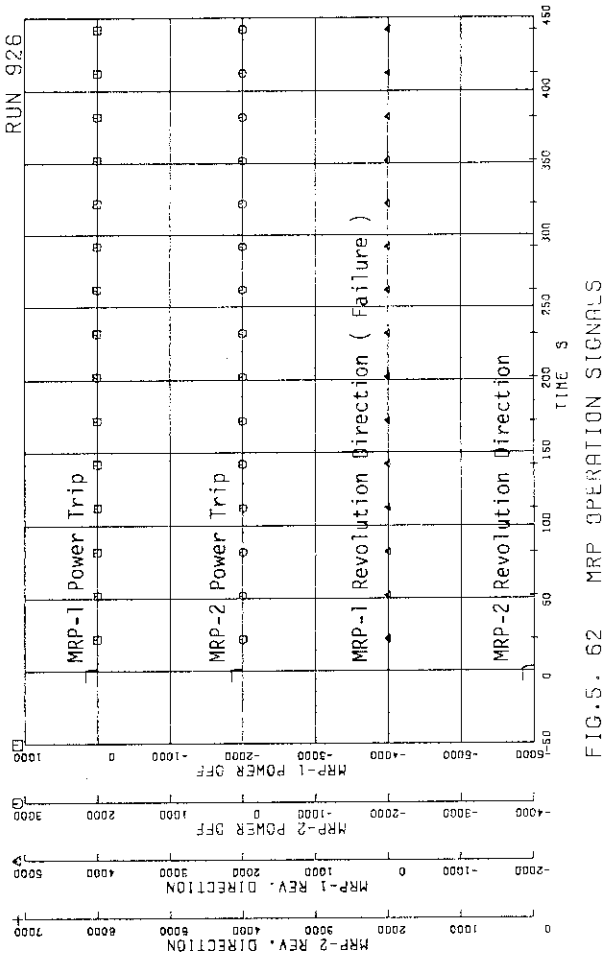

FIG.5. 62 MRP OPERATION SIGNALS

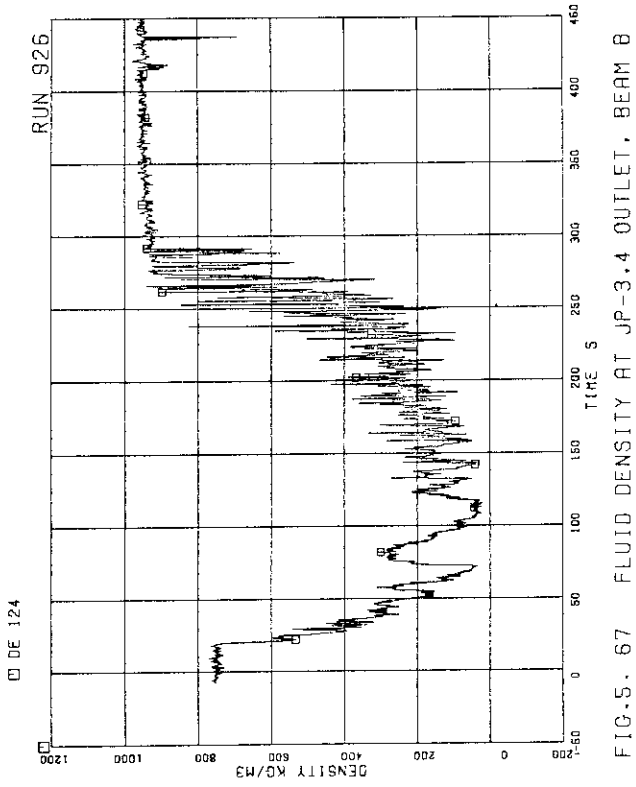

FIG.5. 67 FLUID DENSITY AT JP-3,4 OUTLET, BEAM B

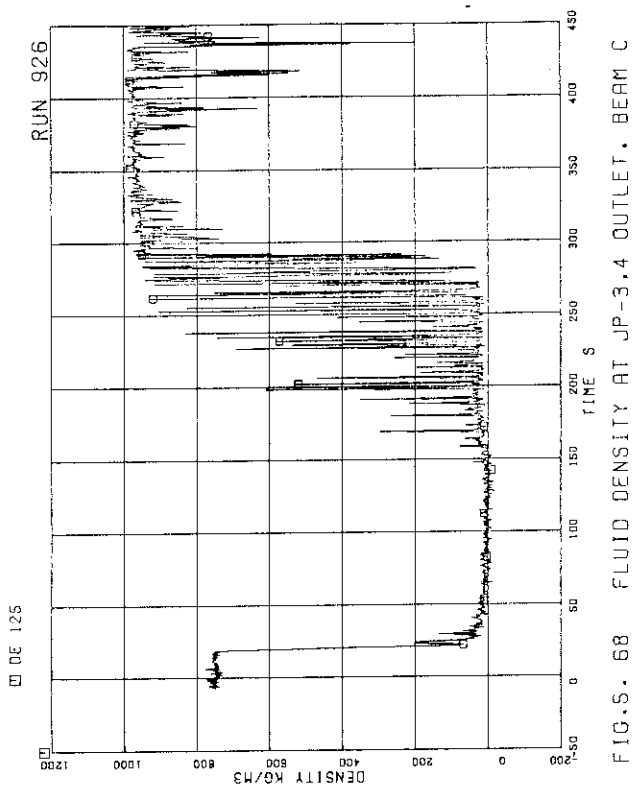

FIG.5. 68 FLUID DENSITY AT JP-3,4 OUTLET, BEAM C

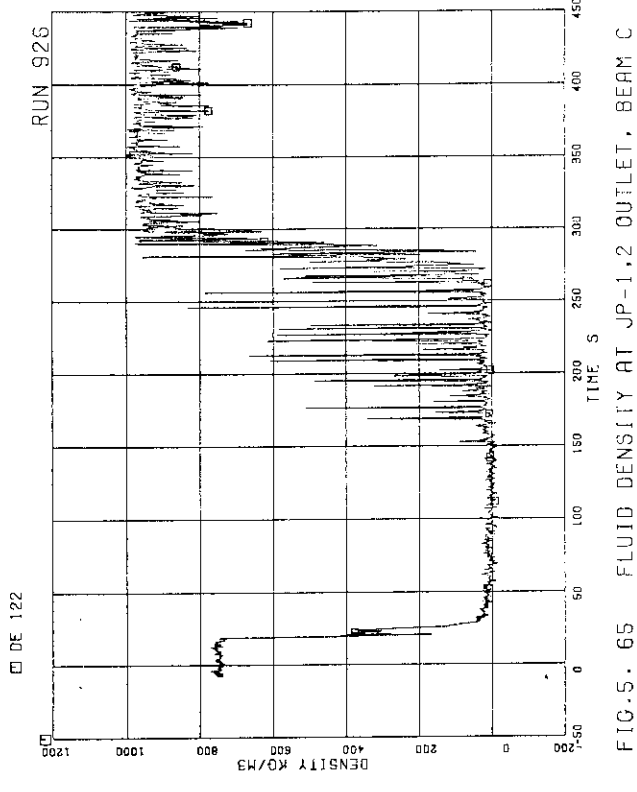

FIG.5. 65 FLUID DENSITY AT JP-1,2 OUTLET, BEAM C

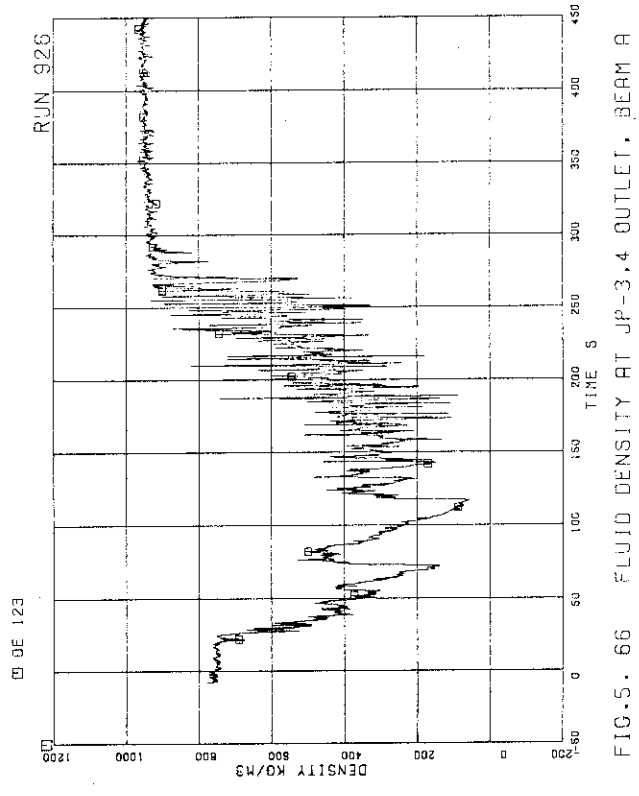

FIG.5. 66 FLUID DENSITY AT JP-3,4 OUTLET, BEAM A

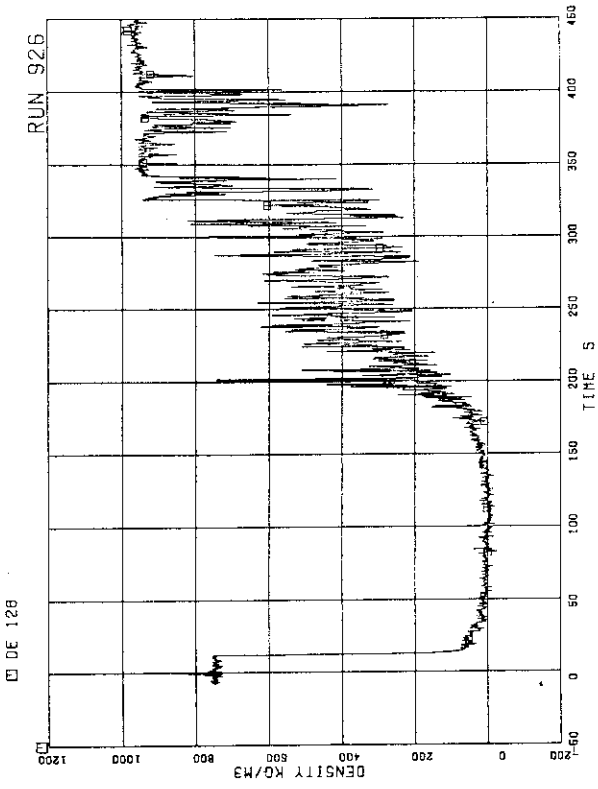

FIG.5. 71 FLUID DENSITY AT PV SIDE OF BREAK, BEAM A

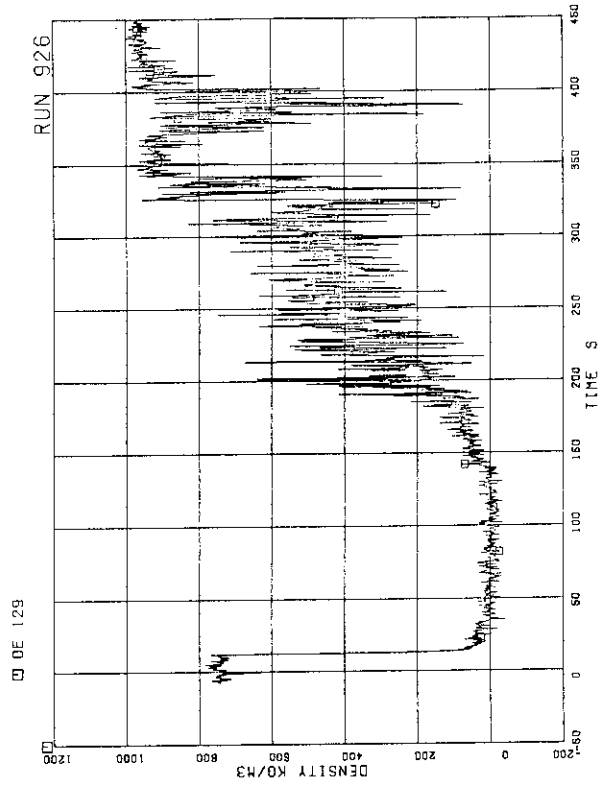

FIG.5. 72 FLUID DENSITY AT PV SIDE OF BREAK, BEAM B

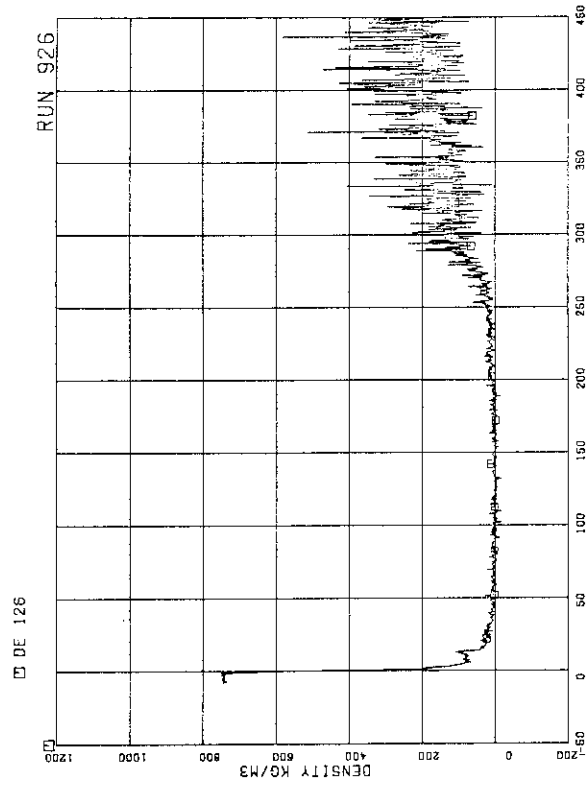

FIG.5. 69 FLUID DENSITY AT MRP SIDE OF BREAK, BEAM A

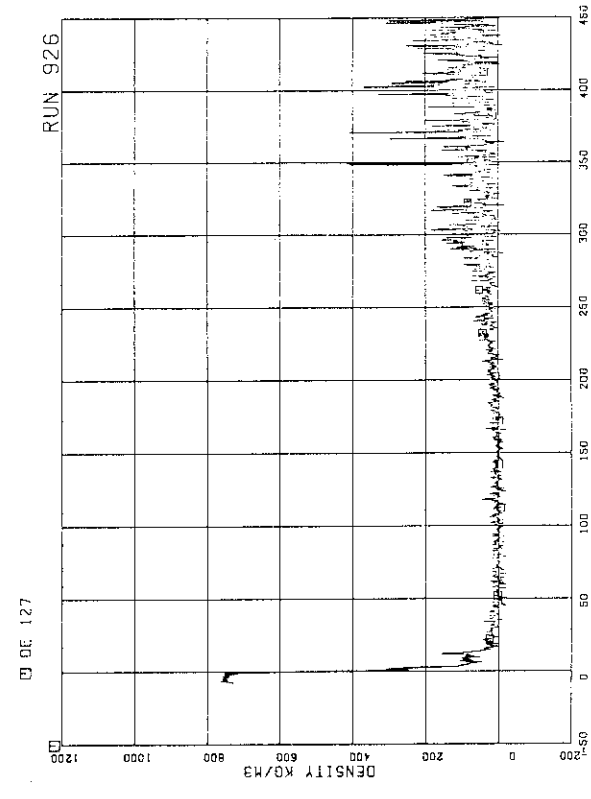

FIG.5. 70 FLUID DENSITY AT MRP SIDE OF BREAK, BEAM B

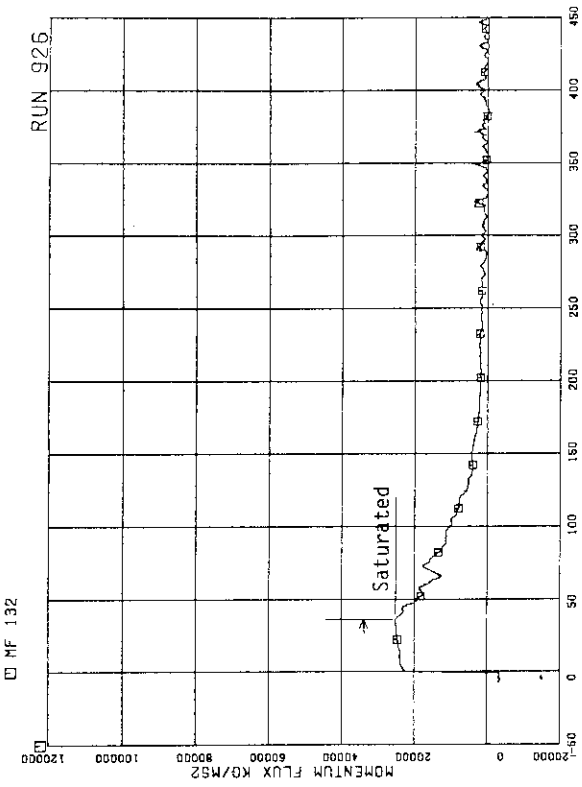

FIG.5. 75 MOMENTUM FLUX AT BREAK A SPOOL PIECE (LOW RANGE)

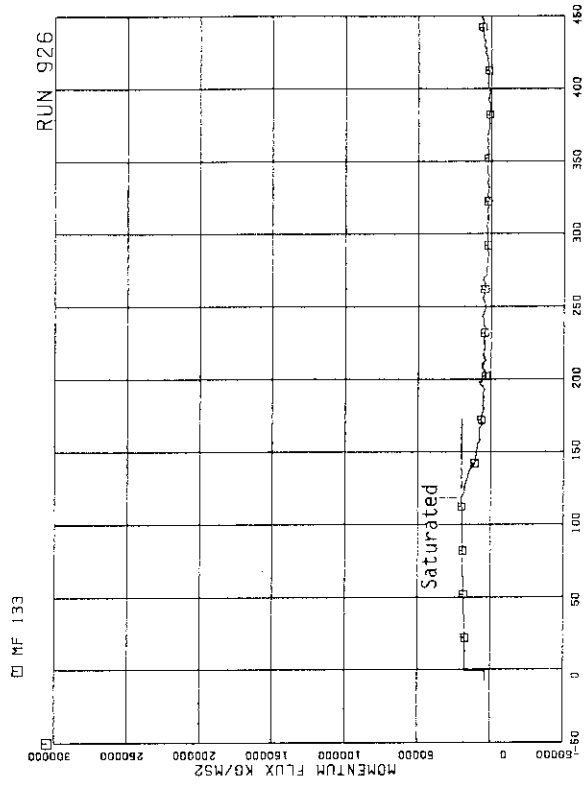

FIG.5. 76 MOMENTUM FLUX AT BREAK B SPOOL PIECE (LOW RANGE)

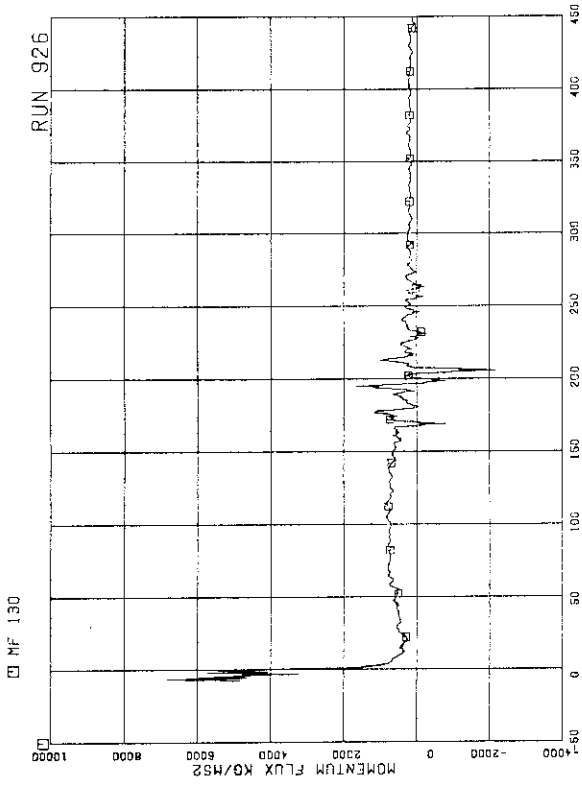

FIG.5. 73 MOMENTUM FLUX AT JP-1,2 OUTLET SPOOL

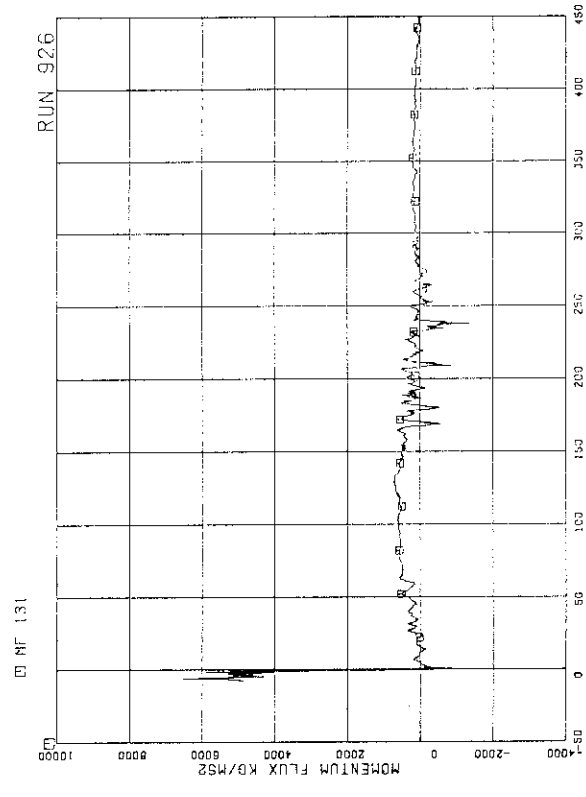

FIG.5. 74 MOMENTUM FLUX AT JP-3,4 OUTLET SPOOL

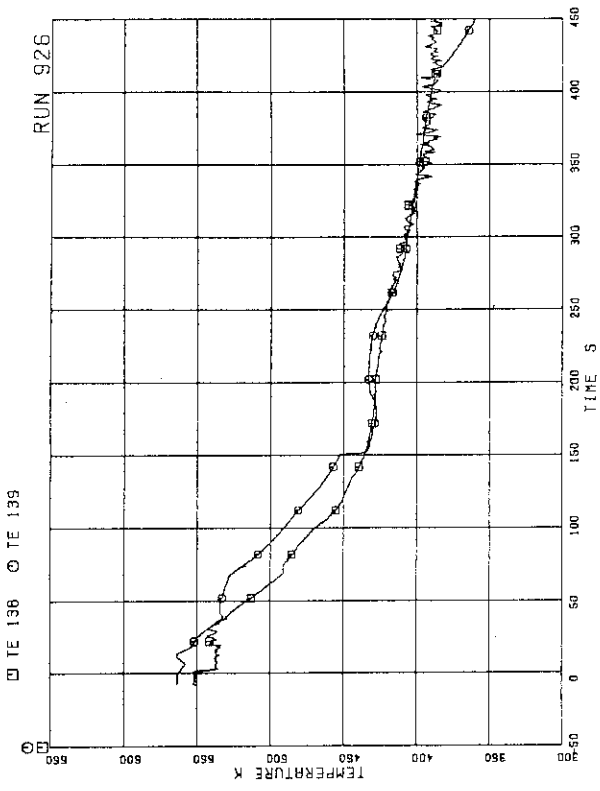

FIG.5. 79 FLUID TEMPERATURES IN LOWER PLENUM AND UPPER PLENUM

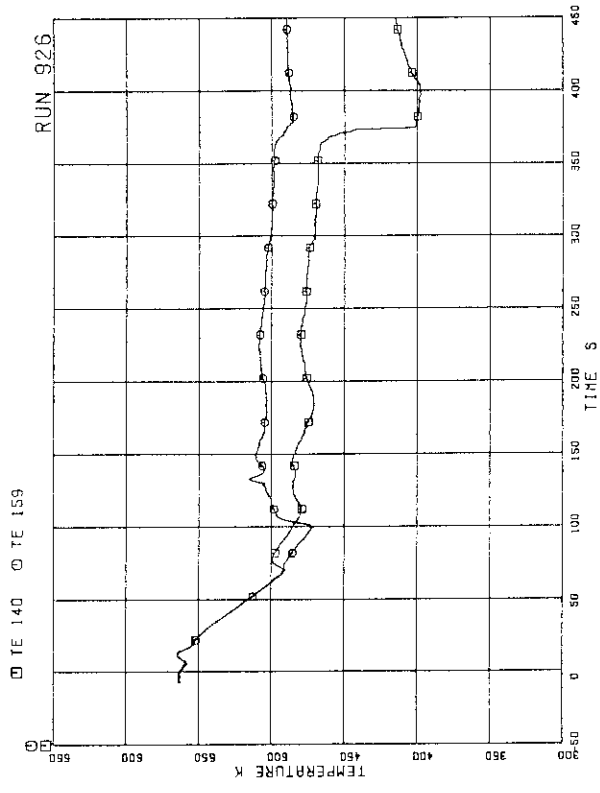

FIG.5. 80 FLUID TEMPERATURES IN STEAM DOME AND MSL

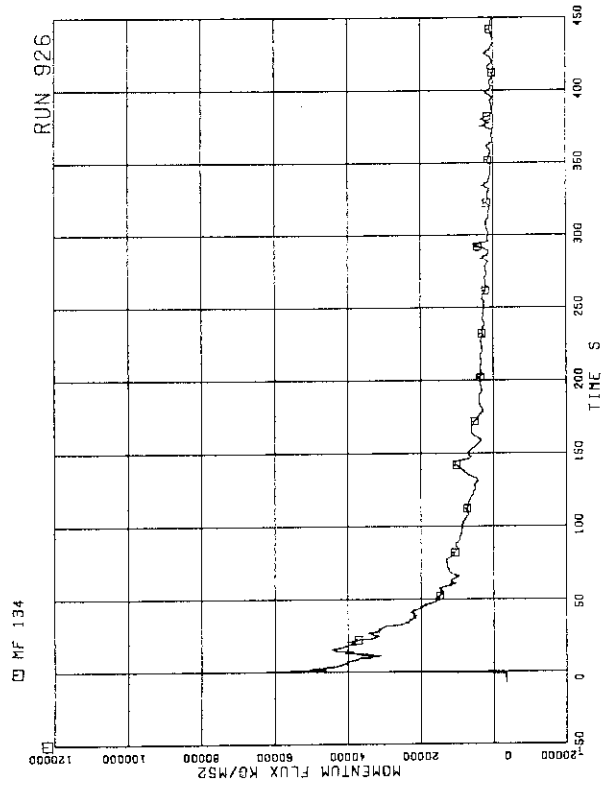

FIG.5. 77 MOMENTUM FLUX AT BREAK A SPOOL PIECE (HIGH RANGE)

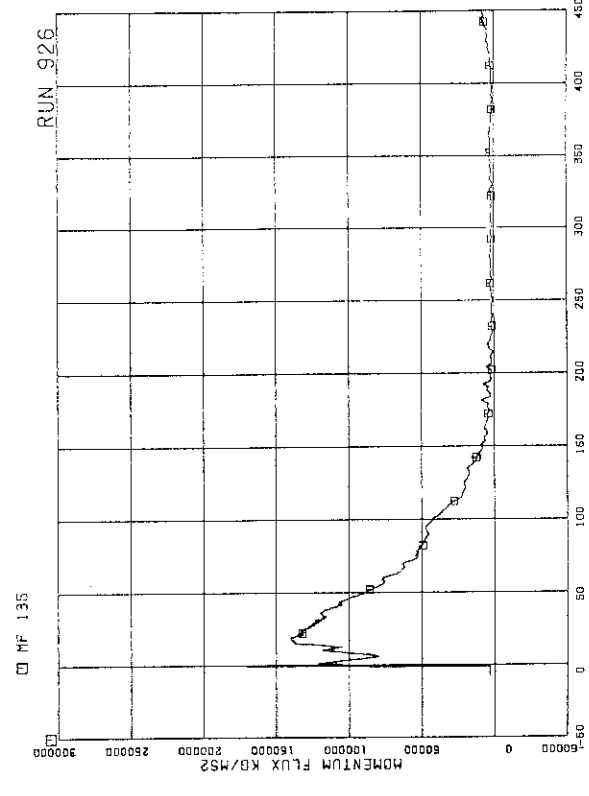

FIG.5. 78 MOMENTUM FLUX AT BREAK B SPOOL PIECE (HIGH RANGE)

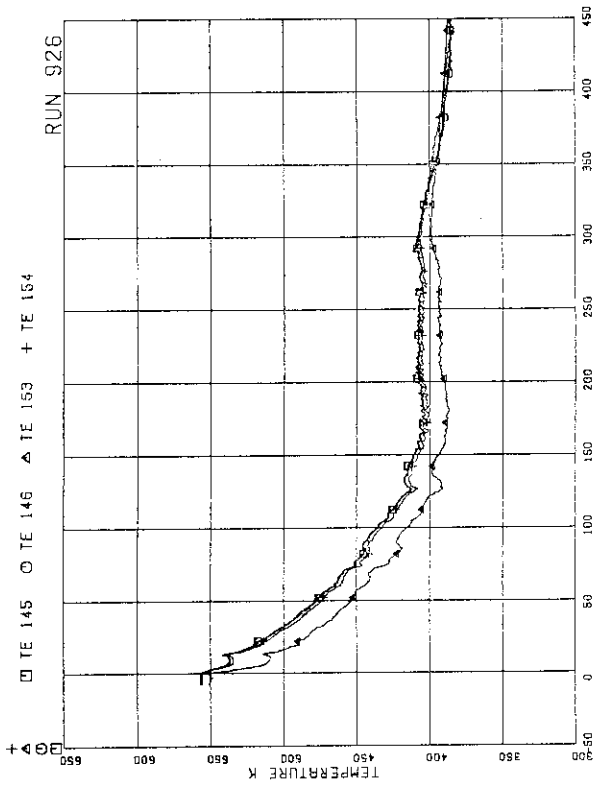

FIG.5. 83 FLUID TEMPERATURES IN BROKEN RECIRCULATION LOOP

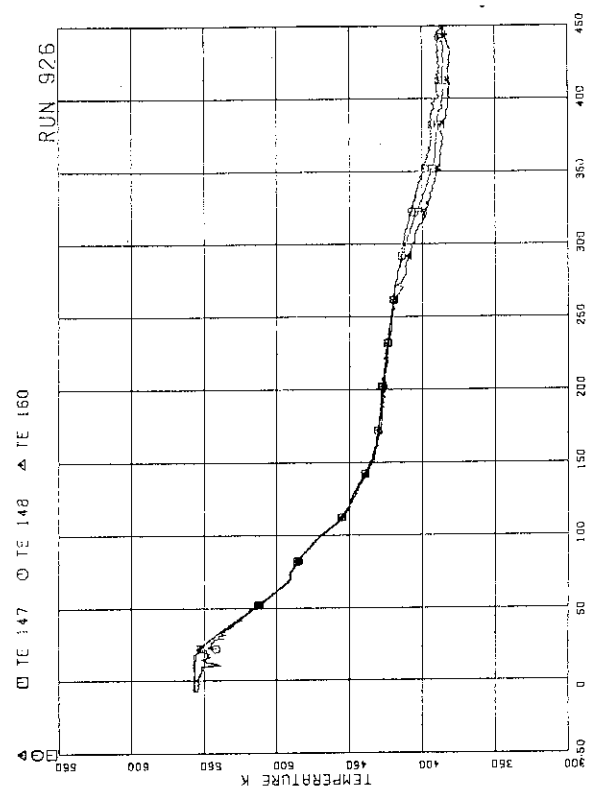

FIG.5. 84 FLUID TEMPERATURES AT JP-1,2 OUTLET

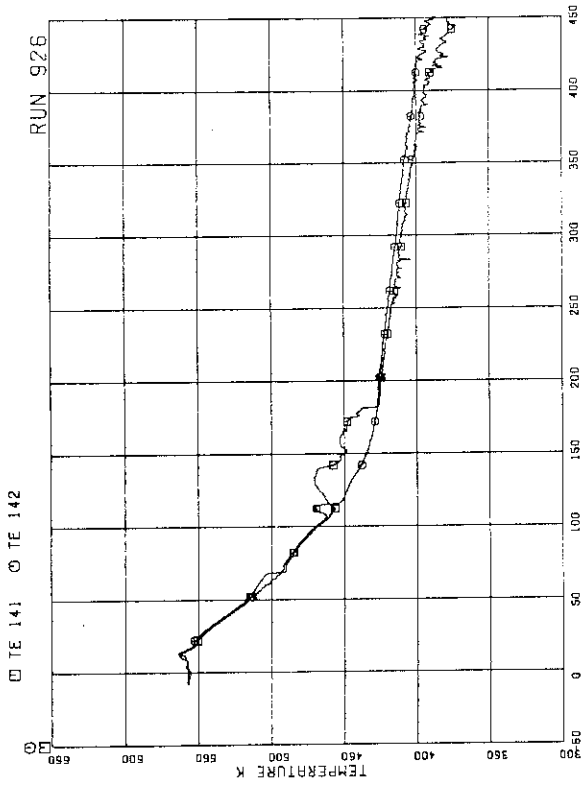

FIG.5. 81 FLUID TEMPERATURES IN DOWNCOMER

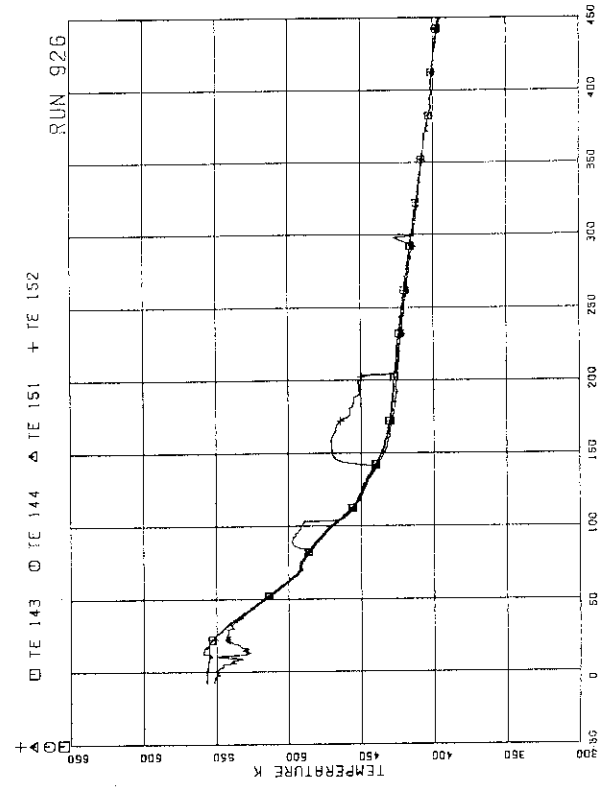

FIG.5. 82 FLUID TEMPERATURES IN INTACT RECIRCULATION LOOP

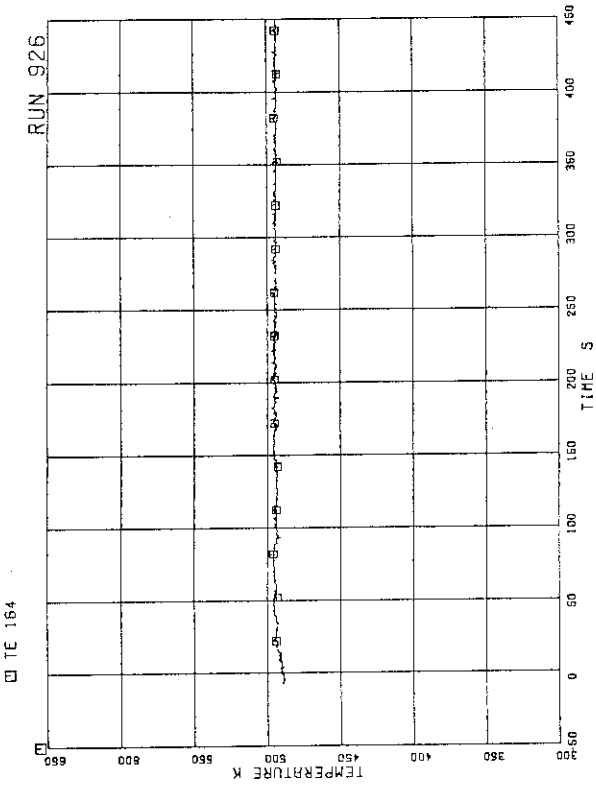

FIG.5. 87 FEEDWATER TEMPERATURE

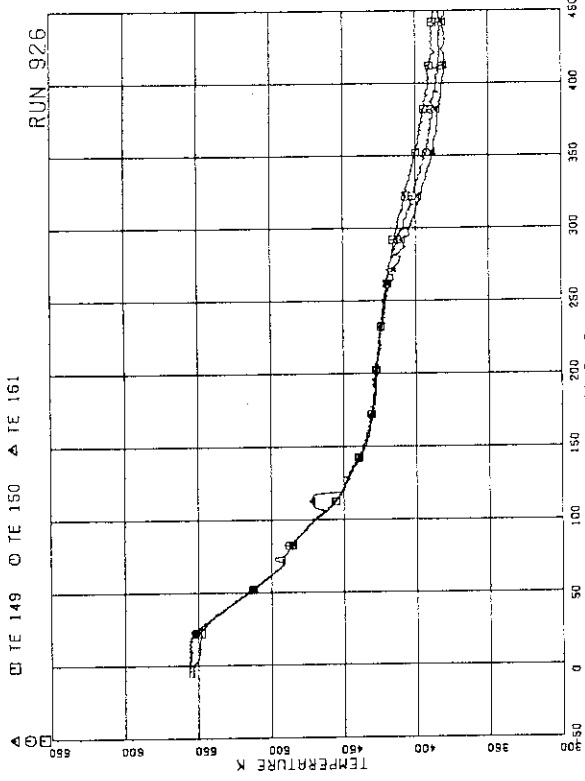

FIG.5. 85 FLUID TEMPERATURES AT JP-3,4 OUTLET

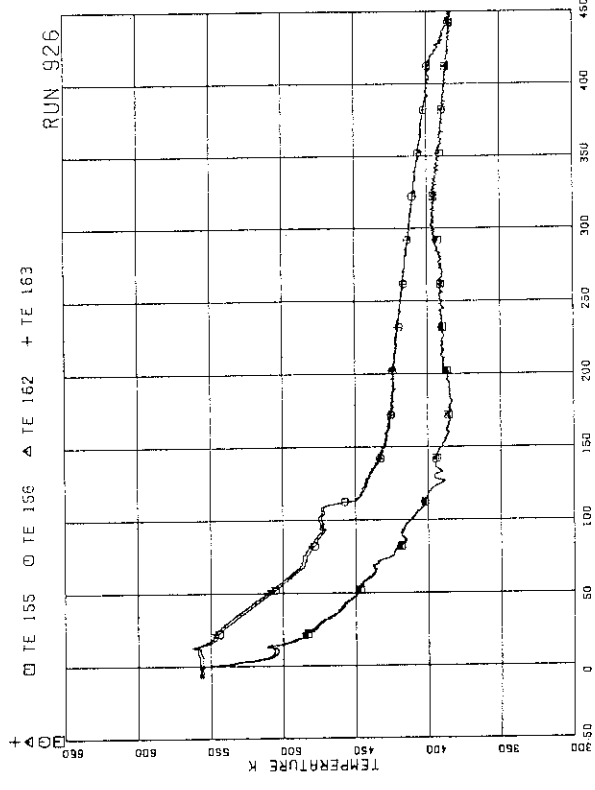

FIG.5. 86 FLUID TEMPERATURES NEAR BREAKS A AND B

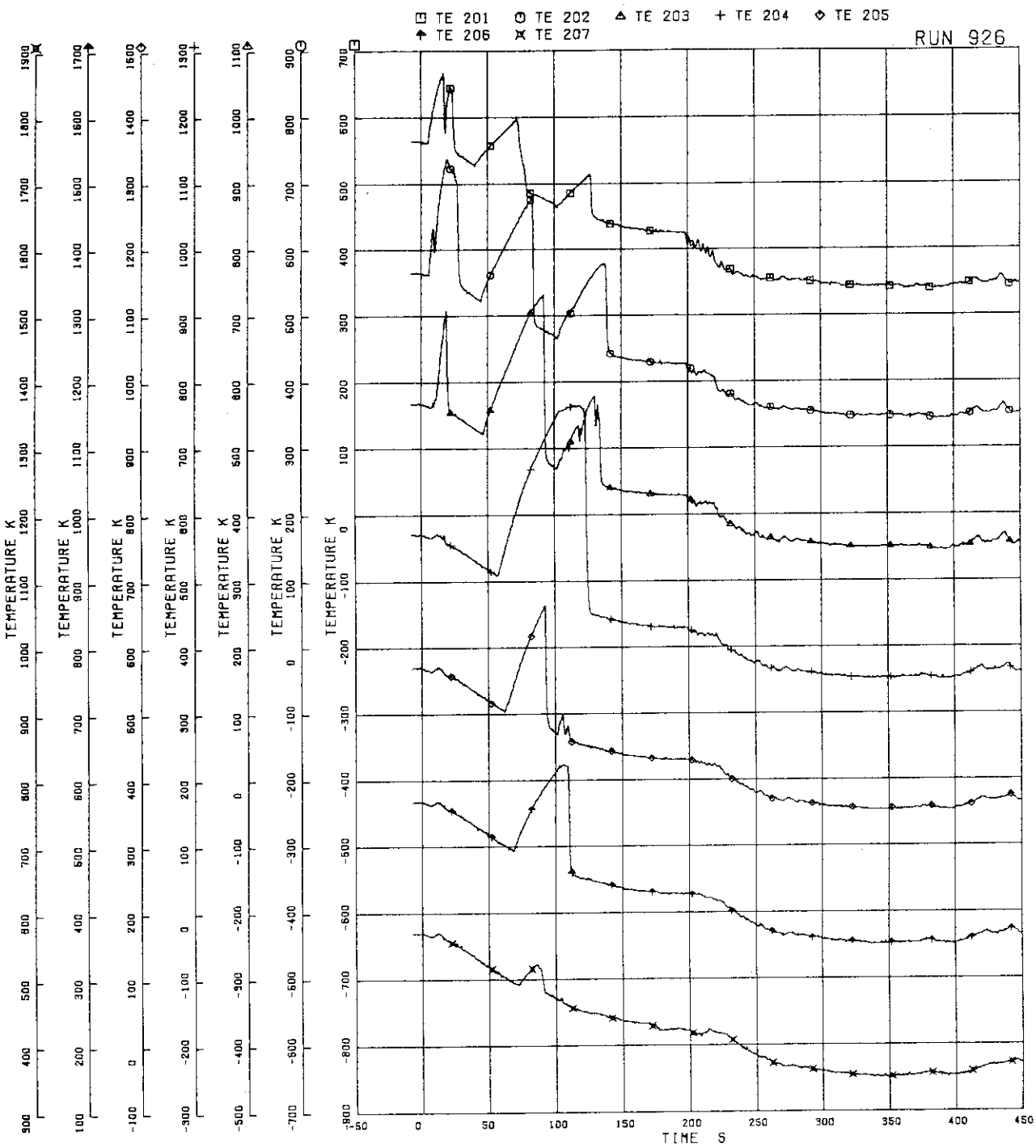

FIG.5. 88 SURFACE TEMPERATURES OF FUEL ROD A11

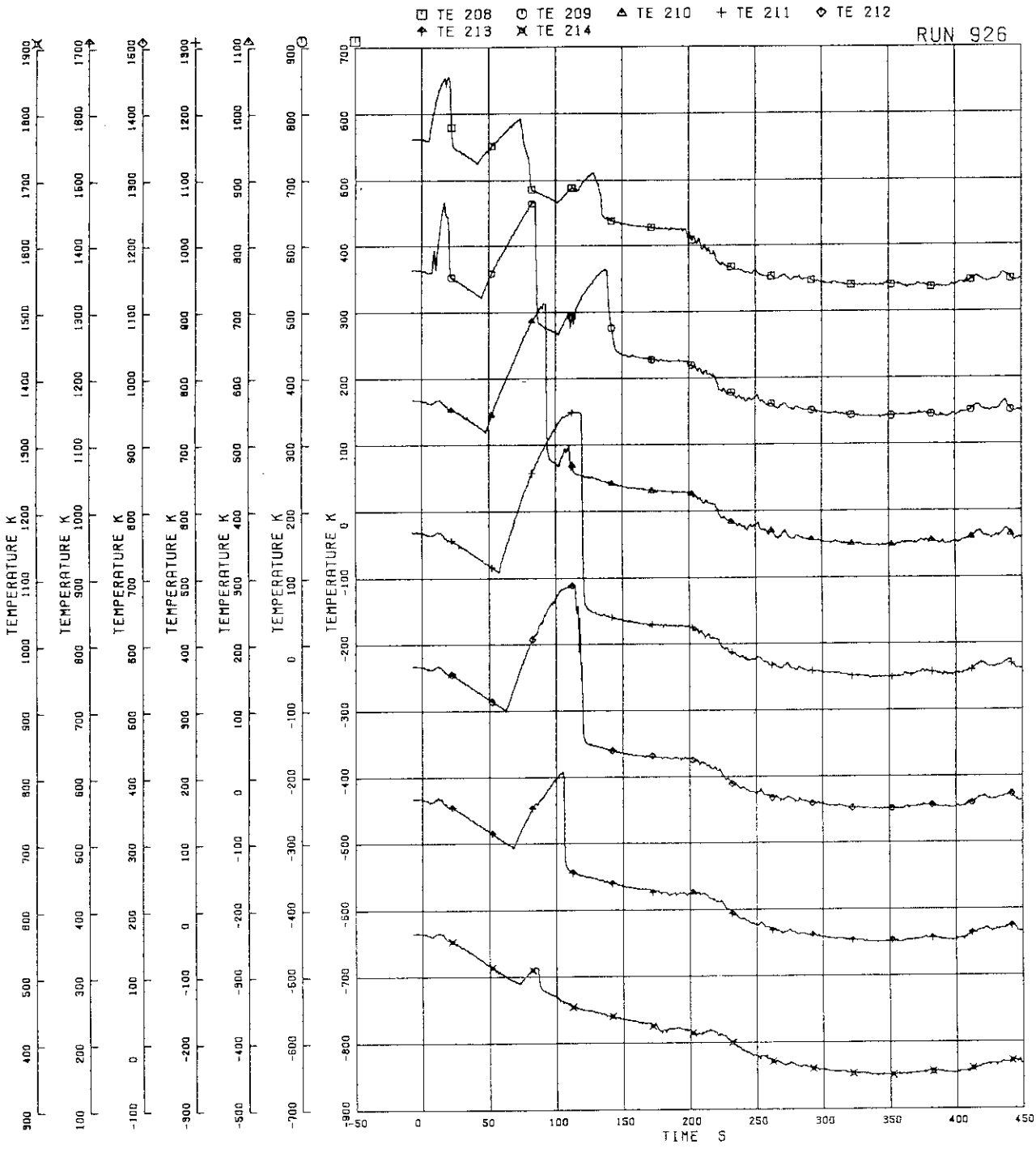

FIG.5. 89 SURFACE TEMPERATURES OF FUEL ROD A12

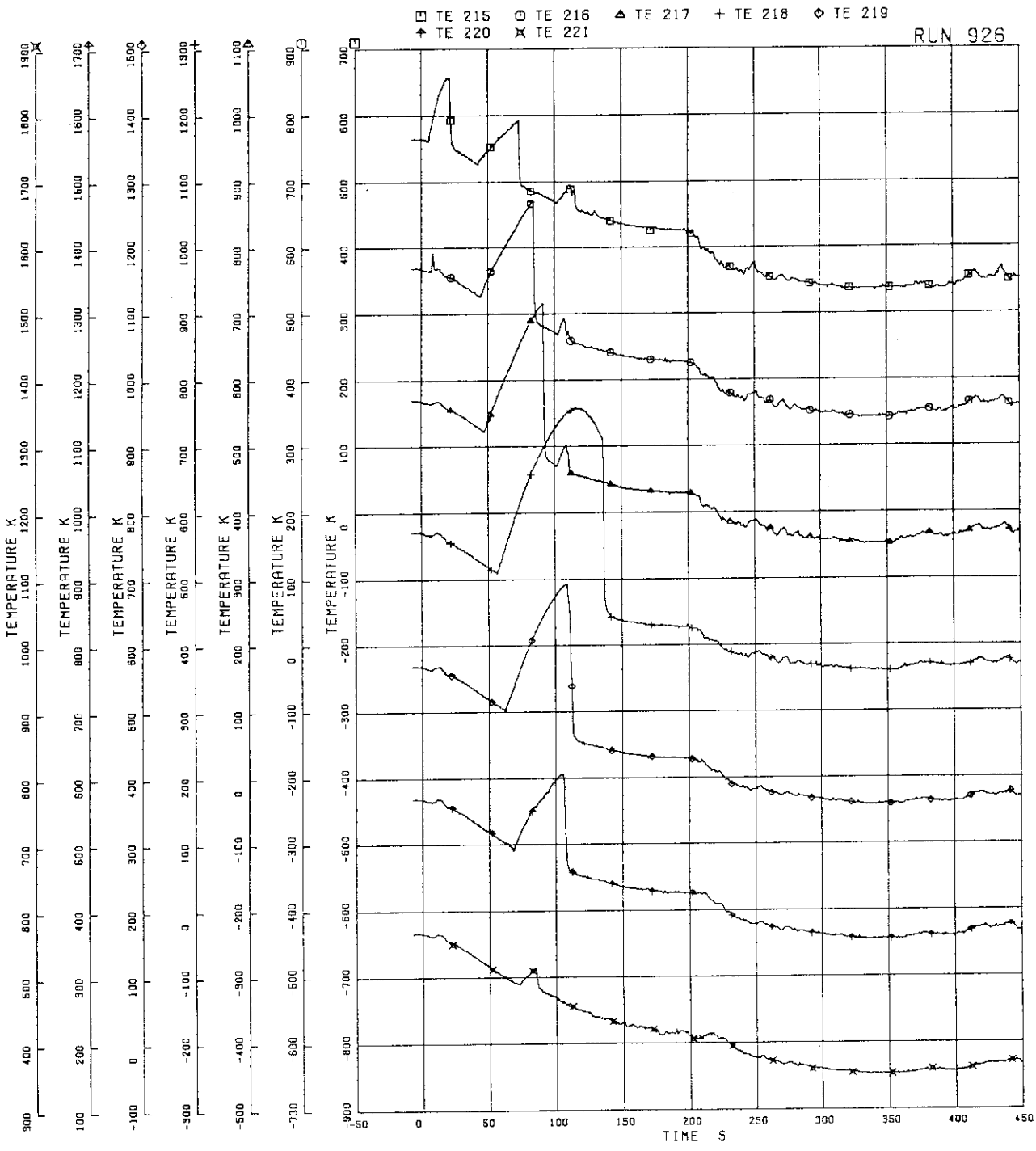

FIG.5. 90 SURFACE TEMPERATURES OF FUEL ROD A13

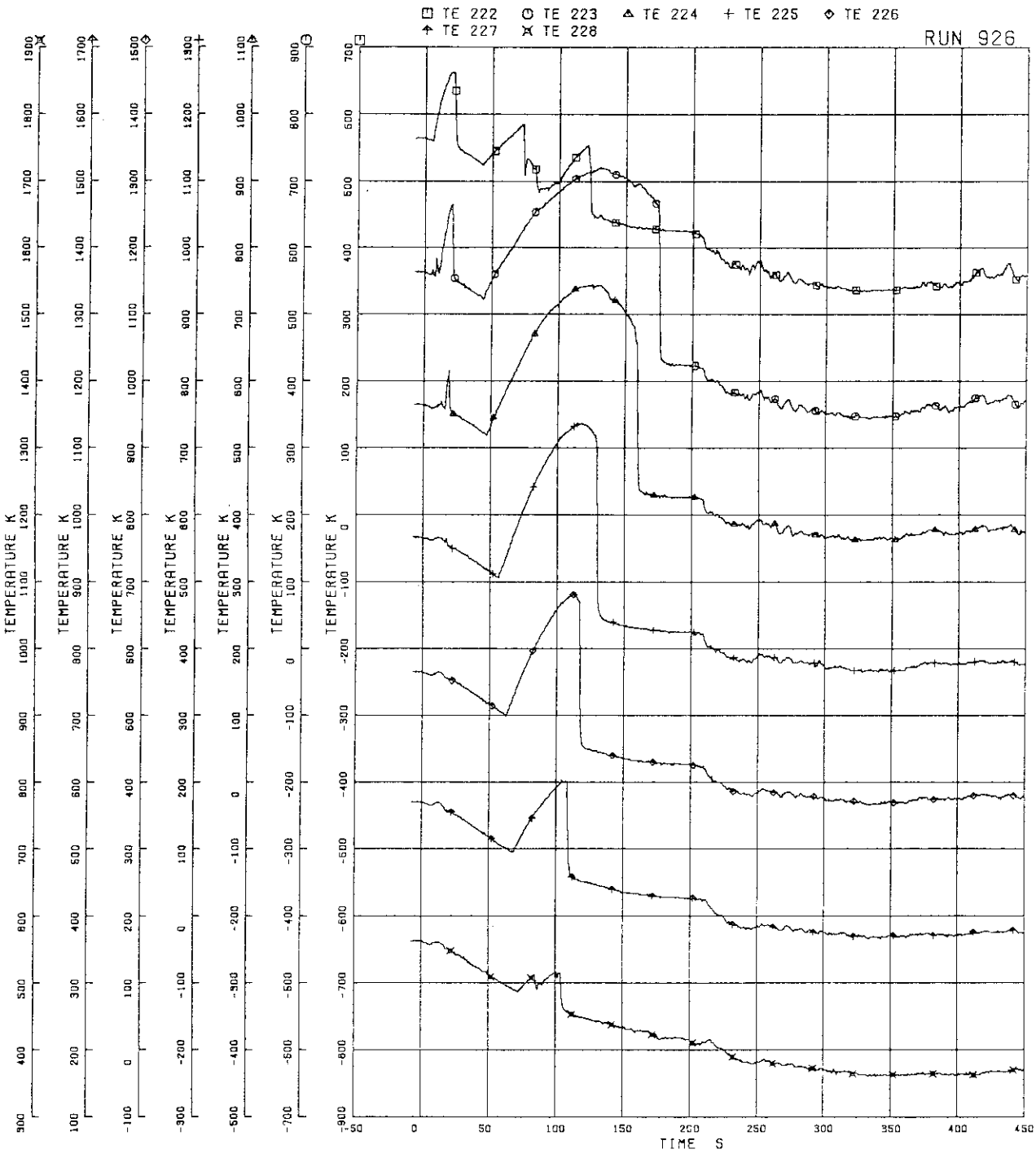

FIG.5. 91 SURFACE TEMPERATURES OF FUEL ROD A14

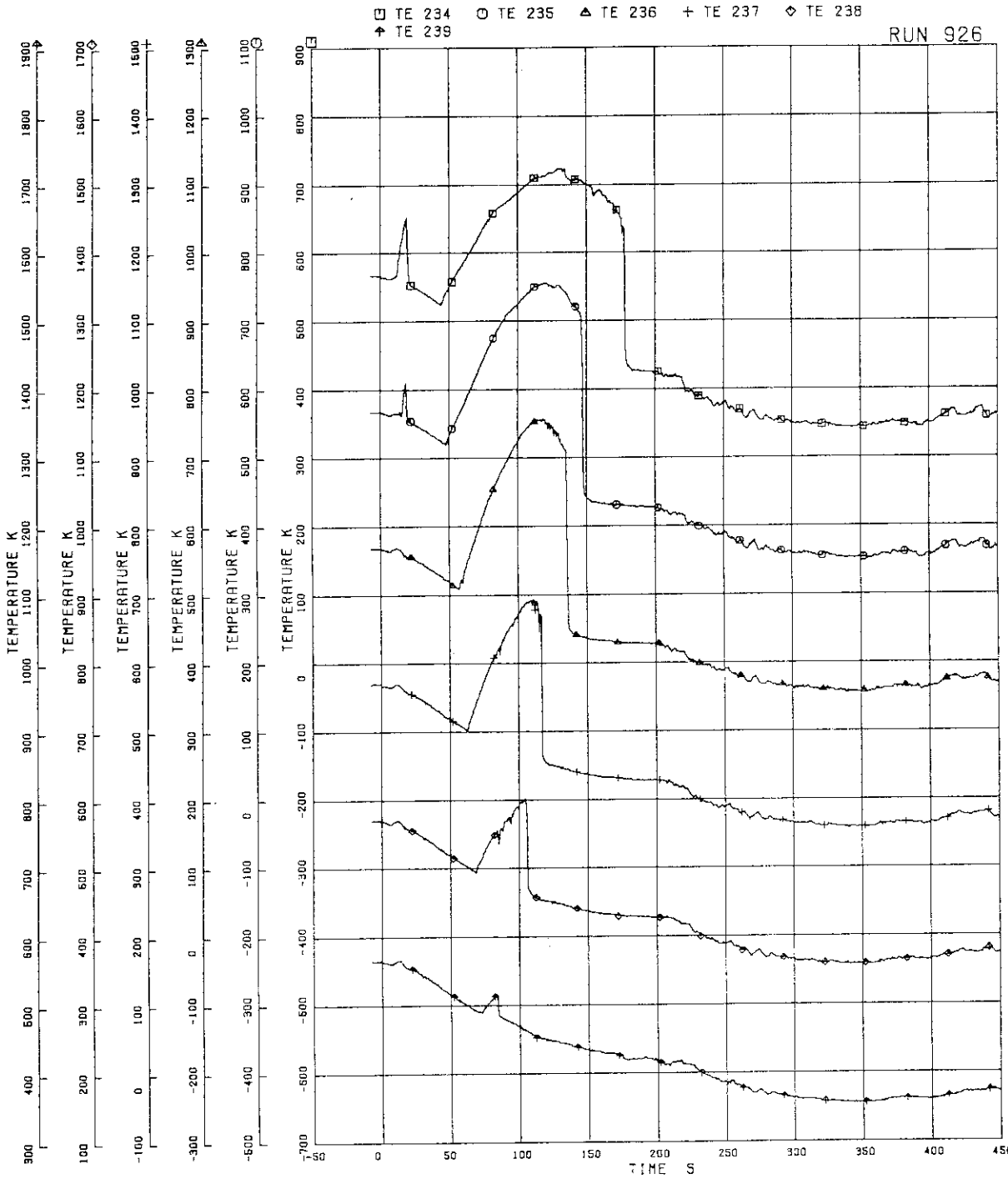

FIG.5. 92 SURFACE TEMPERATURES OF FUEL ROD A15

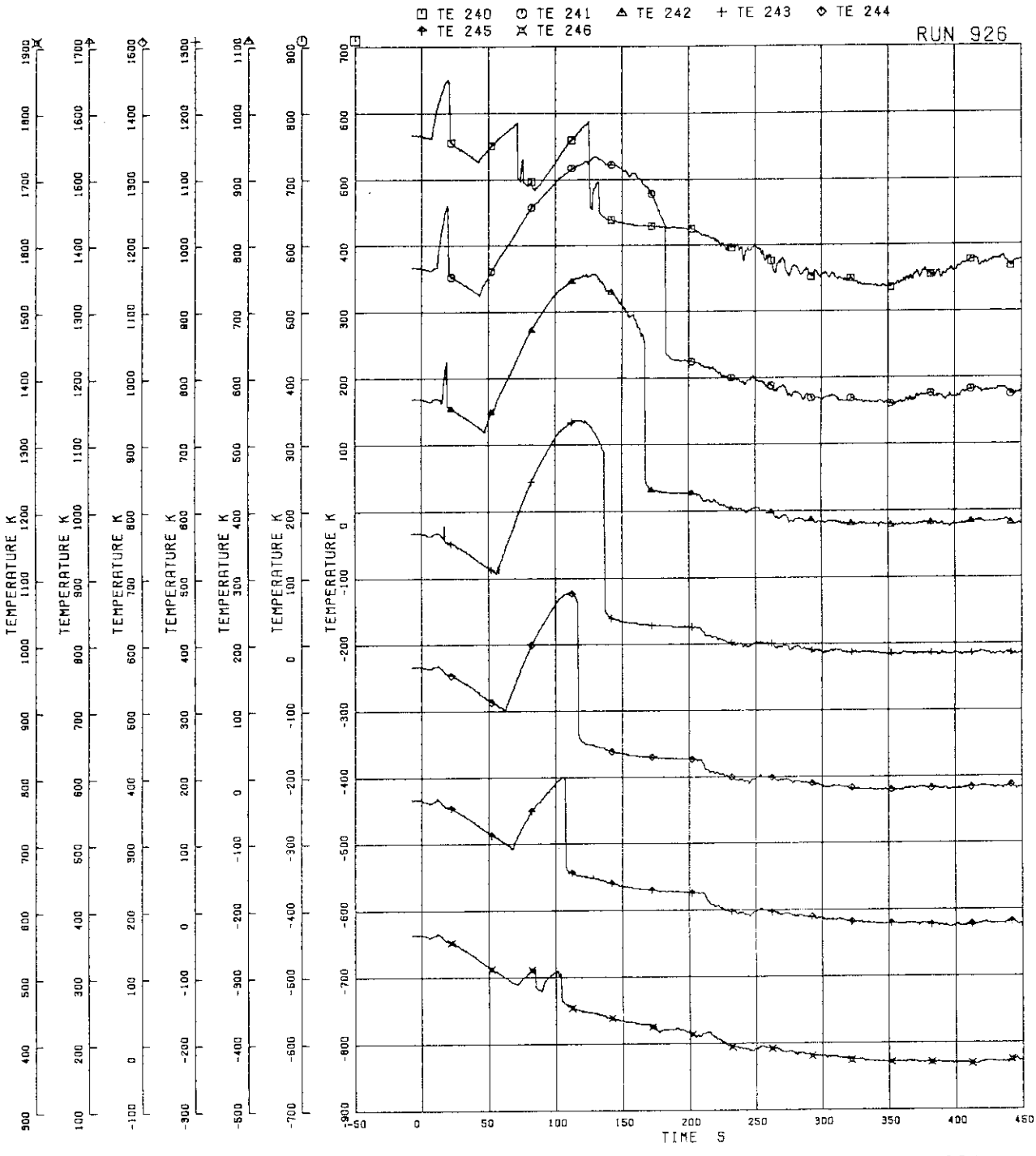

FIG.5. 93 SURFACE TEMPERATURES OF FUEL ROD A24

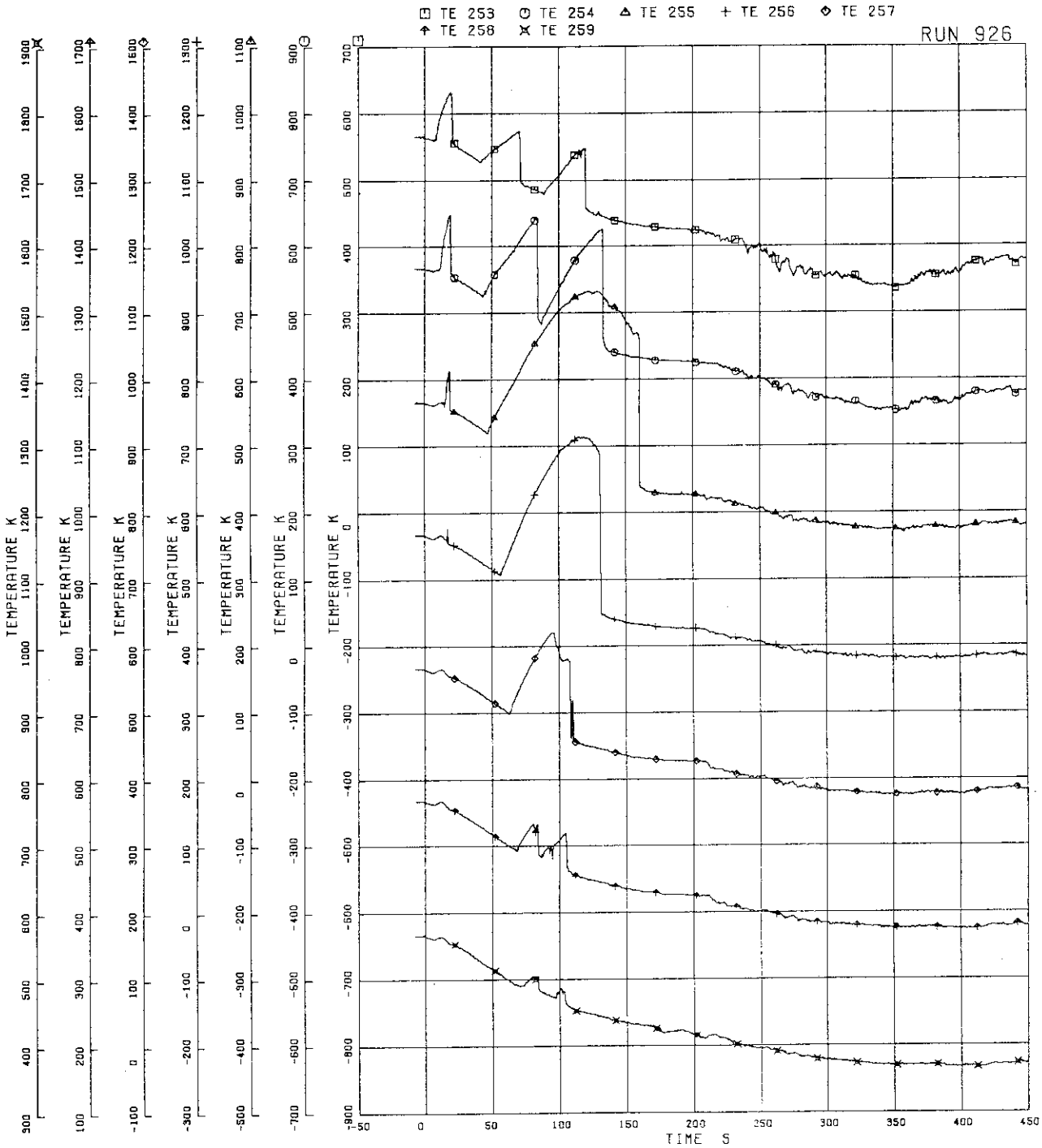

FIG.5. 94 SURFACE TEMPERATURES OF FUEL ROD A33

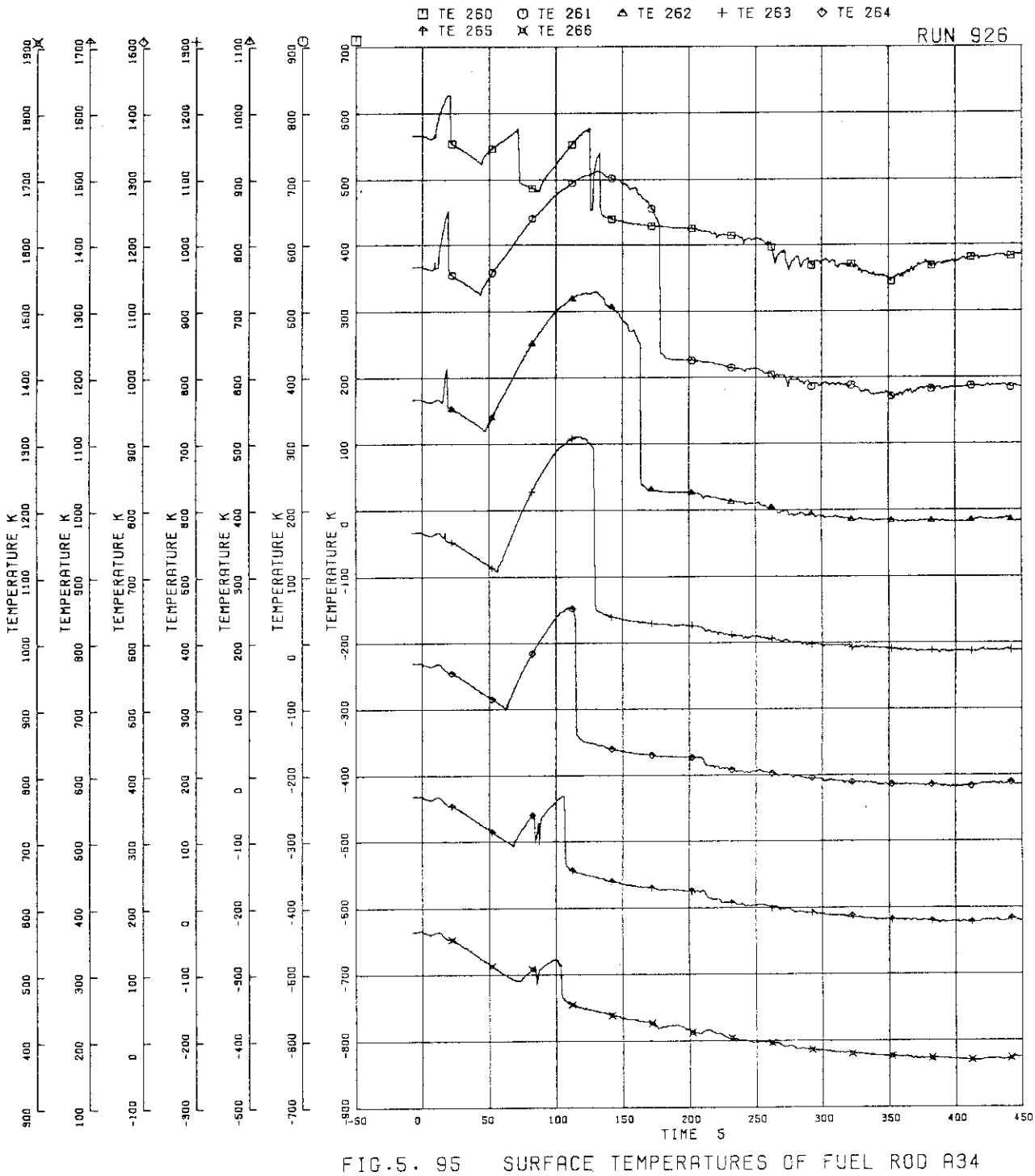

FIG.5. 95 SURFACE TEMPERATURES OF FUEL ROD A34

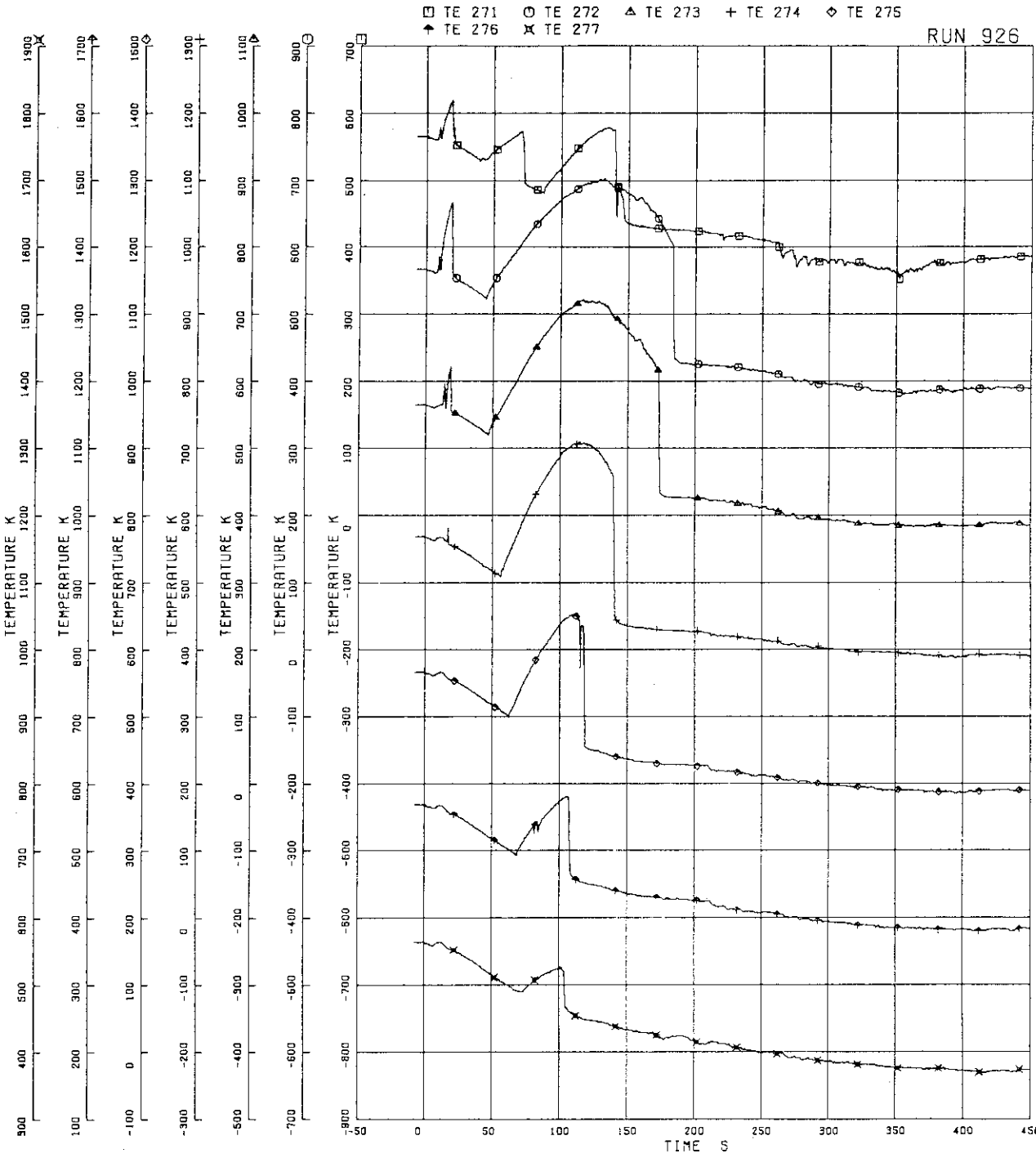

FIG.5. 96 SURFACE TEMPERATURES OF FUEL ROD A44

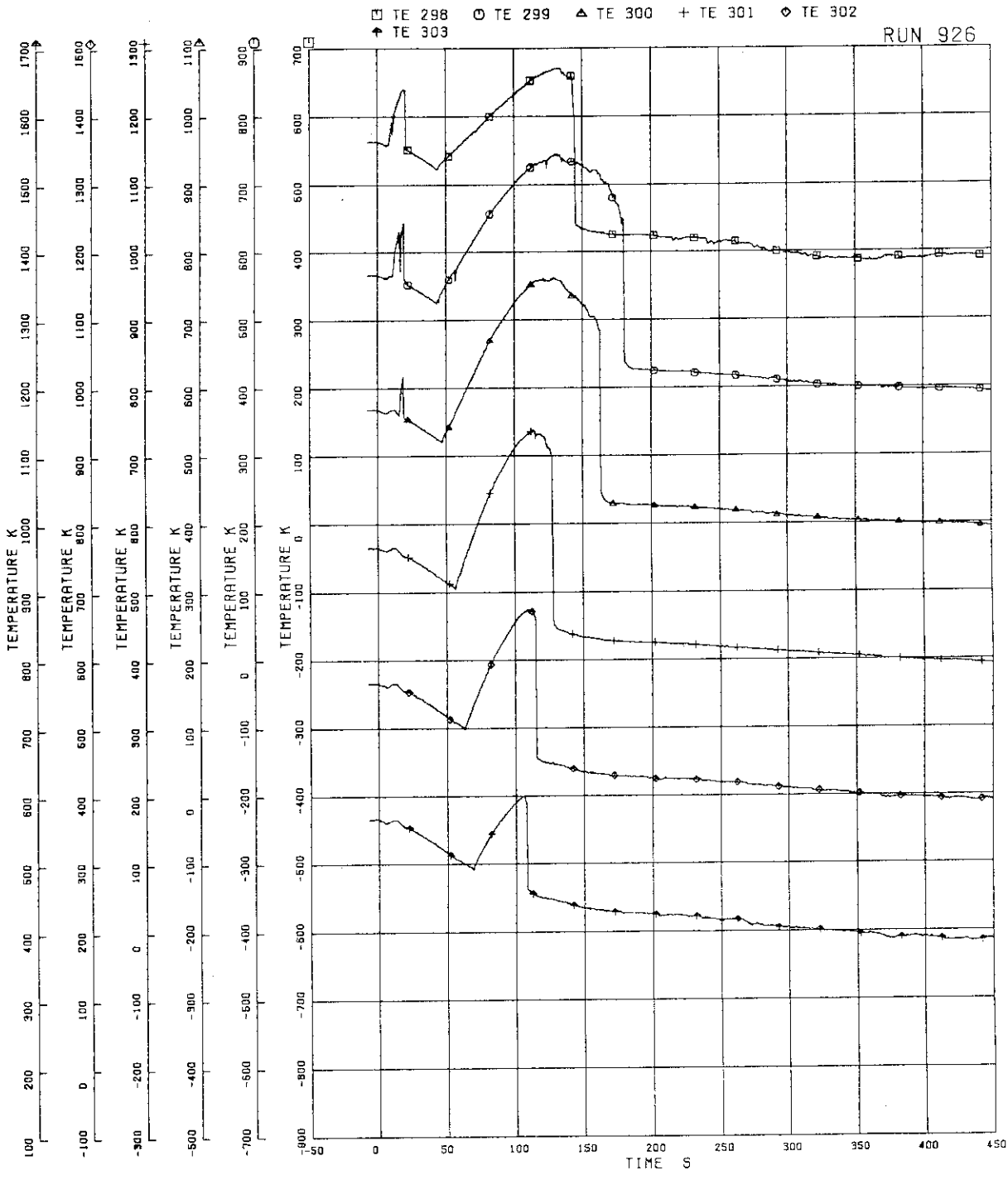

FIG.5. 97 SURFACE TEMPERATURES OF FUEL ROD A77

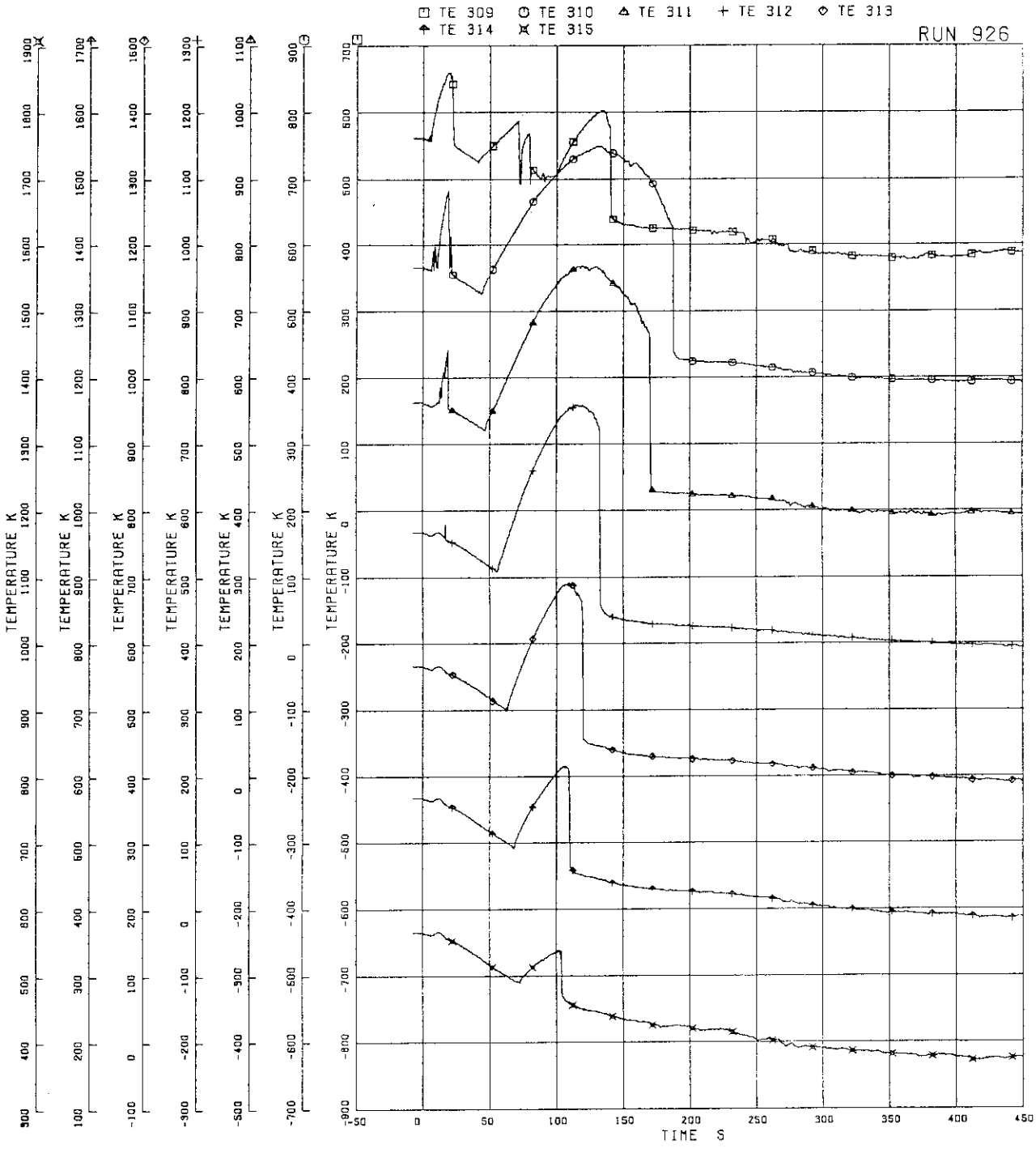

FIG.5. 98 SURFACE TEMPERATURES OF FUEL ROD A85

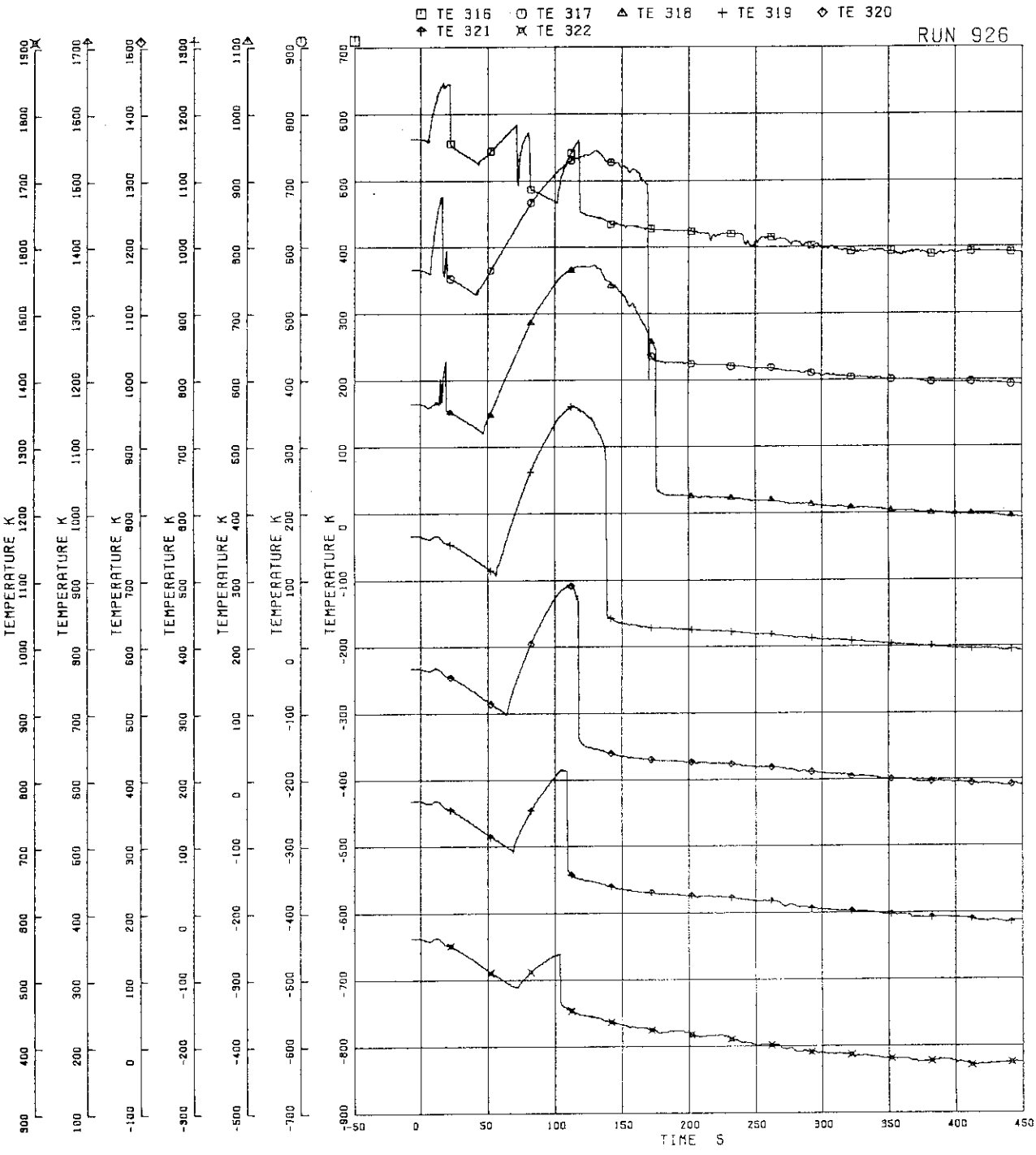

FIG.5. 99 SURFACE TEMPERATURES OF FUEL ROD A87

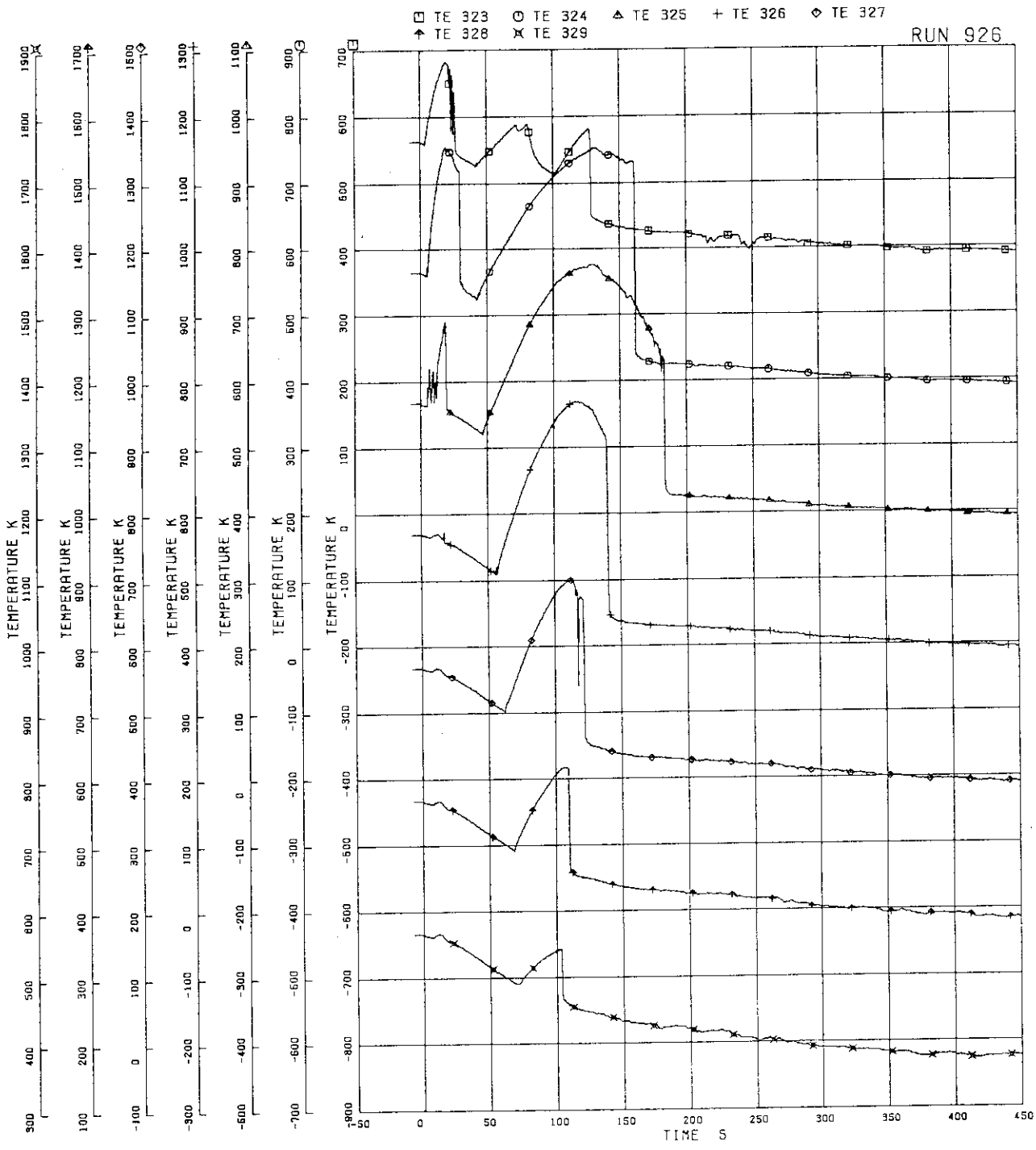

FIG.5.100 SURFACE TEMPERATURES OF FUEL ROD A88

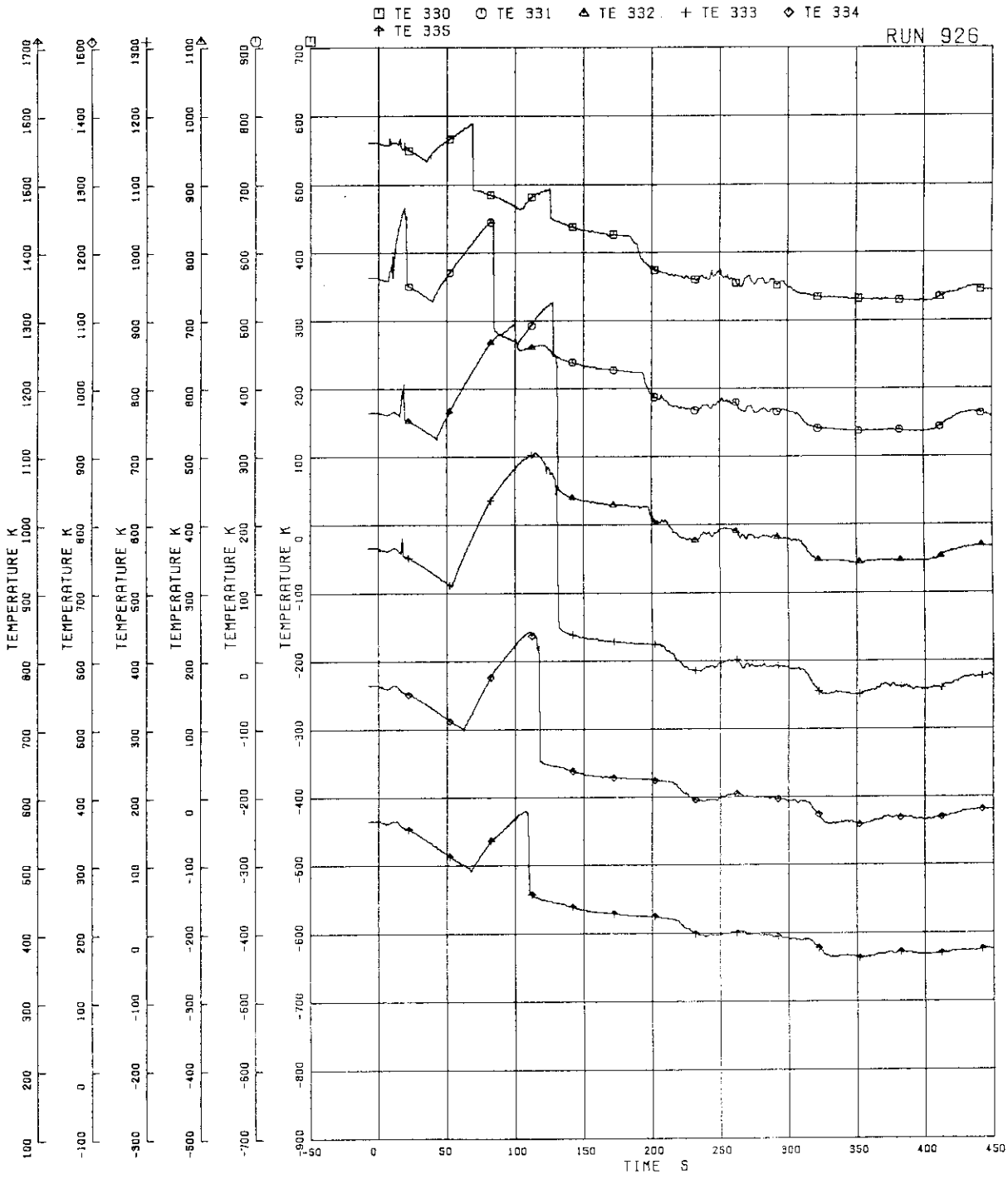

FIG.5.101 SURFACE TEMPERATURES OF FUEL ROD B11

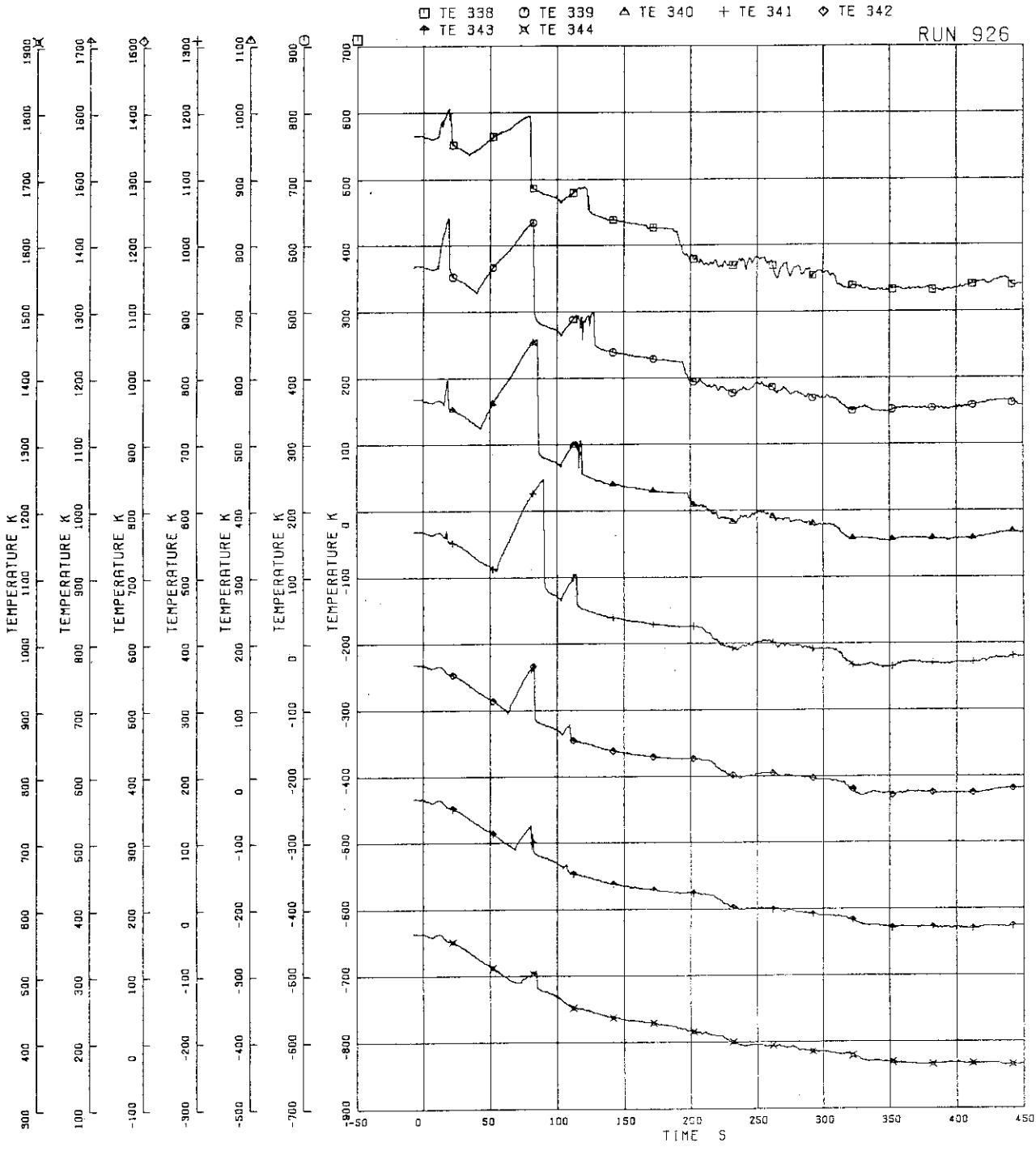

FIG.5.102 SURFACE TEMPERATURES OF FUEL ROD B22

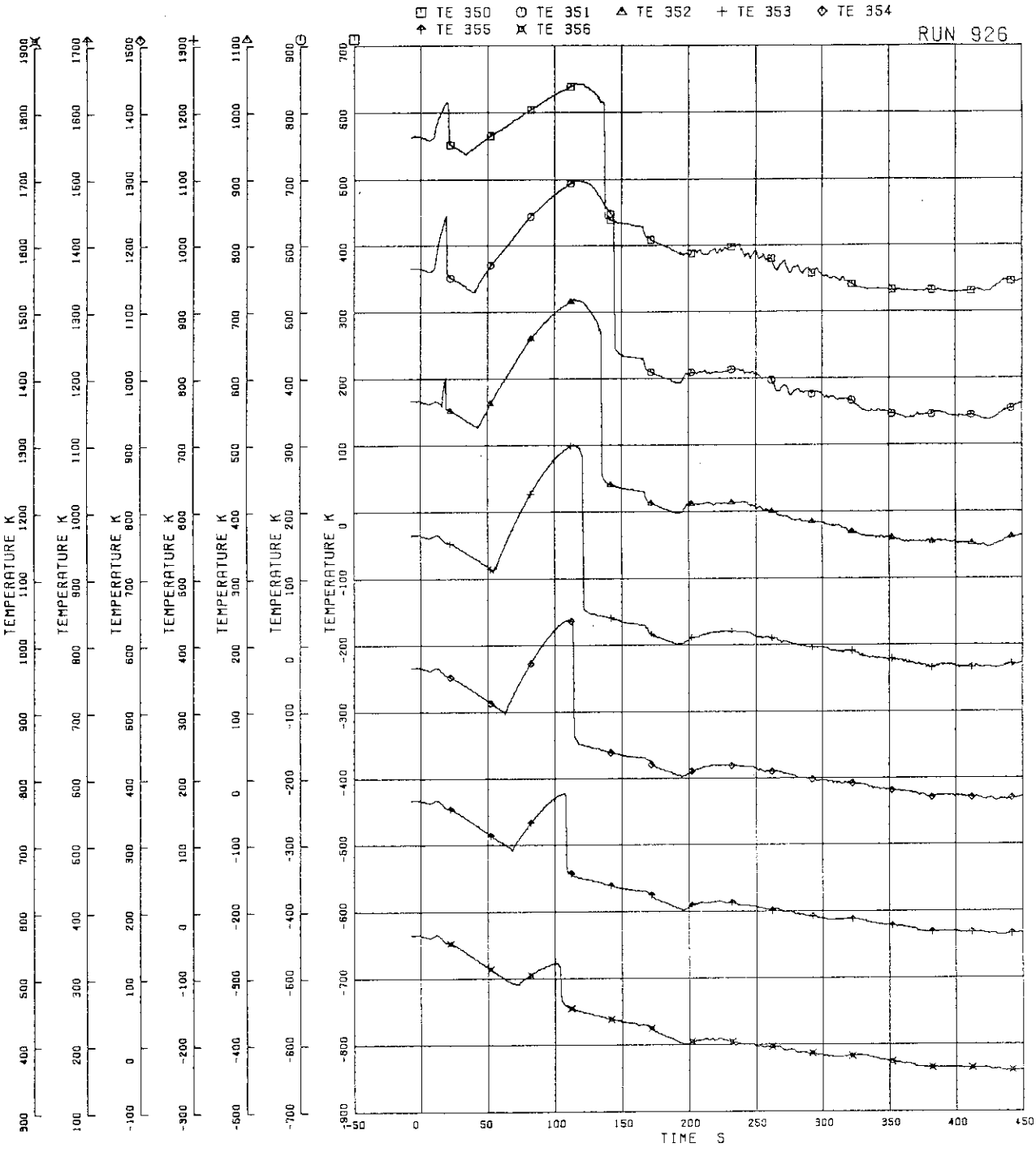

FIG.5.103 SURFACE TEMPERATURES OF FUEL ROD B77

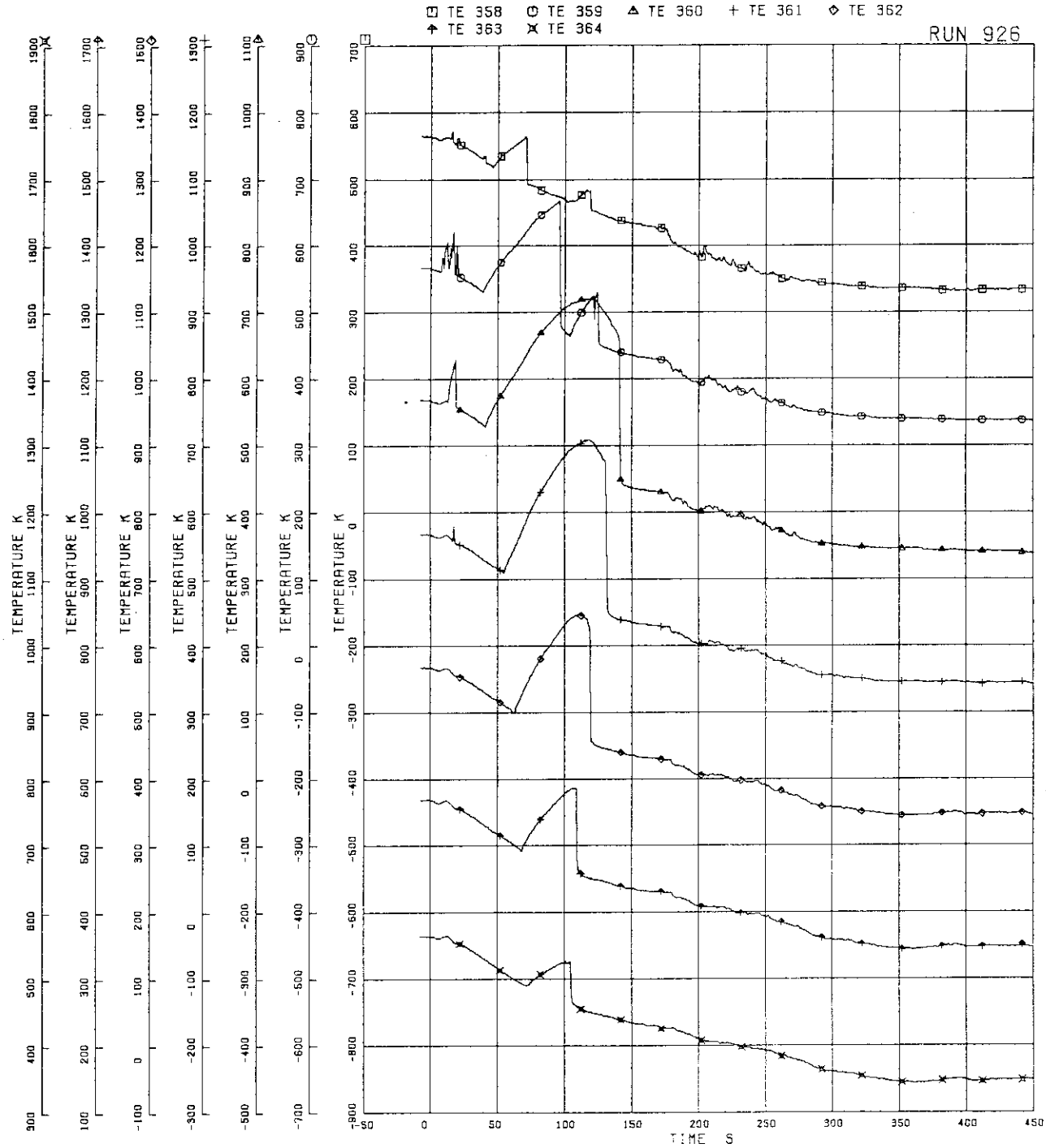

FIG.5.104 SURFACE TEMPERATURES OF FUEL ROD C11

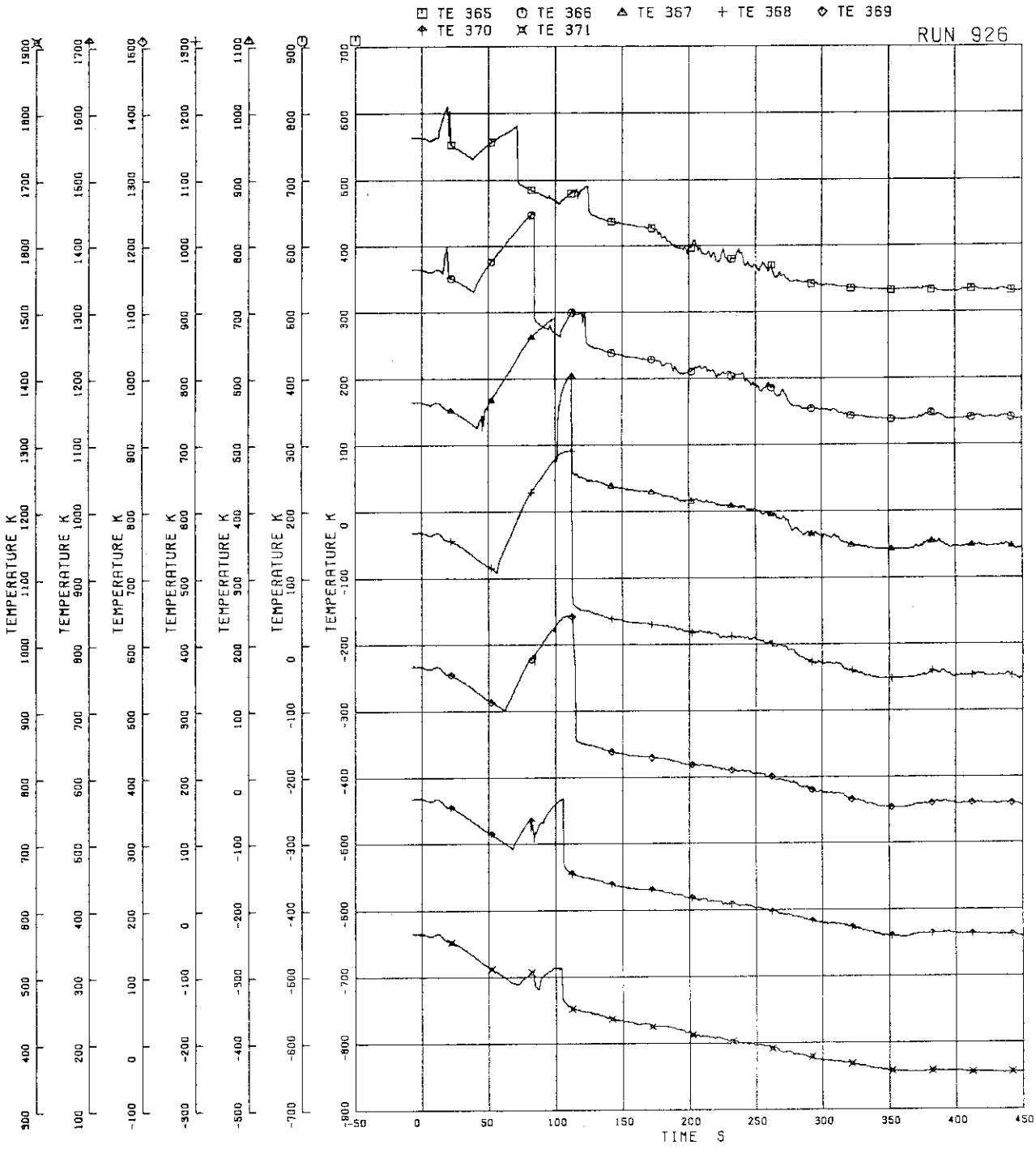

FIG.5.105 SURFACE TEMPERATURES OF FUEL ROD C13

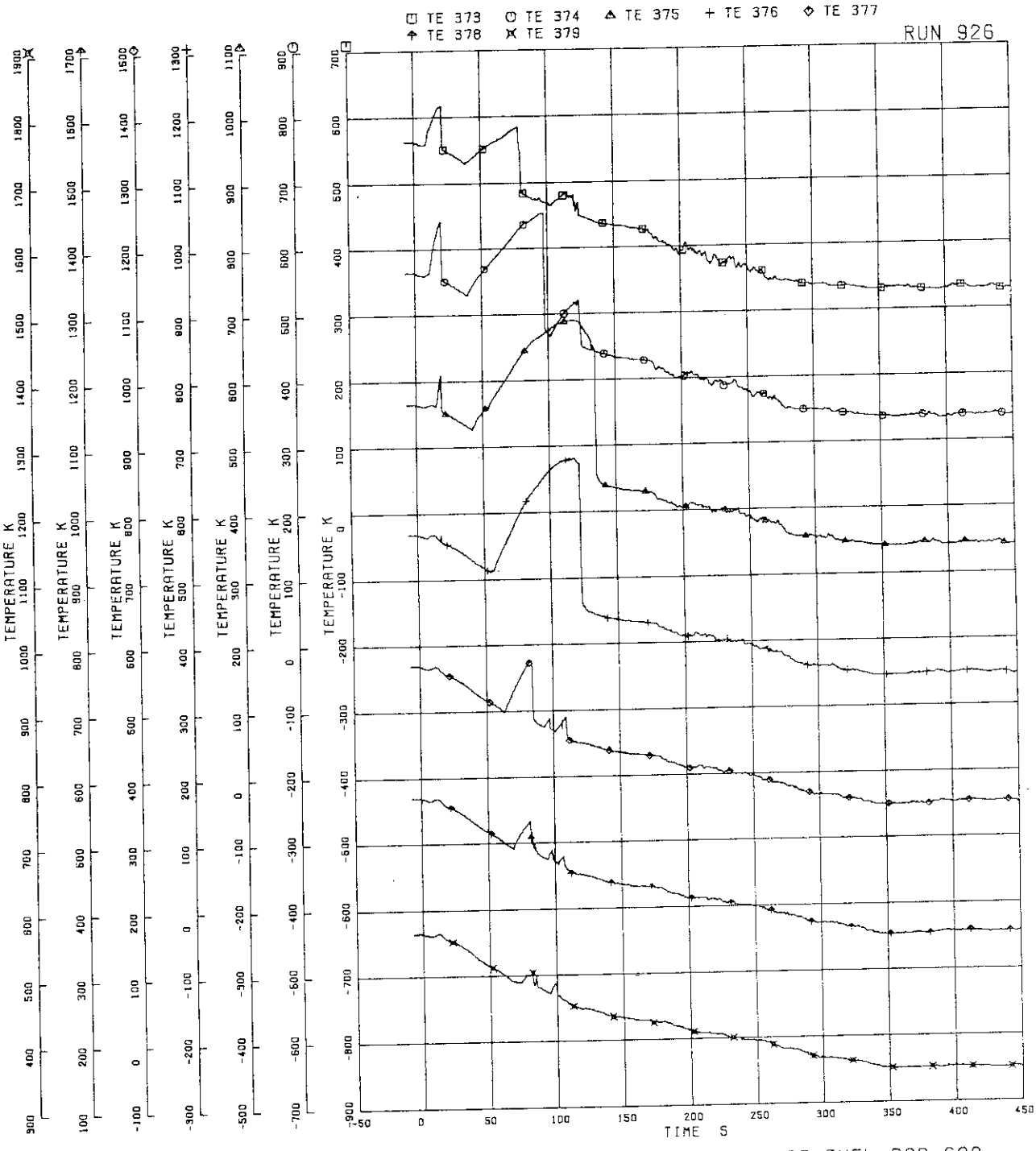

FIG.5.106 SURFACE TEMPERATURES OF FUEL ROD C22

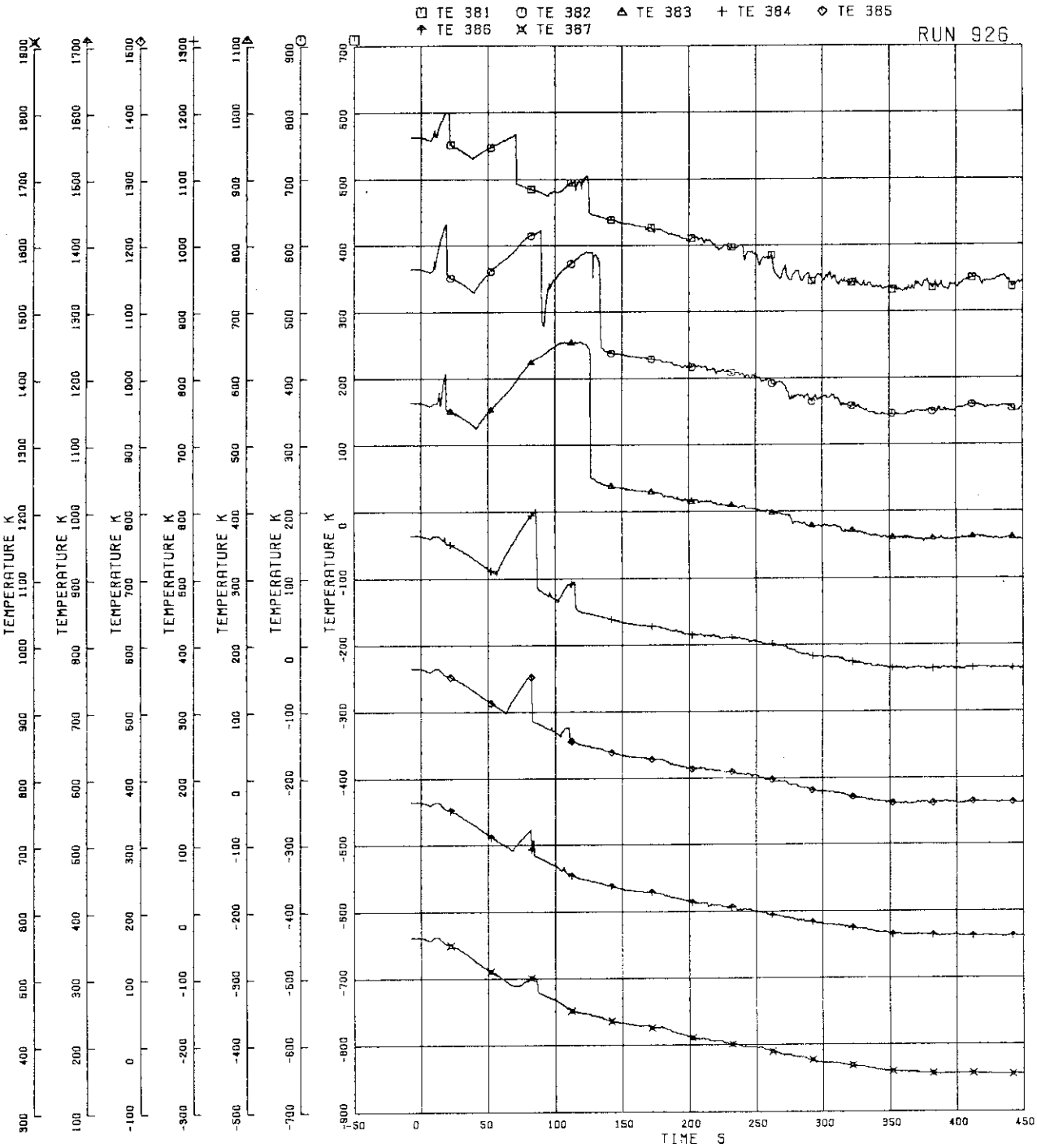

FIG.5.107 SURFACE TEMPERATURES OF FUEL ROD C33

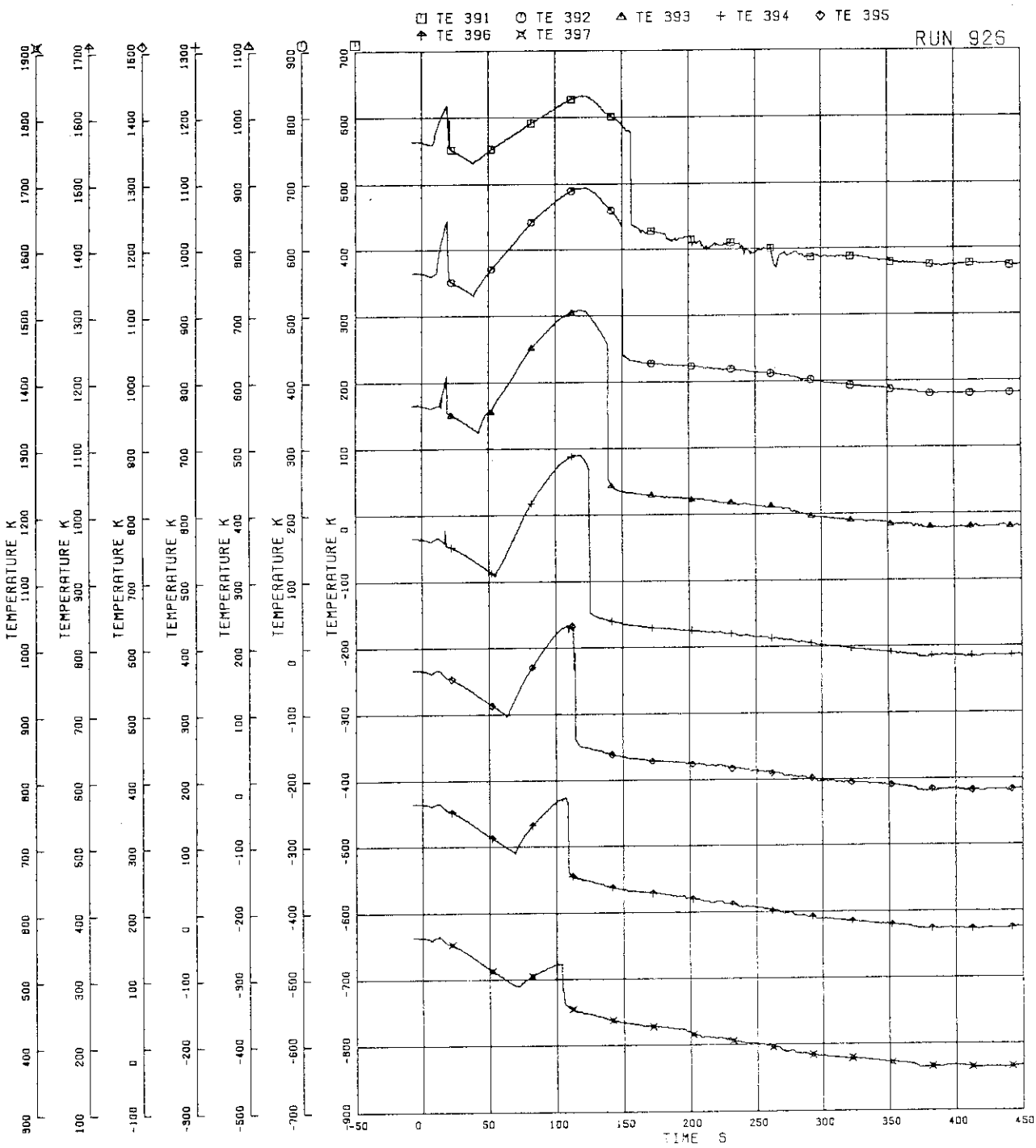

FIG.5.108 SURFACE TEMPERATURES OF FUEL ROD C77

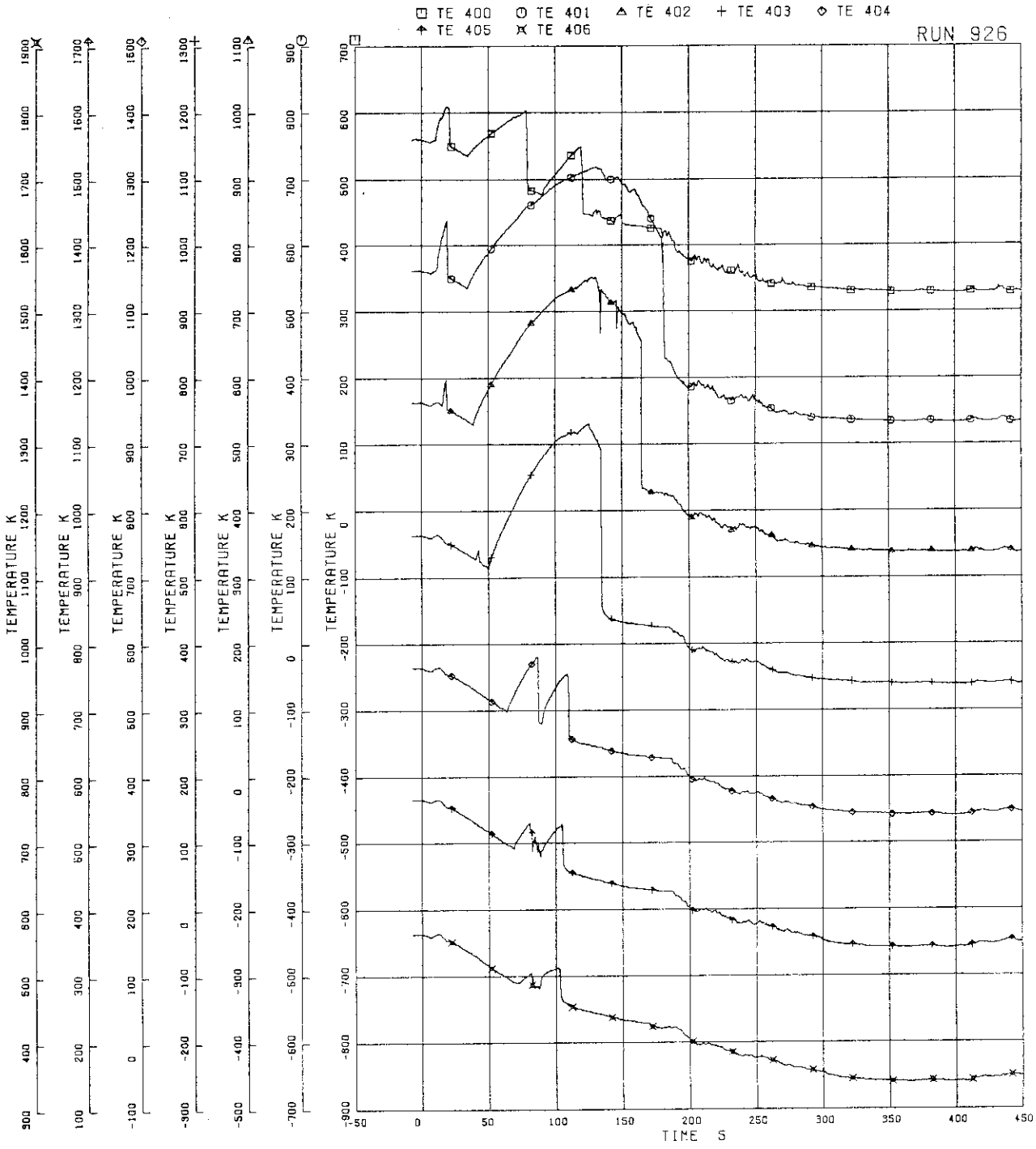

FIG.5.109 SURFACE TEMPERATURES OF FUEL ROD D22

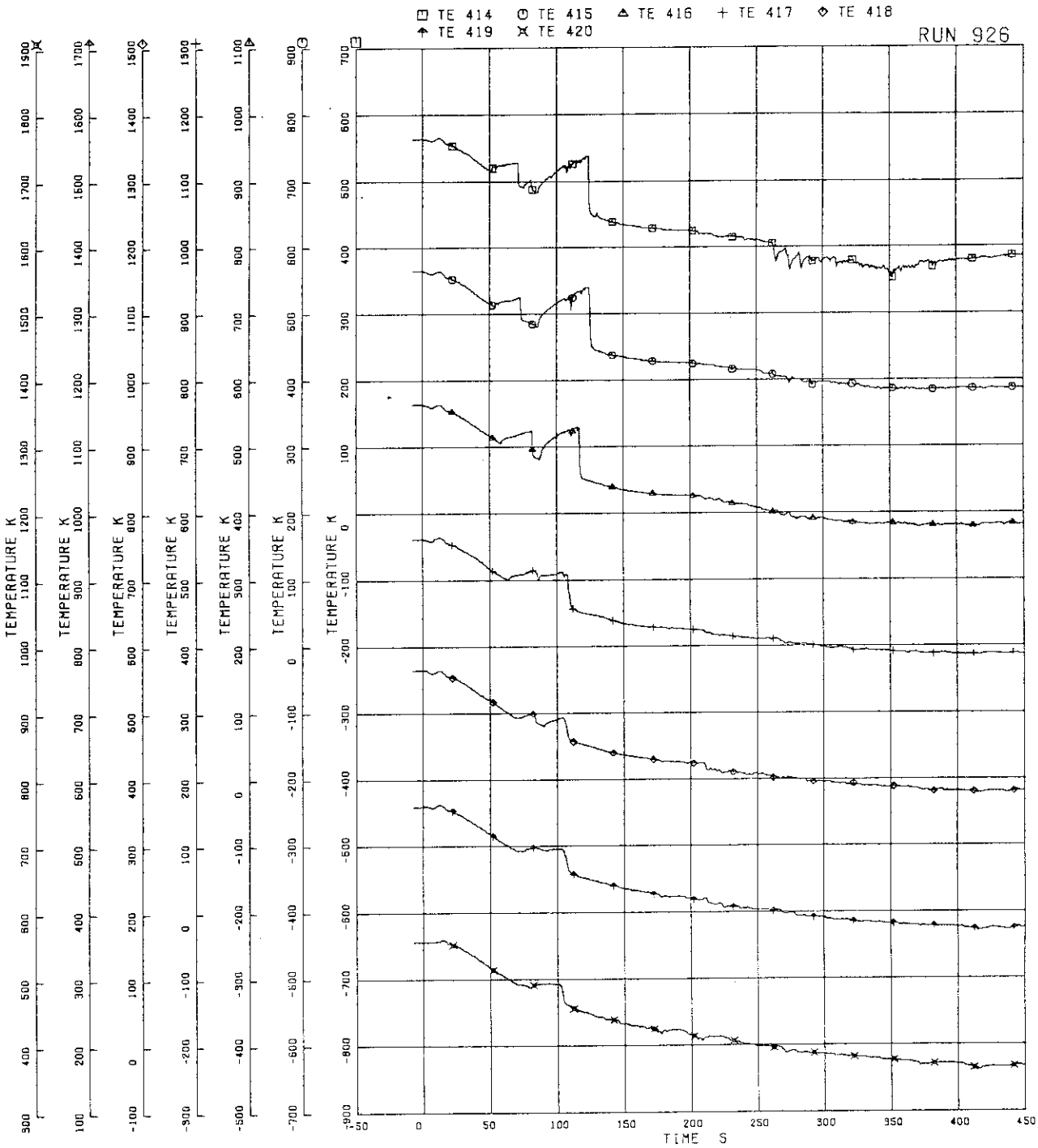

FIG.5-110 SURFACE TEMPERATURES OF WATER ROD SIMULATOR A45

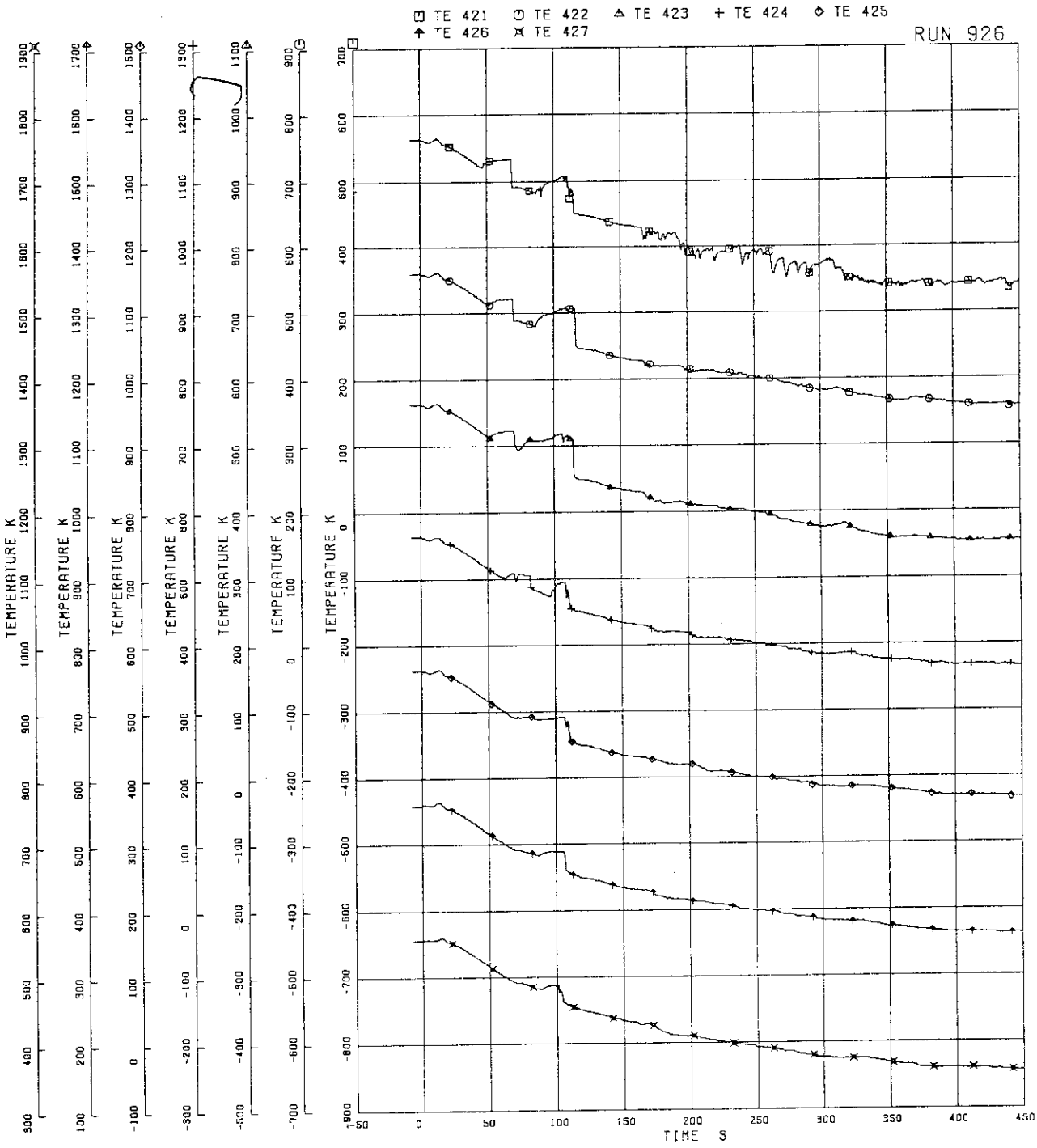

FIG.5.111 SURFACE TEMPERATURES OF WATER ROD SIMULATOR B45

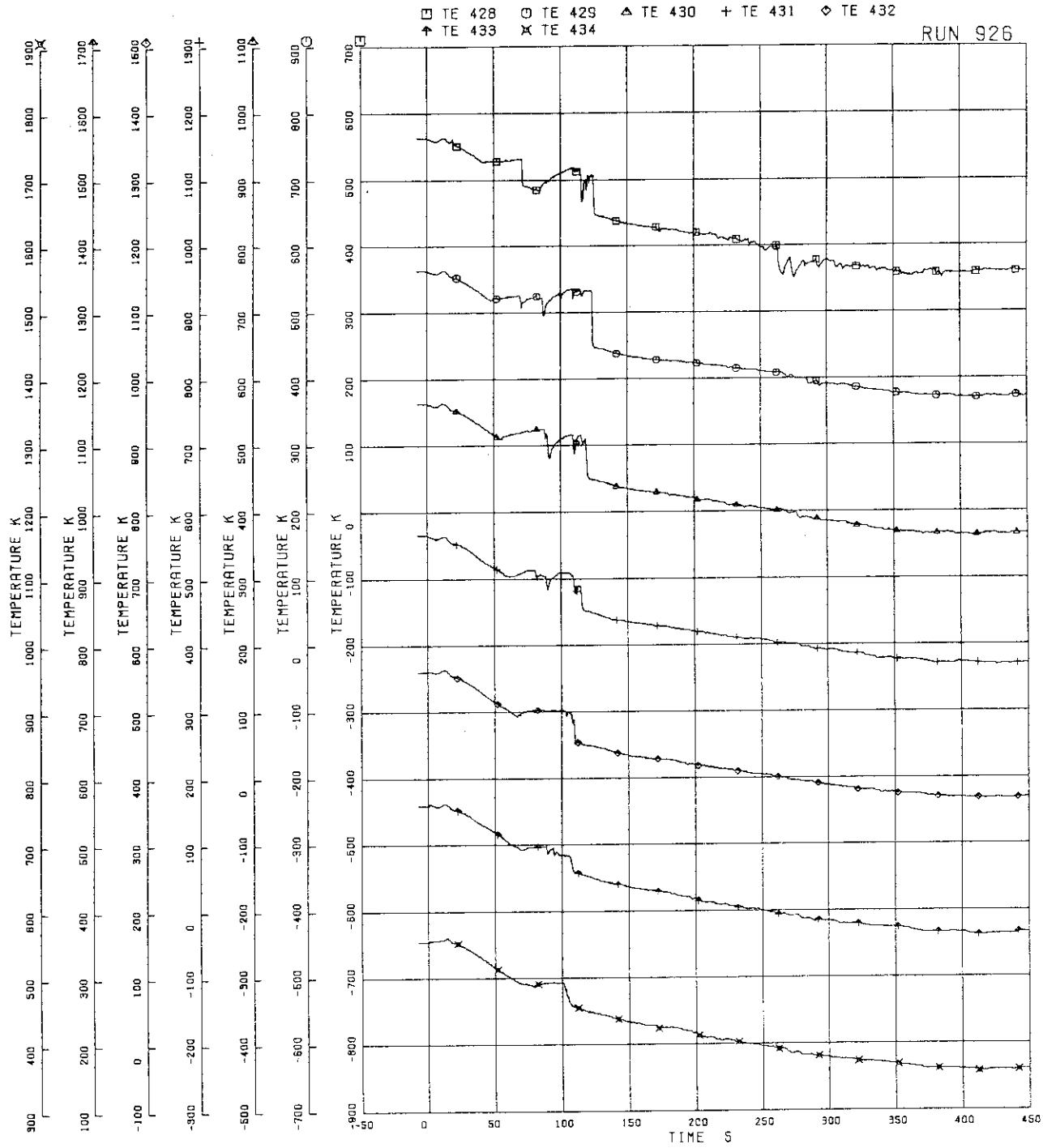

FIG.5.112 SURFACE TEMPERATURES OF WATER ROD SIMULATOR C45

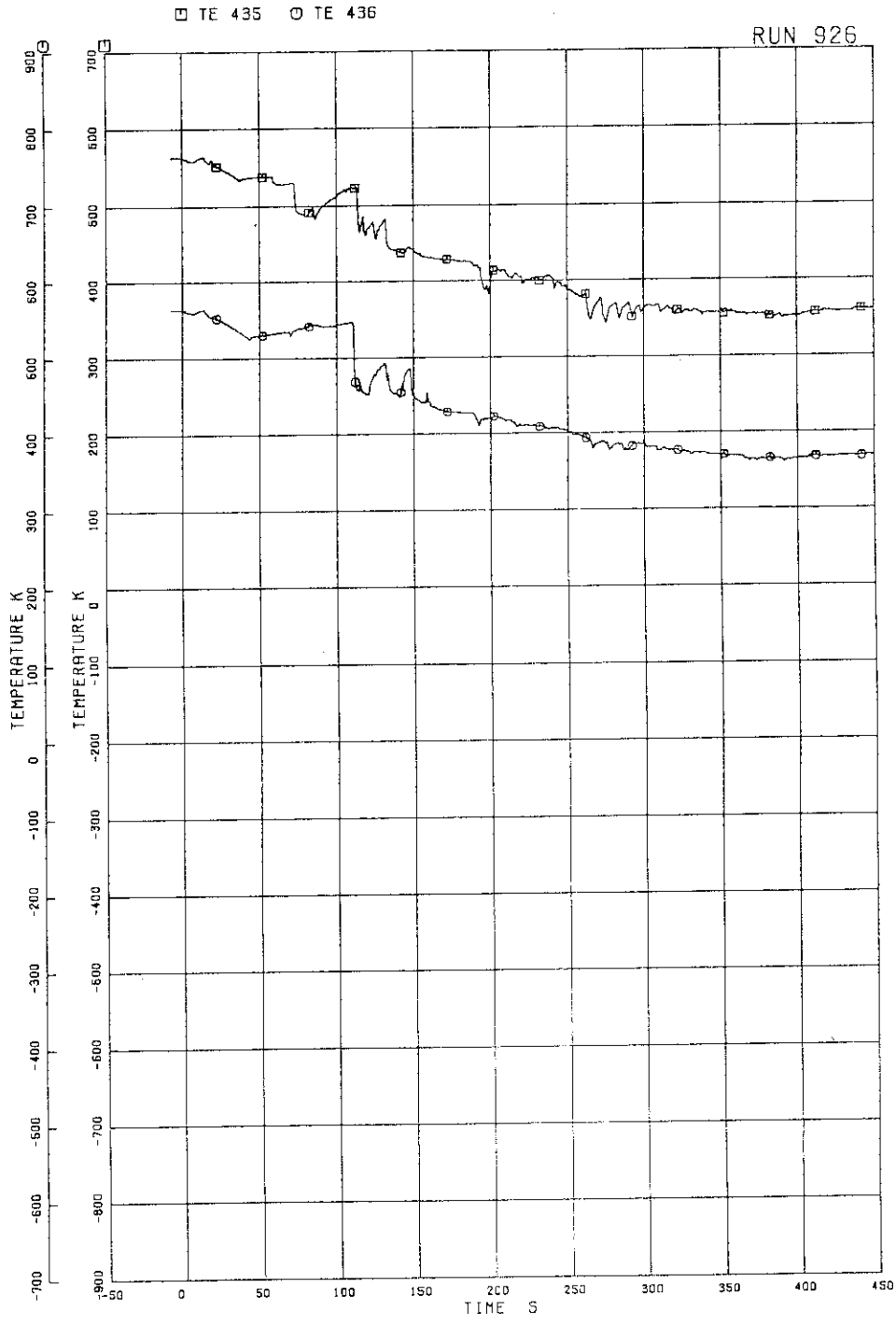

FIG.5.113 SURFACE TEMPERATURES OF WATER ROD SIMULATOR D45

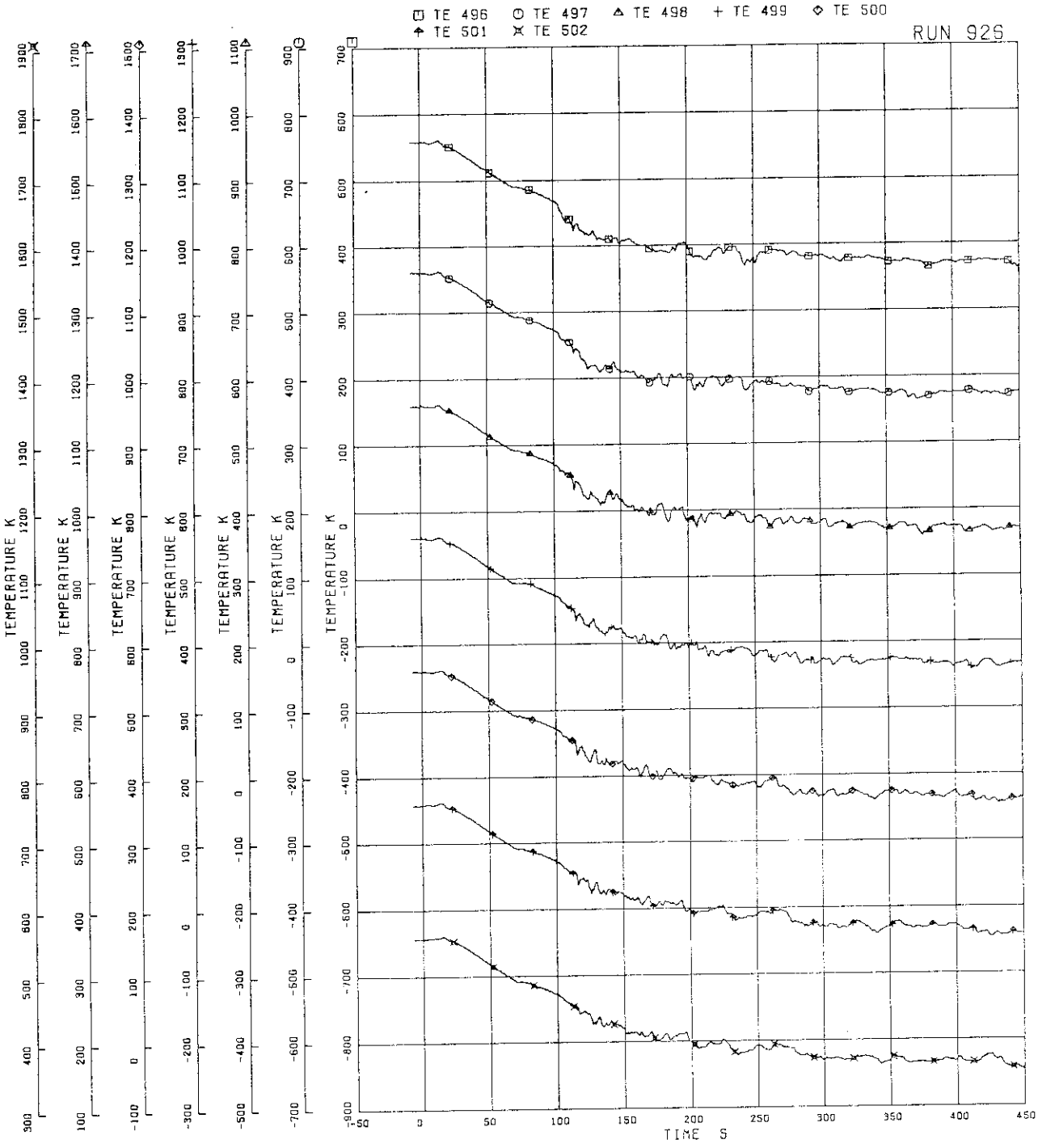

FIG.5.114 INNER SURFACE TEMPERATURES OF CHANNEL BOX A, LOCATION A1

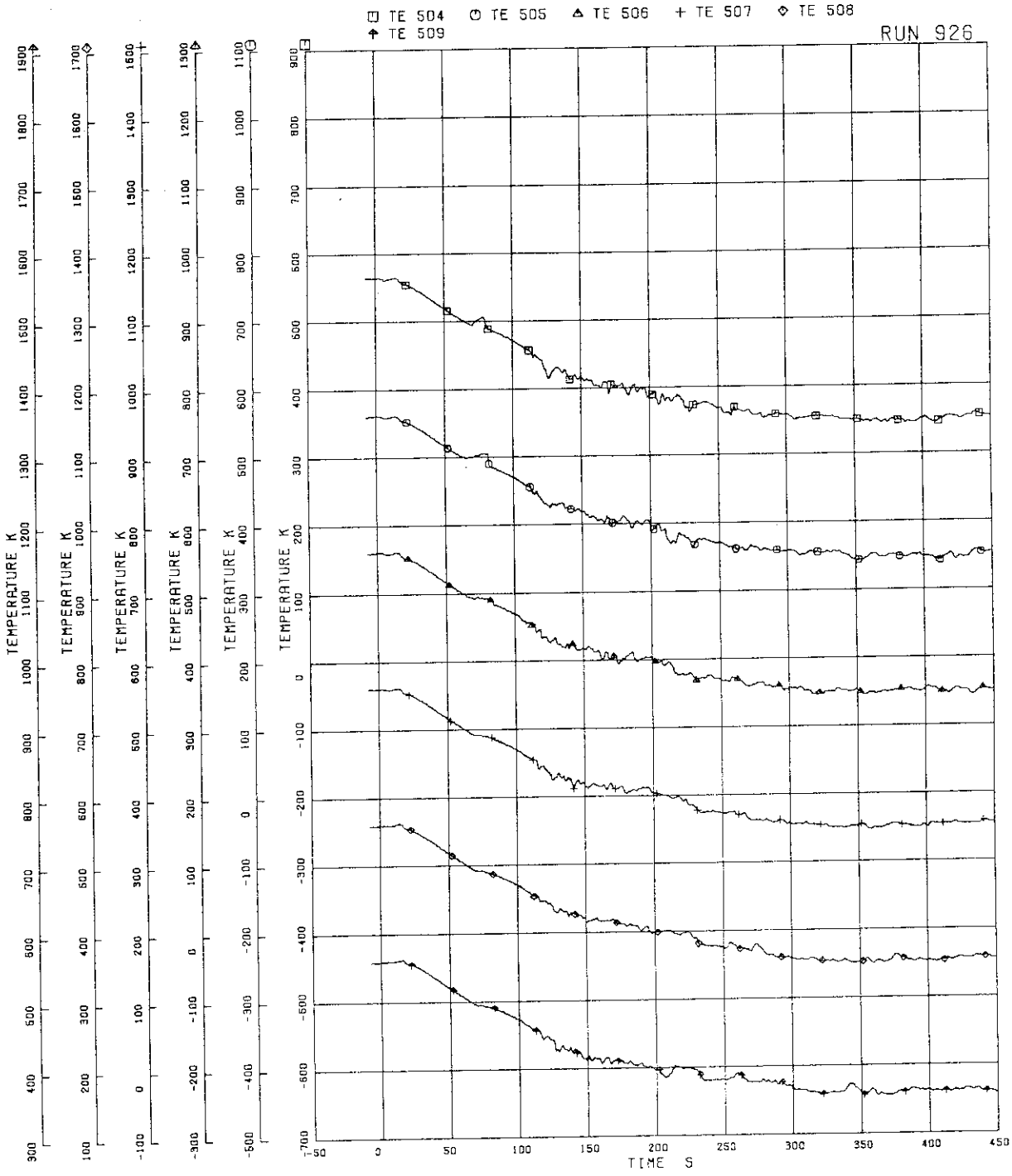

FIG.5.115 INNER SURFACE TEMPERATURES OF CHANNEL BOX A, LOCATION A2

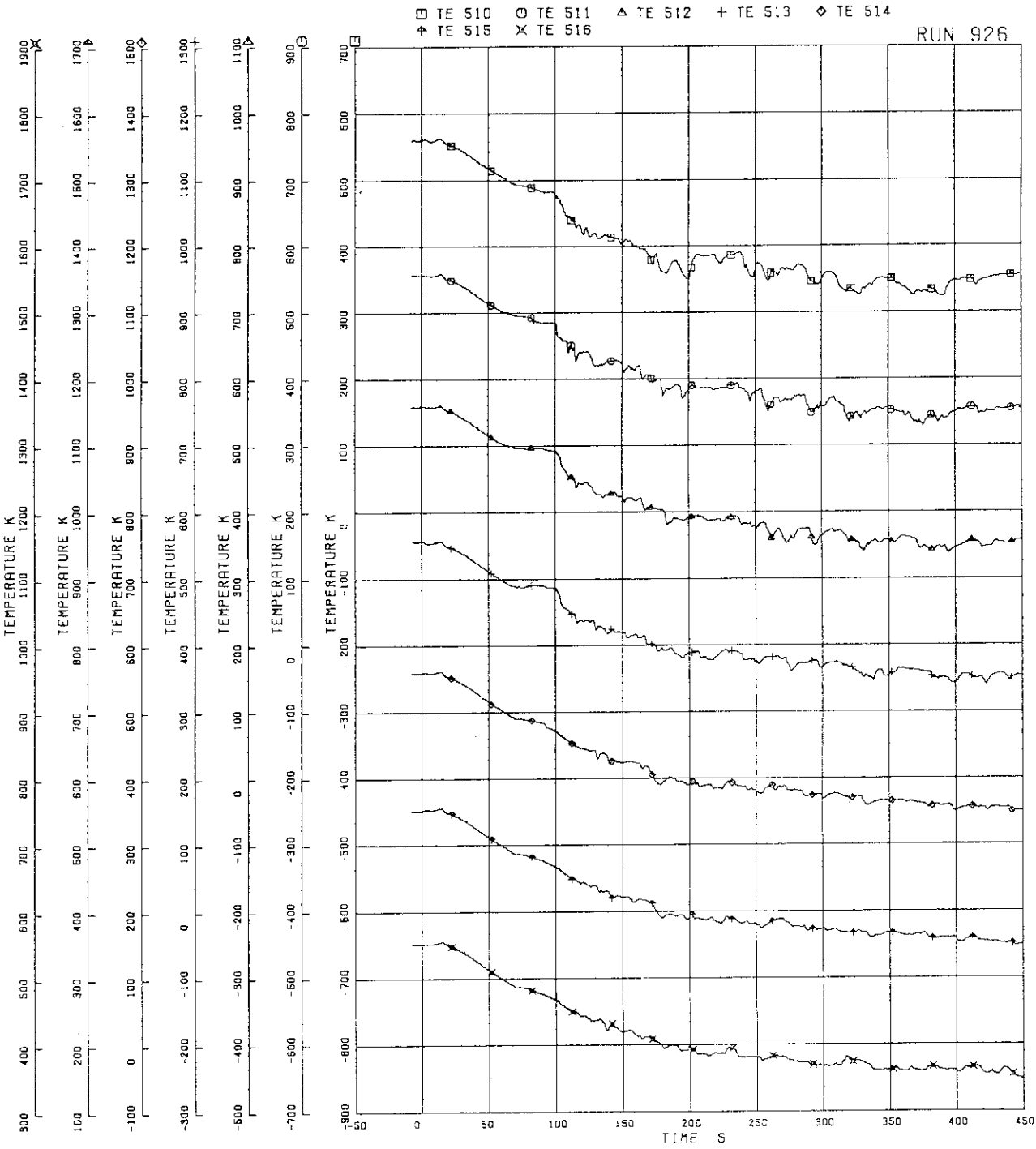

FIG.5.116 INNER SURFACE TEMPERATURES OF CHANNEL BOX B

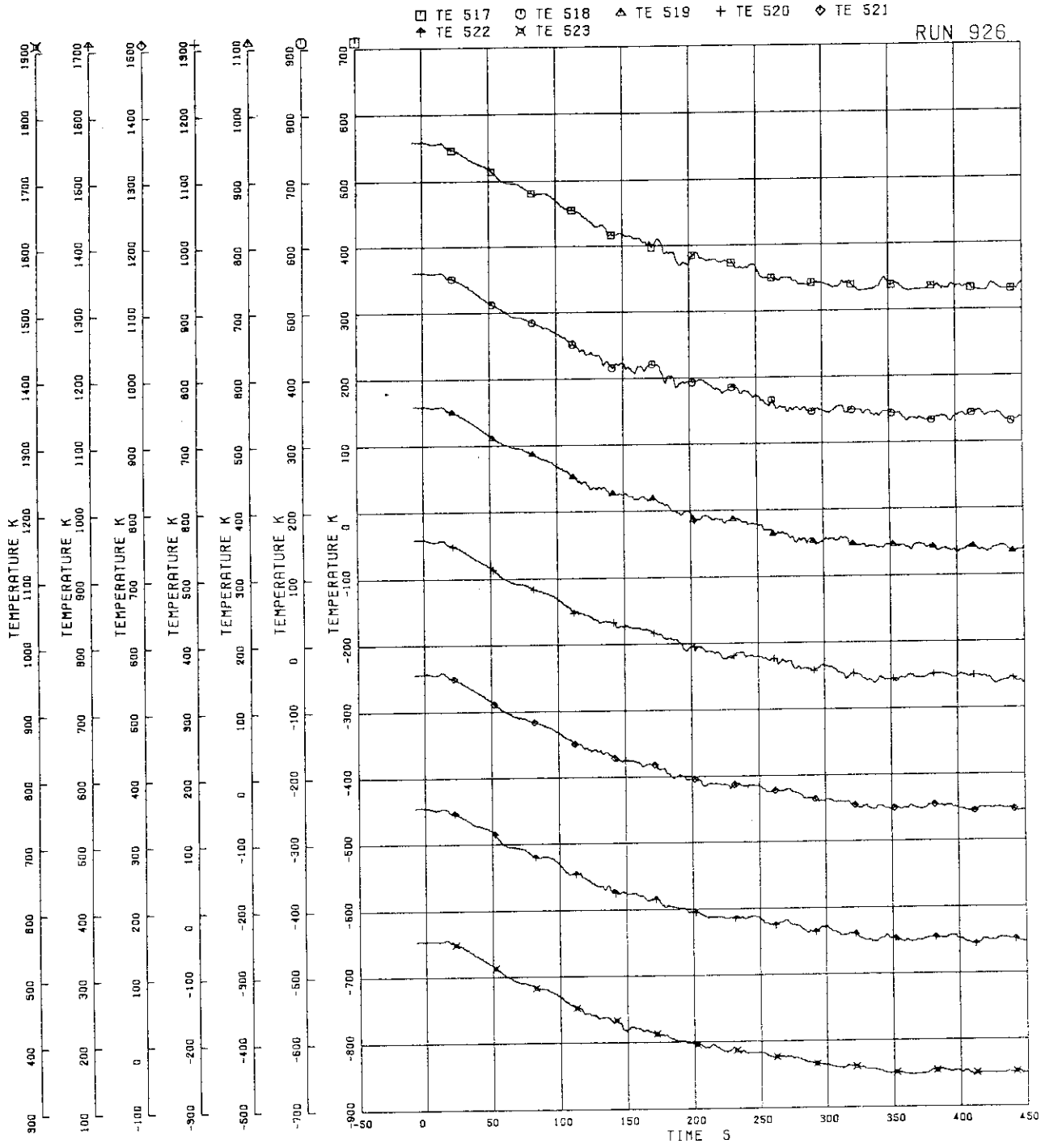

FIG.5.117 INNER SURFACE TEMPERATURES OF CHANNEL BOX C

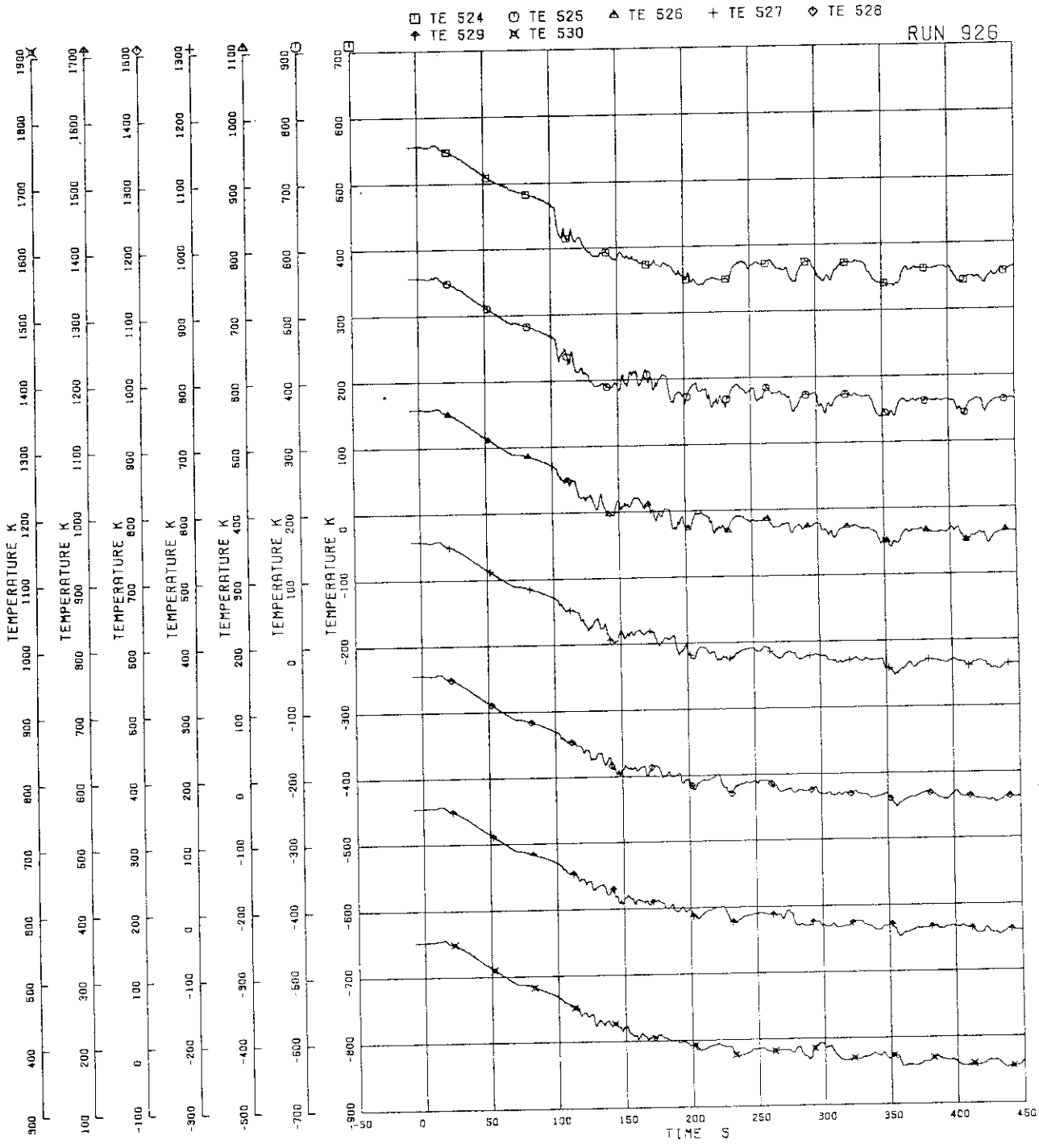

FIG.5.118 INNER SURFACE TEMPERATURES OF CHANNEL BOX D

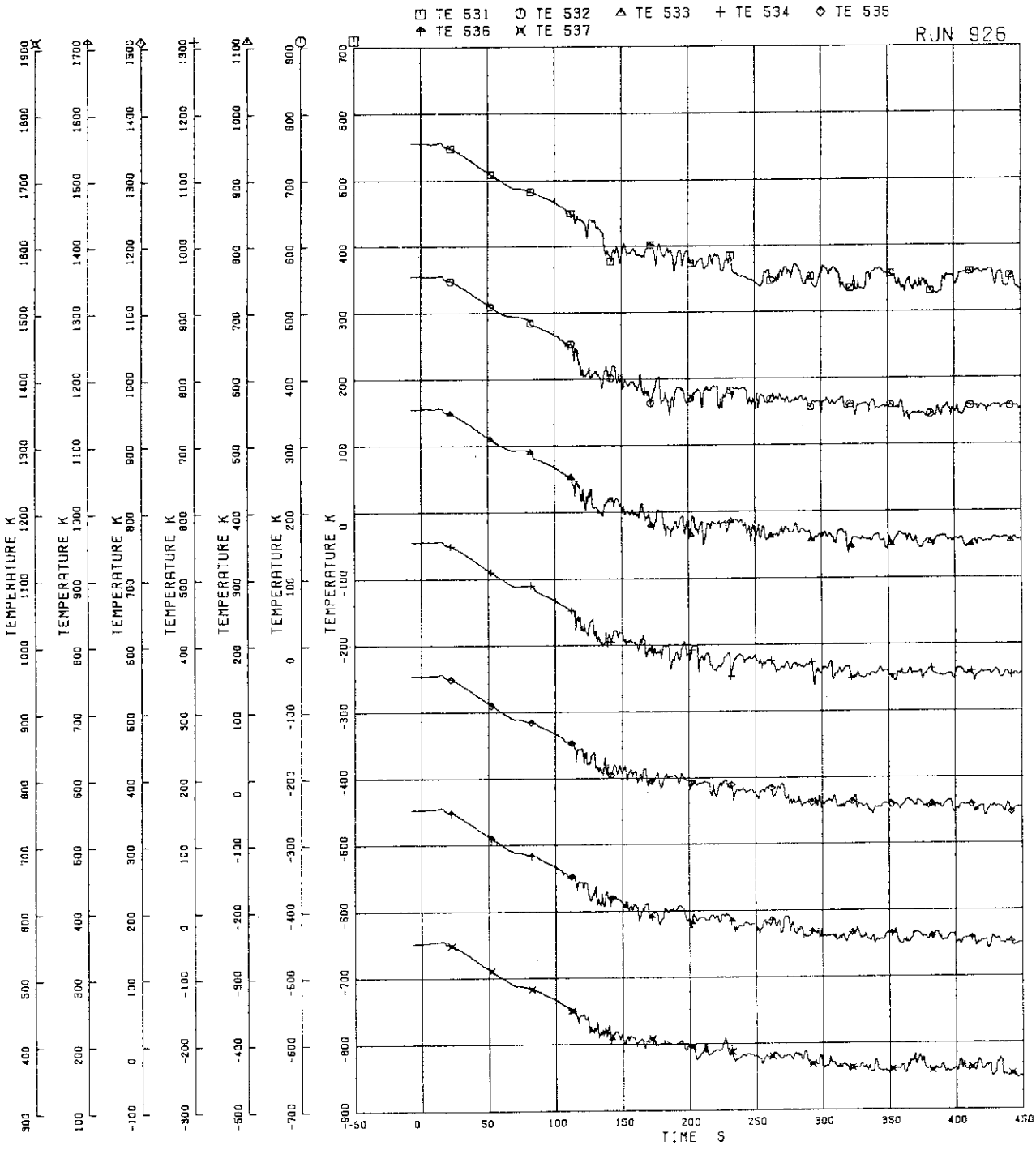

FIG.5.119 OUTER SURFACE TEMPERATURES OF CHANNEL BOX A

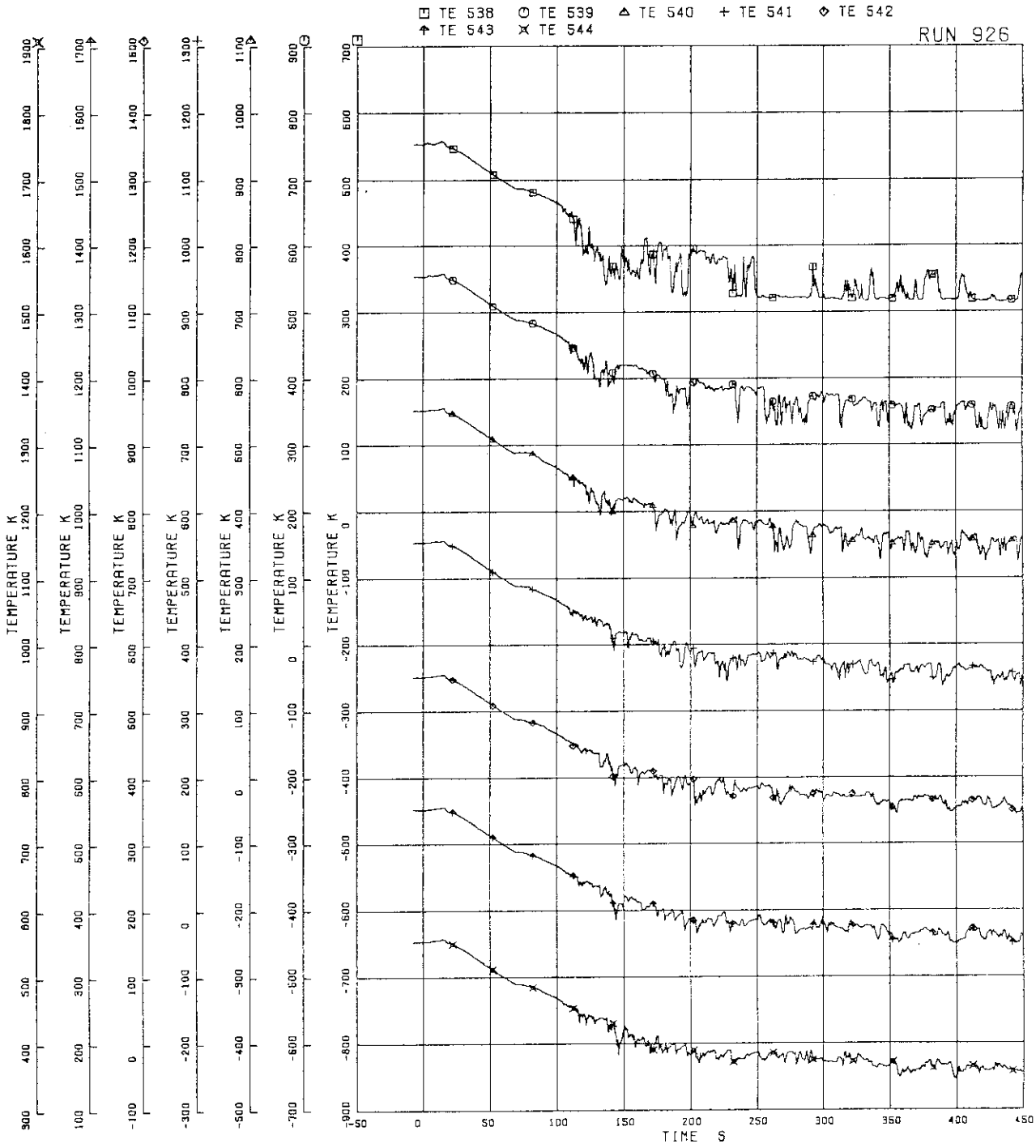

FIG.5.120 OUTER SURFACE TEMPERATURES OF CHANNEL BOX C

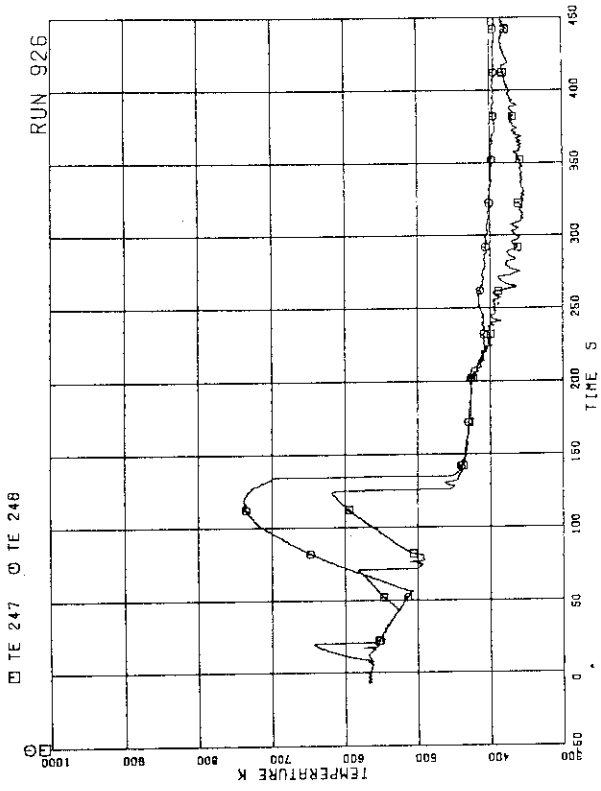

FIG.5.123 SURFACE TEMPERATURES OF FUEL ROD A26 AT POSITIONS 1 AND 4

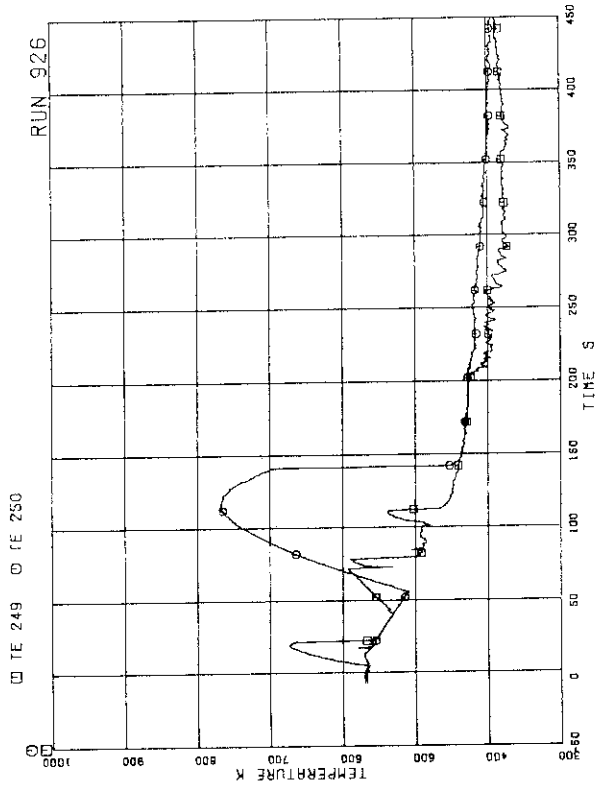

FIG.5.124 SURFACE TEMPERATURES OF FUEL ROD A28 AT POSITIONS 1 AND 4

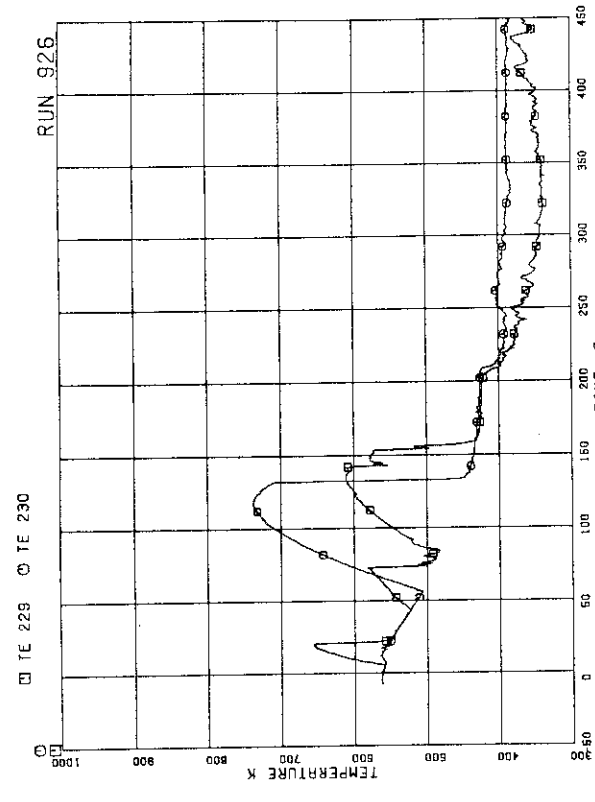

FIG.5.121 SURFACE TEMPERATURES OF FUEL ROD A15 AT POSITIONS 1 AND 4

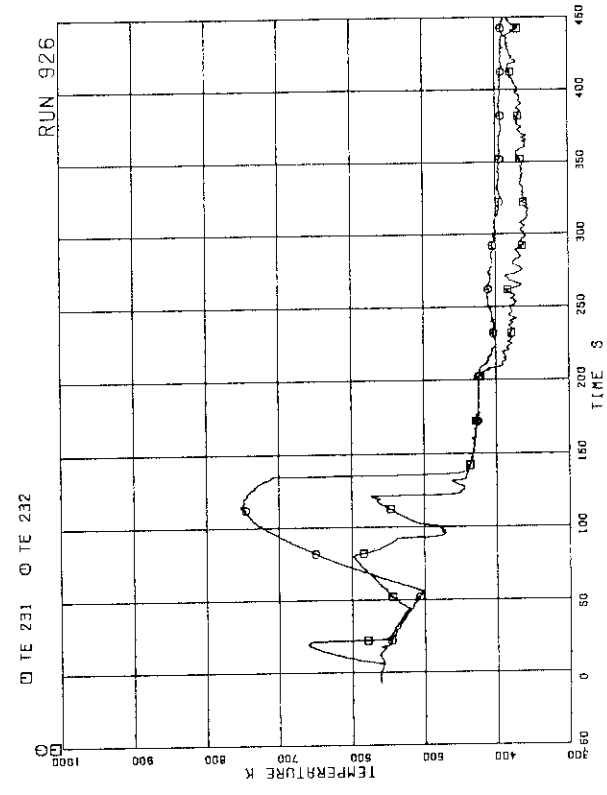

FIG.5.122 SURFACE TEMPERATURES OF FUEL ROD A17 AT POSITIONS 1 AND 4

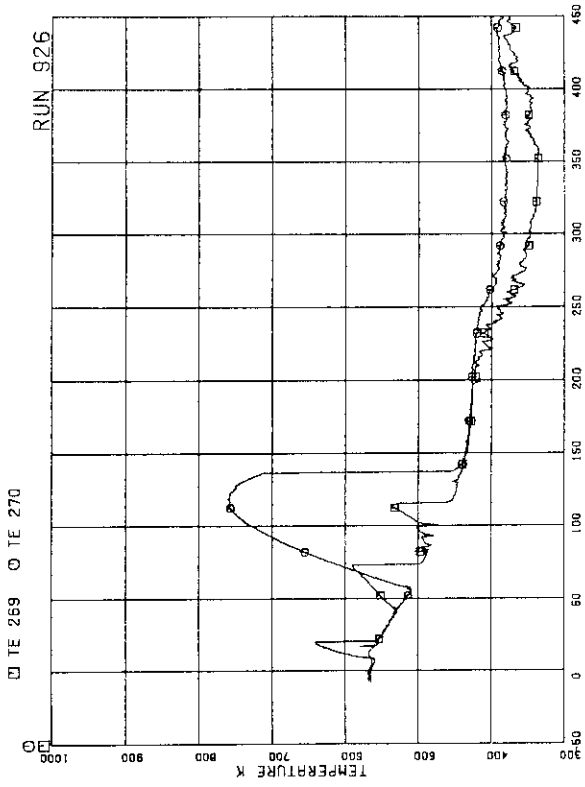

FIG.5.127 SURFACE TEMPERATURES OF FUEL ROD A42
AT POSITIONS 1 AND 4

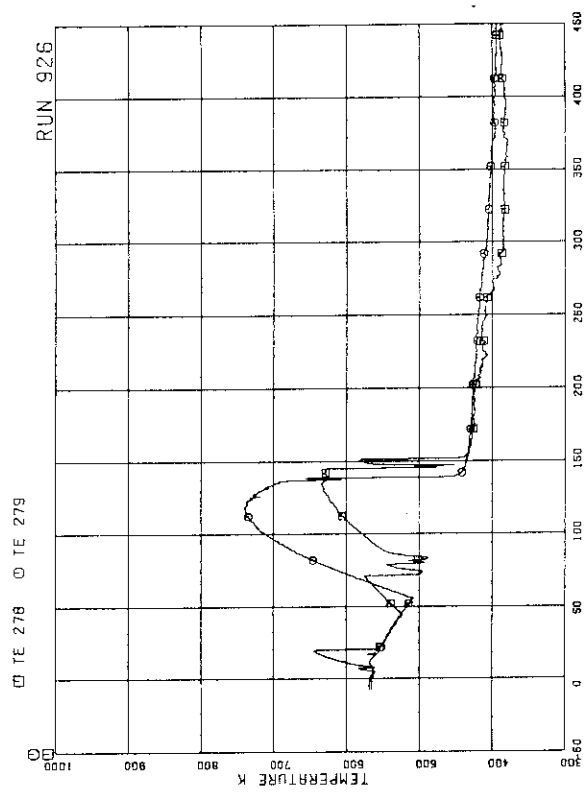

FIG.5.128 SURFACE TEMPERATURES OF FUEL ROD A48
AT POSITIONS 1 AND 4

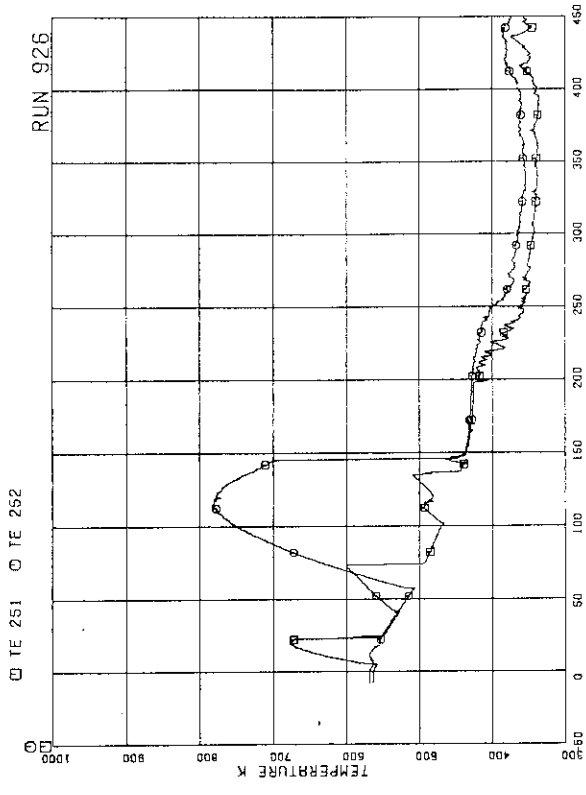

FIG.5.125 SURFACE TEMPERATURES OF FUEL ROD A31
AT POSITIONS 1 AND 4

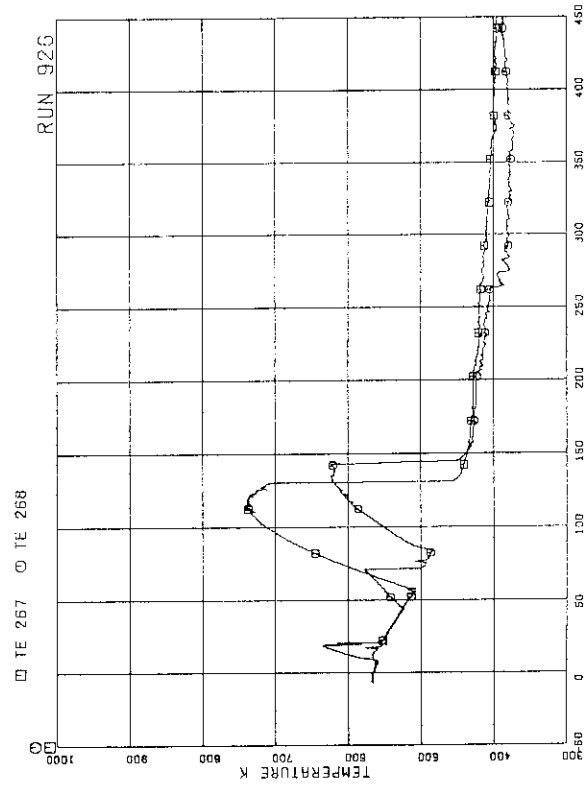

FIG.5.126 SURFACE TEMPERATURES OF FUEL ROD A37
AT POSITIONS 1 AND 4

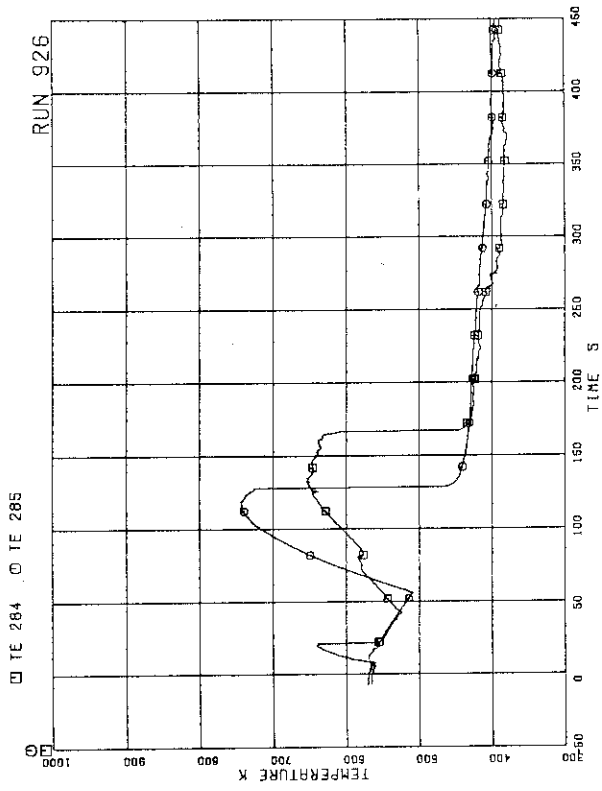

FIG.5.131 SURFACE TEMPERATURES OF FUEL ROD A57
AT POSITIONS 1 AND 4

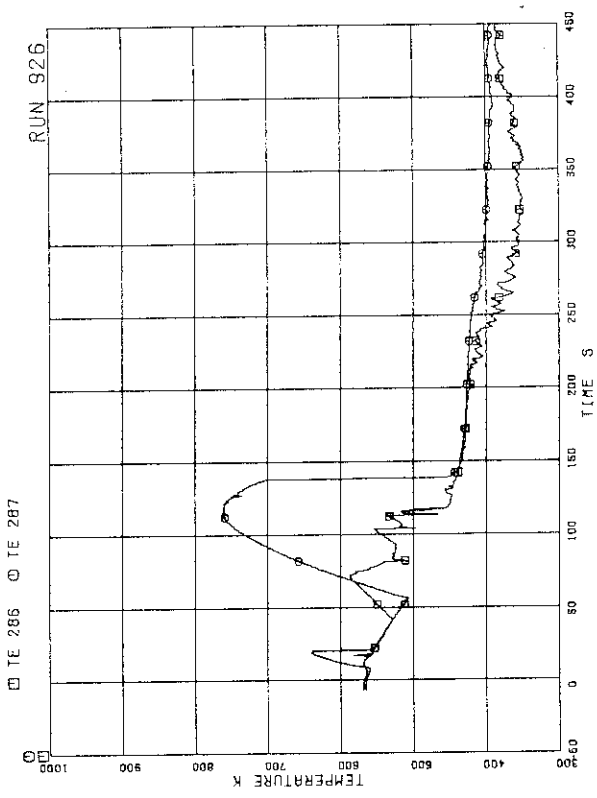

FIG.5.132 SURFACE TEMPERATURES OF FUEL ROD A62
AT POSITIONS 1 AND 4

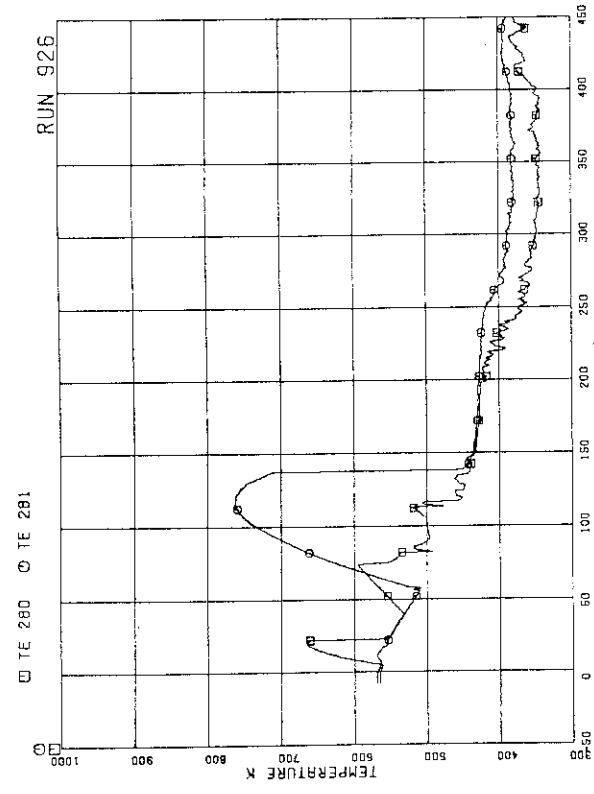

FIG.5.129 SURFACE TEMPERATURES OF FUEL ROD A51
AT POSITIONS 1 AND 4

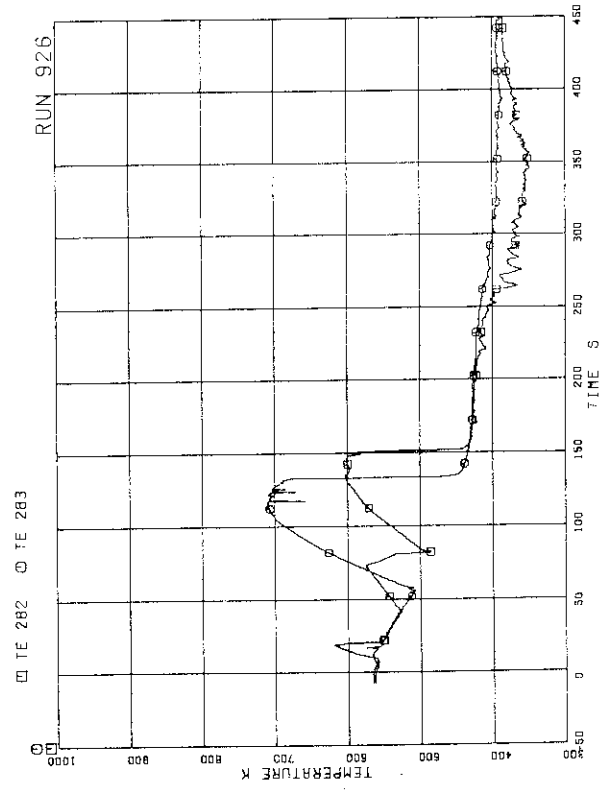

FIG.5.130 SURFACE TEMPERATURES OF FUEL ROD A53
AT POSITIONS 1 AND 4

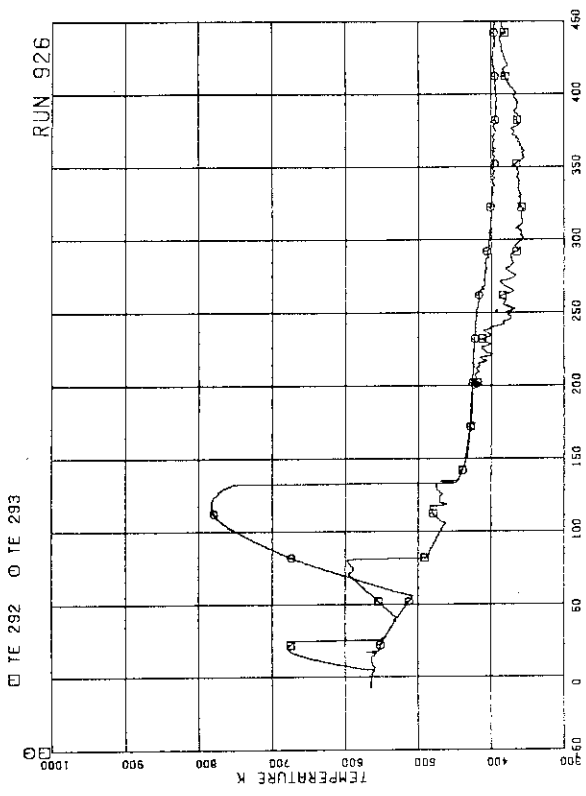

FIG.5.135 SURFACE TEMPERATURES OF FUEL ROD A71
AT POSITIONS 1 AND 4

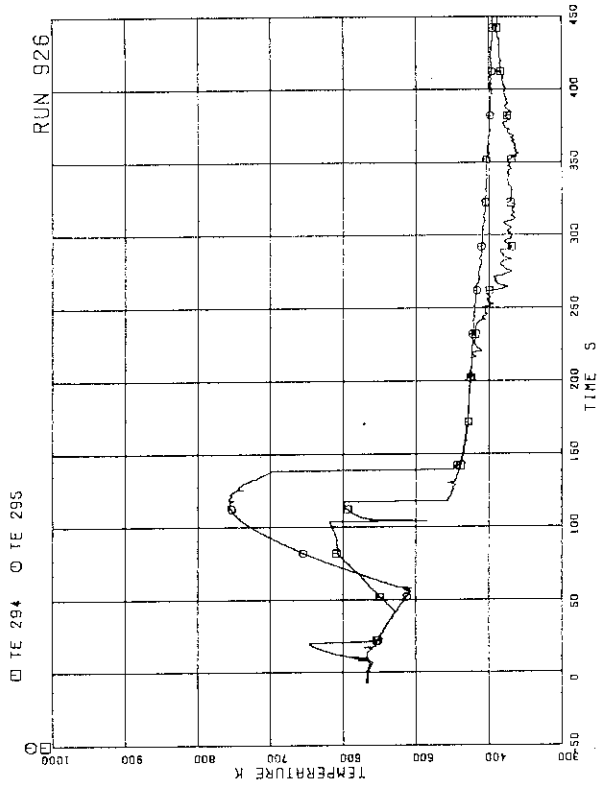

FIG.5.136 SURFACE TEMPERATURES OF FUEL ROD A73
AT POSITIONS 1 AND 4

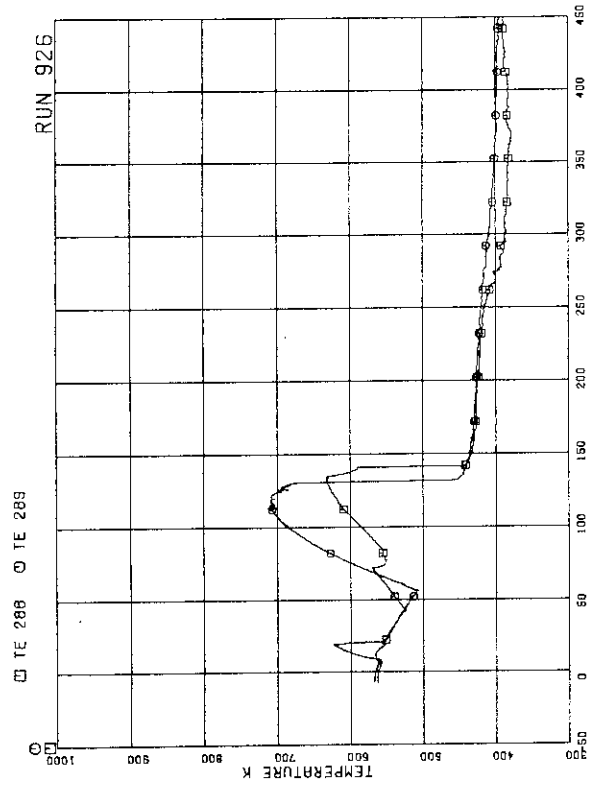

FIG.5.133 SURFACE TEMPERATURES OF FUEL ROD A66
AT POSITIONS 1 AND 4

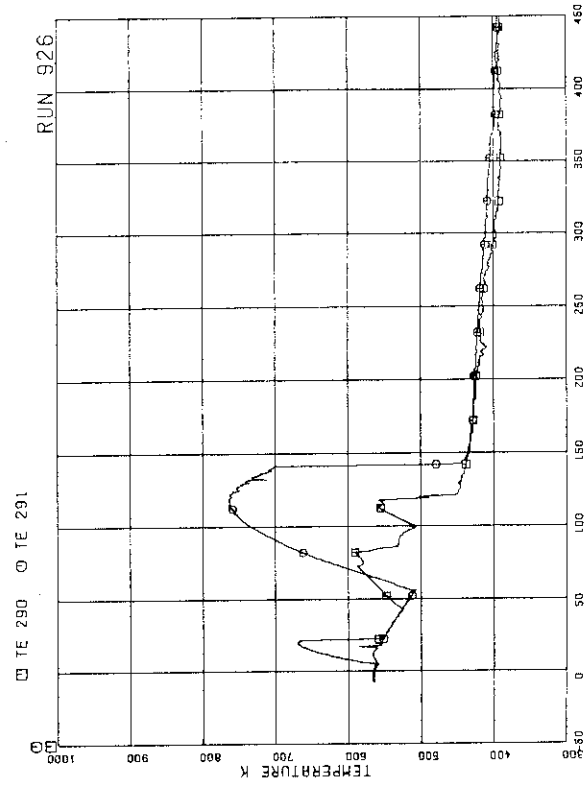

FIG.5.134 SURFACE TEMPERATURES OF FUEL ROD A68
AT POSITIONS 1 AND 4

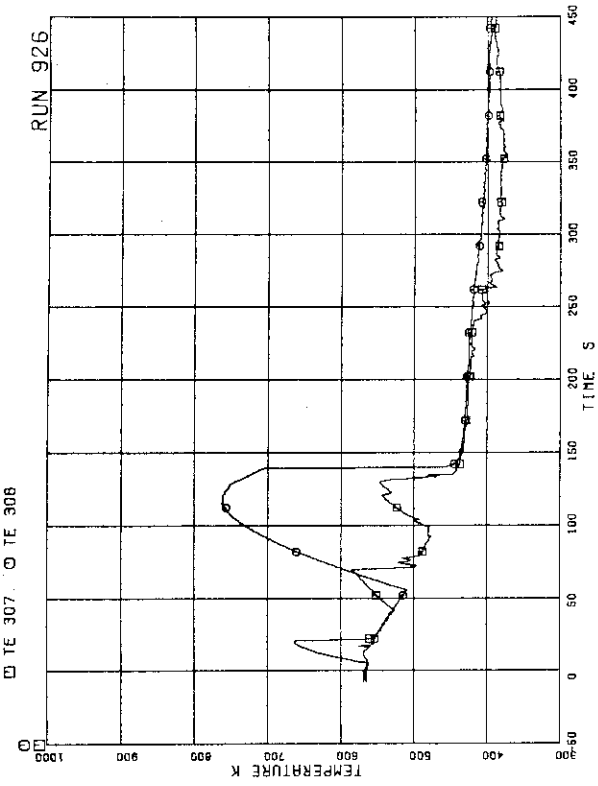

FIG.5.139 SURFACE TEMPERATURES OF FUEL ROD A84
AT POSITIONS 1 AND 4

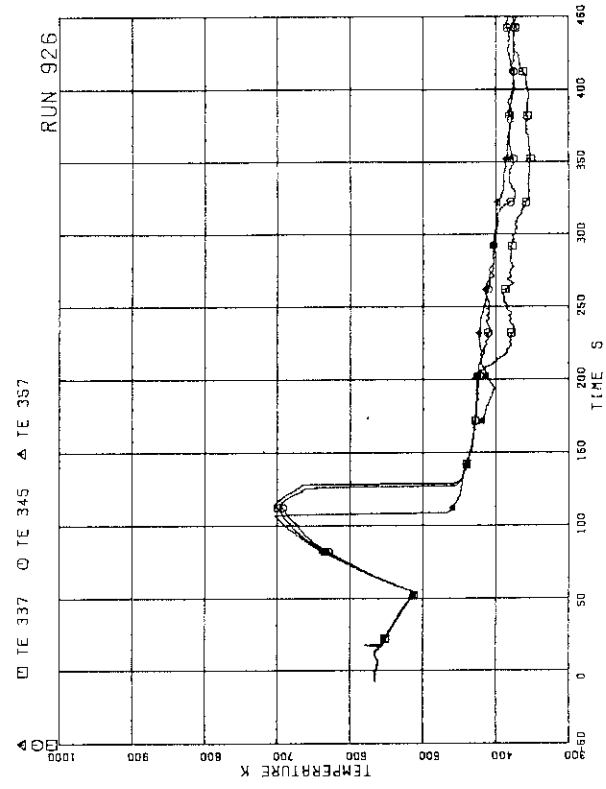

FIG.5.140 SURFACE TEMPERATURES OF FUEL RODS
B13,B31,B86 AT POSITION 4

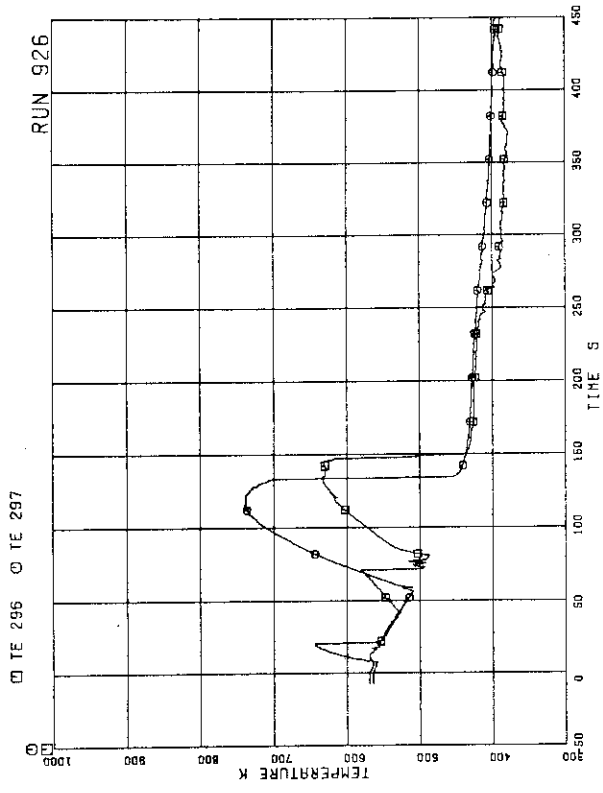

FIG.5.137 SURFACE TEMPERATURES OF FUEL ROD A75
AT POSITIONS 1 AND 4

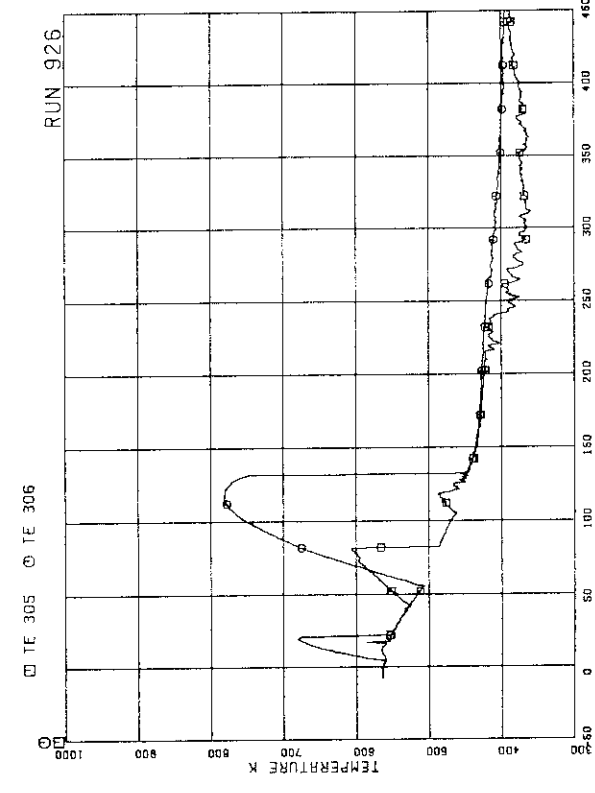

FIG.5.138 SURFACE TEMPERATURES OF FUEL ROD A82
AT POSITIONS 1 AND 4

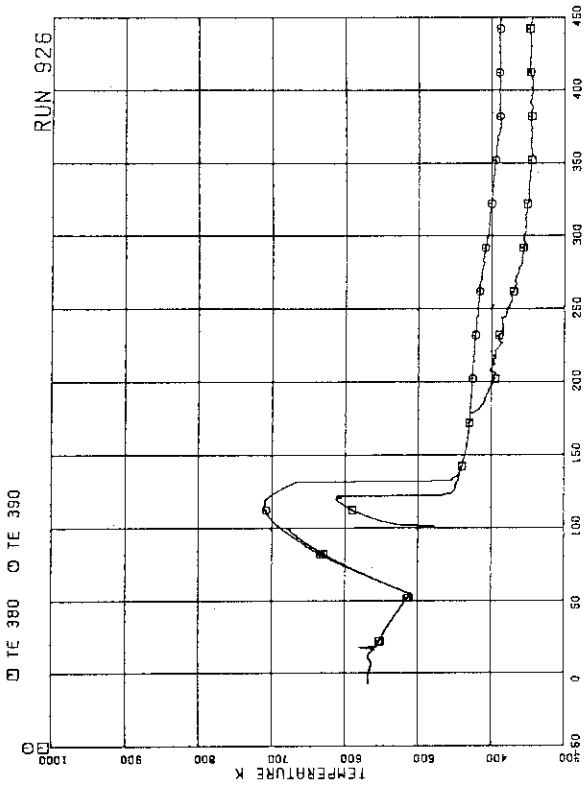

FIG.5.143 SURFACE TEMPERATURES OF FUEL RODS C31,C68 AT POSITION 4

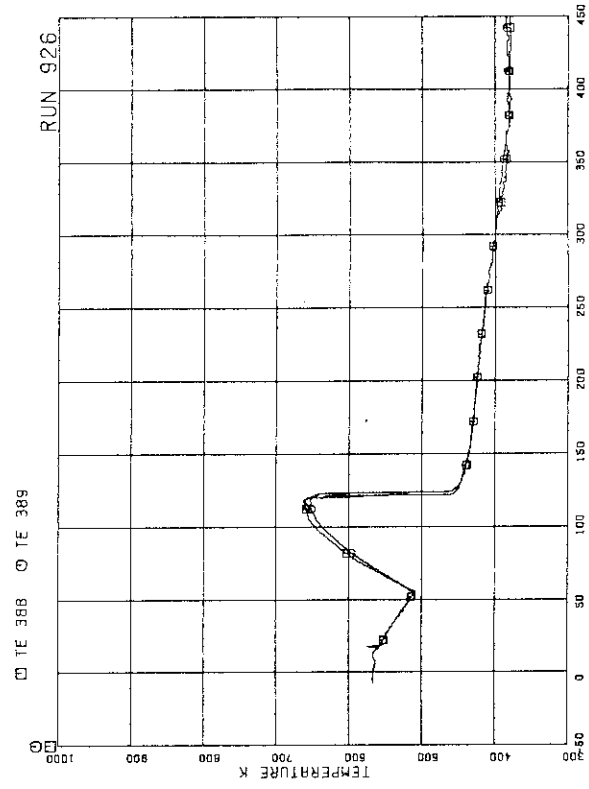

FIG.5.144 SURFACE TEMPERATURES OF FUEL RODS C35,C66 AT POSITION 4

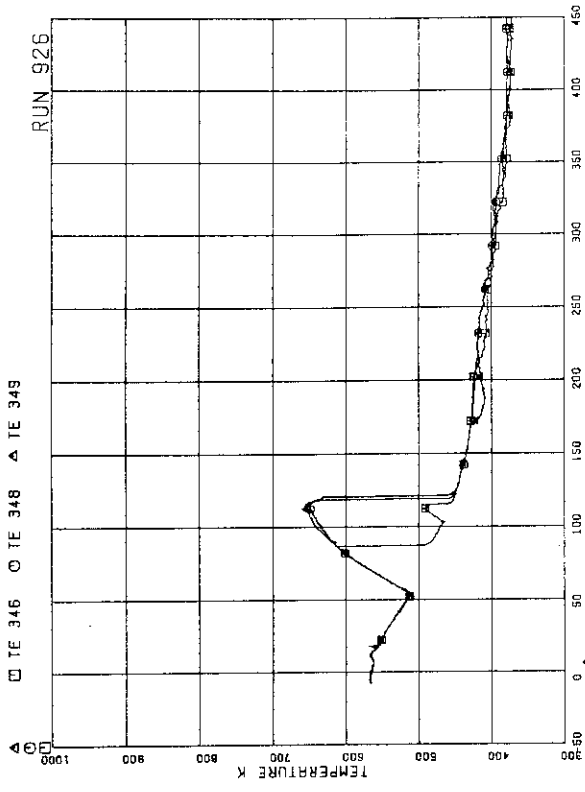

FIG.5.141 SURFACE TEMPERATURES OF FUEL RODS B33,B53,B66 AT POSITION 4

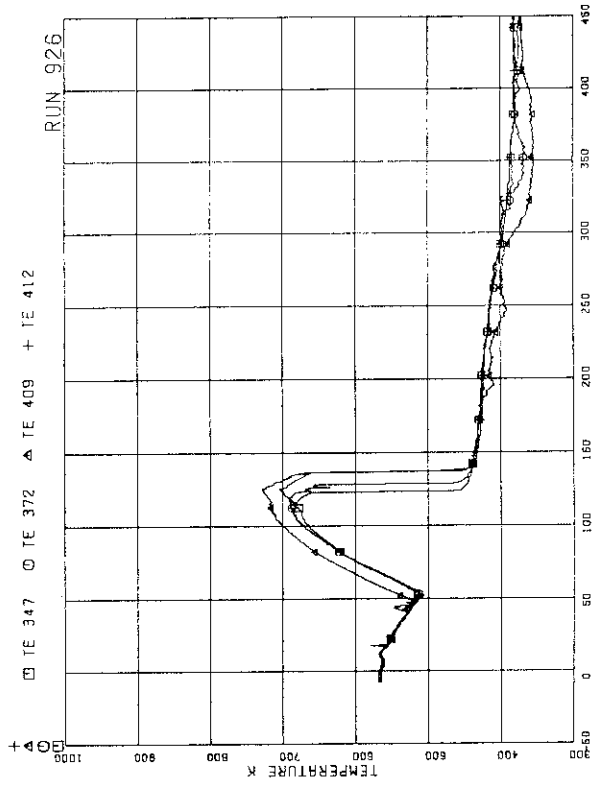

FIG.5.142 SURFACE TEMPERATURES OF FUEL RODS B51,C15,D51,D77 AT POSITION 4

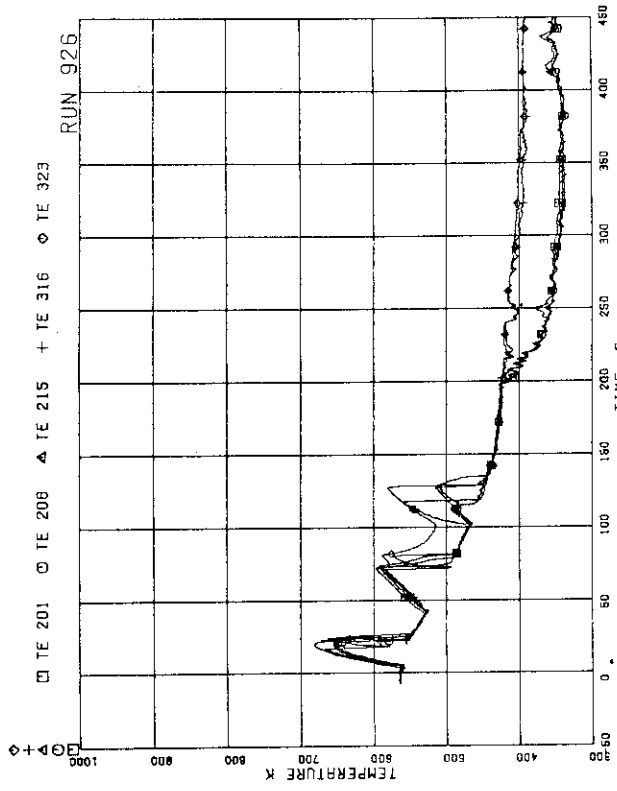

FIG.5.147 SURFACE TEMPERATURES OF FUEL RODS
A11,A12,A13,A87,A88 AT POSITION 1

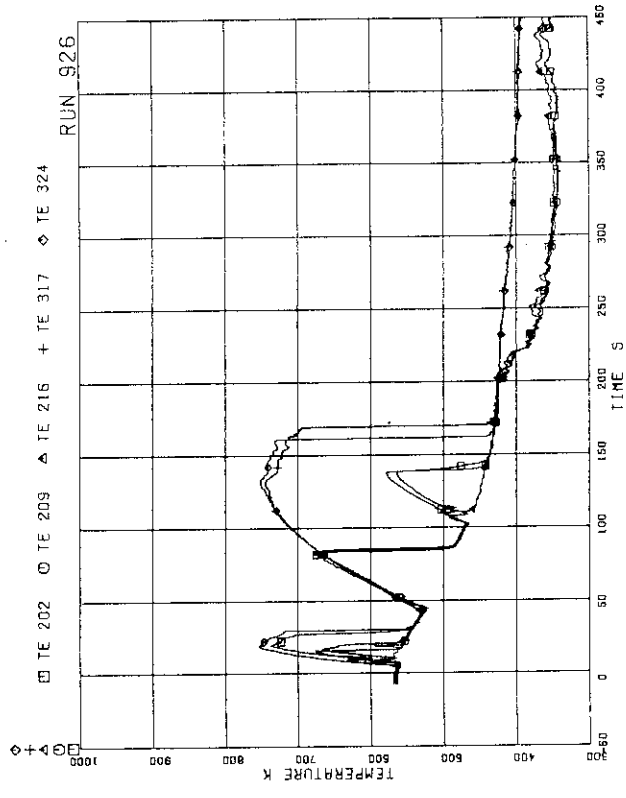

FIG.5.148 SURFACE TEMPERATURES OF FUEL RODS
A11,A12,A13,A87,A88 AT POSITION 2

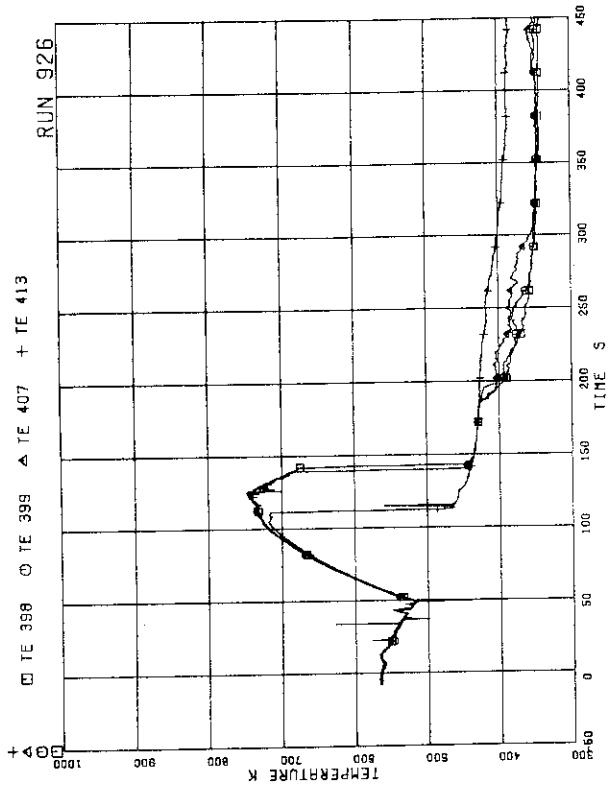

FIG.5.145 SURFACE TEMPERATURES OF FUEL RODS
D11,D13,D31,D86 AT POSITION 4

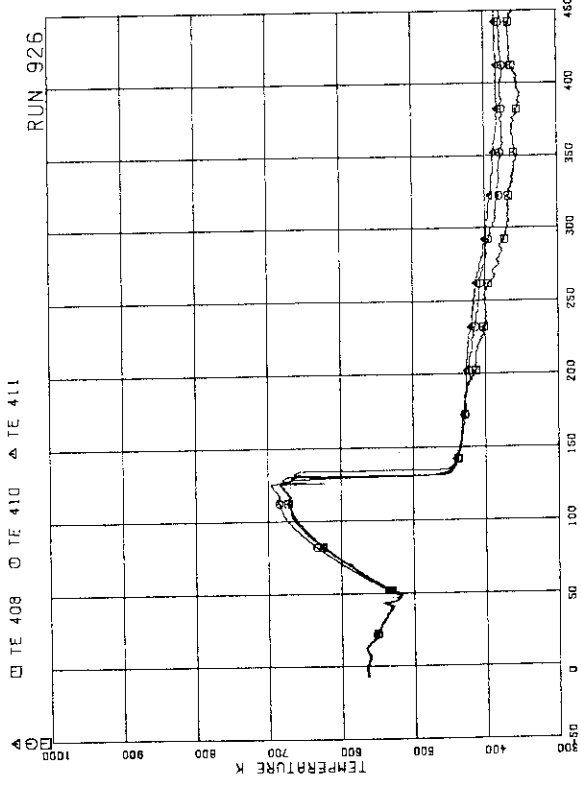

FIG.5.146 SURFACE TEMPERATURES OF FUEL RODS
D33,D53,D66 AT POSITION 4

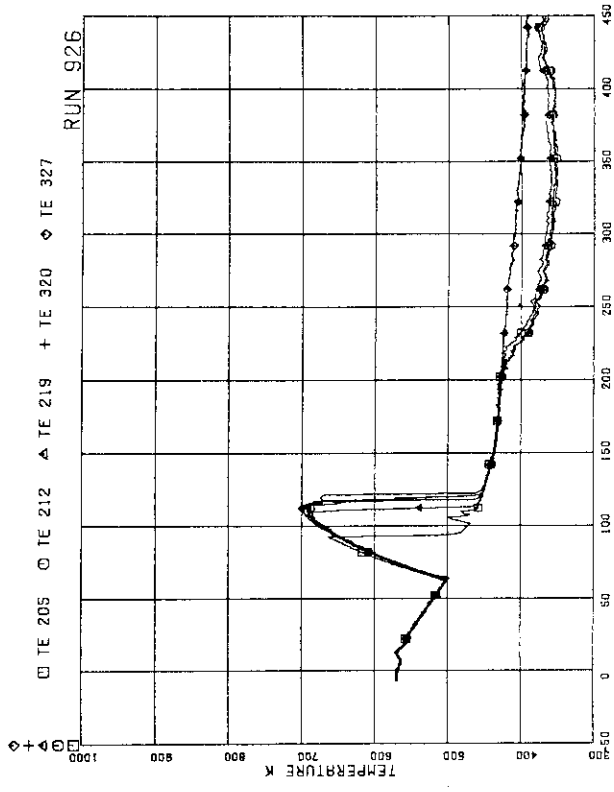

FIG.5.151 SURFACE TEMPERATURE OF FUEL RODS A11,A12,A13,A87,A88 AT POSITION 5

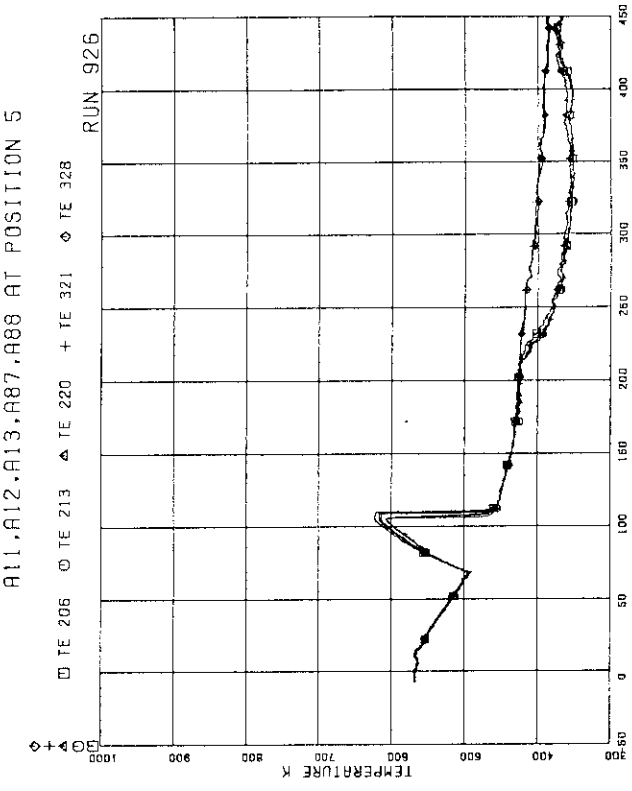

FIG.5.152 SURFACE TEMPERATURES OF FUEL RODS A11,A12,A13,A87,A88 AT POSITION 6

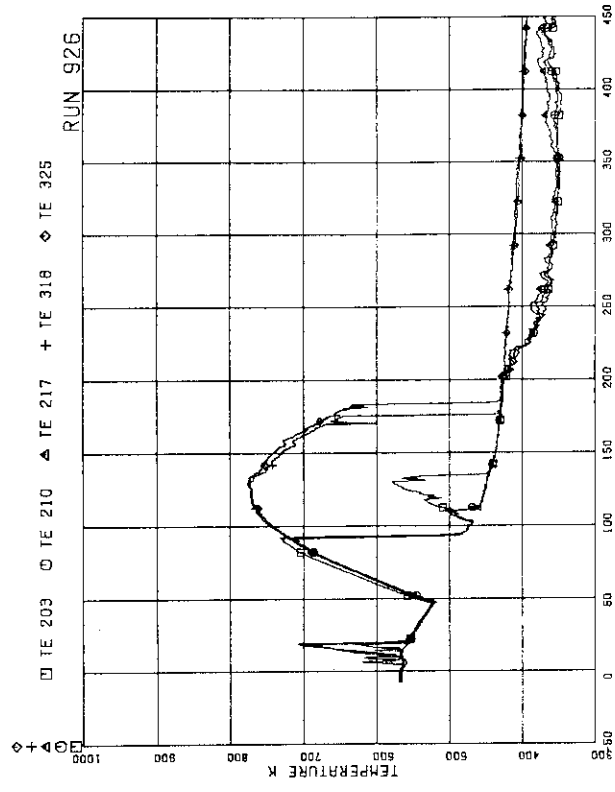

FIG.5.149 SURFACE TEMPERATURES OF FUEL RODS A11,A12,A13,A87,A88 AT POSITION 3

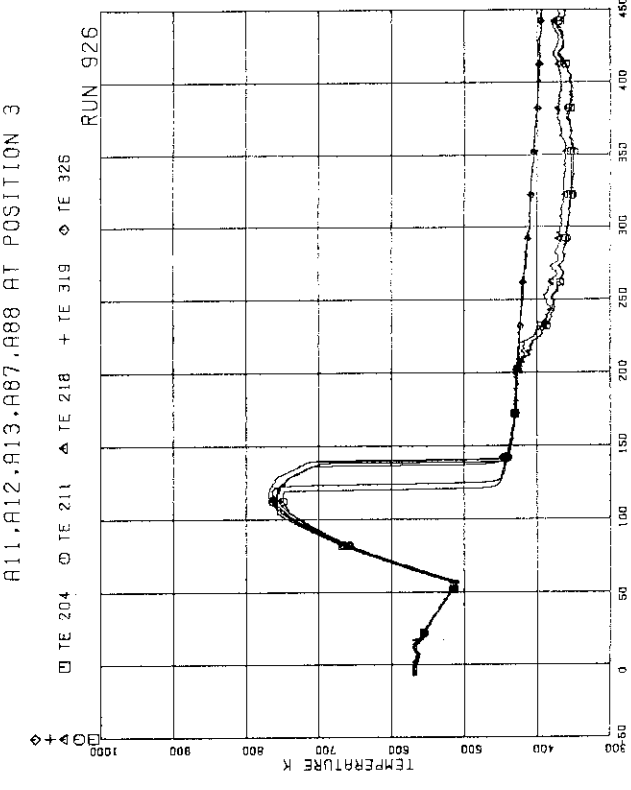

FIG.5.150 SURFACE TEMPERATURES OF FUEL RODS A11,A12,A13,A87,A88 AT POSITION 4

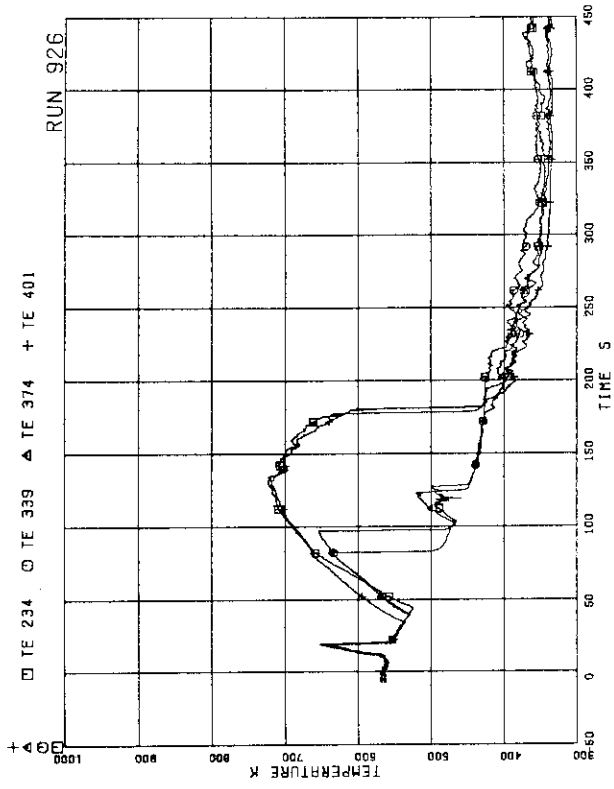

FIG.5.155 SURFACE TEMPERATURES OF FUEL RODS A22,B22,C22,D22 AT POSITION 2

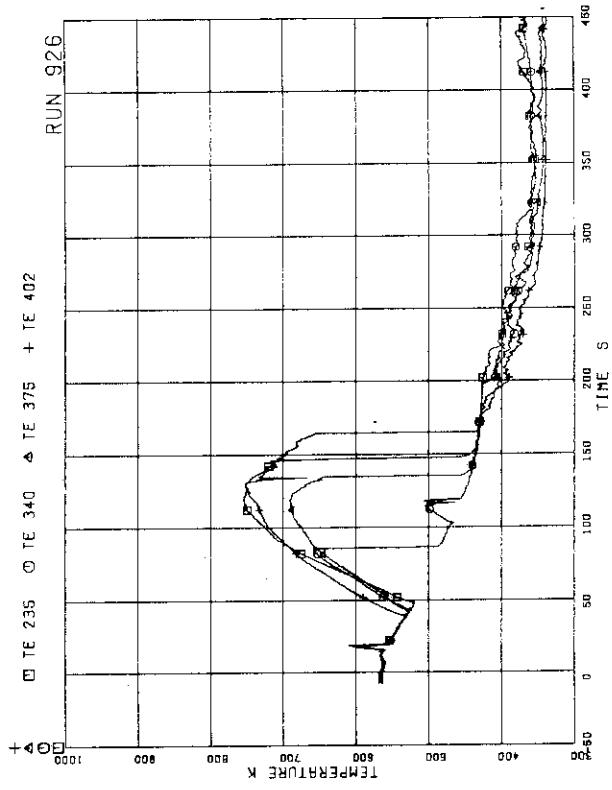

FIG.5.156 SURFACE TEMPERATURES OF FUEL RODS A22,B22,C22,D22 AT POSITION 3

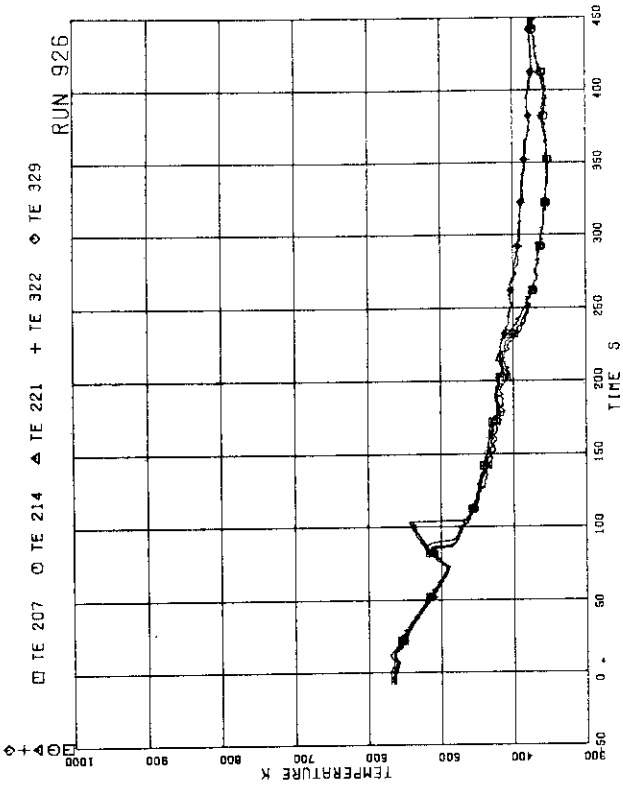

FIG.5.153 SURFACE TEMPERATURES OF FUEL RODS A11,A12,A13,A87,A88 AT POSITION 7

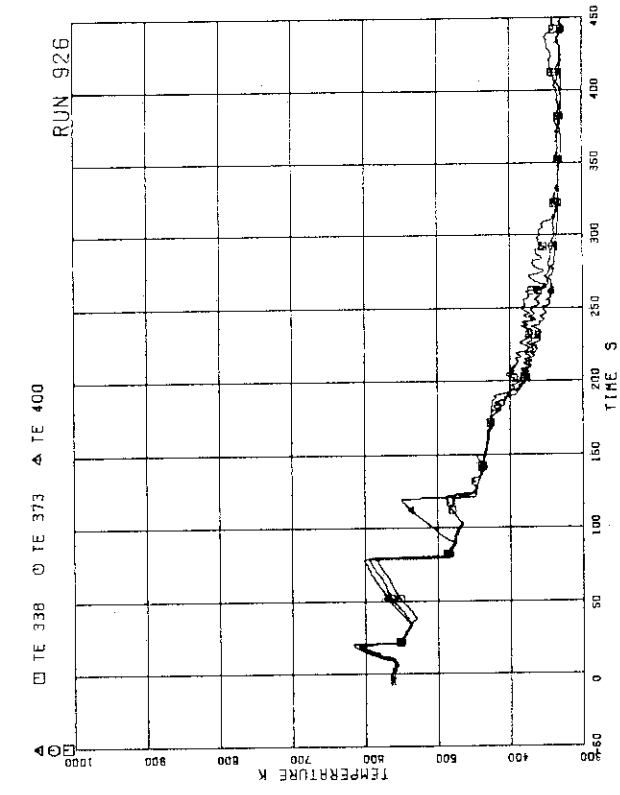

FIG.5.154 SURFACE TEMPERATURES OF FUEL RODS B22,C22,D22 AT POSITION 1

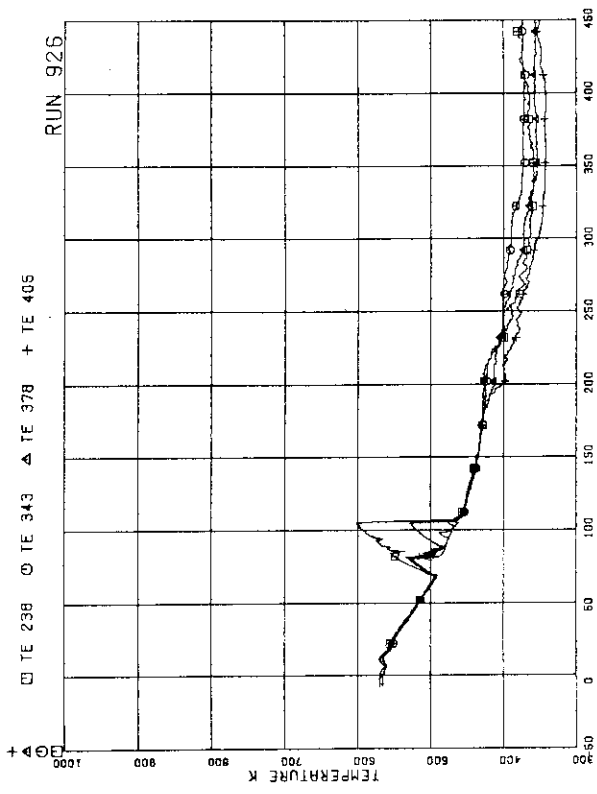

FIG.5.159 SURFACE TEMPERATURES OF FUEL RODS A22,B22,C22,022 AT POSITION 6

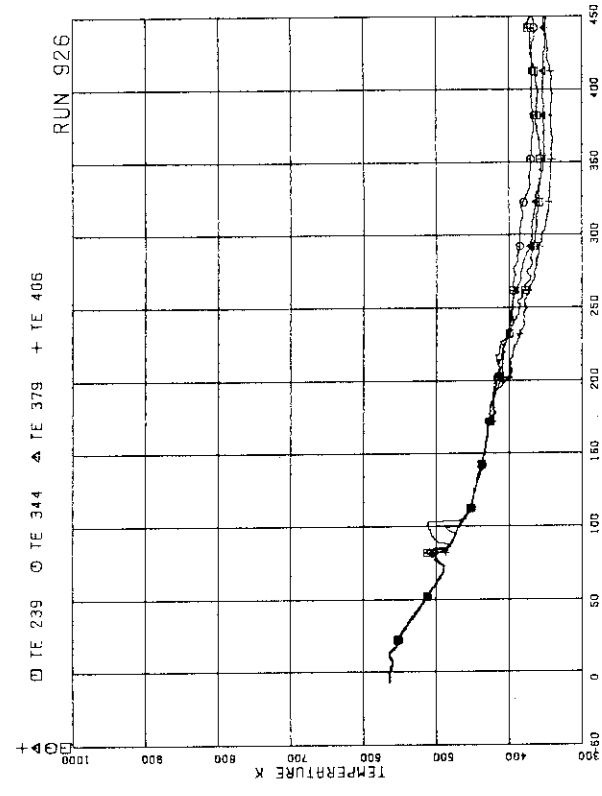

FIG.5.160 SURFACE TEMPERATURES OF FUEL RODS A22,B22,C22,022 AT POSITION 7

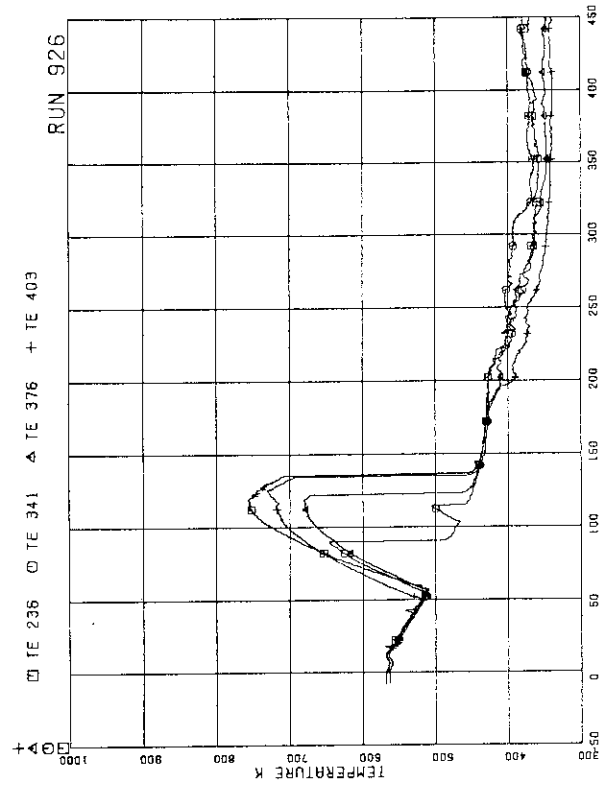

FIG.5.157 SURFACE TEMPERATURES OF FUEL RODS A22,B22,C22,022 RODS AT POSITION 4

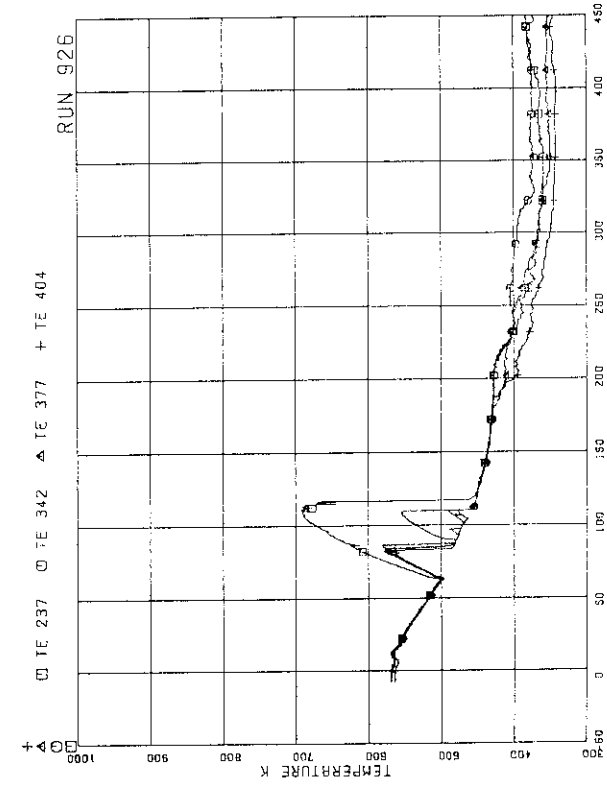

FIG.5.158 SURFACE TEMPERATURES OF FUEL RODS A22,B22,C22,022 AT POSITION 5

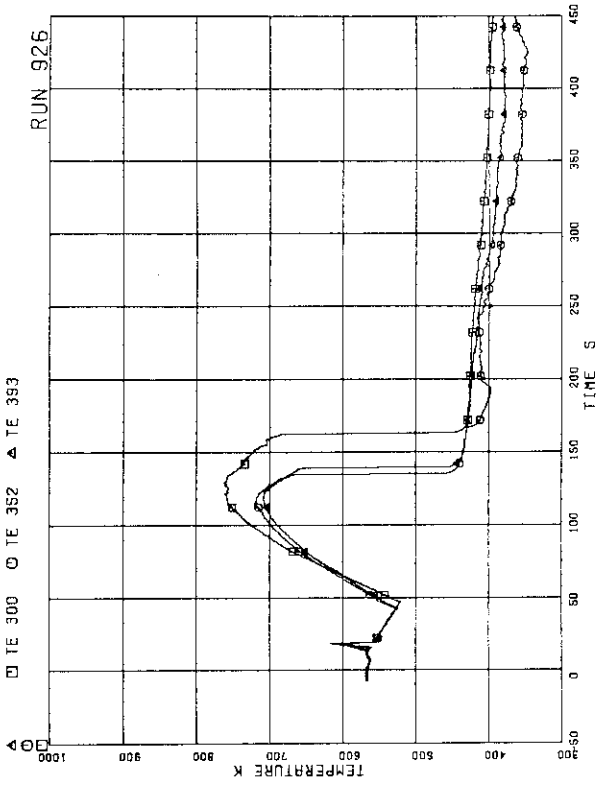

FIG.5.163 SURFACE TEMPERATURES OF FUEL RODS
A77,B77,C77 AT POSITION 3

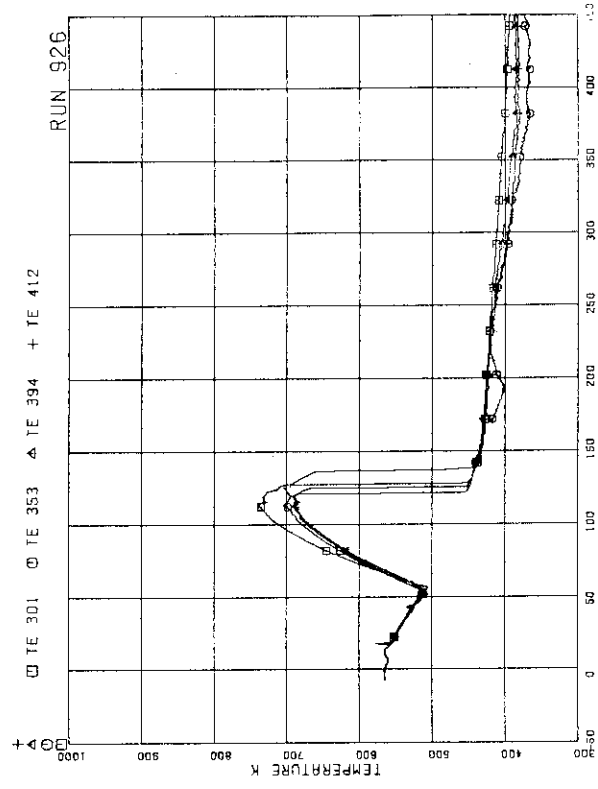

FIG.5.164 SURFACE TEMPERATURES OF FUEL RODS
A77,B77,C77 AT POSITION 4

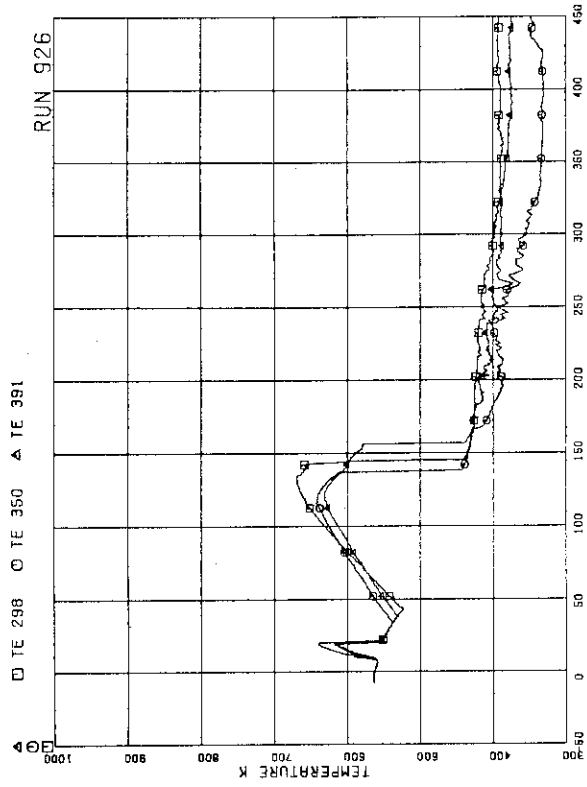

FIG.5.161 SURFACE TEMPERATURES OF FUEL RODS
A77,B77,C77 AT POSITION 1

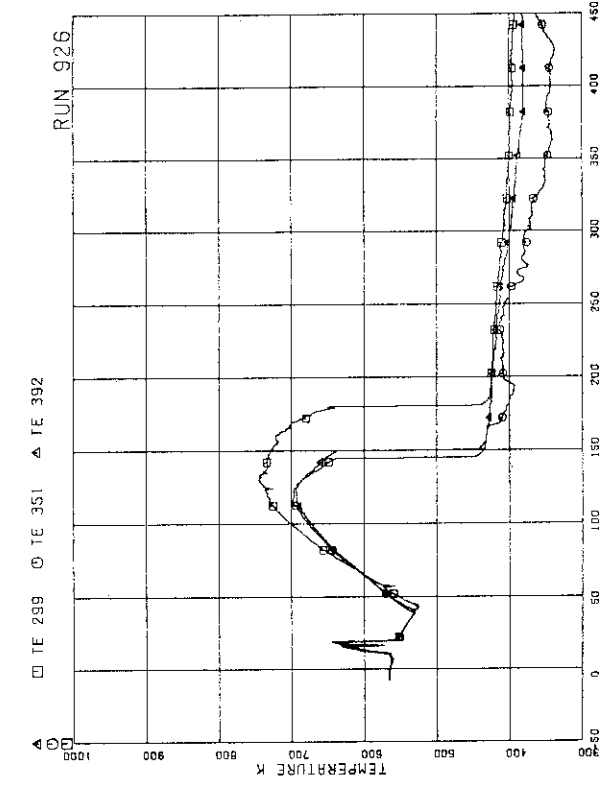

FIG.5.162 SURFACE TEMPERATURES OF FUEL RODS
A77,B77,C77 AT POSITION 2

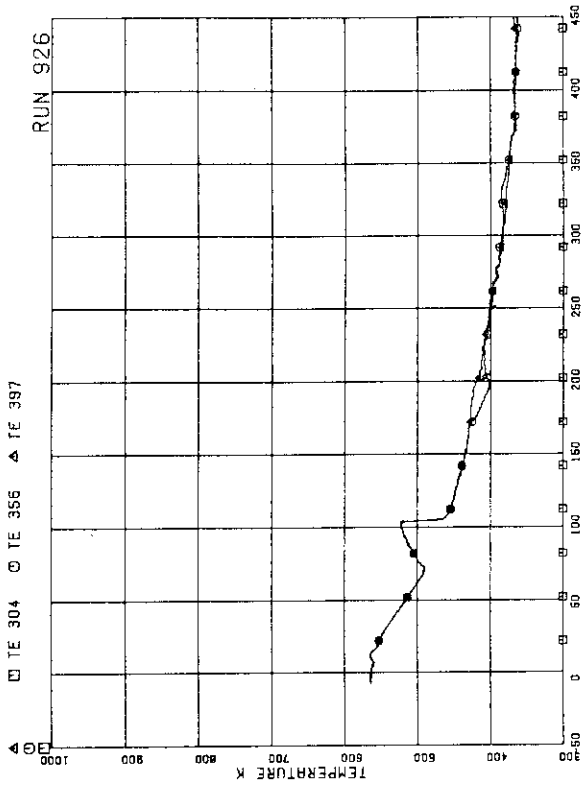

FIG.5.167 SURFACE TEMPERATURES OF FUEL RODS A77,B77,C77 RODS AT POSITION 7

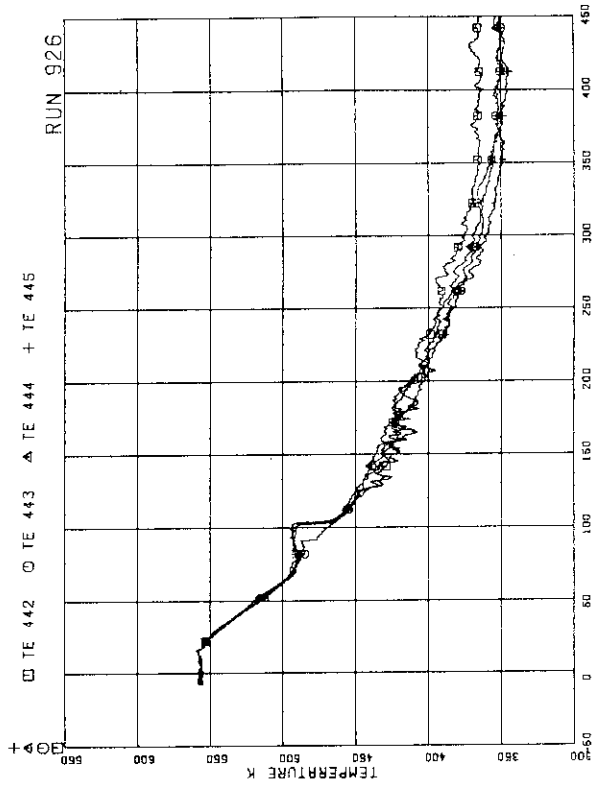

FIG.5.168 FLUID TEMPERATURES AT CHANNEL INLET

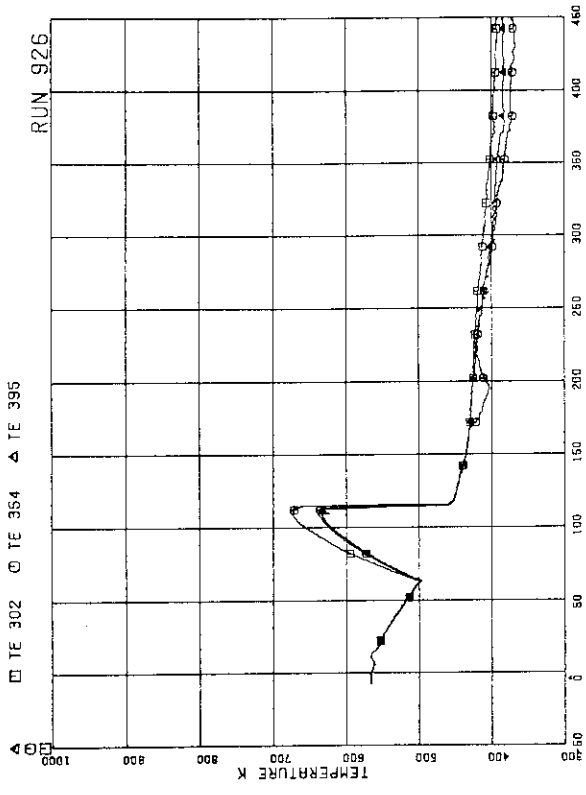

FIG.5.165 SURFACE TEMPERATURES OF FUEL RODS A77,B77,C77 AT POSITION 5

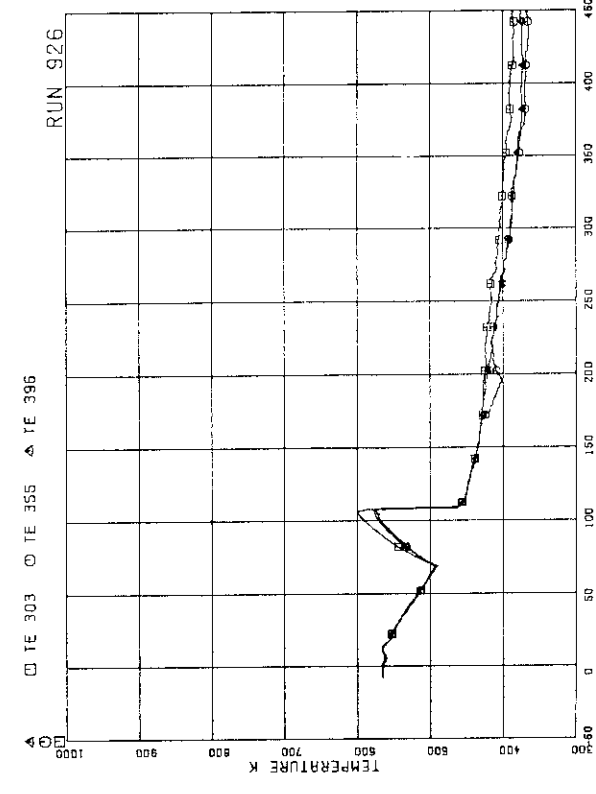

FIG.5.166 SURFACE TEMPERATURES OF FUEL RODS A77,B77,C77 AT POSITION 6

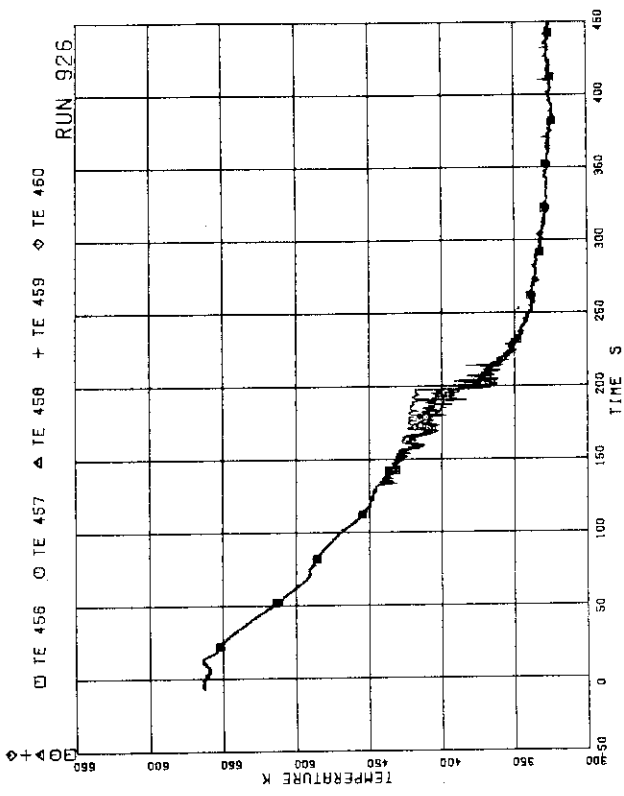

FIG.5.171 FLUID TEMPERATURES ABOVE UTP OF CHANNEL A, OPENINGS 1 TO 5

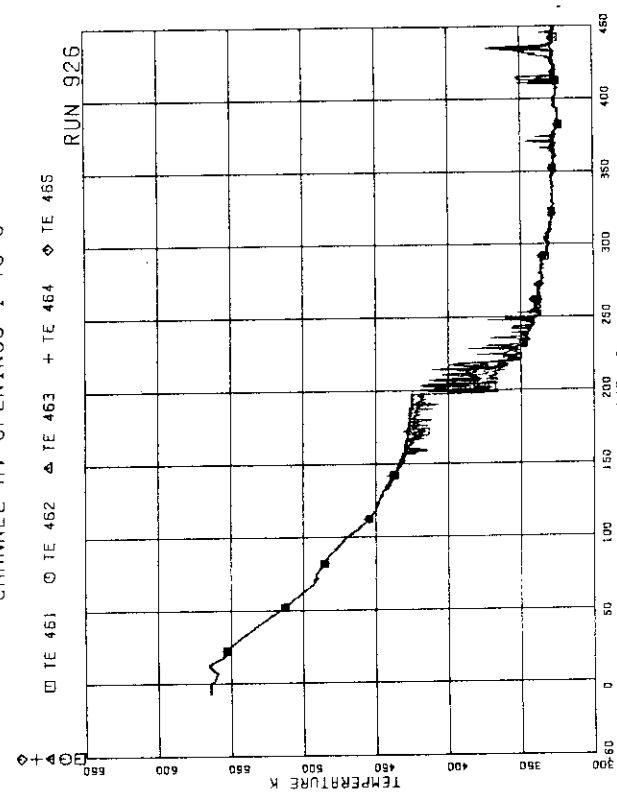

FIG.5.172 FLUID TEMPERATURES ABOVE UTP OF CHANNEL A, OPENINGS 6 TO 10

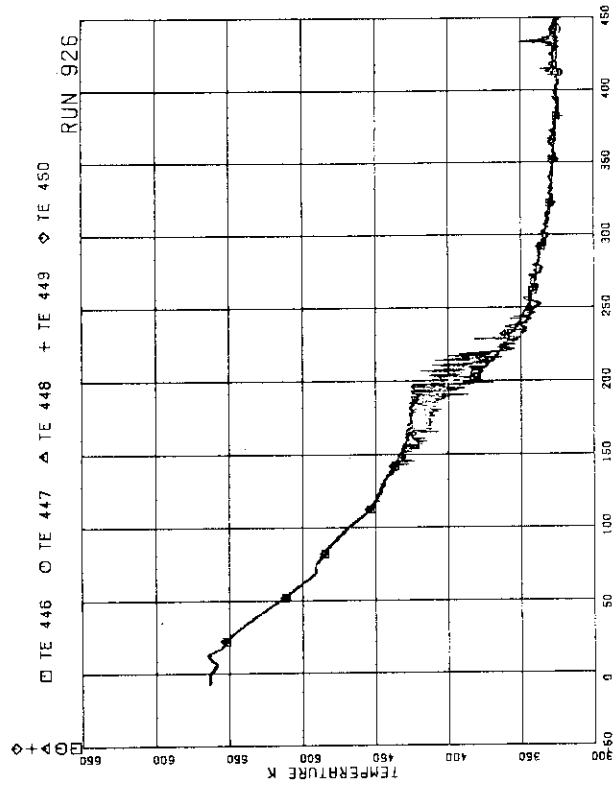

FIG.5.169 FLUID TEMPERATURES AT CHANNEL A OUTLET

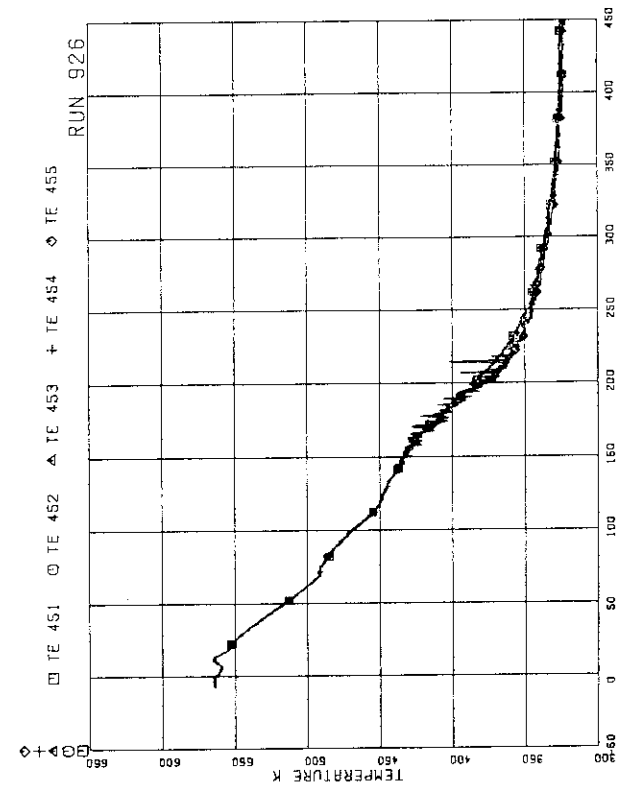

FIG.5.170 FLUID TEMPERATURES AT CHANNEL C OUTLET

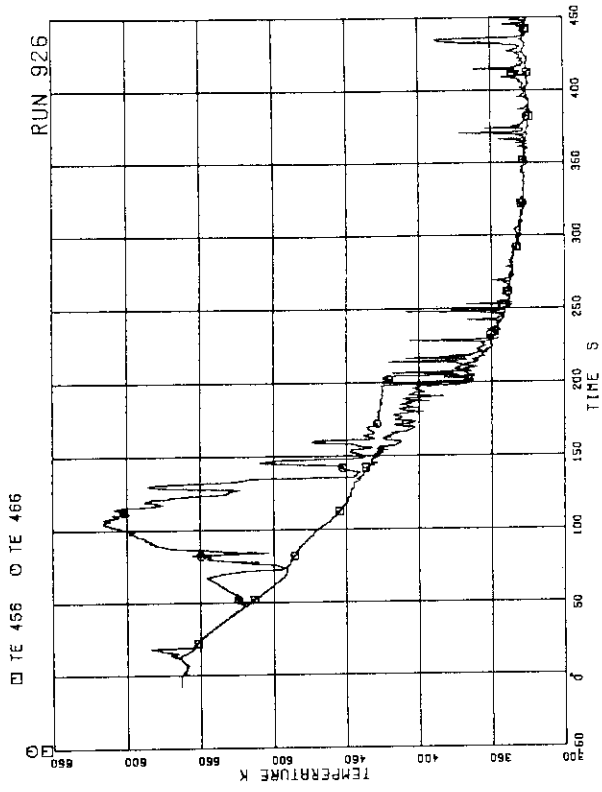

FIG.5.175 FLUID TEMPERATURES AT UTP IN CHANNEL A, OPENING 1

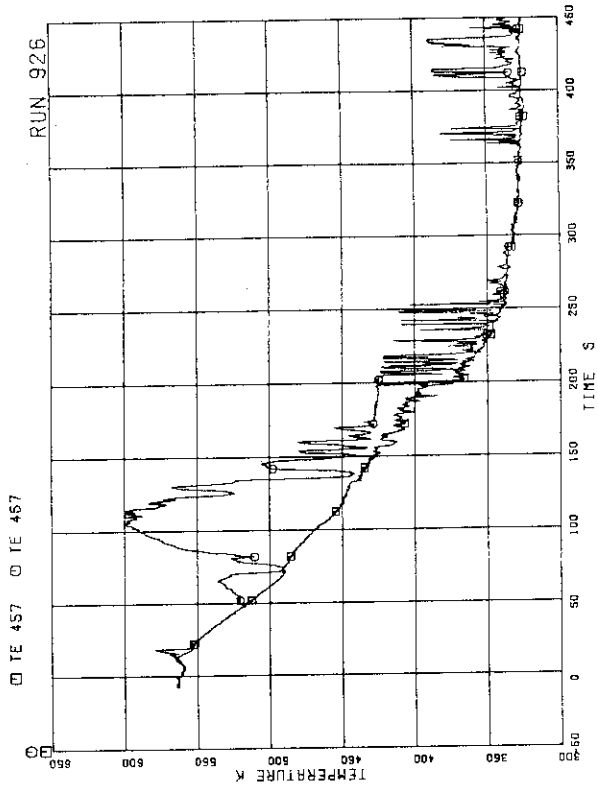

FIG.5.176 FLUID TEMPERATURES AT UTP IN CHANNEL A, OPENING 2

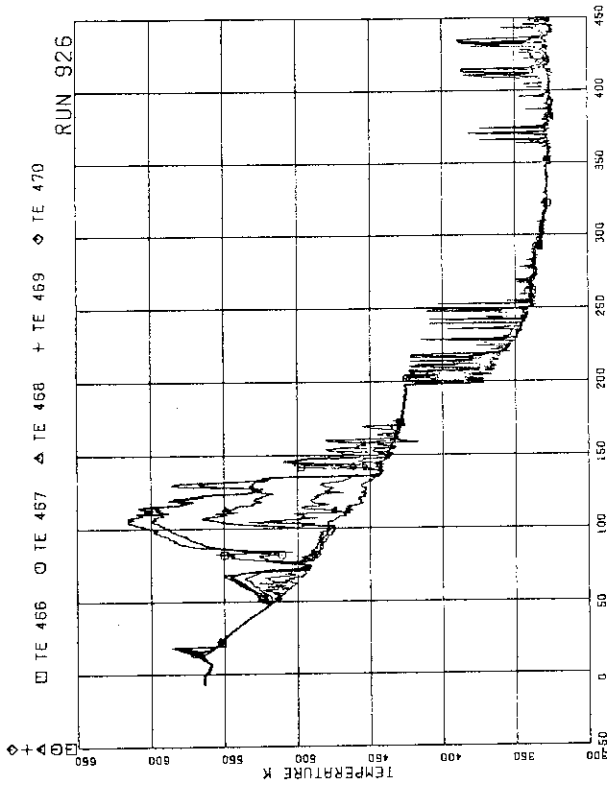

FIG.5.173 FLUID TEMPERATURES BELOW UTP OF CHANNEL A, OPENINGS 1 TO 5

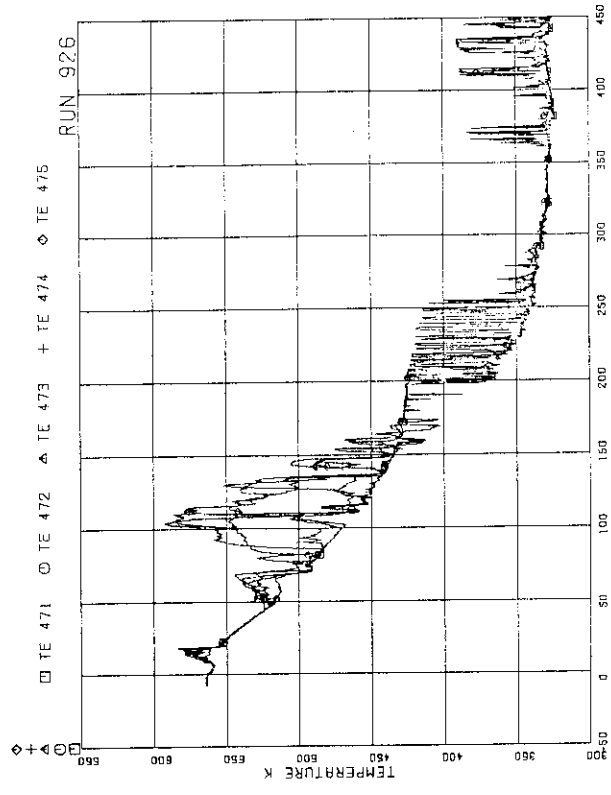

FIG.5.174 FLUID TEMPERATURES BELOW UTP OF CHANNEL A, OPENINGS 6 TO 10

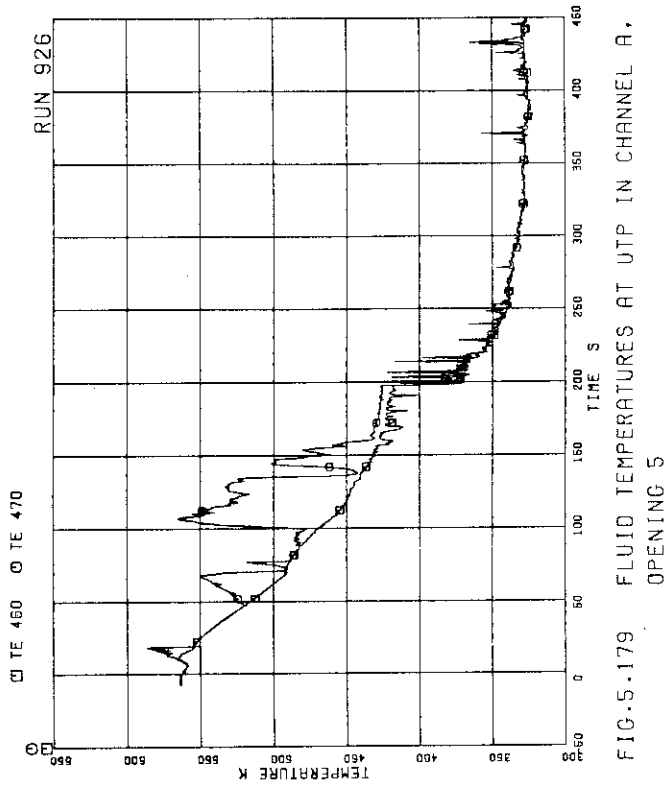

FIG.5.179 FLUID TEMPERATURES AT UTP IN CHANNEL A, OPENING 5

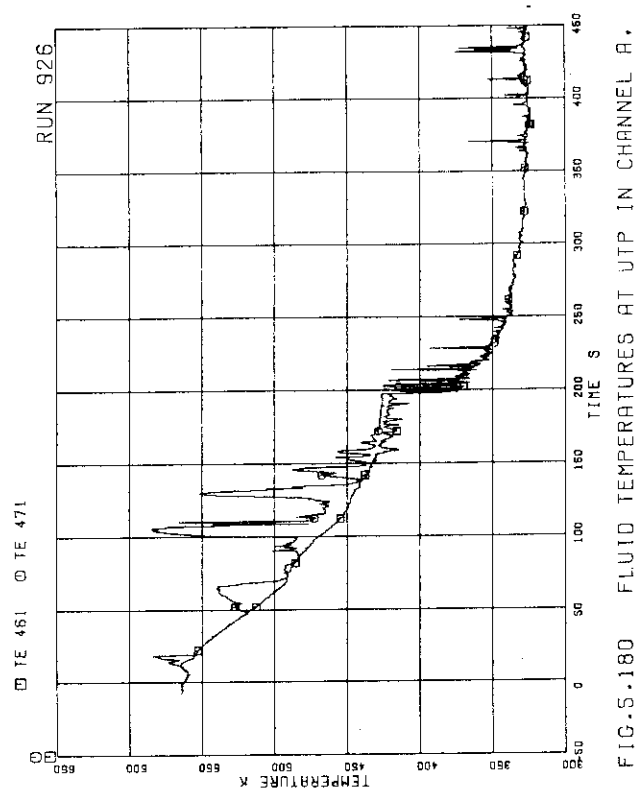

FIG.5.180 FLUID TEMPERATURES AT UTP IN CHANNEL A, OPENING 6

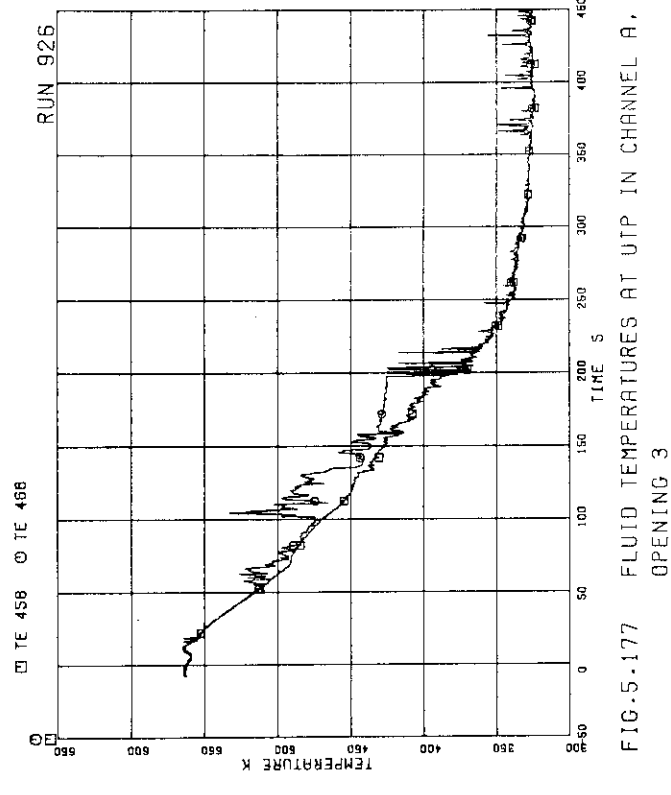

FIG.5.177 FLUID TEMPERATURES AT UTP IN CHANNEL A, OPENING 3

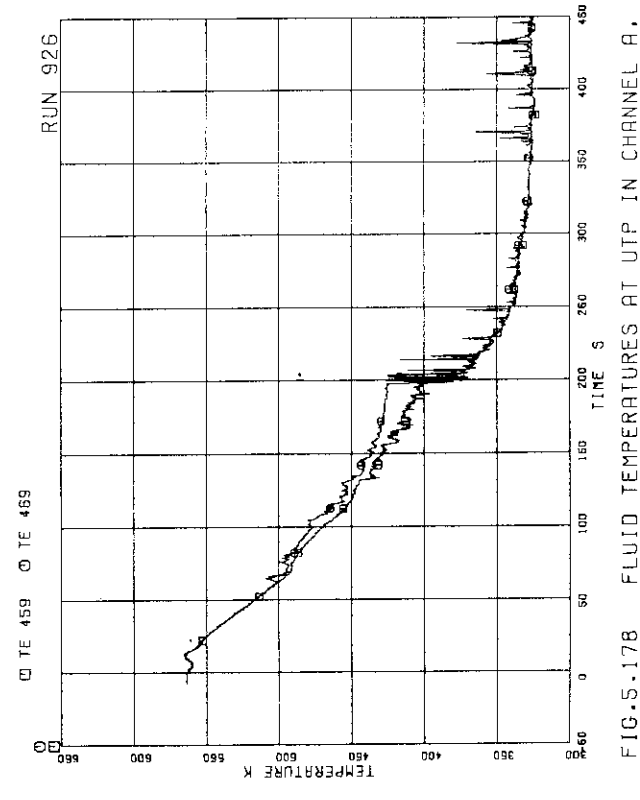

FIG.5.178 FLUID TEMPERATURES AT UTP IN CHANNEL A, OPENING 4

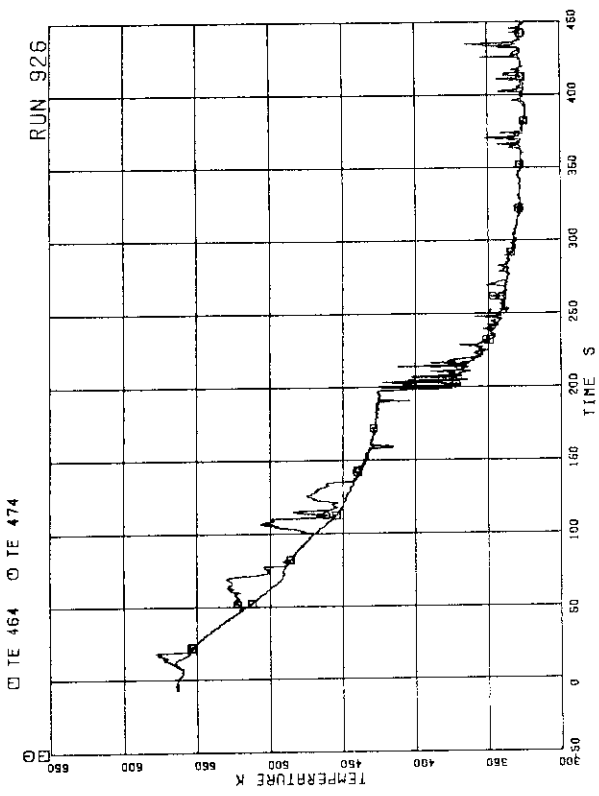

FIG.5.183 FLUID TEMPERATURES AT UTP IN CHANNEL A, OPENING 9

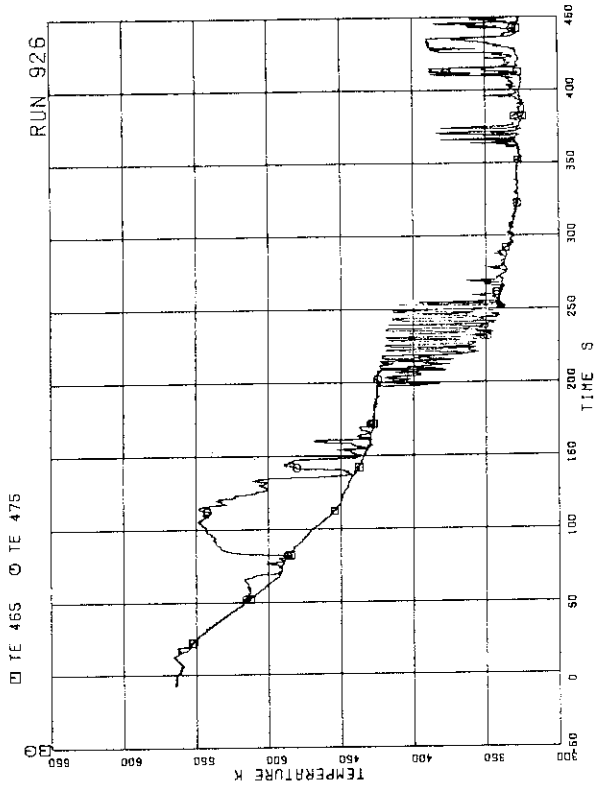

FIG.5.184 FLUID TEMPERATURES AT UTP IN CHANNEL A, OPENING 10

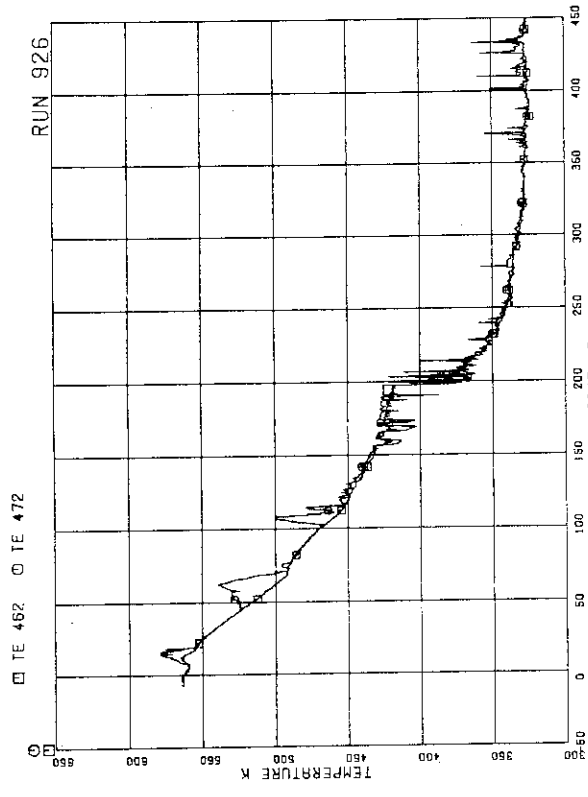

FIG.5.181 FLUID TEMPERATURES AT UTP IN CHANNEL A, OPENING 7

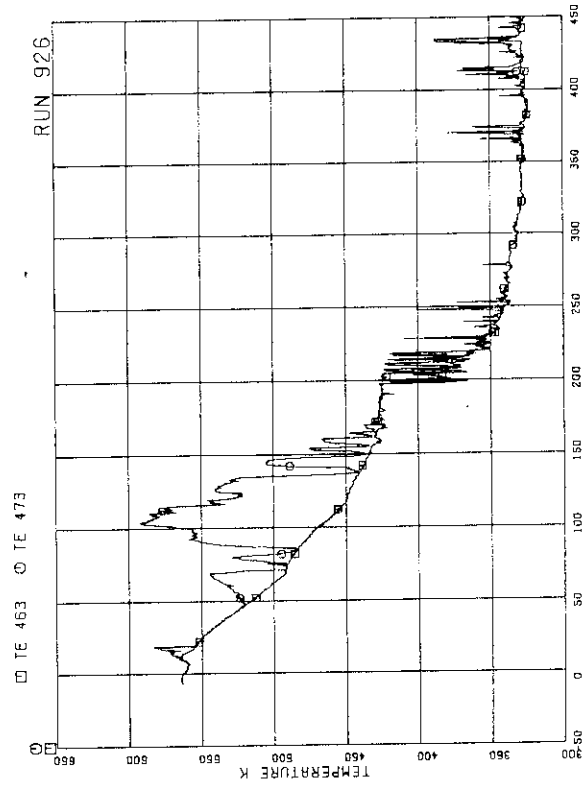

FIG.5.182 FLUID TEMPERATURES AT UTP IN CHANNEL A, OPENING 8

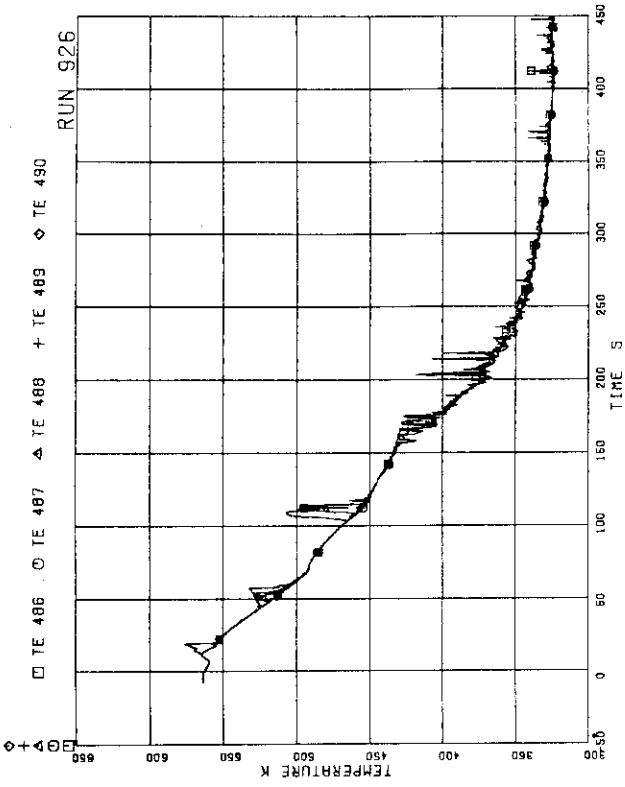

FIG.5.185 FLUID TEMPERATURES ABOVE UTP OF CHANNEL C, OPENINGS 1 TO 5

FIG.5.186 FLUID TEMPERATURES ABOVE UTP OF CHANNEL C, OPENINGS 6 TO 10

FIG.5.187 FLUID TEMPERATURES BELOW UTP OF CHANNEL C, OPENINGS 1 TO 5

FIG.5.188 FLUID TEMPERATURES BELOW UTP OF CHANNEL C, OPENINGS 6 TO 10

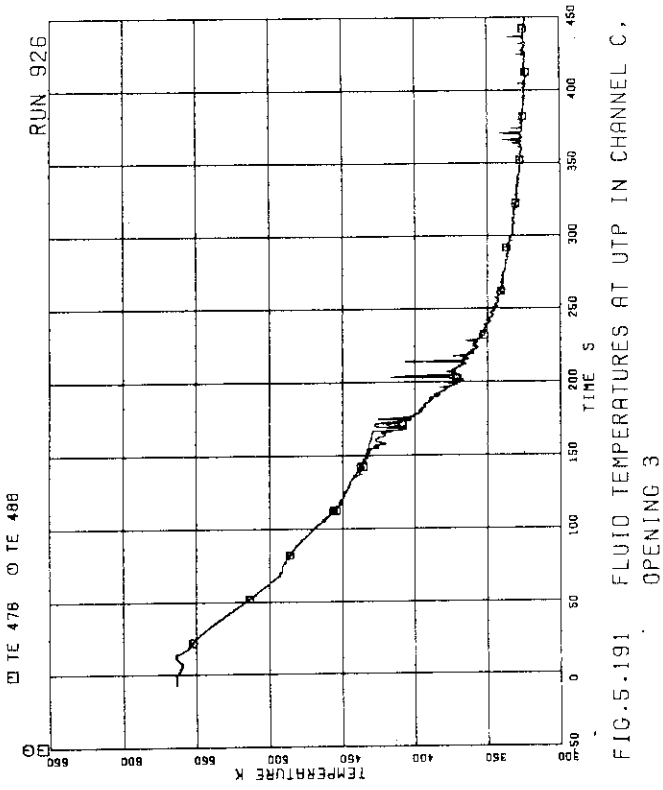

FIG.5.191 FLUID TEMPERATURES AT UTP IN CHANNEL C, OPENING 3

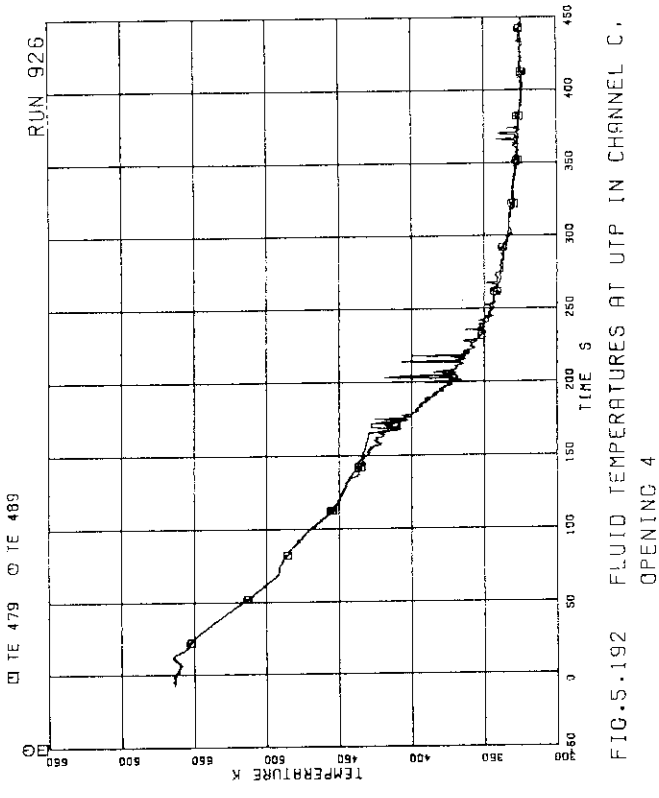

FIG.5.192 FLUID TEMPERATURES AT UTP IN CHANNEL C, OPENING 4

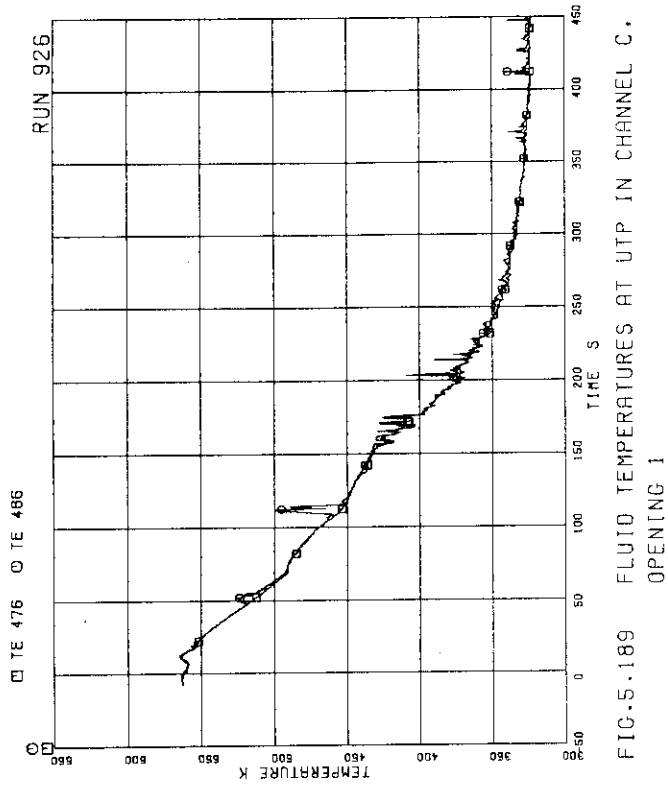

FIG.5.189 FLUID TEMPERATURES AT UTP IN CHANNEL C, OPENING 1

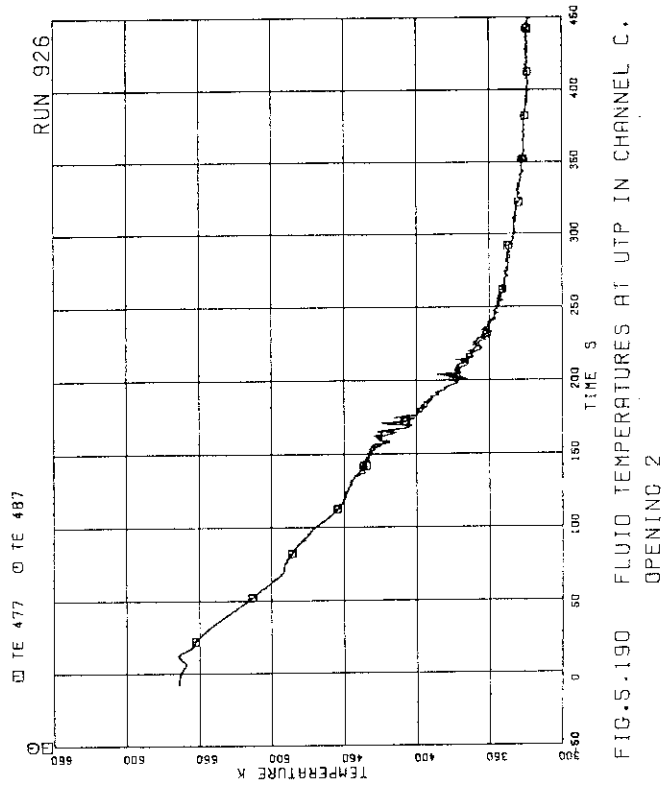

FIG.5.190 FLUID TEMPERATURES AT UTP IN CHANNEL C, OPENING 2

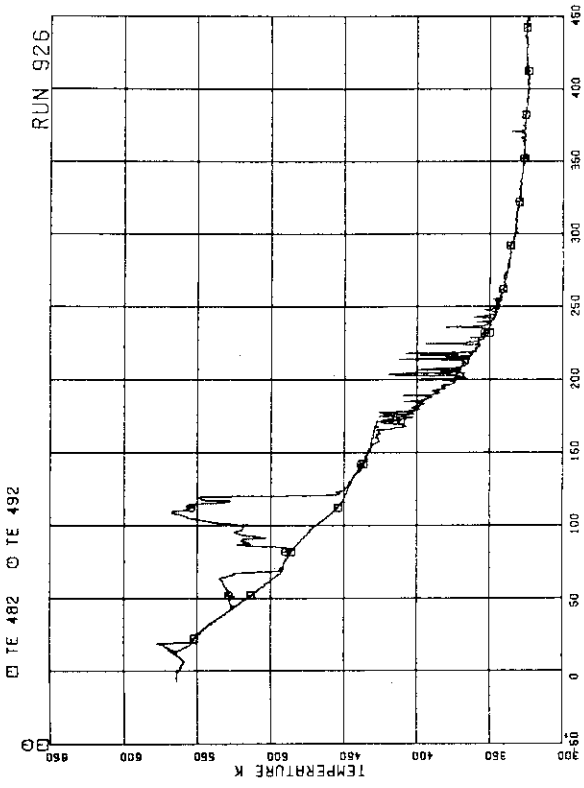

FIG.5.195 FLUID TEMPERATURES AT UTP IN CHANNEL C, OPENING 7

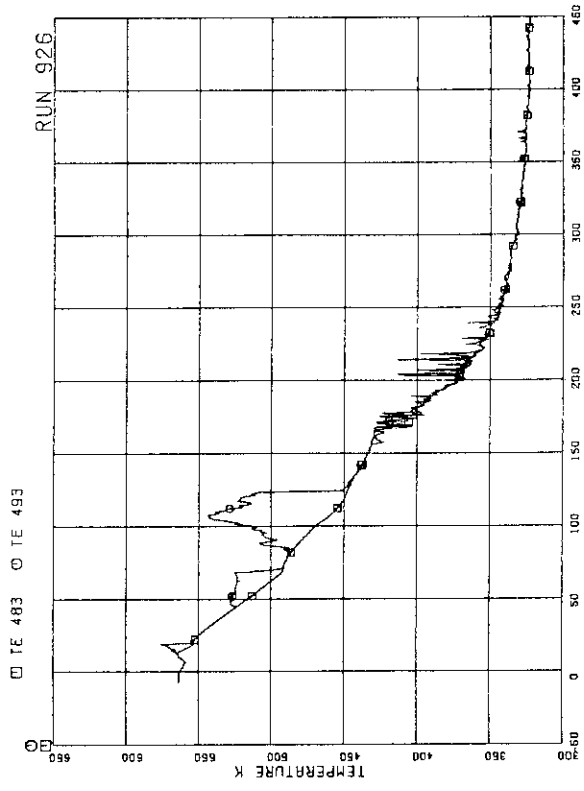

FIG.5.196 FLUID TEMPERATURES AT UTP IN CHANNEL C, OPENING 8

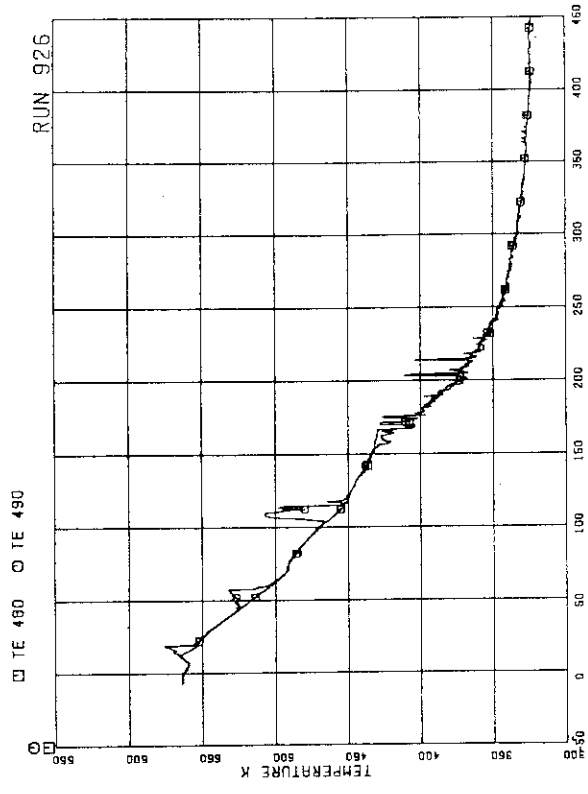

FIG.5.193 FLUID TEMPERATURES AT UTP IN CHANNEL C, OPENING 5

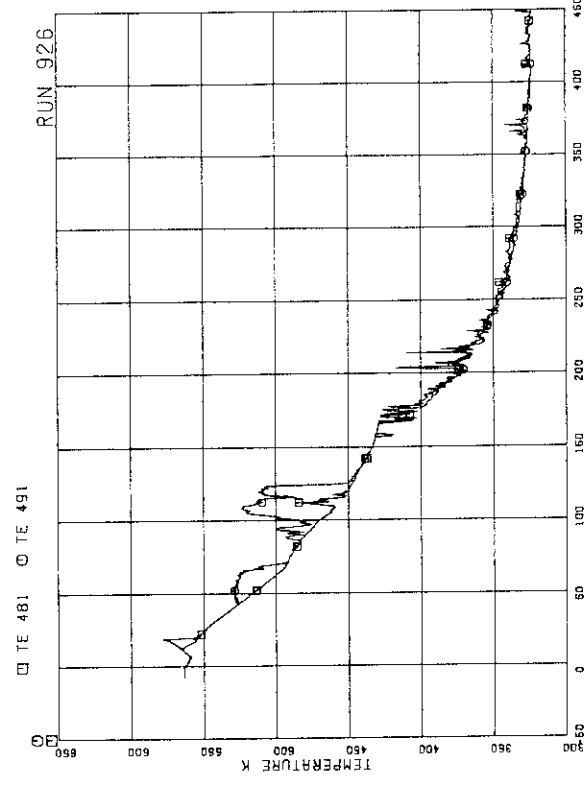

FIG.5.194 FLUID TEMPERATURES AT UTP IN CHANNEL C, OPENING 6

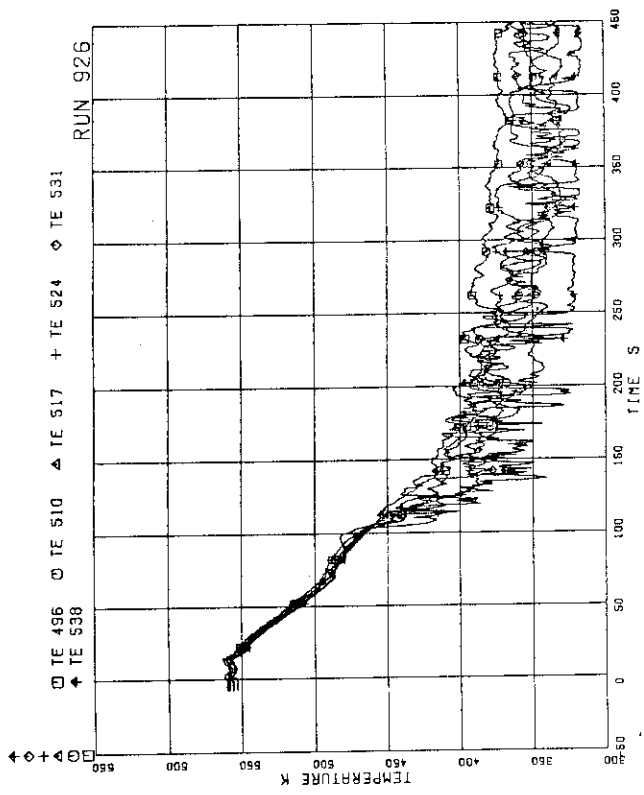

FIG.5.199 INNER AND OUTER SURFACE TEMPERATURES OF CHANNEL BOX AT POS.1

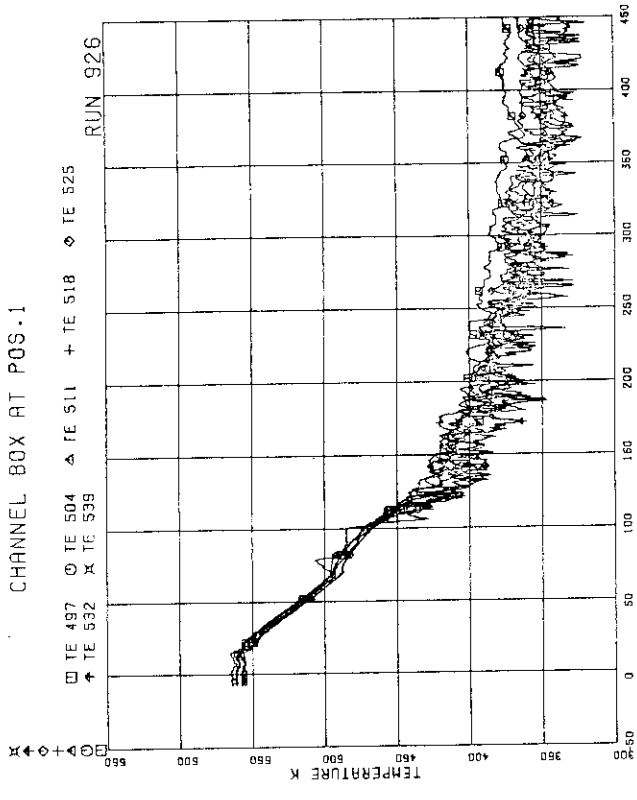

FIG.5.200 INNER AND OUTER SURFACE TEMPERATURES OF CHANNEL BOX AT POS.2

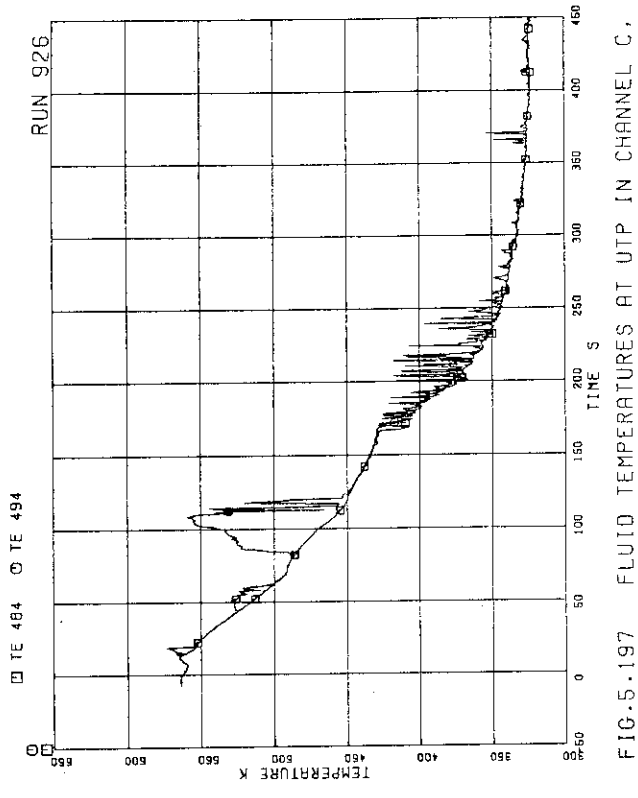

FIG.5.197 FLUID TEMPERATURES AT UTP IN CHANNEL C, OPENING 9

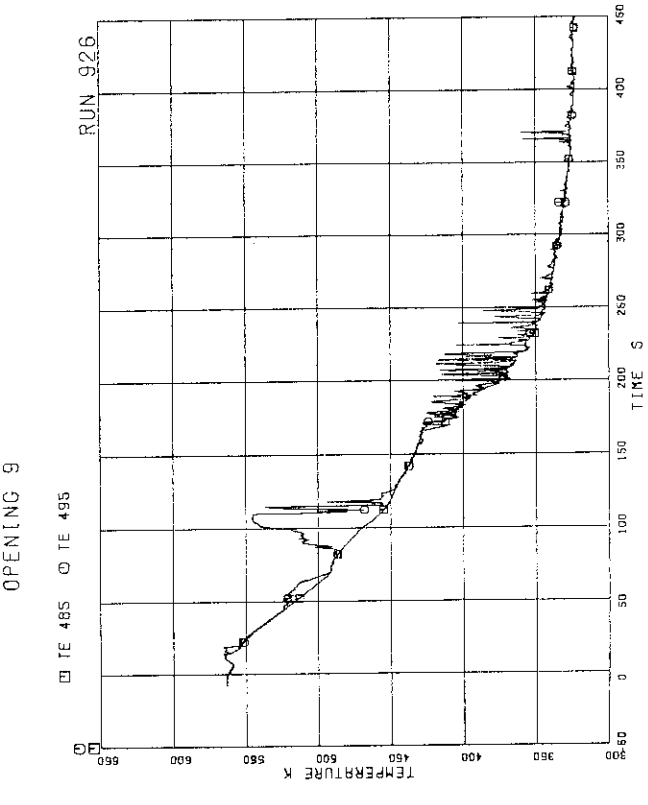

FIG.5.198 FLUID TEMPERATURES AT UTP IN CHANNEL C, OPENING 10

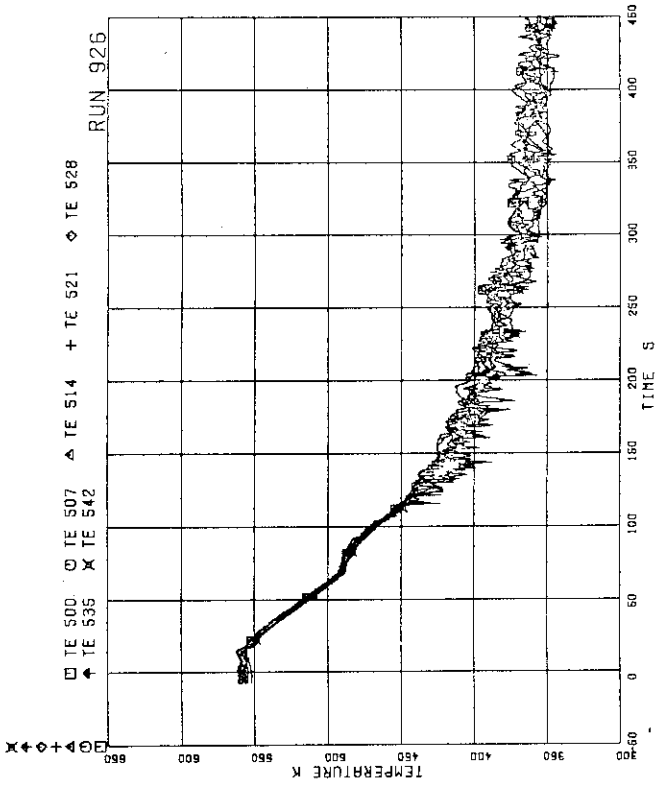

FIG.5.203 INNER AND OUTER SURFACE TEMPERATURES OF CHANNEL BOX AT POS.5

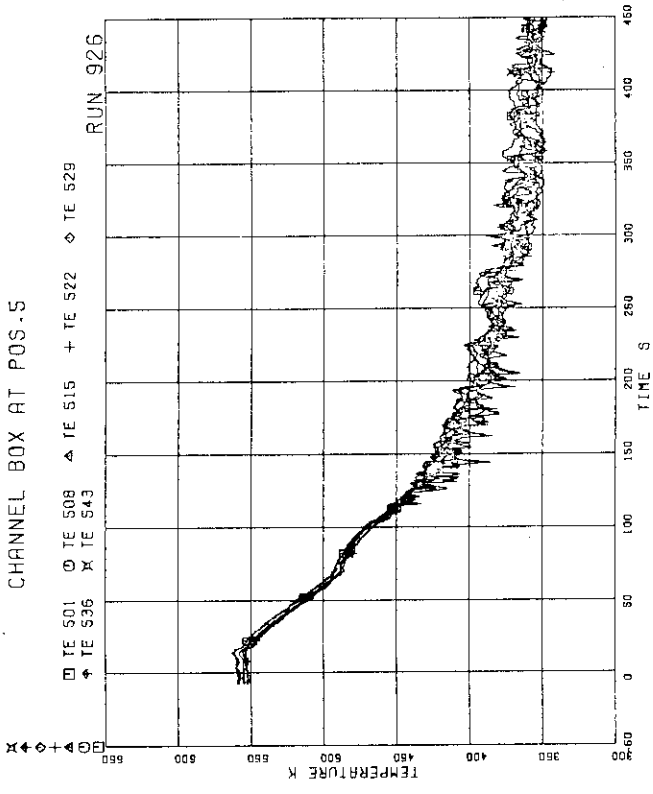

FIG.5.204 INNER AND OUTER SURFACE TEMPERATURES OF CHANNEL BOX AT POS.6

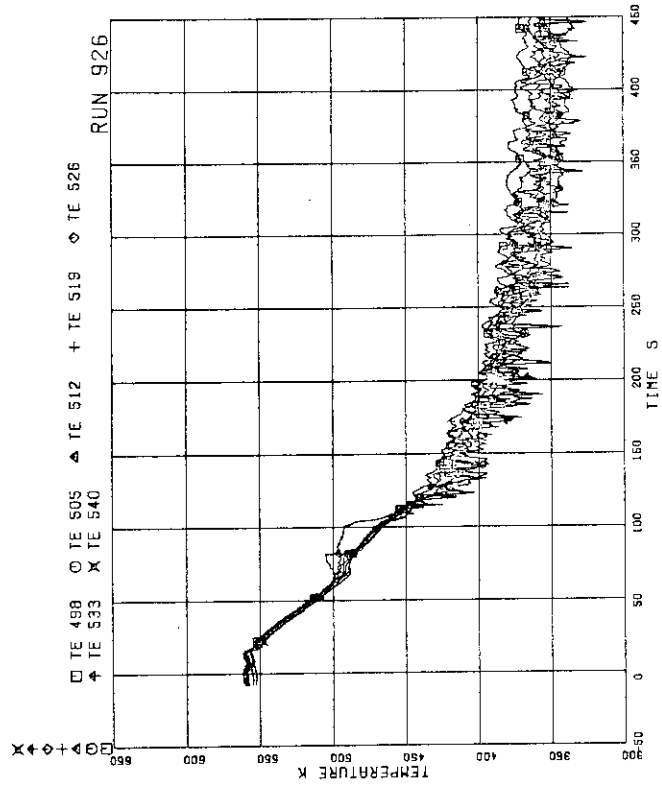

FIG.5.201 INNER AND OUTER SURFACE TEMPERATURES OF CHANNEL BOX AT POS.3

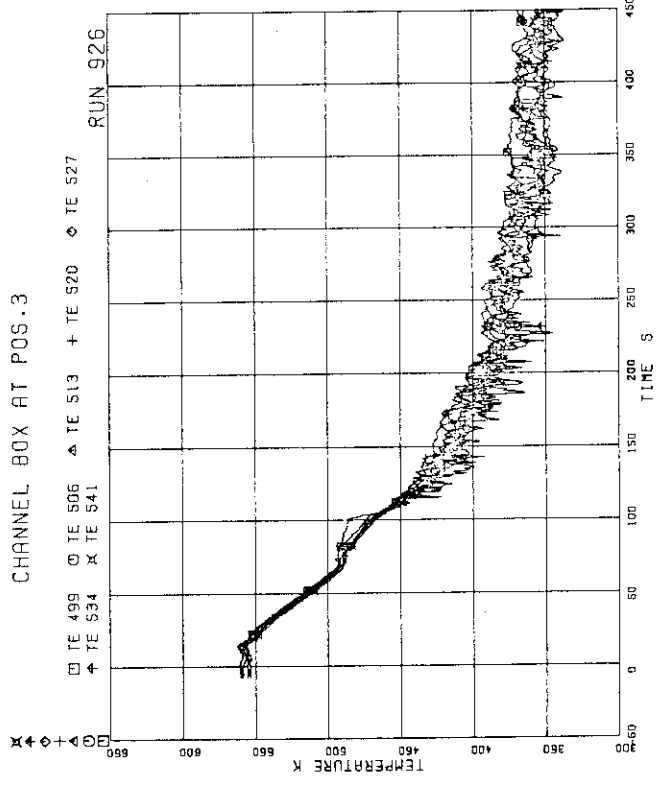

FIG.5.202 INNER AND OUTER SURFACE TEMPERATURES OF CHANNEL BOX AT POS.4

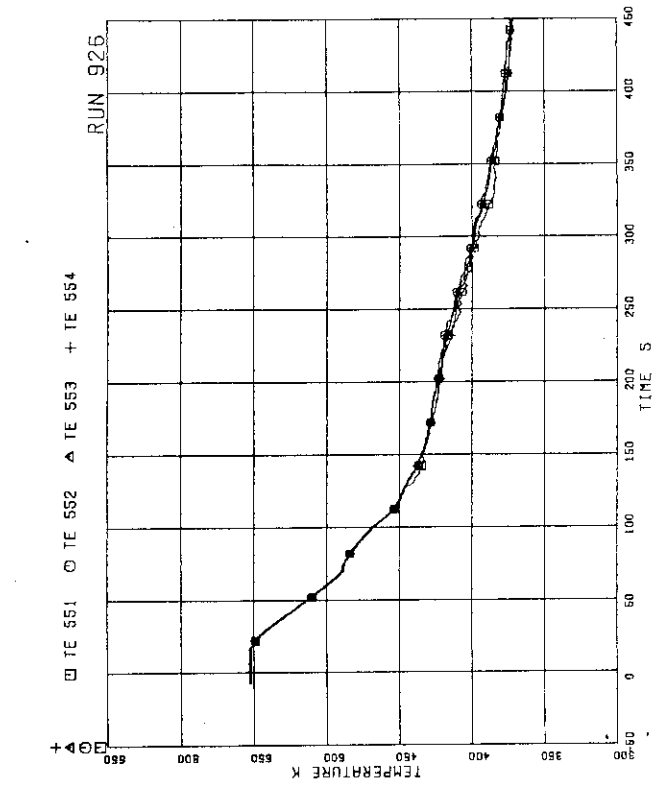

FIG.5.207 FLUID TEMPERATURES IN LOWER PLENUM, NORTH

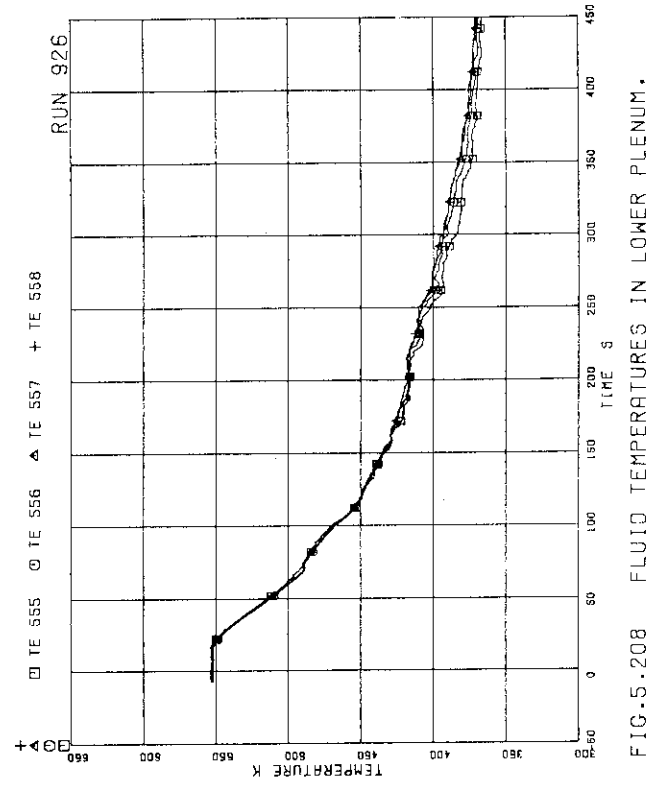

FIG.5.208 FLUID TEMPERATURES IN LOWER PLENUM, SOUTH

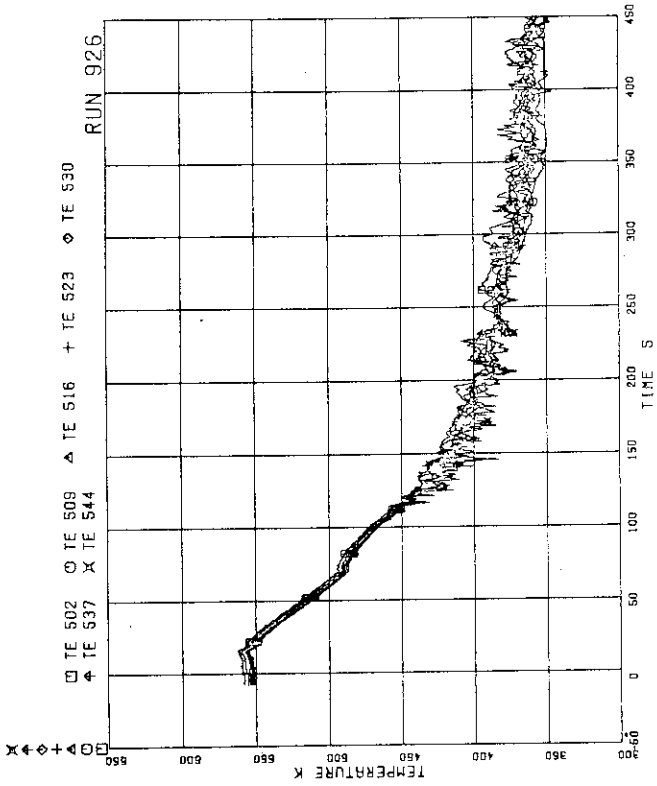

FIG.5.205 INNER AND OUTER SURFACE TEMPERATURES OF CHANNEL BOX AT POS.7

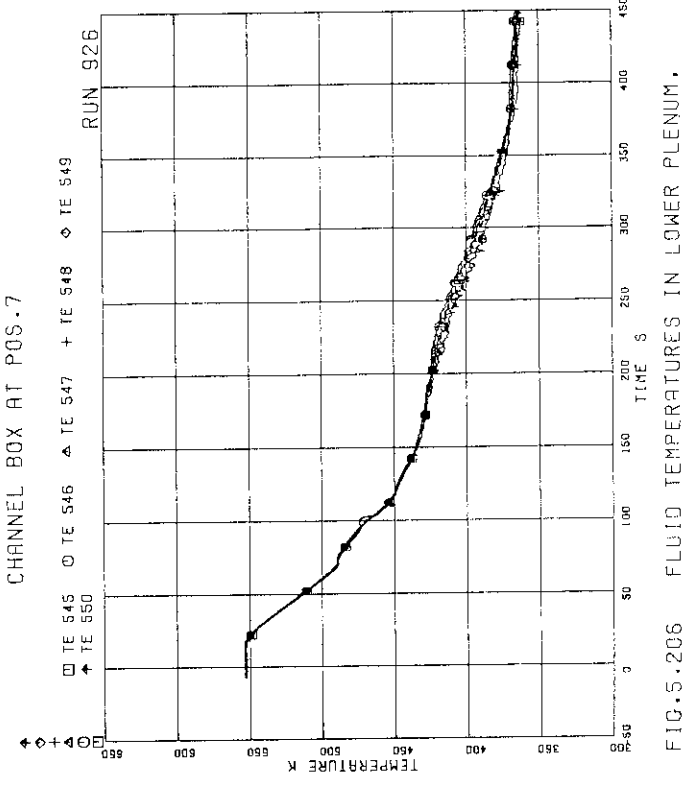

FIG.5.206 FLUID TEMPERATURES IN LOWER PLENUM, CENTER

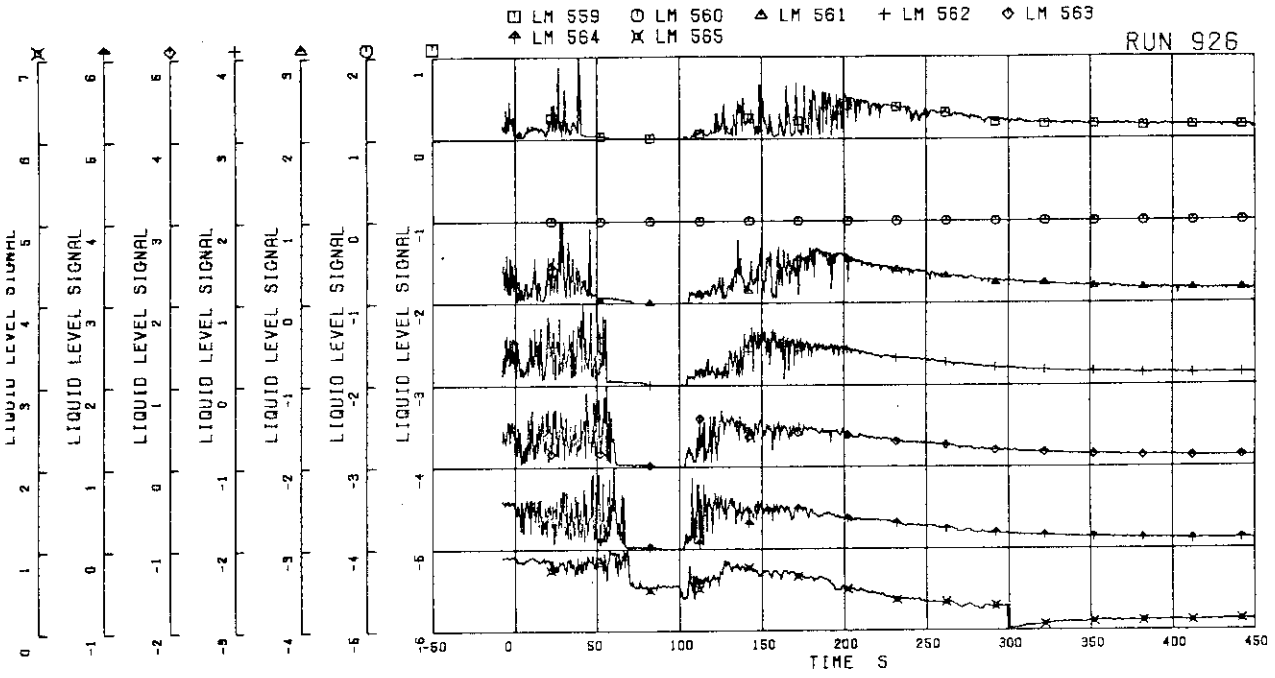

FIG.5.209 LIQUID LEVEL SIGNALS IN CHANNEL BOX A, LOCATION A1

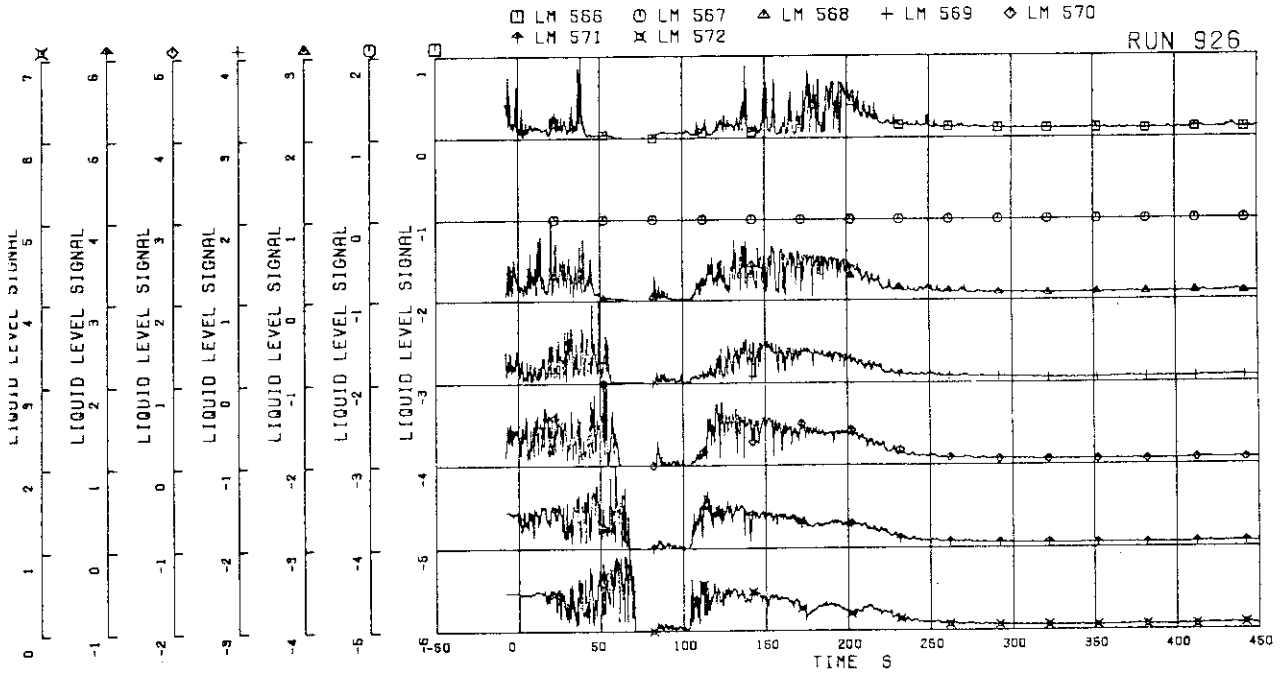

FIG.5.210 LIQUID LEVEL SIGNALS IN CHANNEL BOX A, LOCATION A2

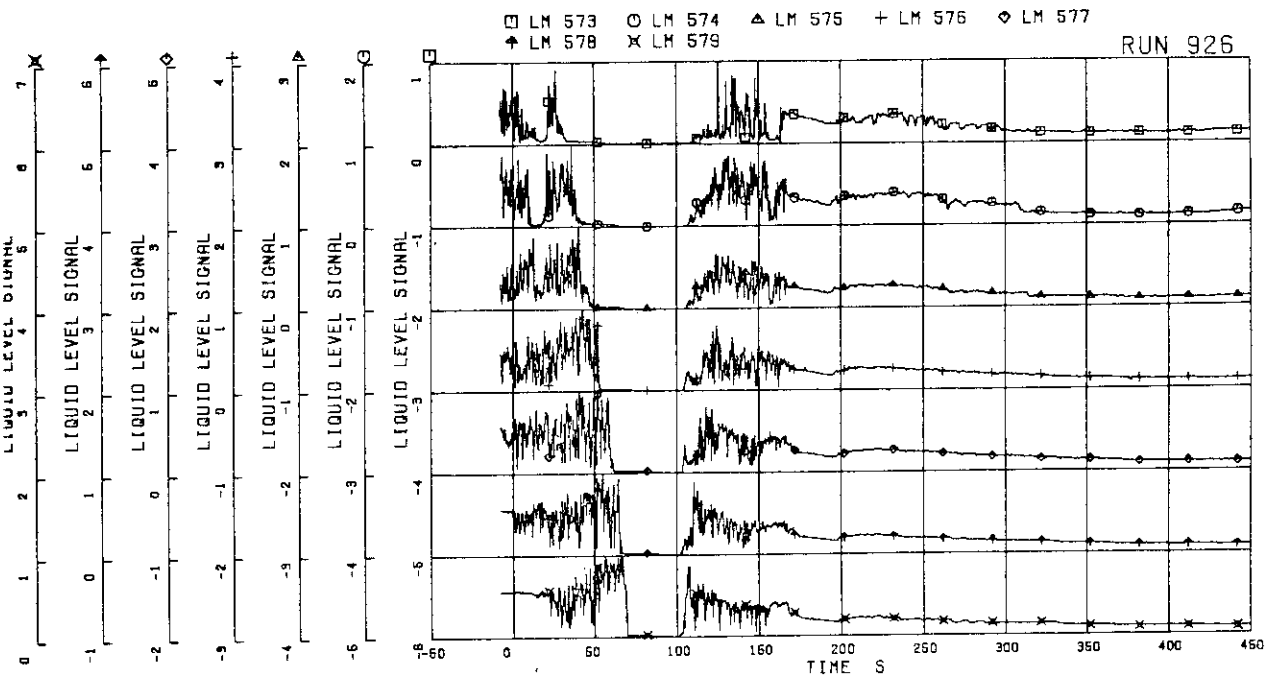

FIG.5.211 LIQUID LEVEL SIGNALS IN CHANNEL BOX B

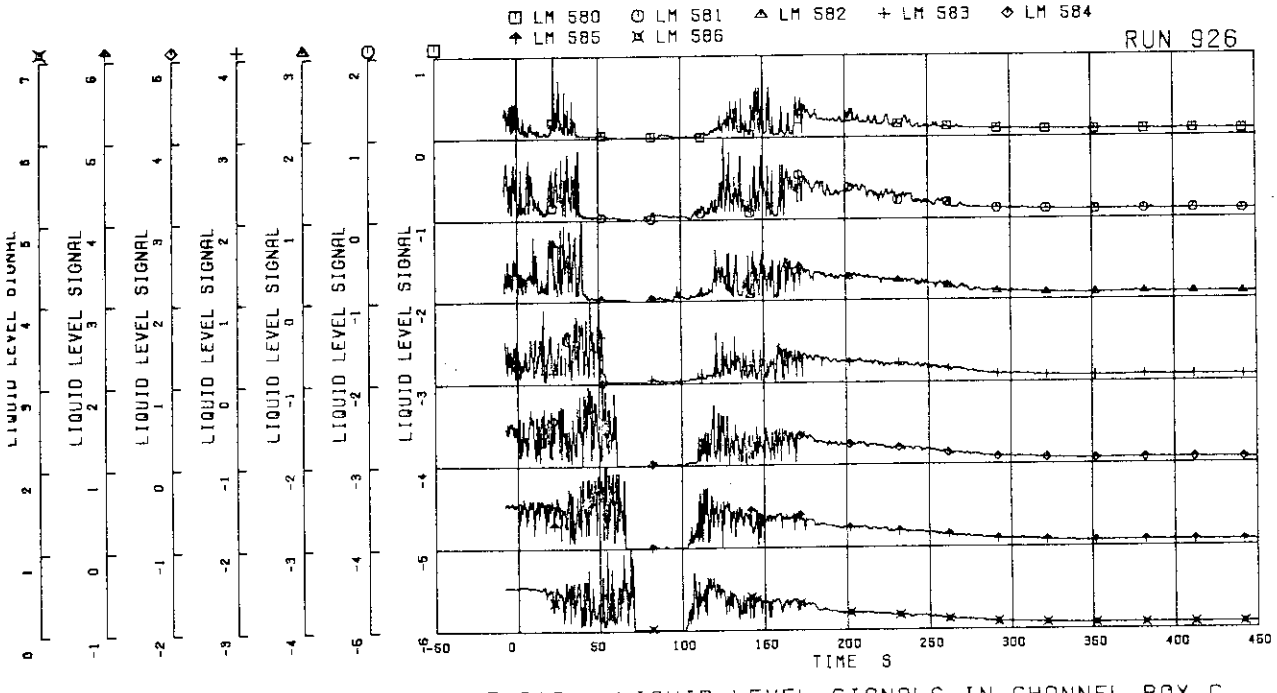

FIG.5.212 LIQUID LEVEL SIGNALS IN CHANNEL BOX C

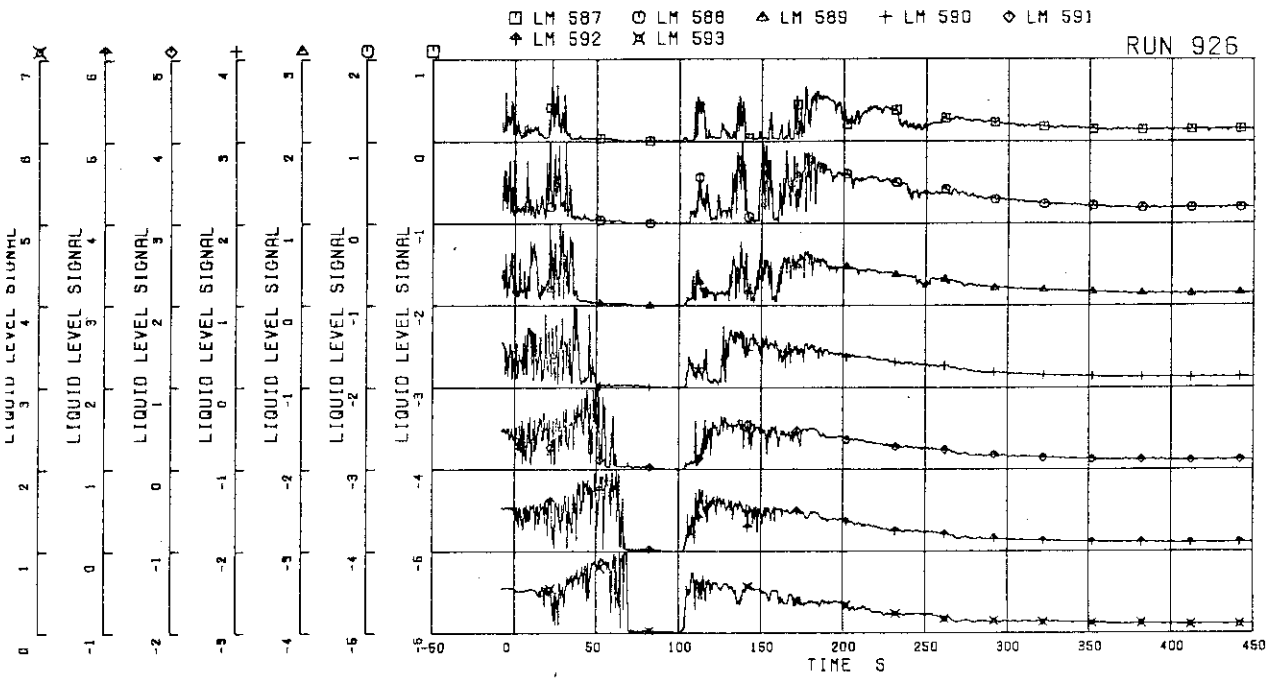

FIG.5.213 LIQUID LEVEL SIGNALS IN CHANNEL BOX D

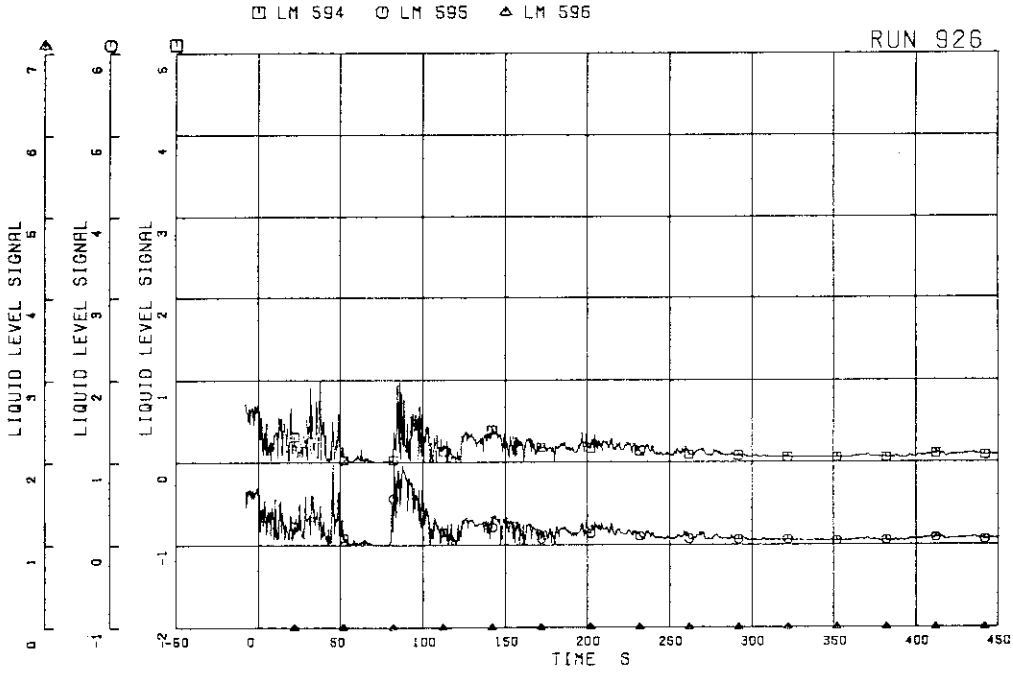

FIG.5.214 LIQUID LEVEL SIGNALS IN CHANNEL A OUTLET LOCATION A1

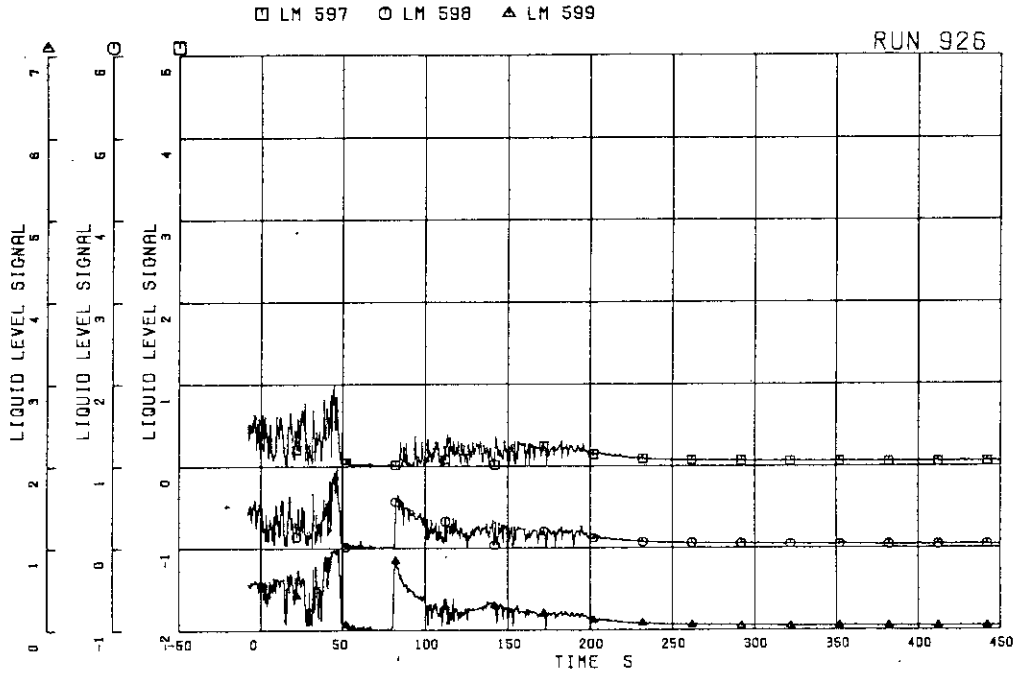

FIG.5.215 LIQUID LEVEL SIGNALS IN CHANNEL A OUTLET LOCATION A2

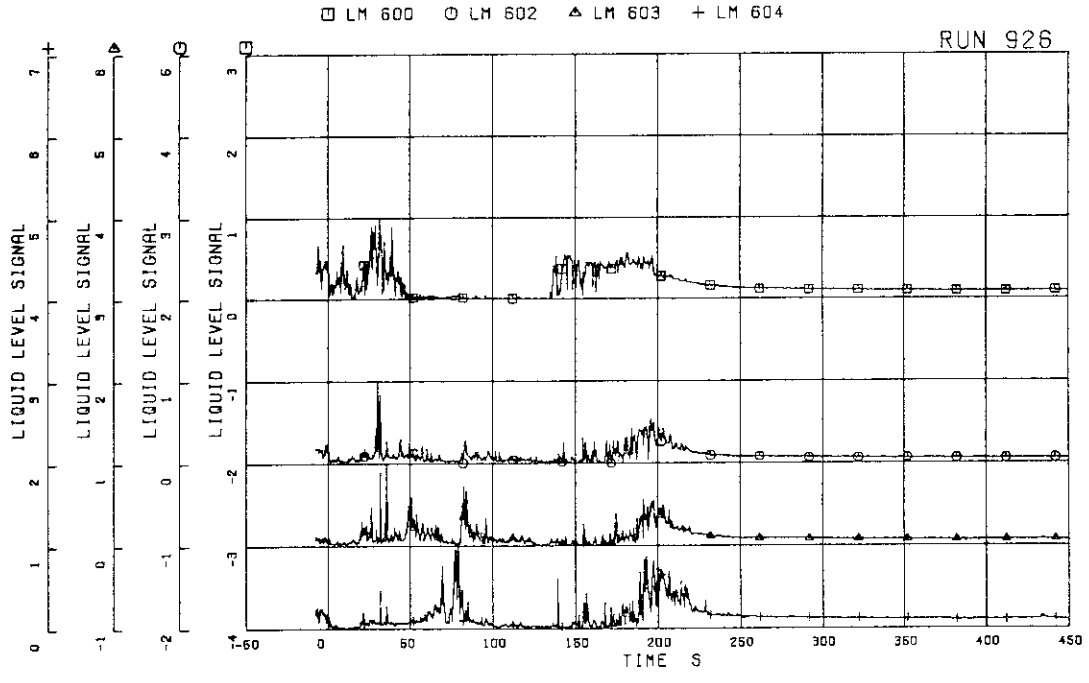

FIG.5.216 LIQUID LEVEL SIGNALS IN CHANNEL A OUTLET CENTER

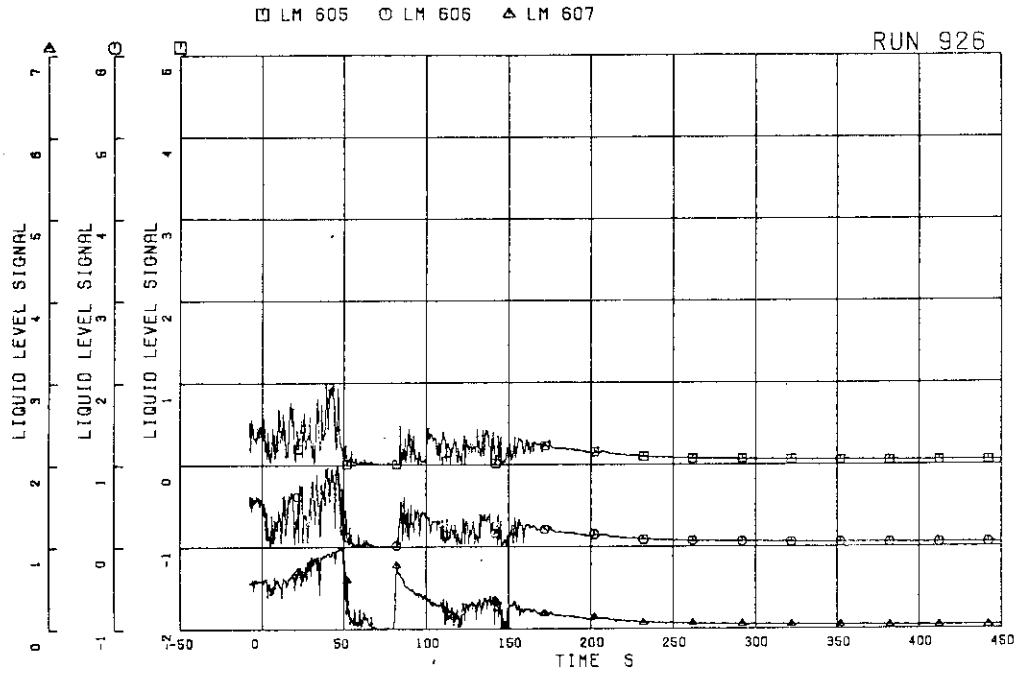

FIG.5.217 LIQUID LEVEL SIGNALS IN CHANNEL C OUTLET LOCATION C1

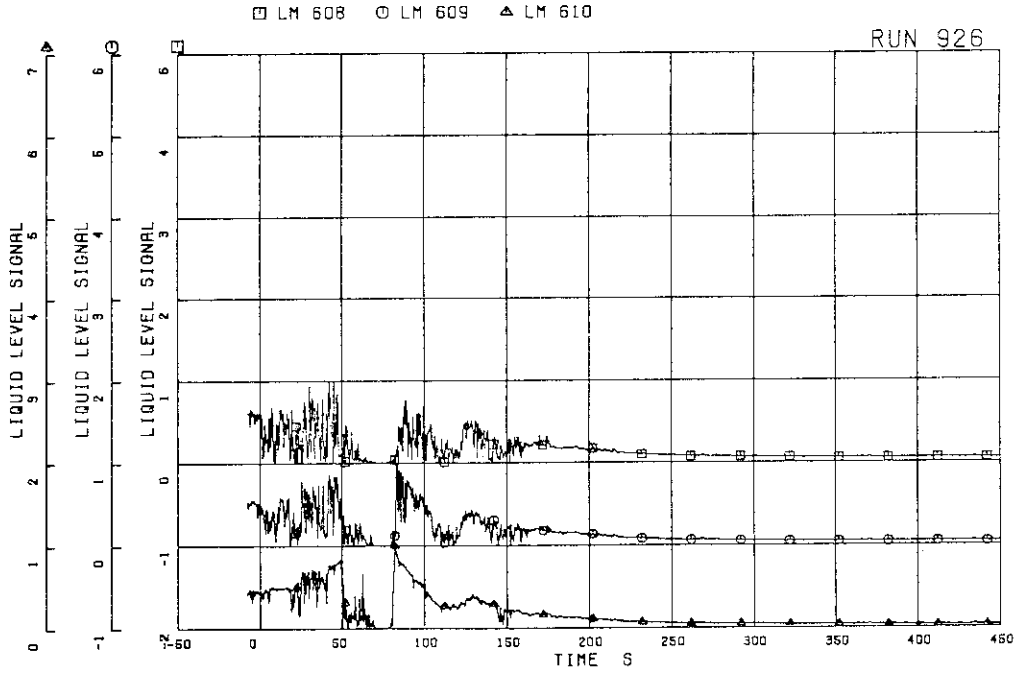

FIG.5.218 LIQUID LEVEL SIGNALS IN CHANNEL C OUTLET LOCATION C2

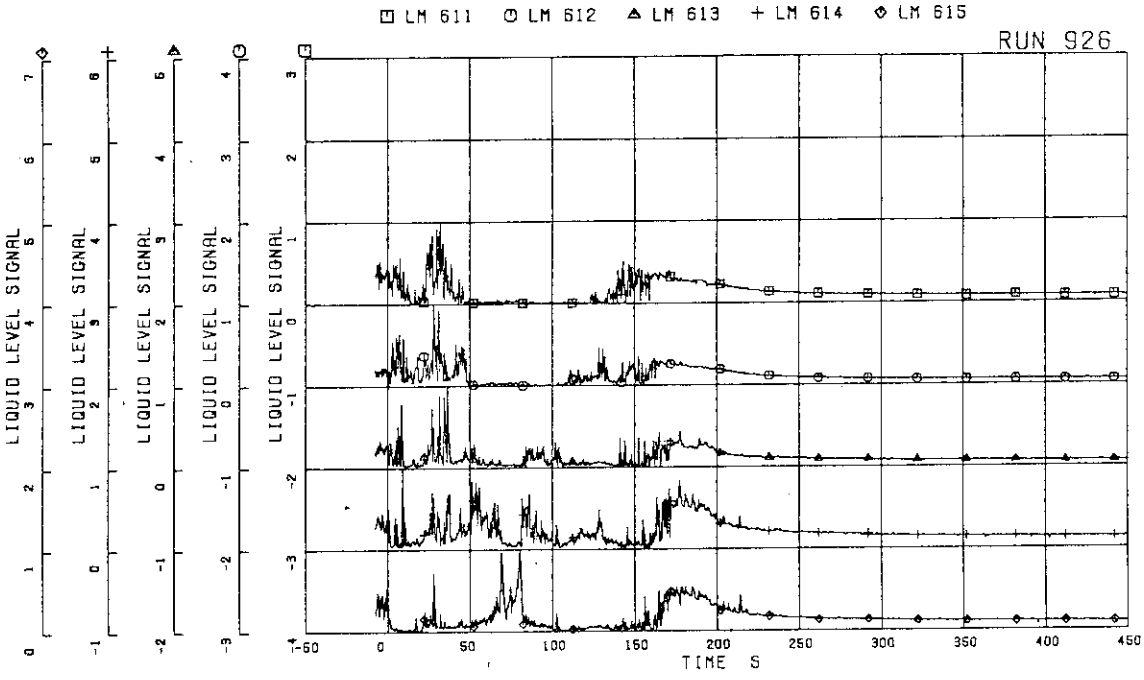

FIG.5.219 LIQUID LEVEL SIGNALS IN CHANNEL C OUTLET CENTER

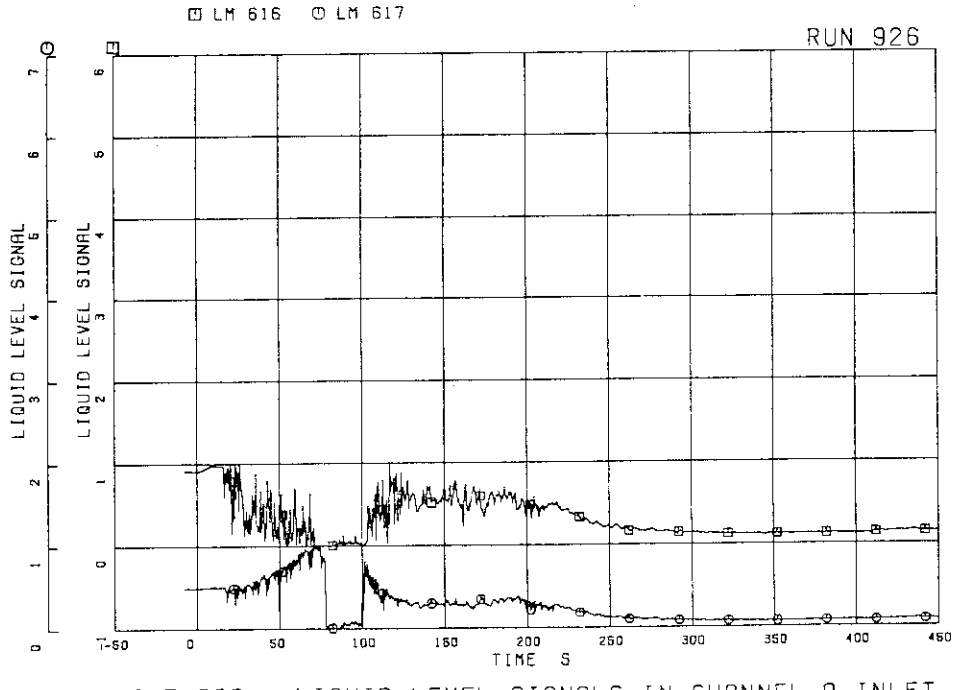

FIG.5.220 LIQUID LEVEL SIGNALS IN CHANNEL A INLET

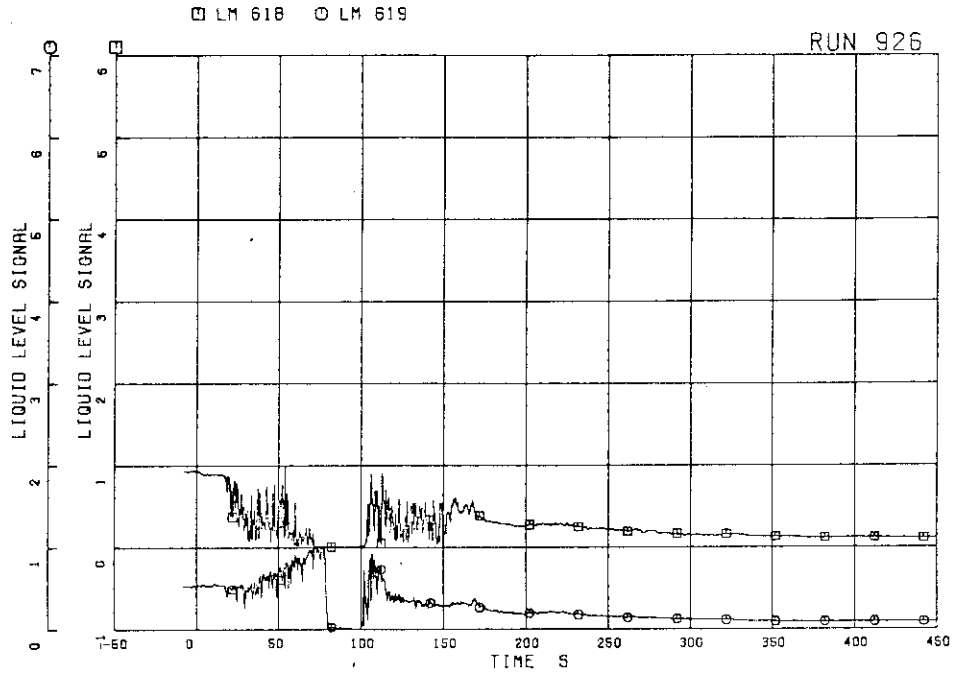

FIG.5.221 LIQUID LEVEL SIGNALS IN CHANNEL B INLET

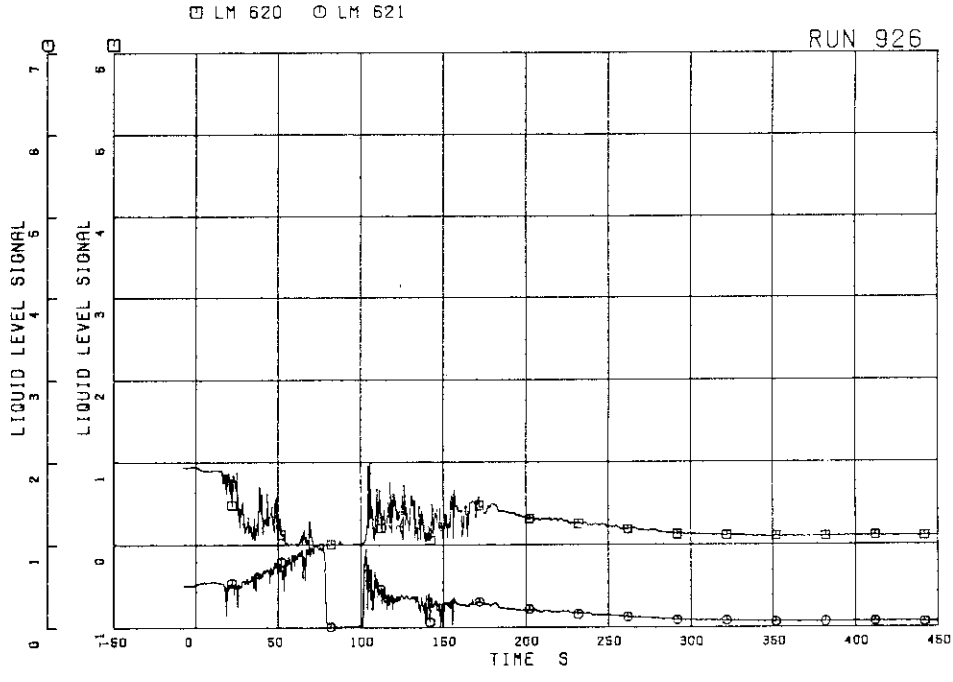

FIG.5.222 LIQUID LEVEL SIGNALS IN CHANNEL C INLET

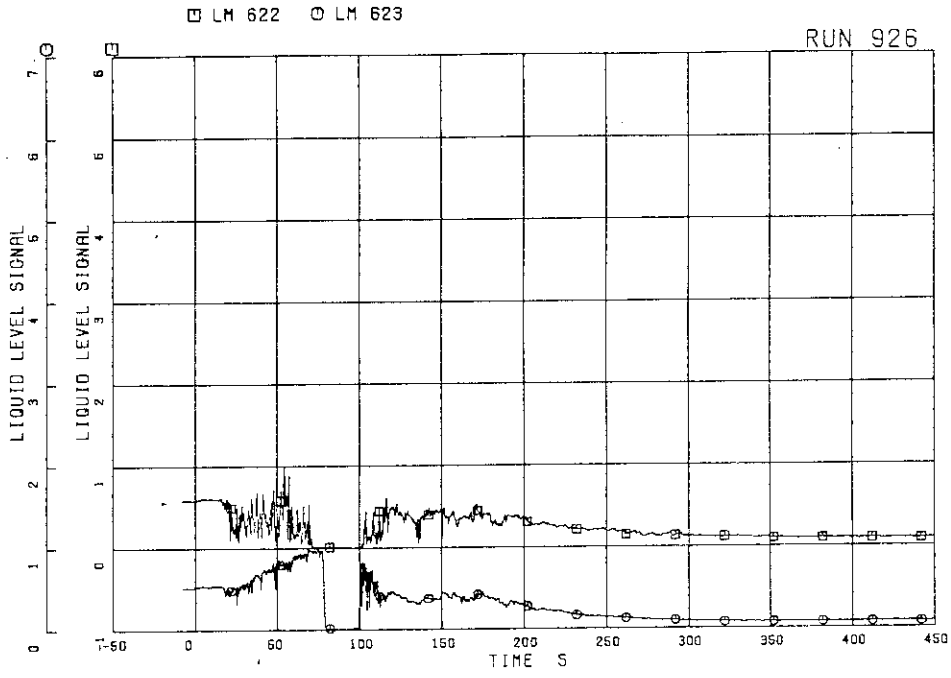

FIG.5.223 LIQUID LEVEL SIGNALS IN CHANNEL D INLET

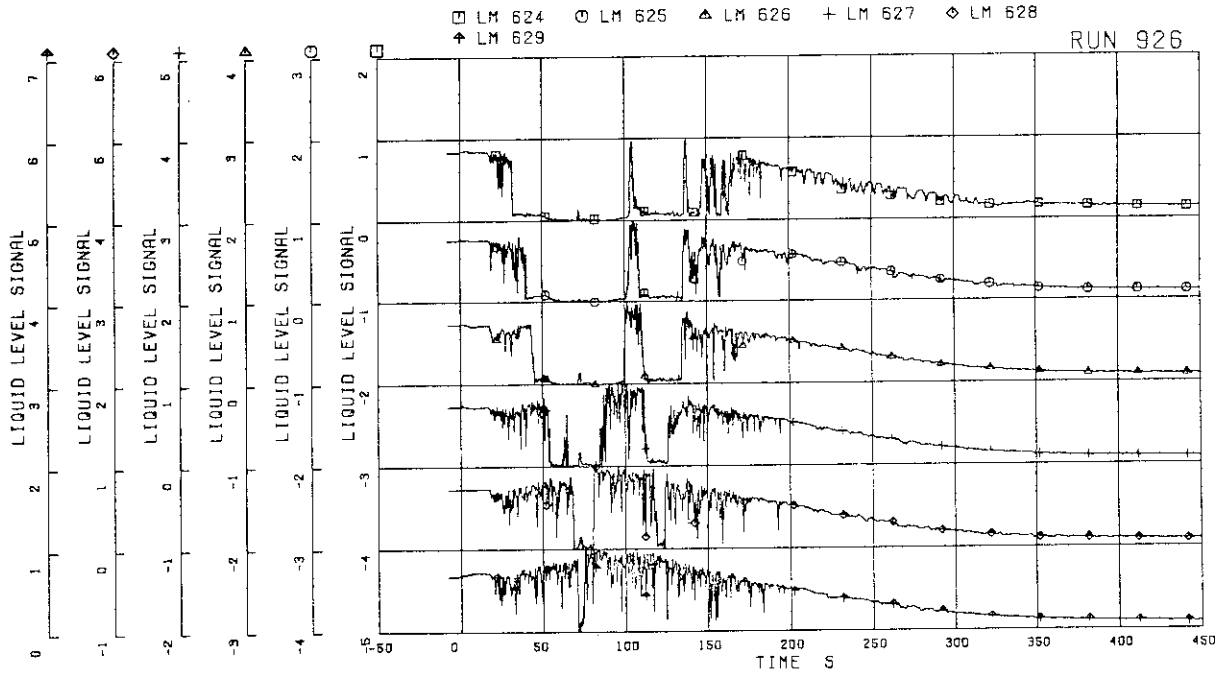

FIG.5.224 LIQUID LEVEL SIGNALS IN LOWER PLENUM, NORTH

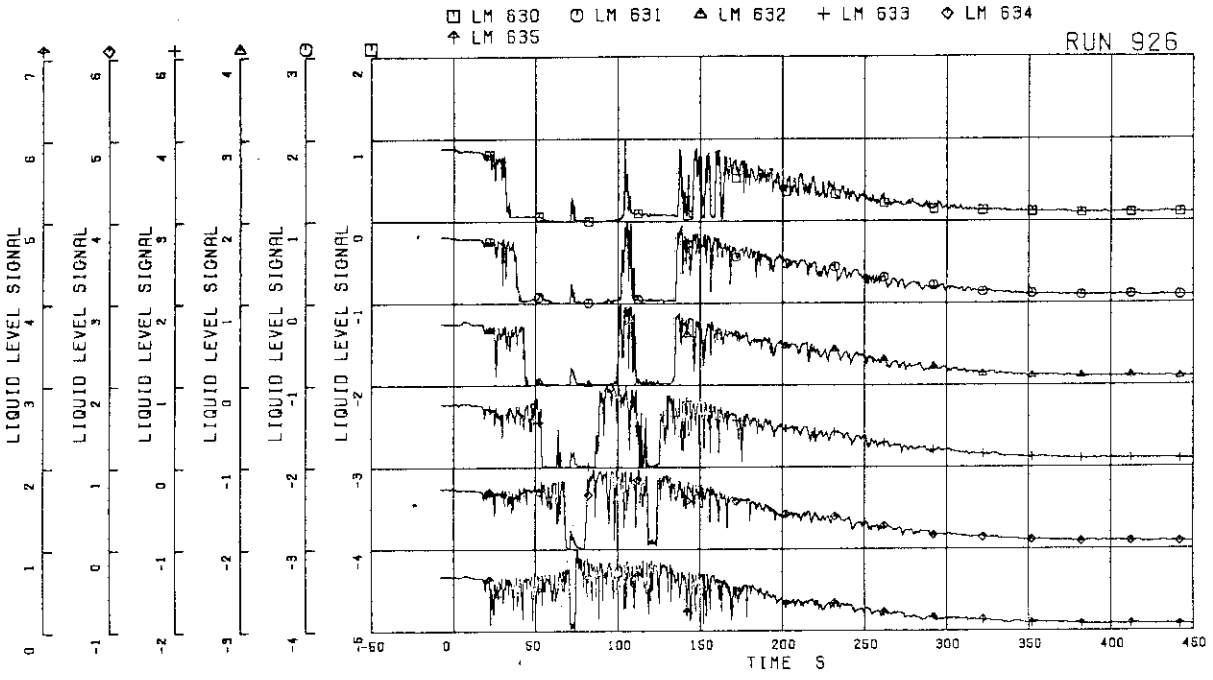

FIG.5.225 LIQUID LEVEL SIGNALS IN LOWER PLENUM, SOUTH

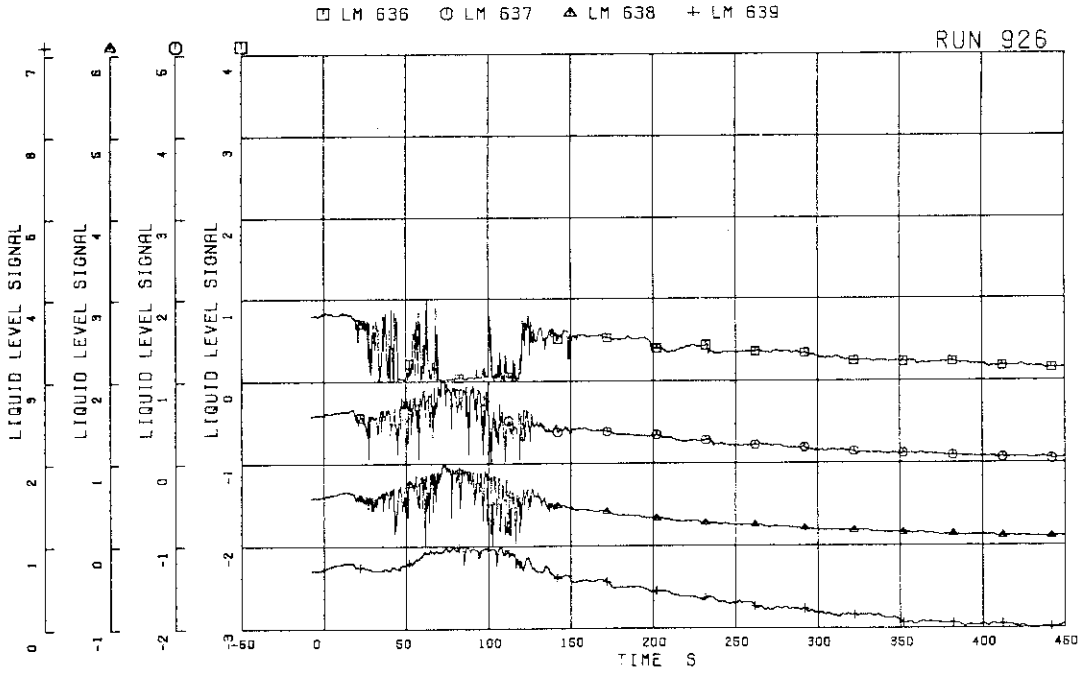

FIG.5.226 LIQUID LEVEL SIGNALS IN GUIDE TUBE, NORTH

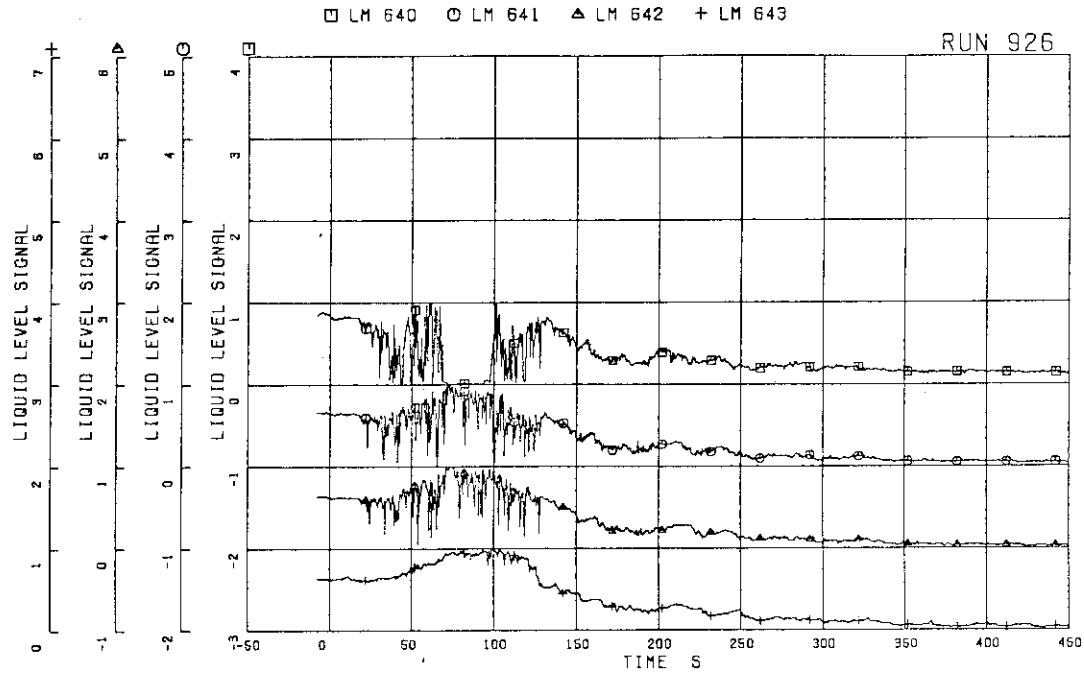

FIG.5.227 LIQUID LEVEL SIGNALS IN GUIDE TUBE, SOUTH

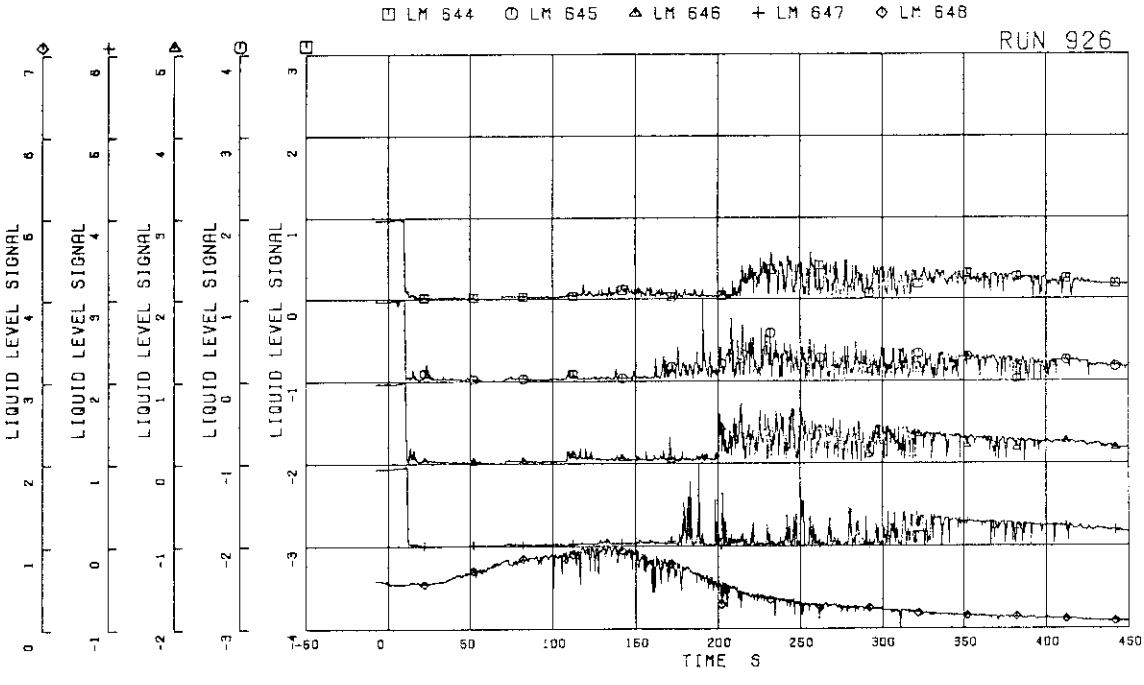

FIG.5.228 LIQUID LEVEL SIGNALS IN DOWNCOMER, D SIDE

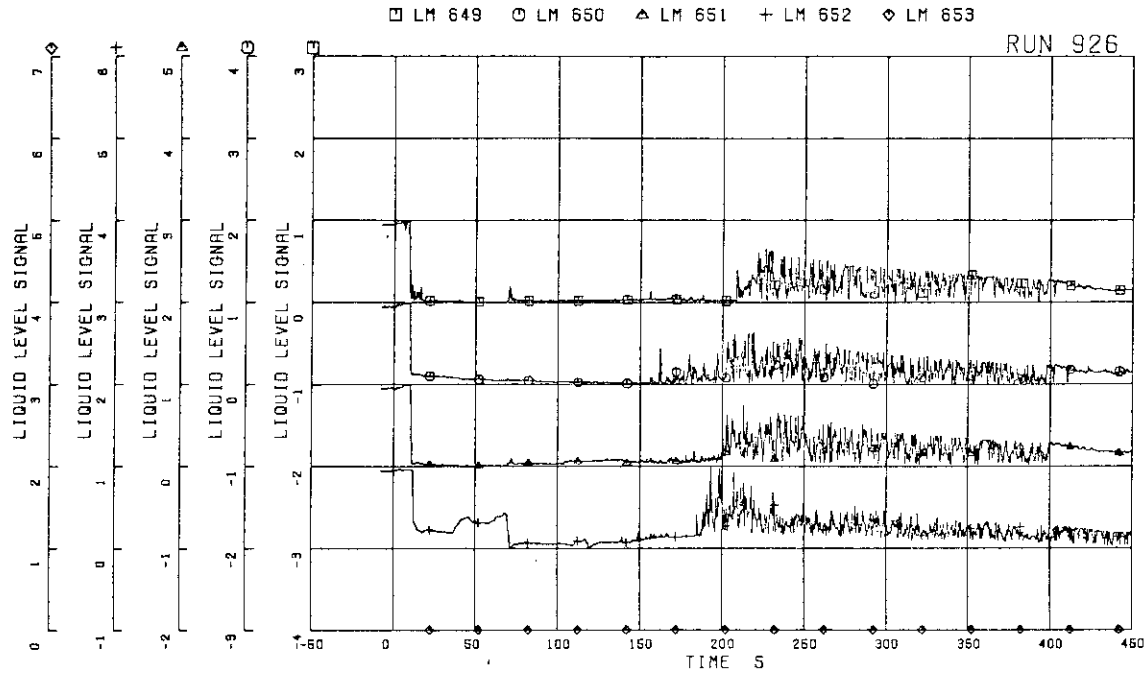

FIG.5.229 LIQUID LEVEL SIGNALS IN DOWNCOMER, B SIDE

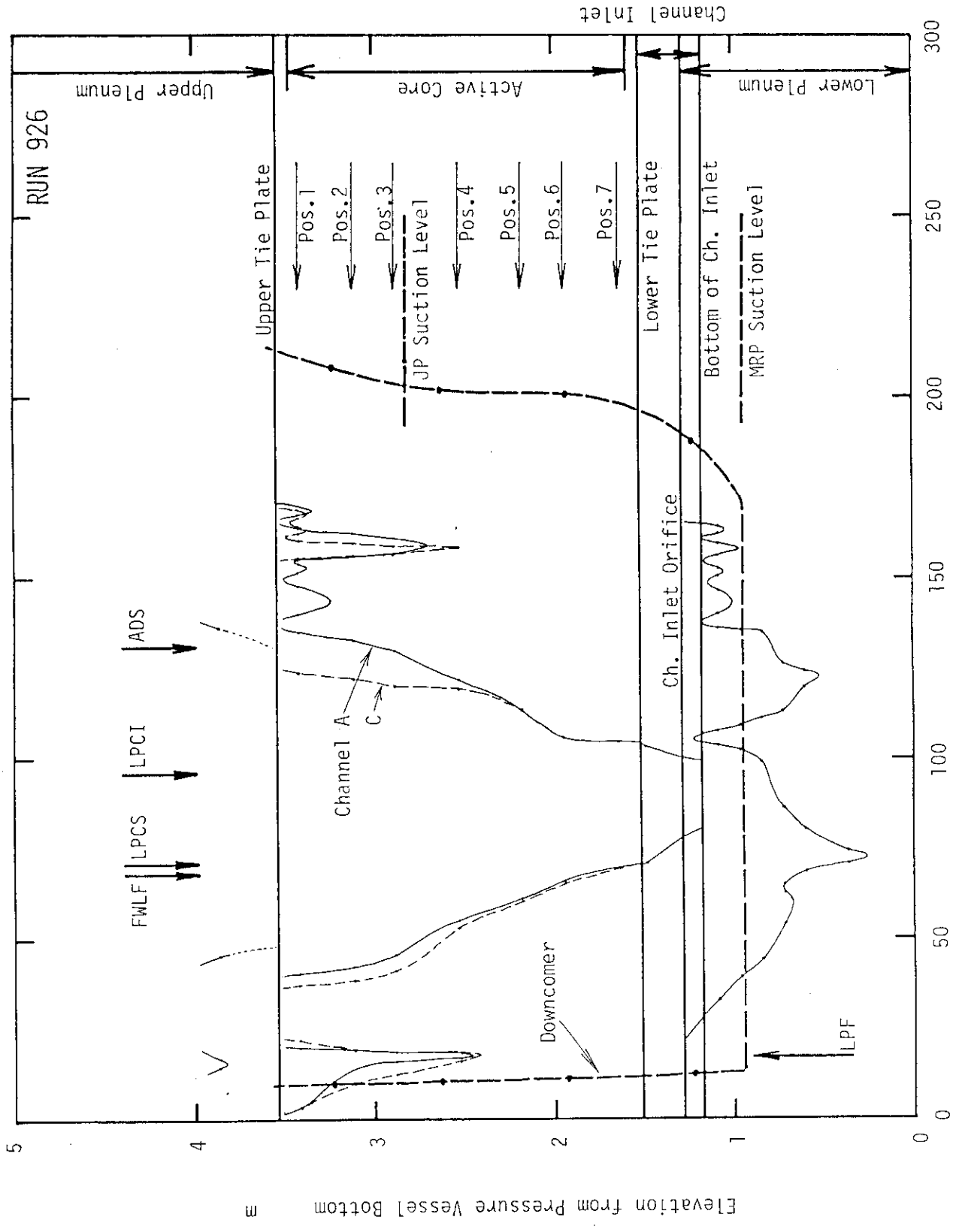

Fig. 5.230 Estimated Liquid Level in Pressure Vessel

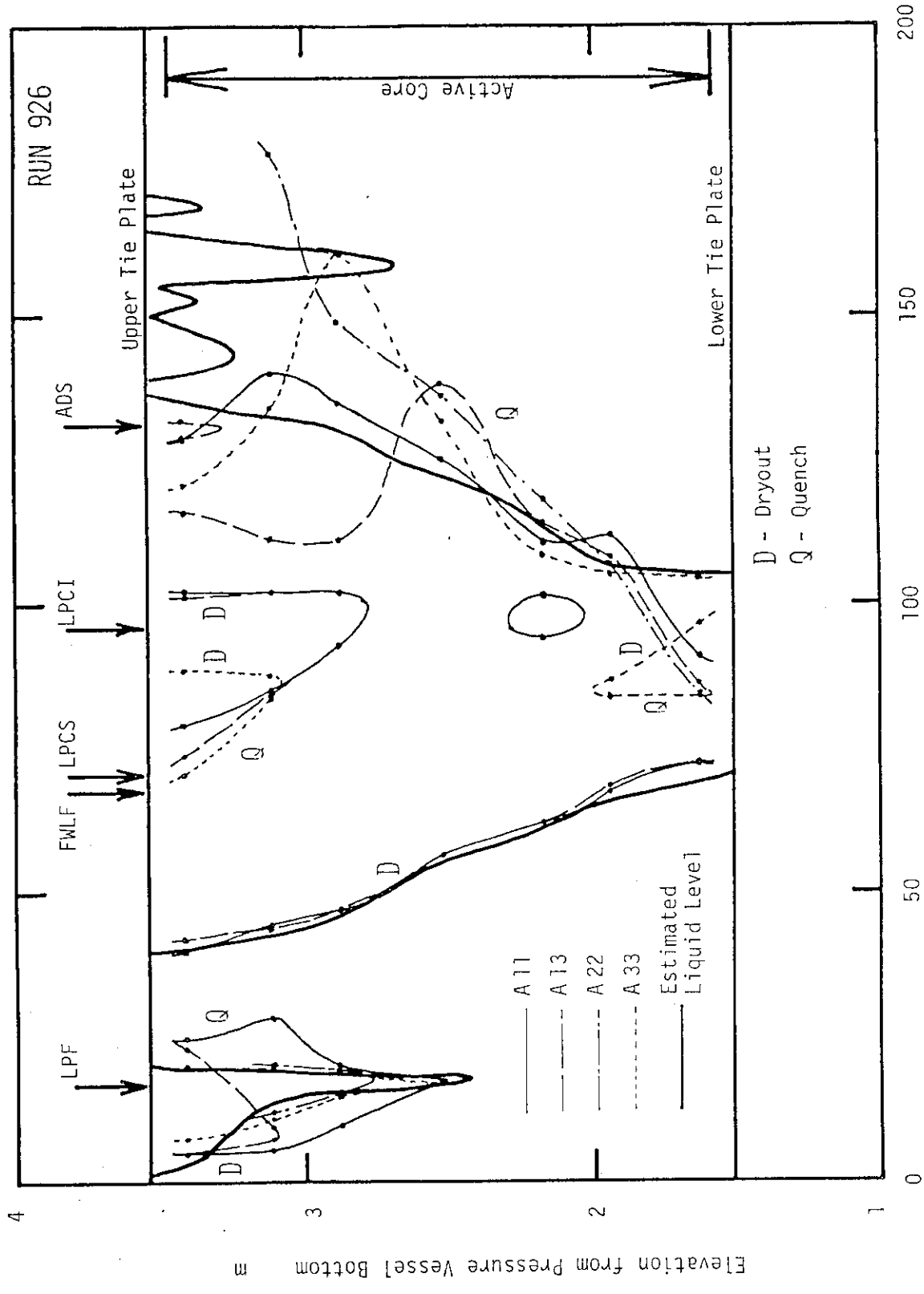

Fig. 5.231 Dryout and Quench Transients in Channel A

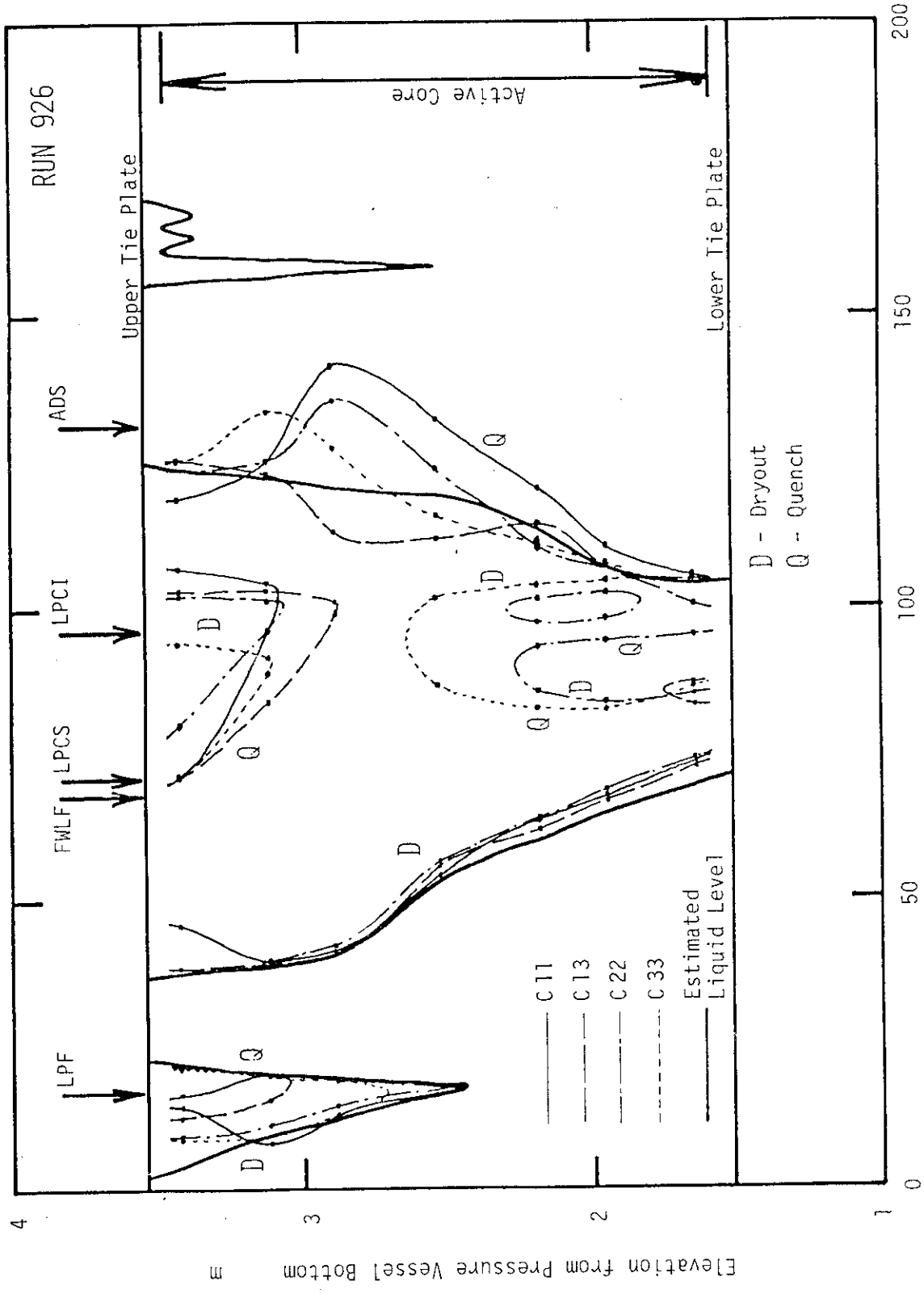

Fig. 5.232 Dryout and Quench Transients in Channel C

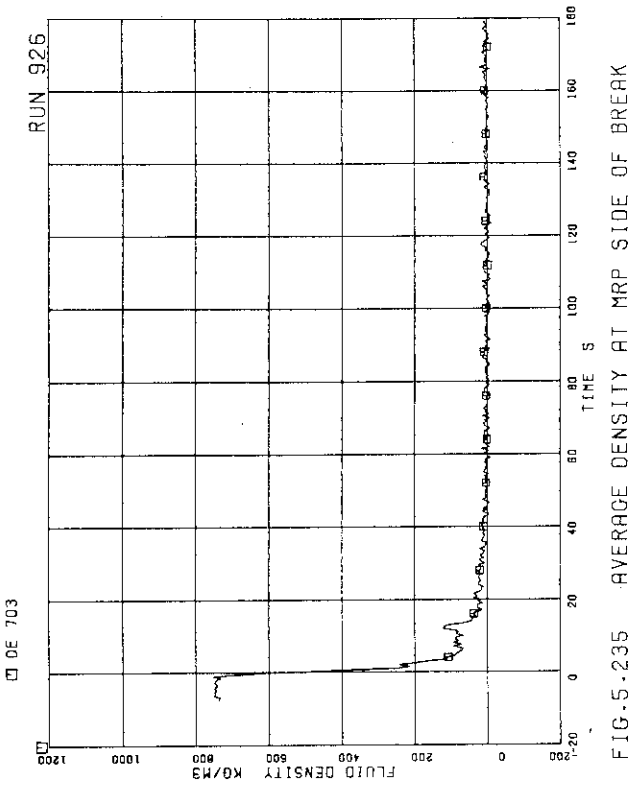

FIG.5.235 AVERAGE DENSITY AT MRP SIDE OF BREAK

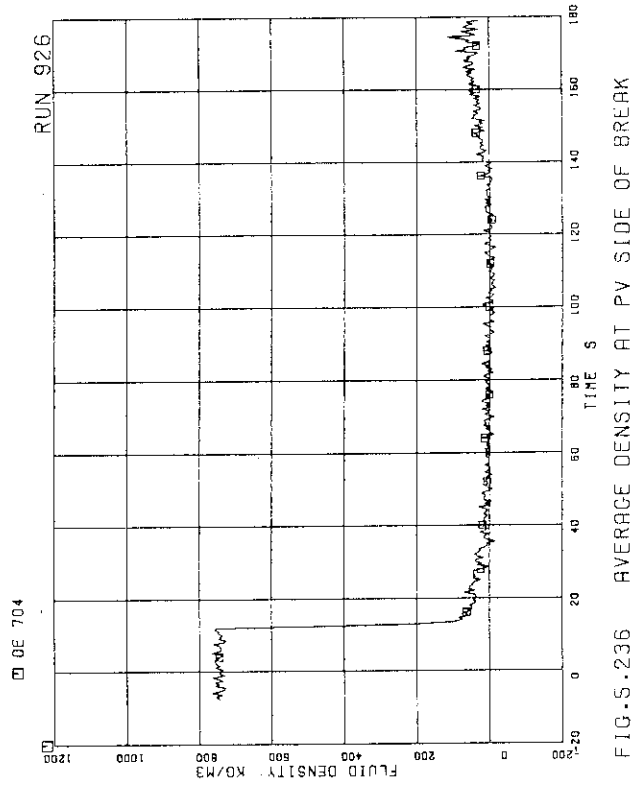

FIG.5.236 AVERAGE DENSITY AT PV SIDE OF BREAK

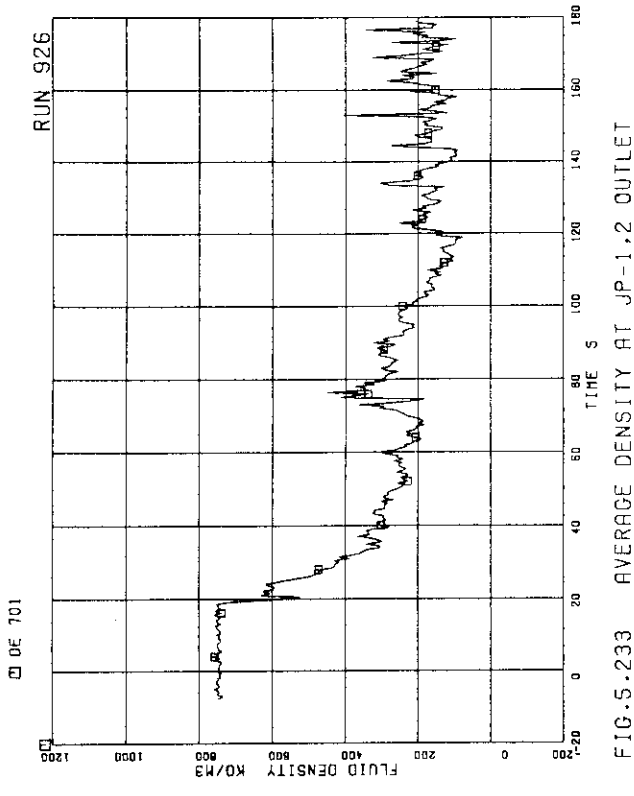

FIG.5.233 AVERAGE DENSITY AT JP-1,2 OUTLET

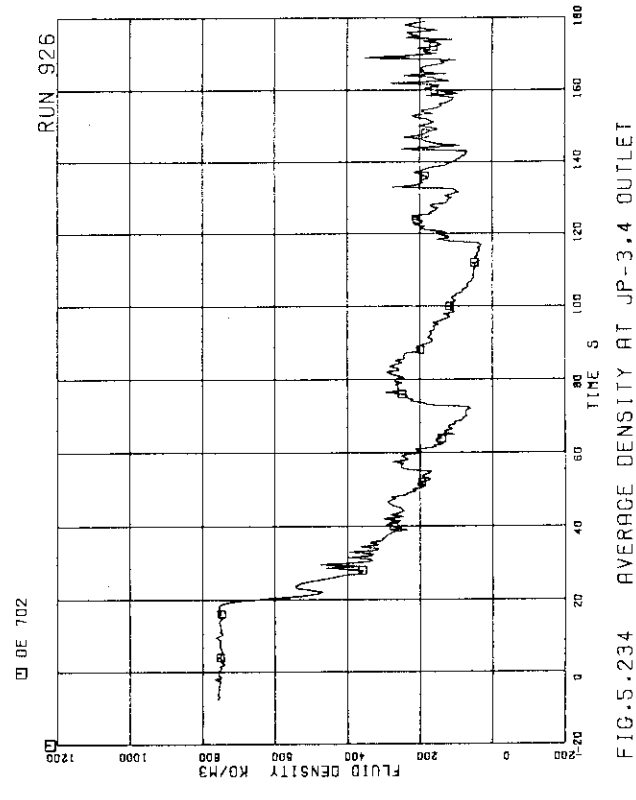

FIG.5.234 AVERAGE DENSITY AT JP-3,4 OUTLET

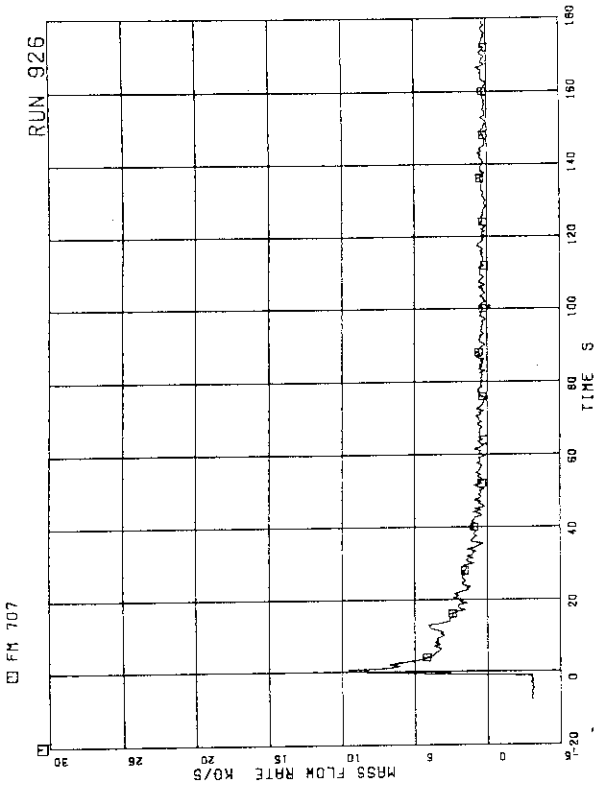

FIG.5.239 FLOW RATE AT MRP SIDE OF BREAK
(BASED ON HIGH RANGE DRAG DISK DATA)

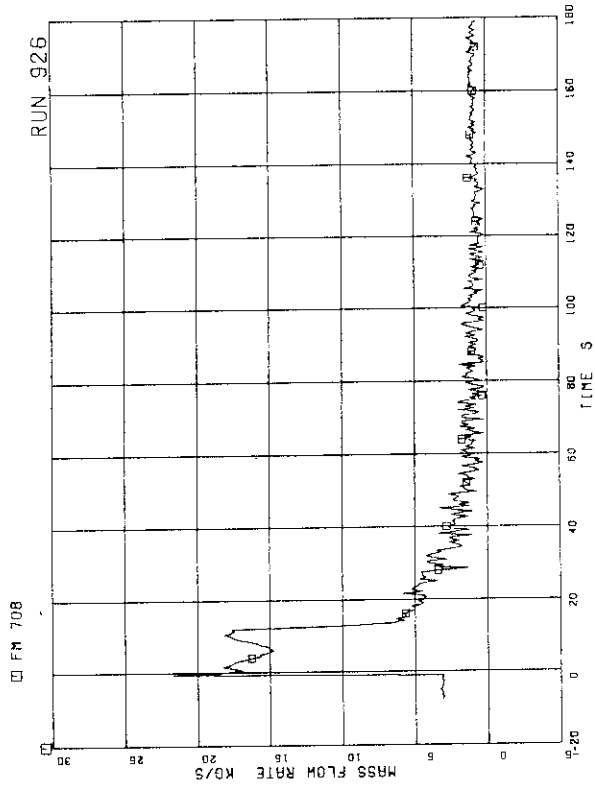

FIG.5.240 FLOW RATE AT PV SIDE OF BREAK
(BASED ON HIGH RANGE DRAG DISK DATA)

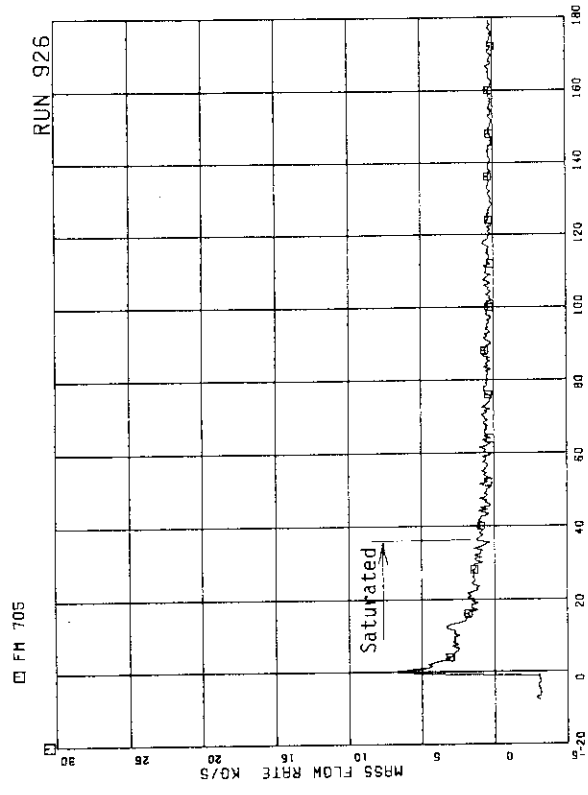

FIG.5.237 FLOW RATE AT MRP SIDE OF BREAK
(BASED ON LOW RANGE DRAG DISK DATA)

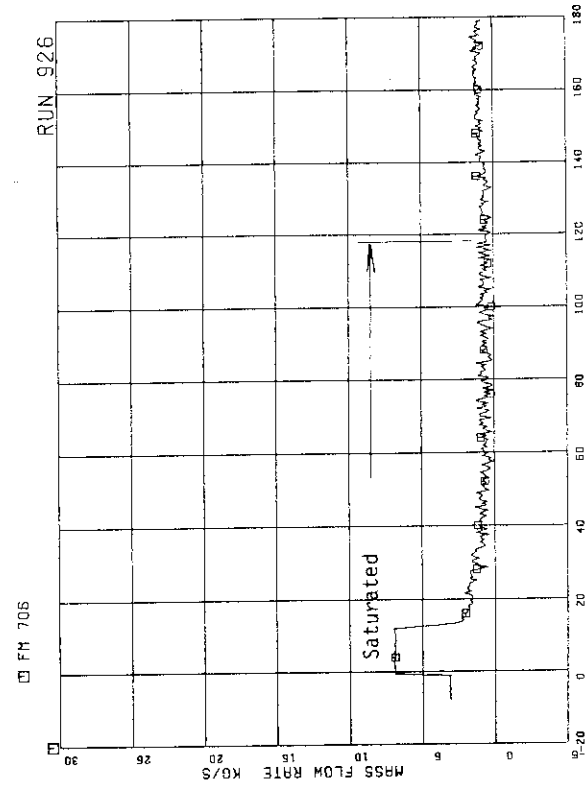

FIG.5.238 FLOW RATE AT PV SIDE OF BREAK
(BASED ON LOW RANGE DRAG DISK DATA)

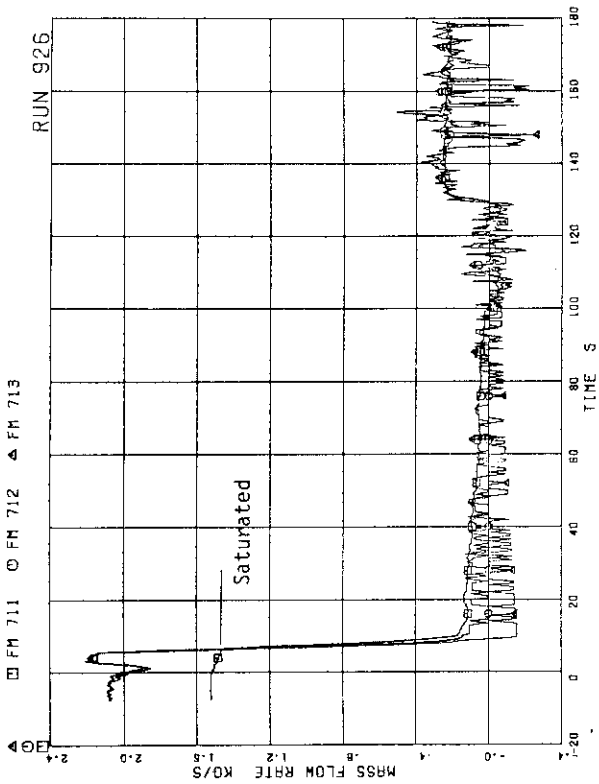

FIG.5.243 STEAM DISCHARGE FLOW RATE THROUGH MSL

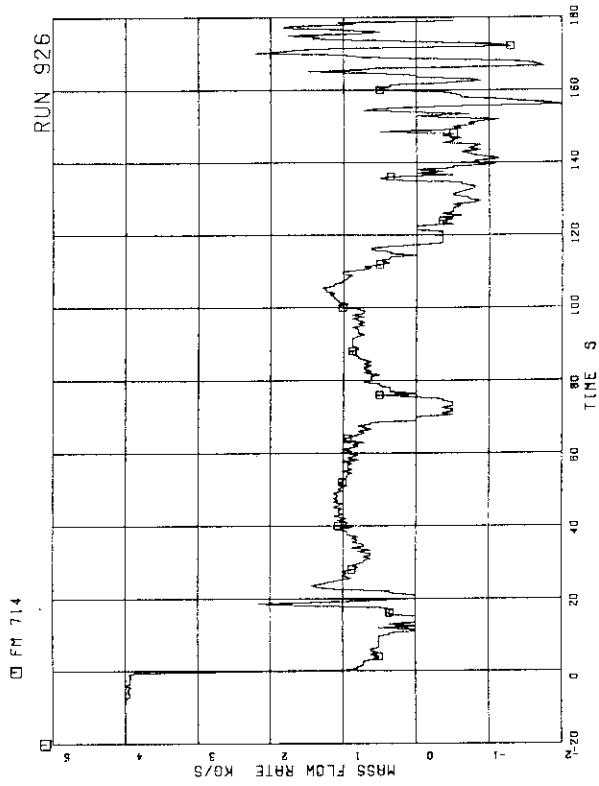

FIG.5.244 FLOW RATE AT CHANNEL A INLET

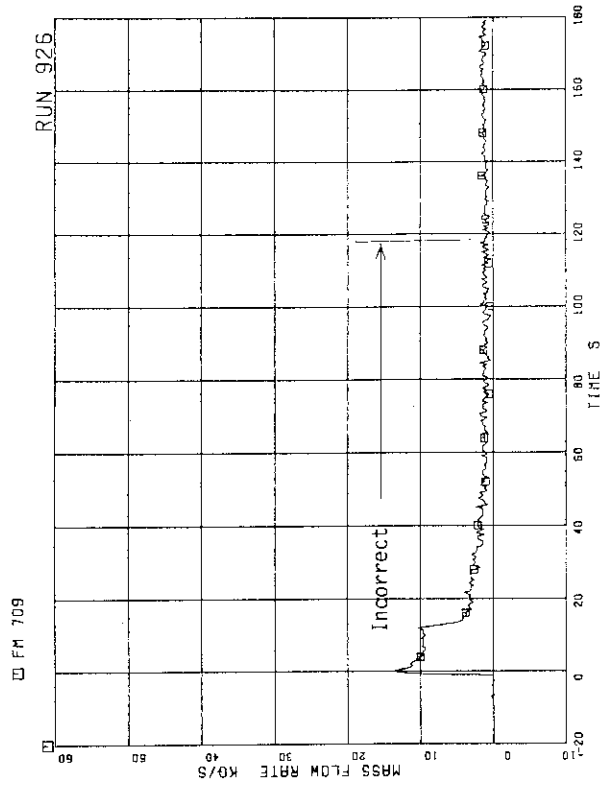

FIG.5.241 TOTAL DISCHARGE FLOW RATE FROM BREAK (BASED ON LOW RANGE DRAG DISK DATA)

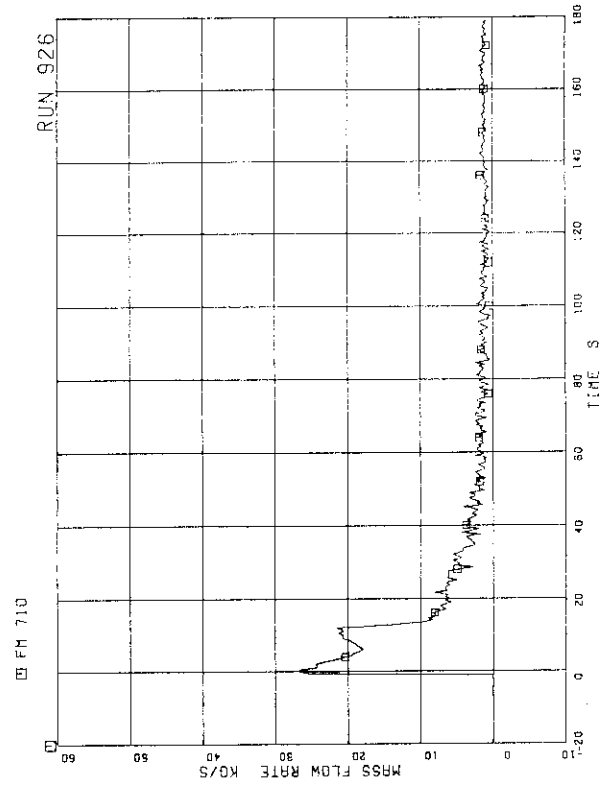

FIG.5.242 TOTAL DISCHARGE FLOW RATE FROM BREAK (BASED ON HIGH RANGE DRAG DISK DATA)

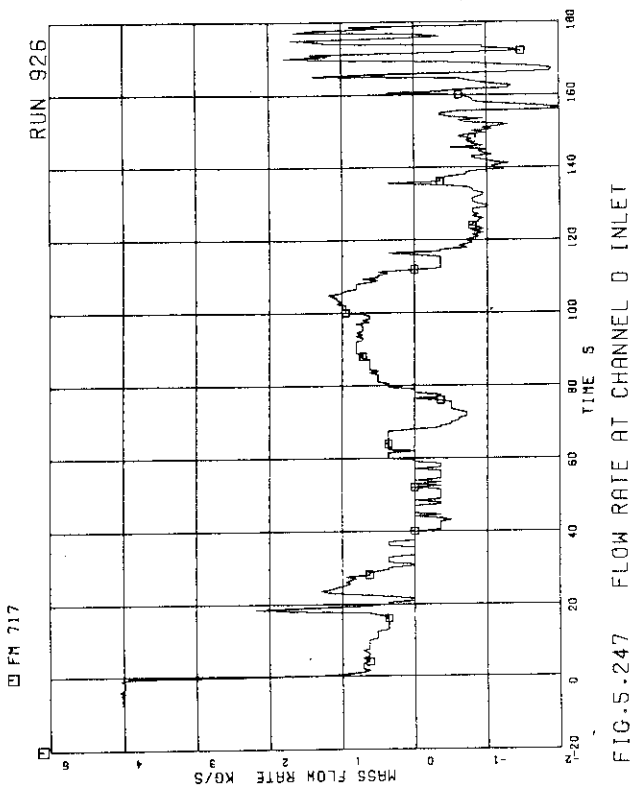

FIG.5.247 FLOW RATE AT CHANNEL D INLET

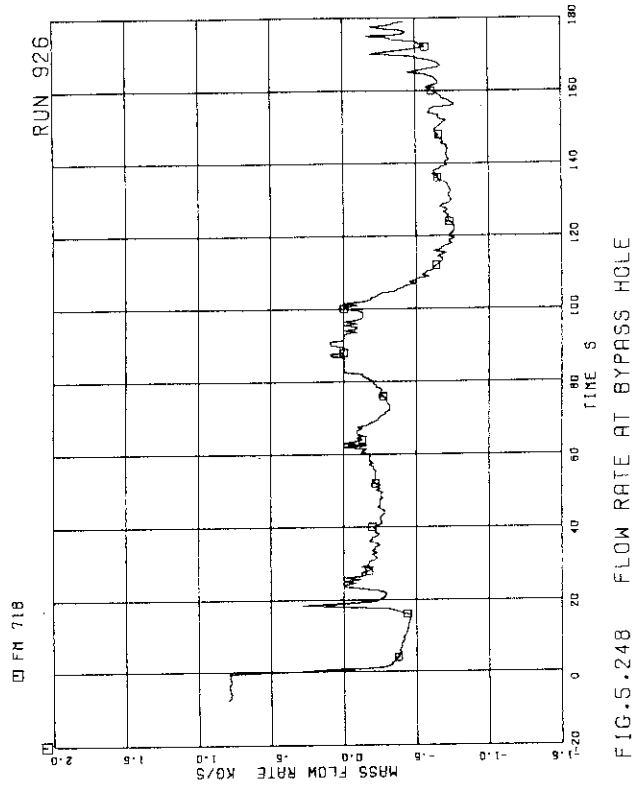

FIG.5.248 FLOW RATE AT BYPASS HOLE

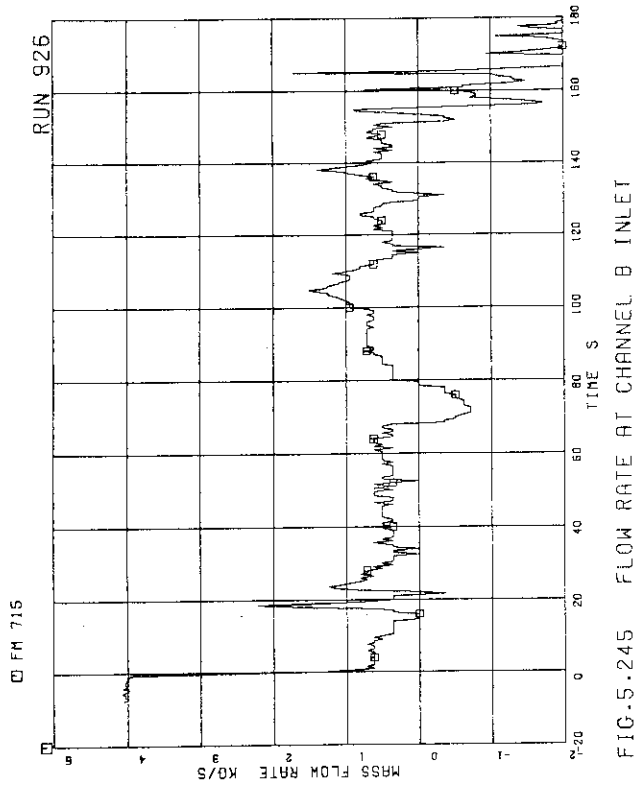

FIG.5.245 FLOW RATE AT CHANNEL B INLET

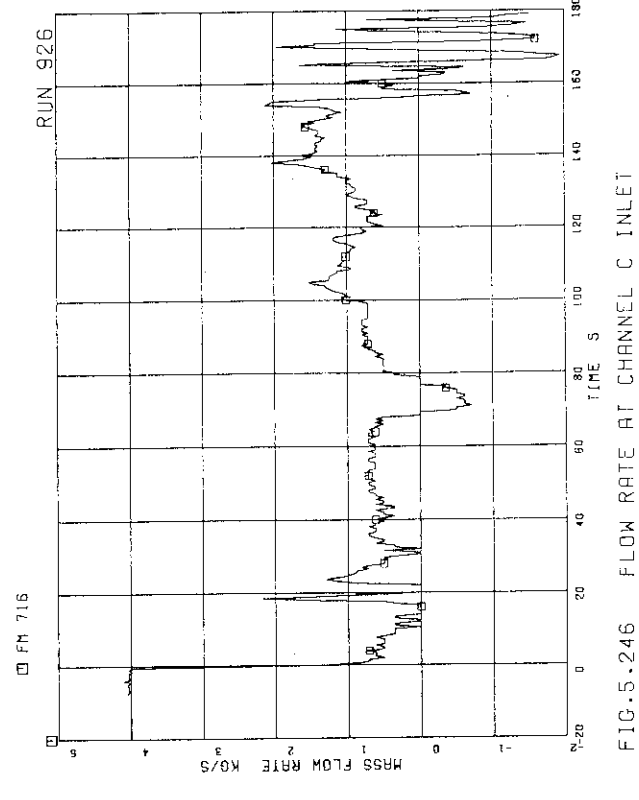

FIG.5.246 FLOW RATE AT CHANNEL C INLET

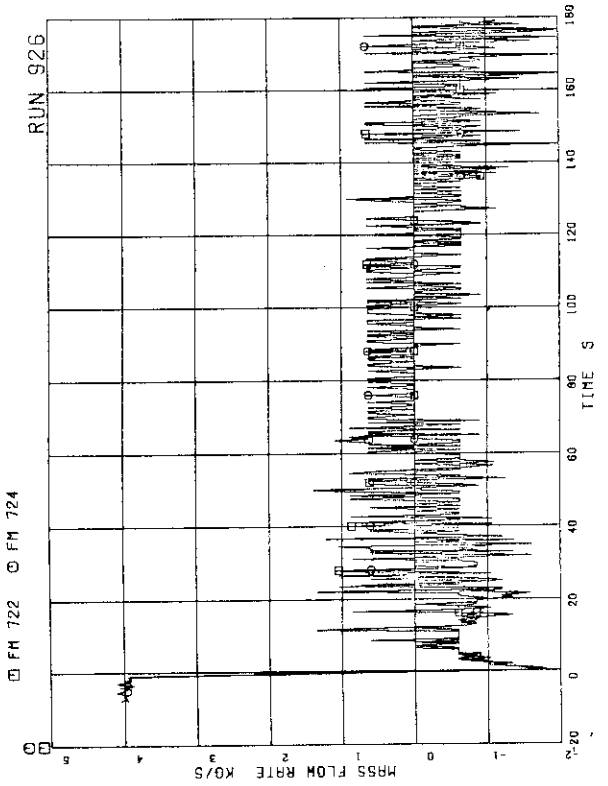

FIG.5.251 FLOW RATE AT JP-3,4 OUTLET (HIGH RANGE)

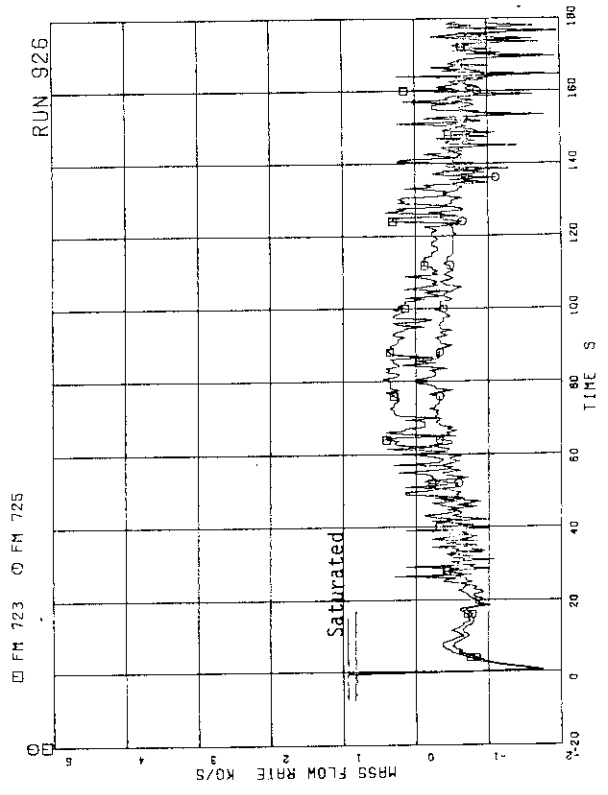

FIG.5.252 FLOW RATE AT JP-3,4 OUTLET (LOW RANGE)

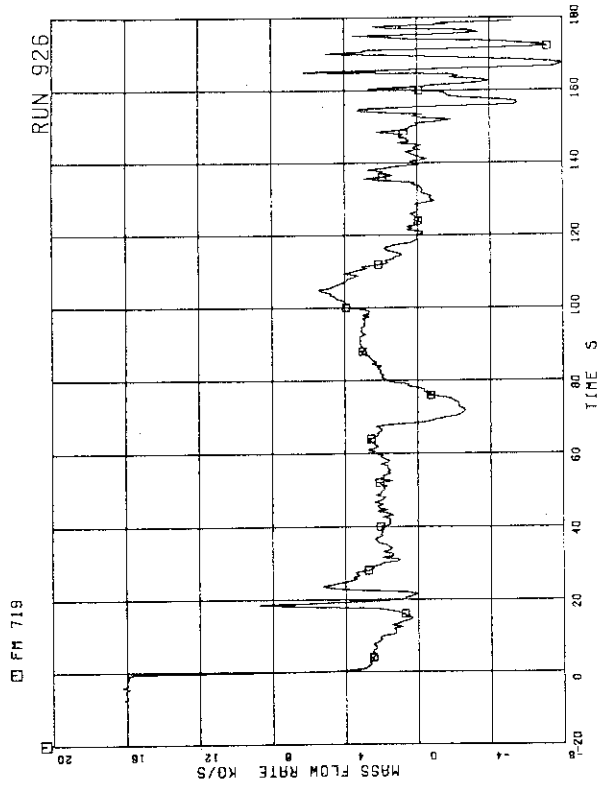

FIG.5.249 TOTAL CHANNEL INLET FLOW RATE

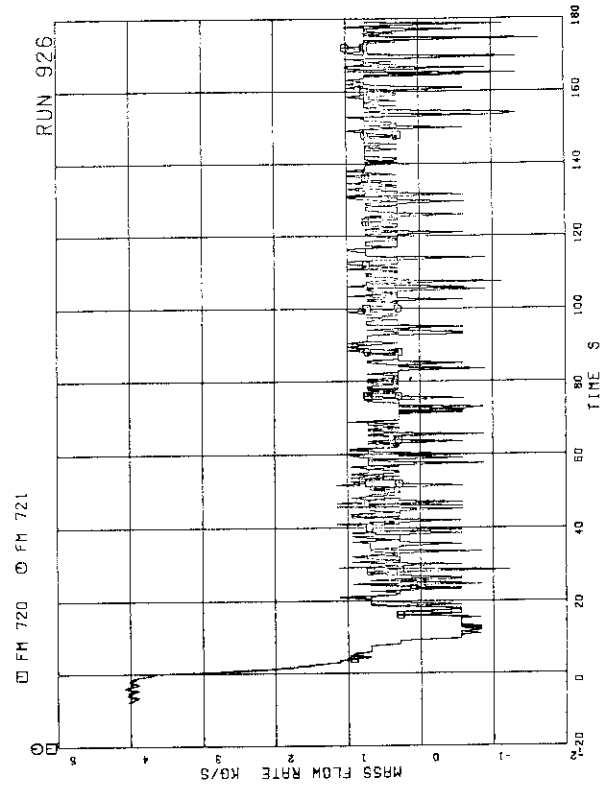

FIG.5.250 FLOW RATE AT JP-1,2 OUTLET (HIGH RANGE)

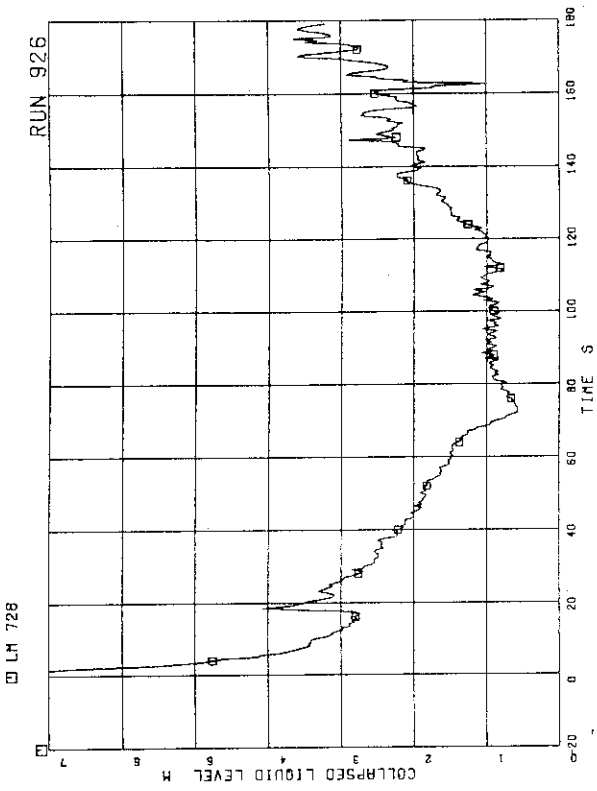

FIG.5.255 COLLAPSED LIQUID LEVEL INSIDE CORE SHROUD

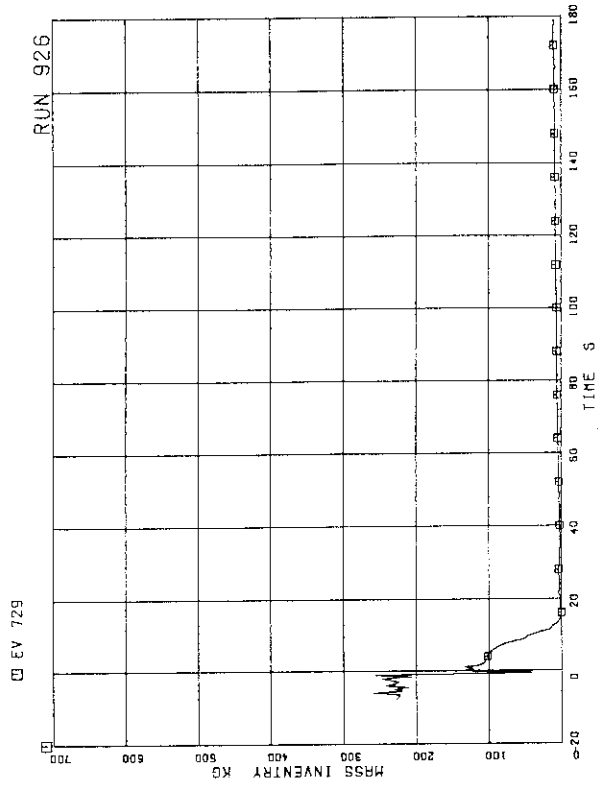

FIG.5.256 FLUID INVENTORY IN DOWNCOMER

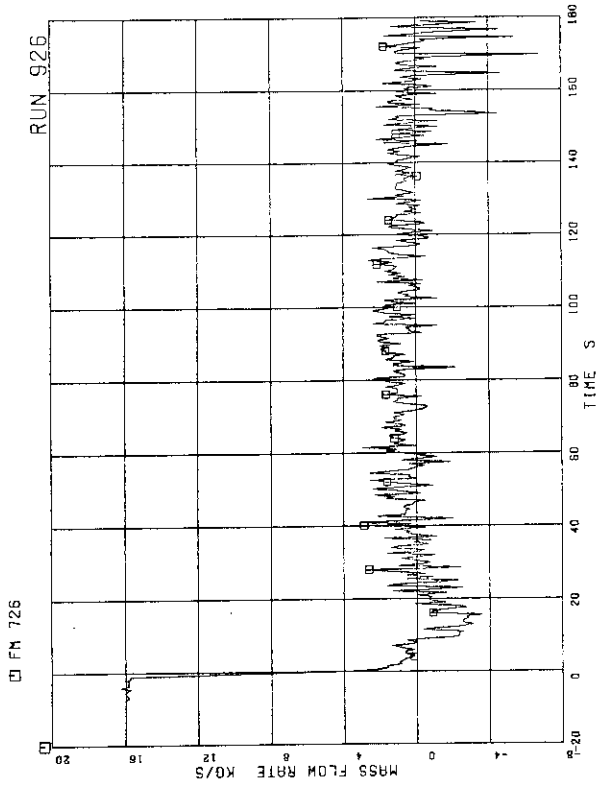

FIG.5.253 TOTAL JP OUTLET FLOW RATE (HIGH RANGE)

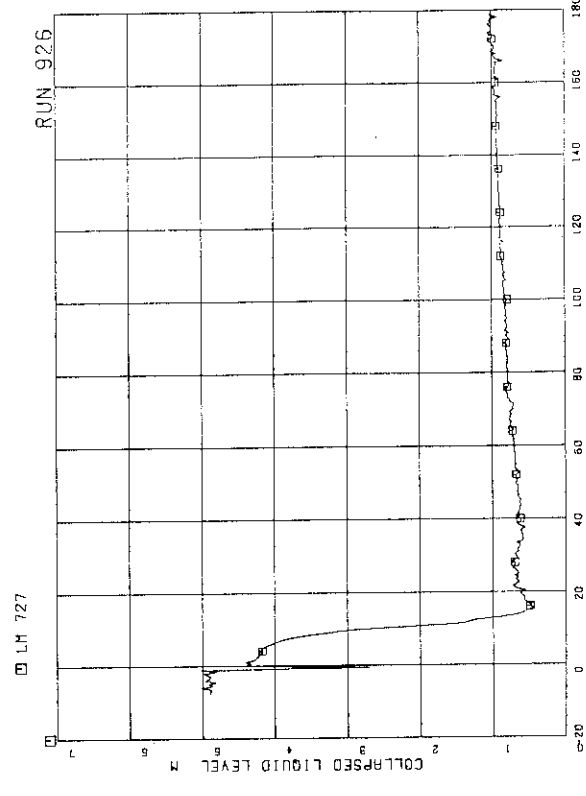

FIG.5.254 COLLAPSED LIQUID LEVEL IN DOWNCOMER

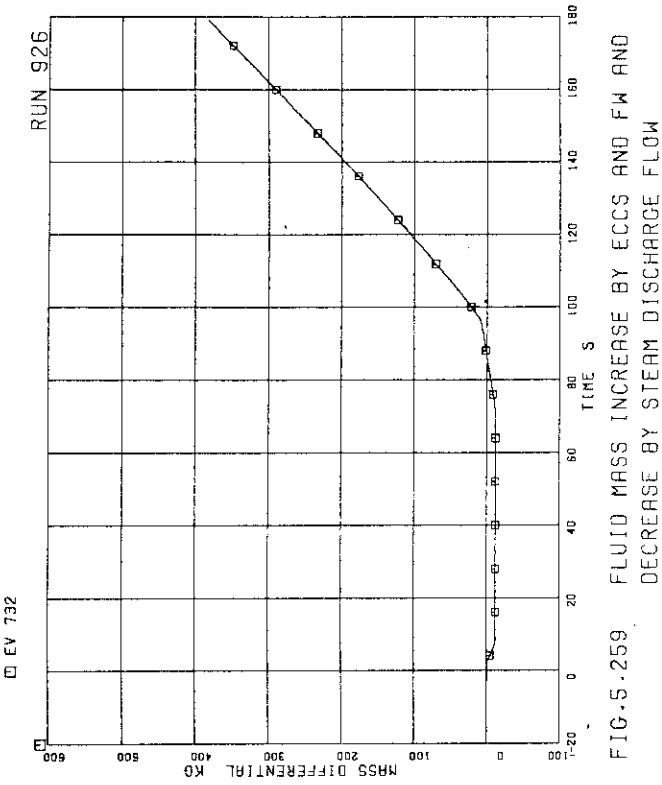

FIG.5.259 FLUID MASS INCREASE BY ECCS AND FW AND DECREASE BY STEAM DISCHARGE FLOW

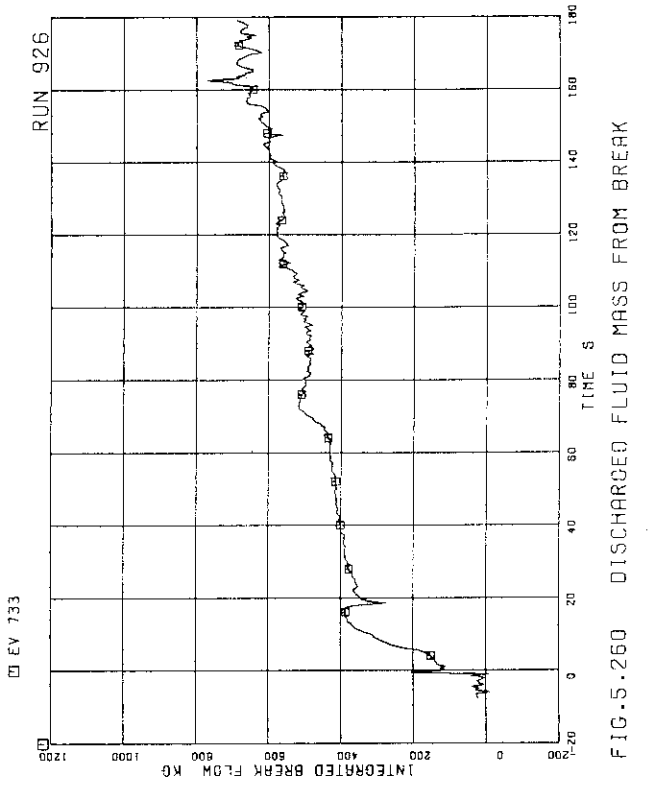

FIG.5.260 DISCHARGED FLUID MASS FROM BREAK

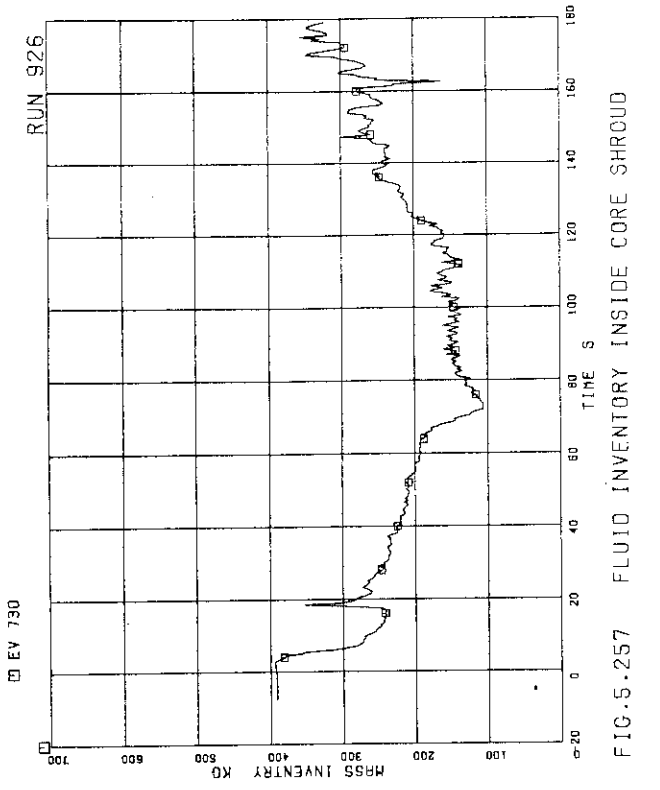

FIG.5.257 FLUID INVENTORY INSIDE CORE SHROUD

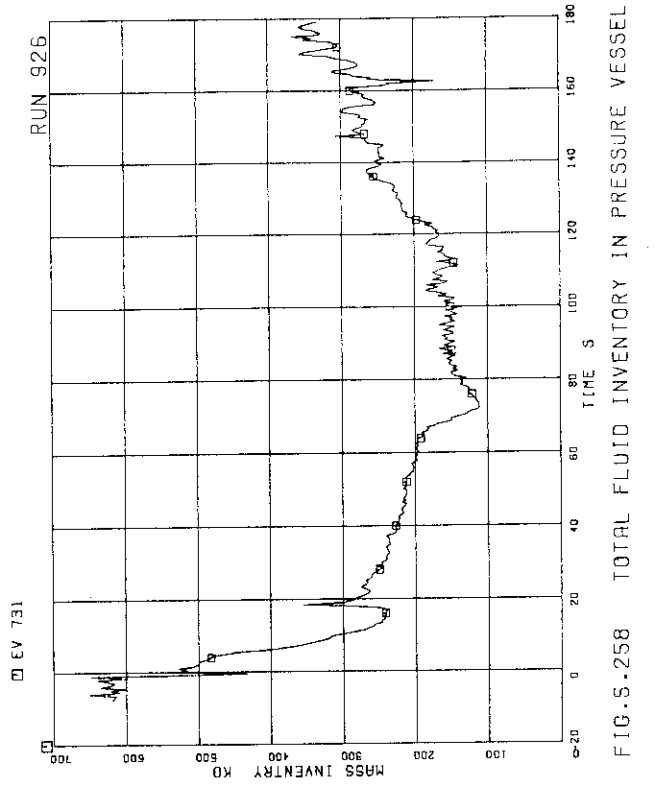

FIG.5.258 TOTAL FLUID INVENTORY IN PRESSURE VESSEL

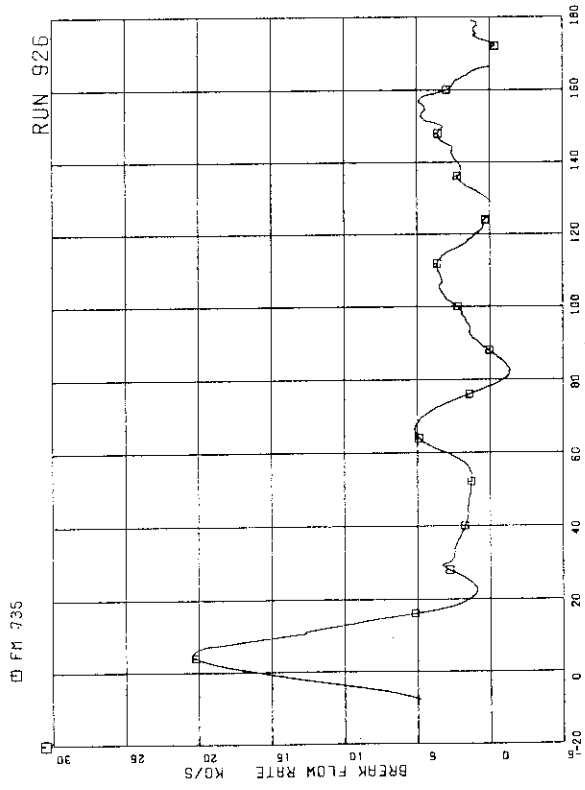

FIG.5.261 DISCHARGED FLOW RATE FROM BREAK

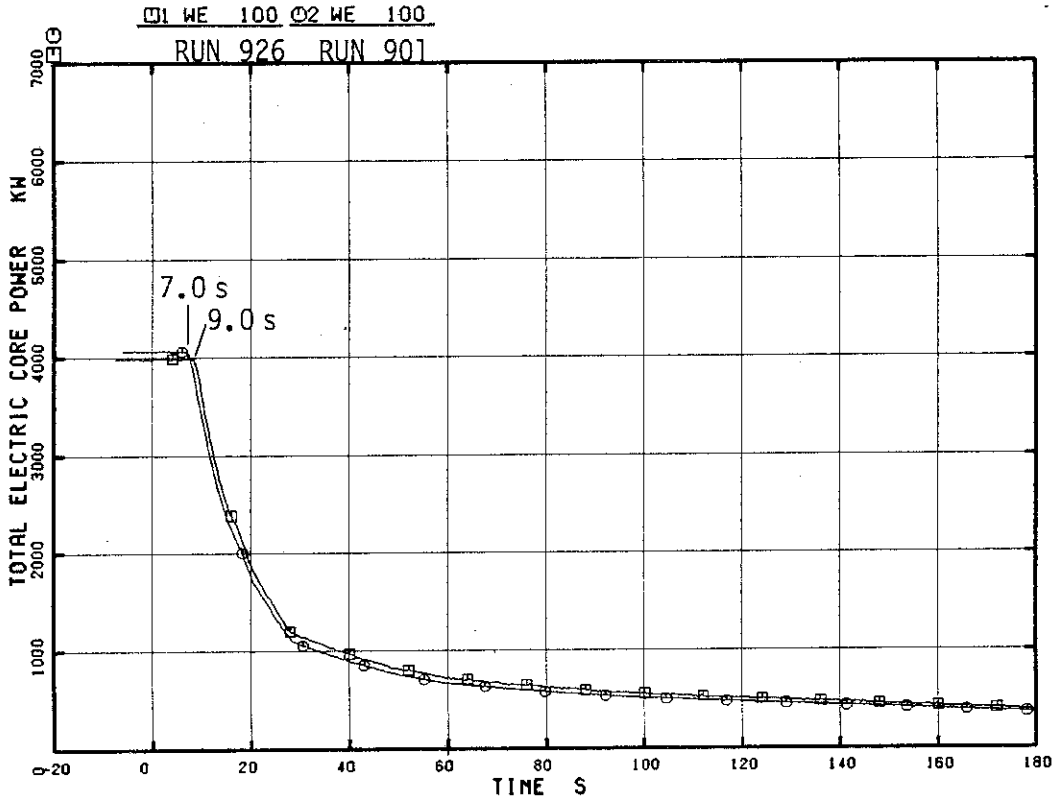

Fig. 6.1 Total Electric Core Power in RUN 926 and RUN 901

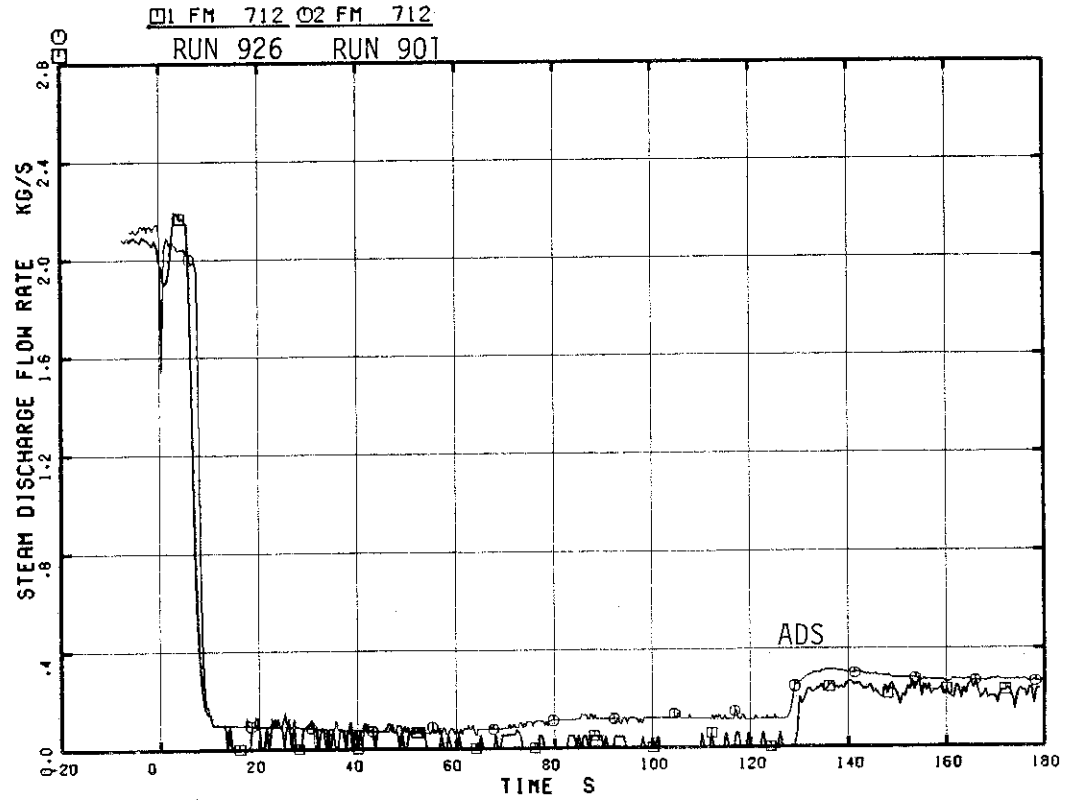

Fig. 6.2 Steam Discharge Flow Rate in RUN 926 and RUN 901

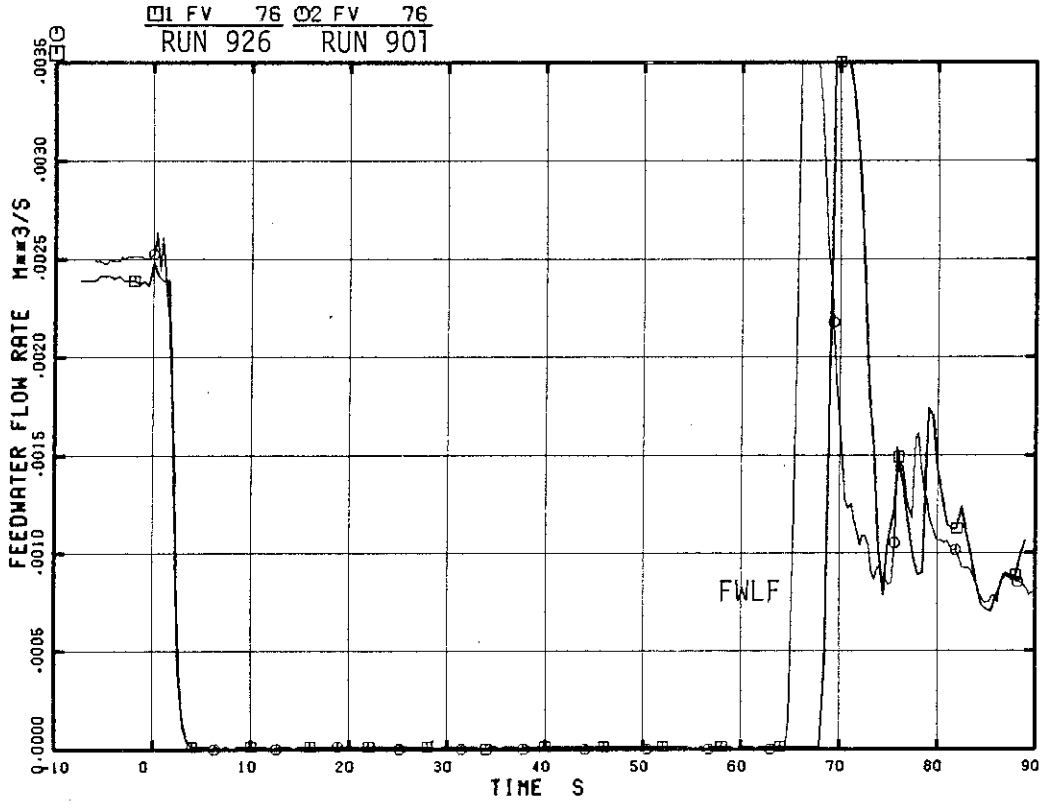

Fig. 6.3 Feedwater Flow Rate in RUN 926 and RUN 901

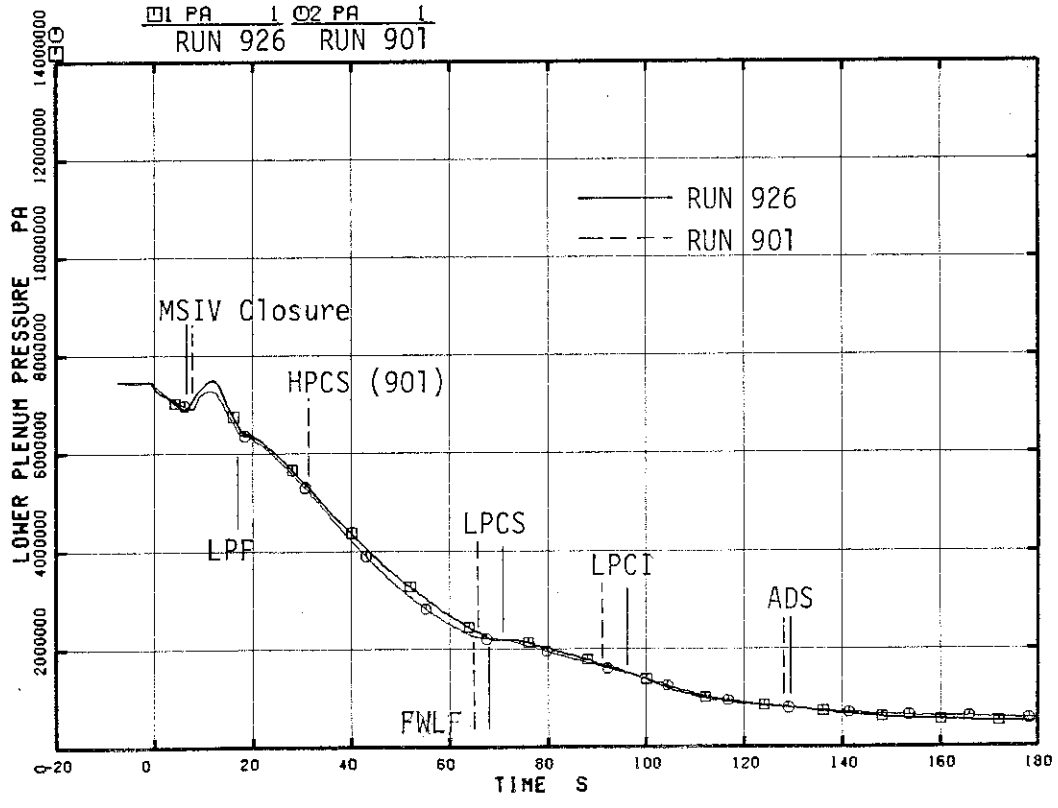

Fig. 6.4 Lower Plenum Pressure in RUN 926 and RUN 901

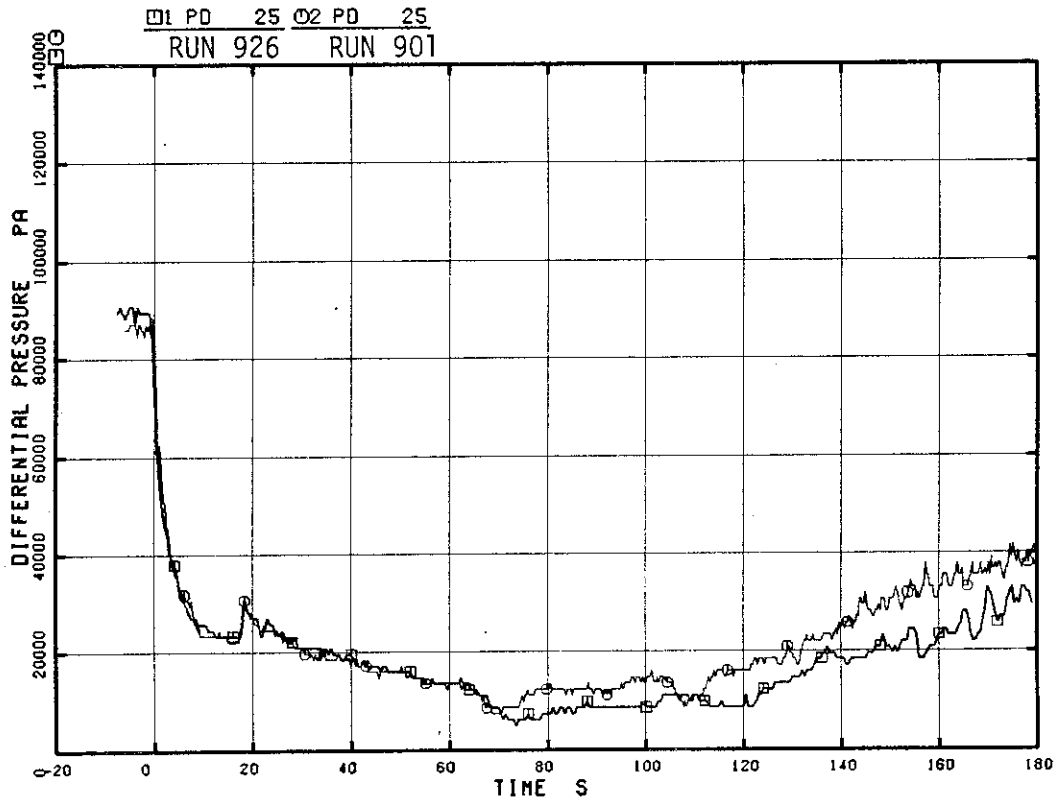

Fig. 6.5 Differential Pressure between Top and Bottom of Pressure Vessel in RUN 926 and RUN 901

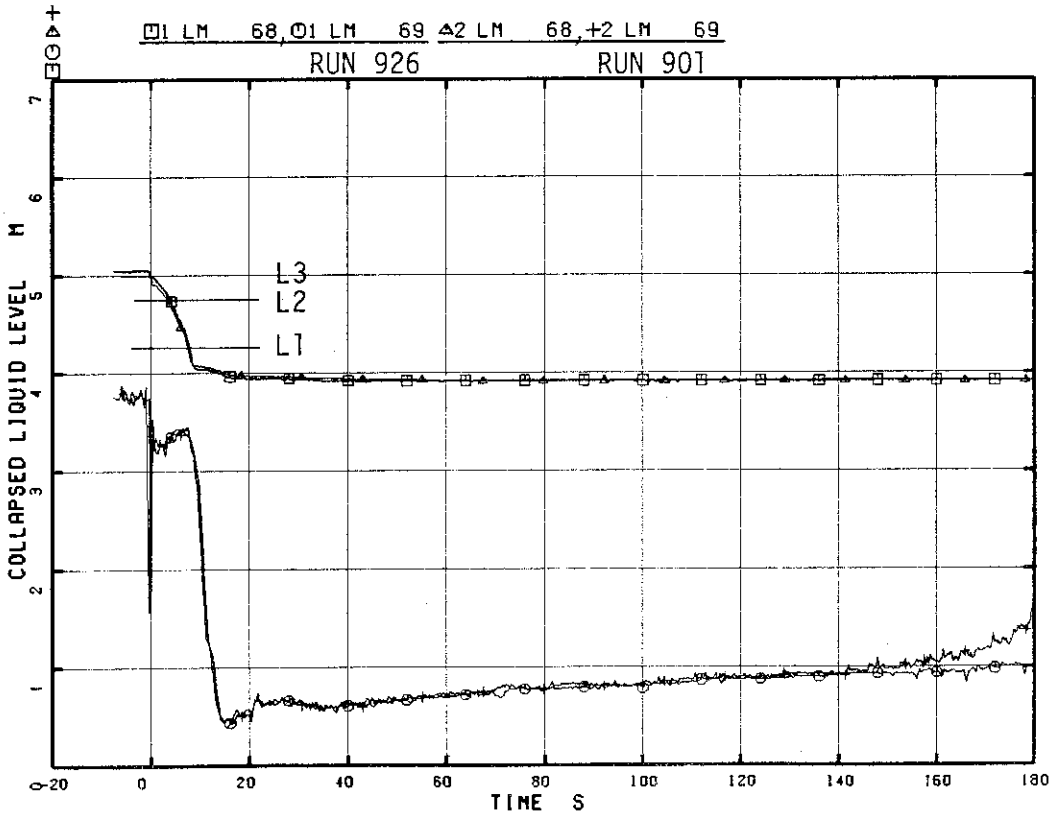

Fig. 6.6 Collapsed Liquid Level in Downcomer in RUN 926 and RUN 901

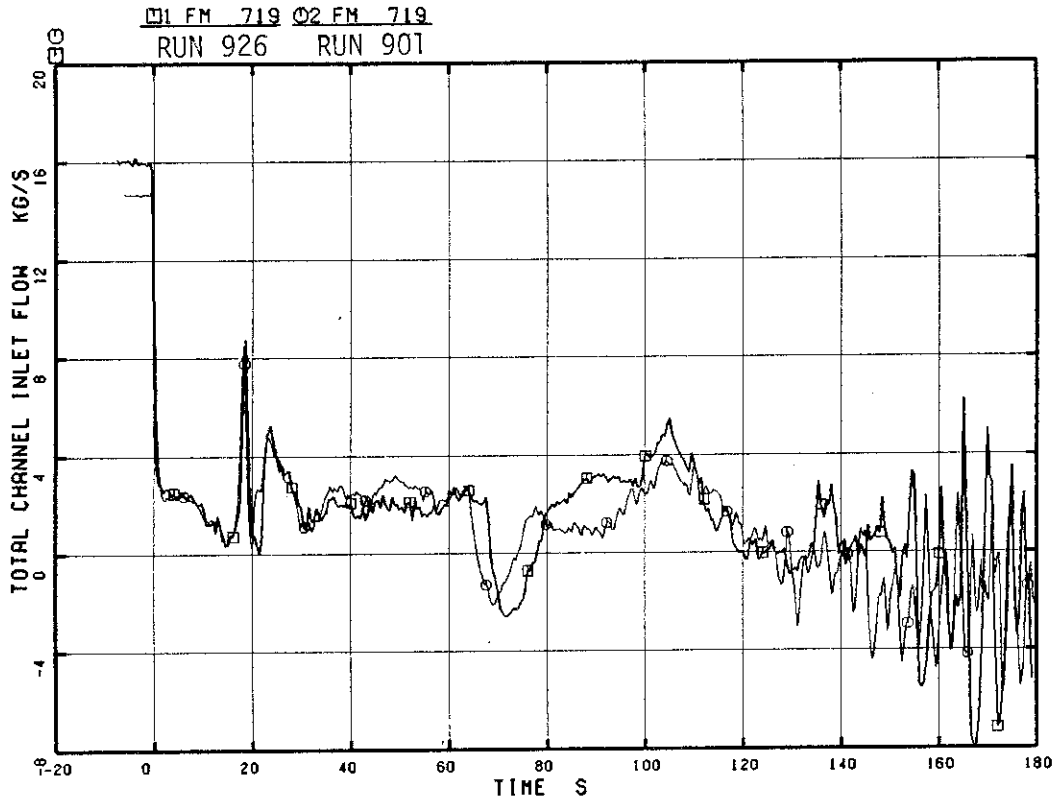

Fig. 6.7 Total Flow Rate through Channel Inlet Orifices in RUN 926 and RUN 901

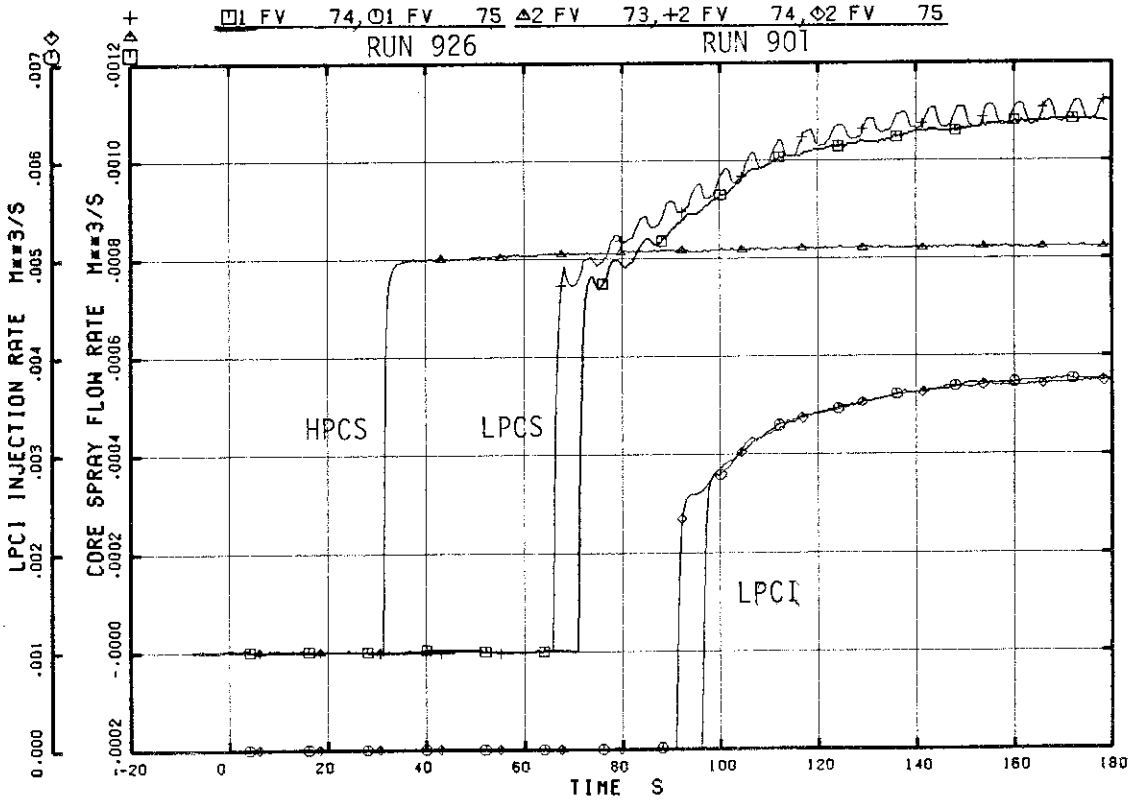

Fig. 6.8 ECCS Flow Rate in RUN 926 and RUN 901

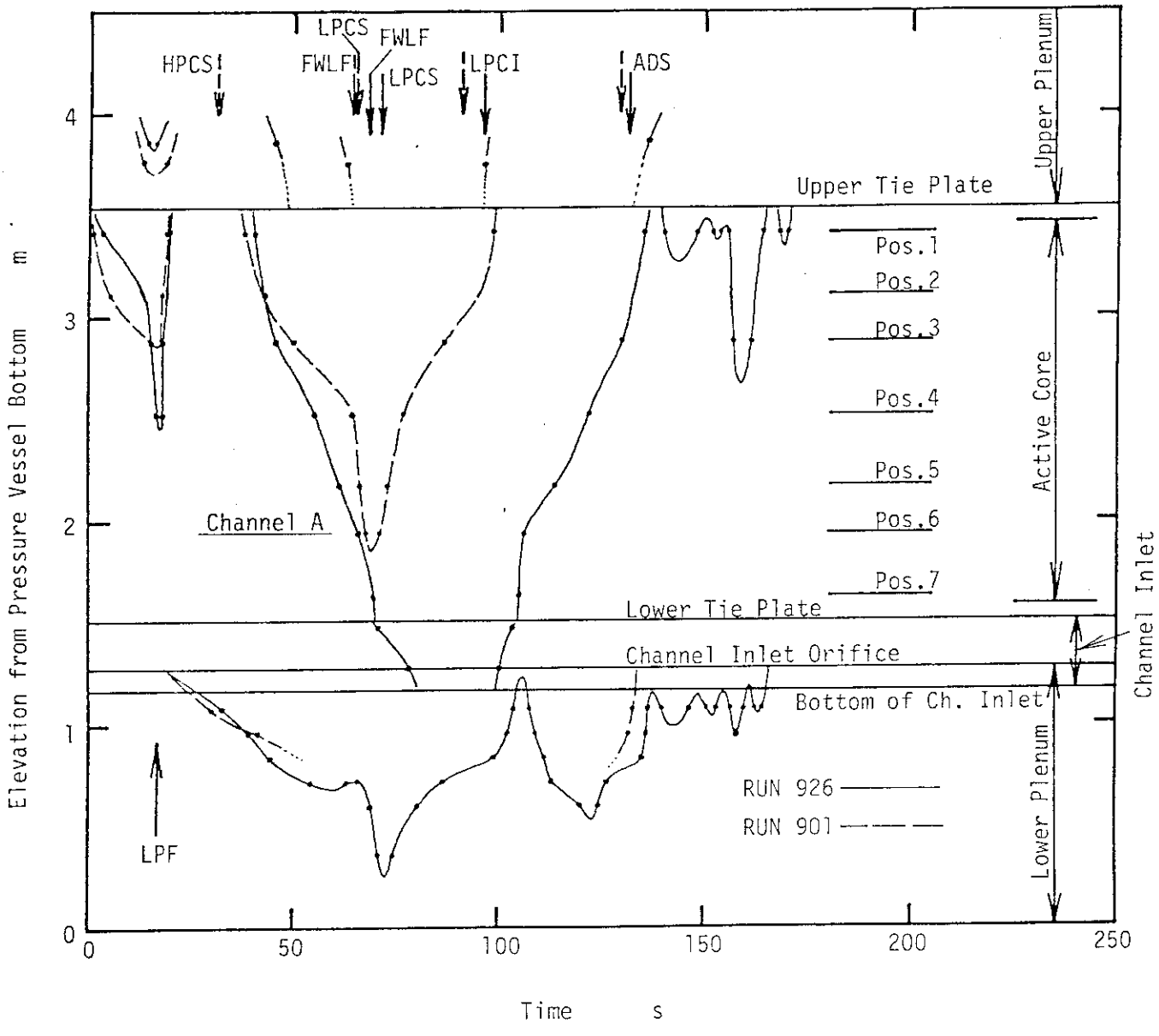

Fig. 6.9 Liquid Levels inside Core Shroud in RUN 926 and RUN 901

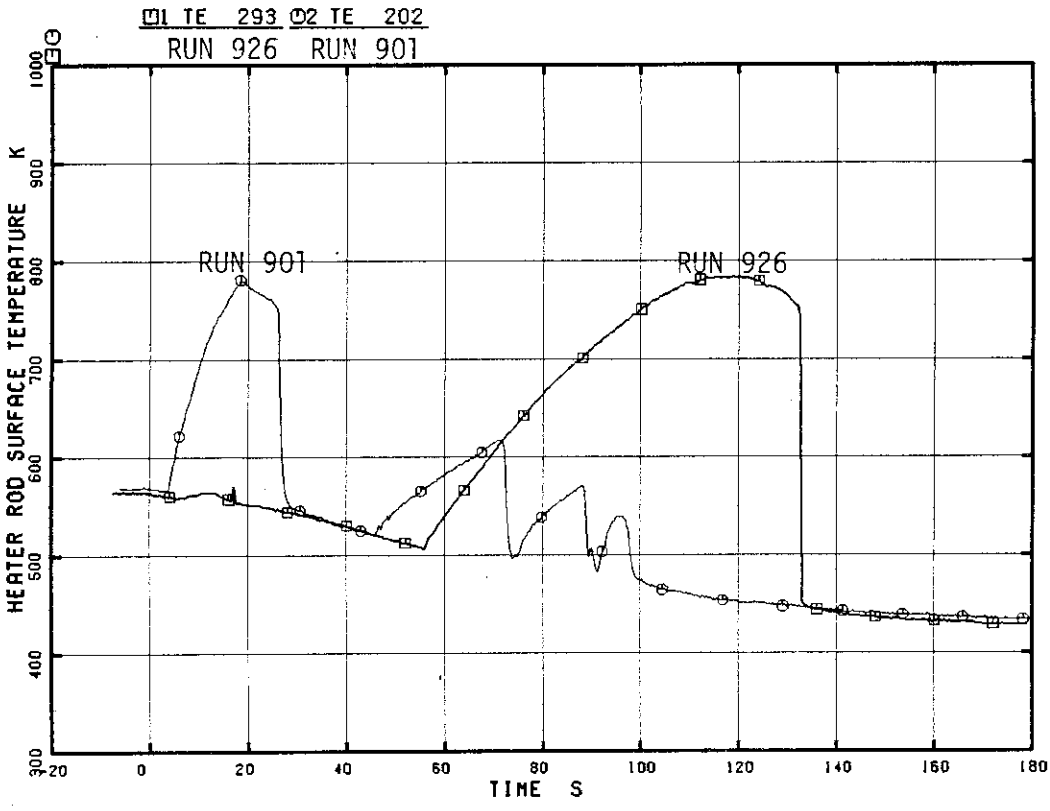

Fig. 6.10 Surface Temperature History of Fuel Rod recorded PCT in RUN 926 and RUN 901